The role of septins during vaccinia virus spread

Julia Pfanzelter

University College London

and

The Francis Crick Institute

PhD Supervisor: Dr Michael Way

A thesis submitted for the degree of

Doctor of Philosophy

University College London

October 2017

Declaration

I, Julia Pfanzelter, confirm that the work presented in this thesis is my own. Where information has been derived from other sources, I confirm that this has been indicated in the thesis.

Abstract

Septins are highly conserved components of the cytoskeleton found in animals and fungi. They play a variety of roles in key cellular processes including cell division, cell migration and membrane trafficking. During host-pathogen interactions, septins inhibit bacterial infection by forming cage-like structures around pathogens such as *Shigella*. In addition, two recent genome-wide RNAi screens demonstrated that septins play an undefined role during vaccinia virus replication. Utilizing cell-based assays and microscopy I set out to determine the role of septins in vaccinia infected cells. I found that septins are recruited to vaccinia virus immediately following its fusion with the plasma membrane during viral egress. Live cell imaging reveals that septins are lost from beneath the virus once the virus stimulates Arp2/3 complex-dependent actin polymerization to enhance its cell-to-cell spread. Virus-induced actin polymerization involves the phosphorylation of the viral protein A36, leading to the recruitment of Cdc42, Nck, Grb2, WIP and N-WASP, which activate the Arp2/3 complex. Chemical or genetic inhibition of A36 phosphorylation dramatically increases the number of virus particles co-localizing with septins. Further experiments demonstrate that the recruitment of Nck and subsequently dynamin, but not Grb2, WIP:N-WASP or the Arp2/3-complex, promote the loss of septins from virions. RNAi-mediated depletion of septins increases virus release, accelerates cell-to-cell spread, and induces more robust actin tails.

Collectively, my results demonstrate that septins limit the spread of vaccinia infection in cell monolayers and the recruitment of dynamin downstream of Nck enables the virus to overcome septin-mediated restriction. This is the first example of septins having an anti-viral effect and my work identifies a new role for septins in host defence.

Impact Statement

Vaccinia virus has been demonstrated to be an effective tool to study a diverse range of cell biological processes such as apoptosis, vesicle transport or actin dynamics (Nichols et al., 2017, Leite and Way, 2015, Frischknecht and Way, 2001, Traktman, 1990). Here, I have utilized vaccinia to gain new insights into the regulation of a cytoskeletal component known as septins.

The work presented in this thesis reveals a novel anti-viral role for septins in host-cell defence, namely that septins suppress the release and spread of the vaccinia virus. I have investigated the mechanism by which vaccinia overcomes this repressive function of septins and have uncovered a new link between the cytoskeletal proteins dynamin, formins and septins. The new potential connection between dynamin and formin-dependent actin polymerization will likely be relevant to cell biologists studying questions outside the context of virus biology. As septins are a highly conserved component of the cytoskeleton and fulfil a variety of vital functions in the cell, their dysregulation is associated with several diseases such as cancer, neuronal diseases, male sterility or platelet defects (Shen et al., 2017, Koch et al., 2015, Yu et al., 2016, Marttinen et al., 2015, Ageta-Ishihara et al., 2013b, Gozal et al., 2011, Bartsch et al., 2011, Shahhoseini et al., 2015). Hence my basic research has potential to contribute to the understanding and treatment of these diseases. Additionally, the community will also benefit from the reagents and methods I have developed, which are applicable to a broad range of scientific questions.

Vaccinia virus has many useful applications in clinical medicine. A modified version of vaccinia is used as an agent for vaccination against, among others, malaria, Ebola virus, HIV, tuberculosis, influenza or coronaviruses (Voigt et al., 2016, Iyer and Amara, 2014, Ohimain, 2016, Volz and Sutter, 2017). In addition, it could also serve as protection against biological weapons derived from smallpox. Describing new mechanisms by which the spread of vaccinia virus can be modulated will be of great interest for future vaccine development to minimize side effects of vaccination and increase efficacy.

Furthermore, increasing the release of virus to optimize vaccine production could be very beneficial, especially for diseases such as malaria or tuberculosis that are commonly associated with resource poor, developing countries.

Apart from being a vaccine agent, vaccinia is also used as an oncolytic virus (Buijs et al., 2015, Turnbull et al., 2015, Fukuhara et al., 2016). Its intrinsic ability to preferentially target cancer cells makes vaccinia an attractive therapeutic agent. Again, the insights provided in this thesis, into how host cells limits virus spread and how the pathogen overcomes such restrictions, can be used to further optimize vaccinia as an oncolytic therapeutic.

Finally, a large portion of my thesis work is being published in the Journal of Cell Biology (in revision), a specialist, well-respected journal with a large readership. Fluorescence images from my work have also been used in print media such as a journal cover (Journal of Cell Science, 128(13), 2015) and as advertising material for international meetings. These visually aesthetic images of septins and vaccinia will be useful for highlighting their importance during future public engagement events.

Acknowledgement

First of all, I would like to thank Michael for all the support and advice and the opportunity to work in his lab for the last four years. You helped me grow and now I feel ready to run and not just walk.
Big thanks go to Serge, for introducing me to the world of septins. Your passion is contagious and helped me through times of trouble.

My deep gratitude goes to the whole Way lab.
Antonio, you introduced me to vaccinia, asked the right questions at the right times and your dry jokes made me chuckle more than once. Theresa, you were the good soul of the lab and now you even look after a whole quadrant, thanks for everything! Jazz, you were the dream post-doc and a joy to work with. Ashley and Joe, thank you for the advice how to survive in the Way lab. Dave, thanks for bringing us all together over beer and more beer and thanks for being such a reliable source of reason and dark humour. Thanks to Xenia and Chiara, it was a great pleasure working, dancing and singing with you in the lab. Flavia, thank you very much for being such a good friend and mentor and I'm sure you'll be a wonderful mum in science. A big thank you also goes to Caitlin, you are the queen of pull-downs and you helped me fight with those bloody phospho-blots. Your advice and support throughout the years was totally "septin"! Lesley, thank you for answering all our burning questions regarding the wonders of birth. Davide, I hope you keep your enthusiasm and stay curious. Angika, thanks for making post-doc interviews look so easy. I'm sure you'll smash your project. I would also like to welcome Amadeus and I wish you in the name of all future PhD students (some of you might do me the honour and flick through the following pages) a great time… you can do it!

Thanks to everyone who read bits and pieces of this work, you helped me through the last few days and hours of my thesis writing.

I would also like to thank Nicola, you are a great friend and flatmate. Going through this "PhD-adventure" together with you was amazeballs. Anne, you have made my time in London very colourful and exciting and thanks to you I now know many quirky parts of this city. Nicki and Sophia, thanks a lot for your friendship across time and space, I'm already looking forward to our next reunion over a glass of glühwein.

Filled with gratitude and love I would like to say "Danke Lars".
Danke für Alles. Danke dafür, dass du meine Leidenschaften teilst und meine Verrücktheiten erträgst, danke für deine Unterstützung bei all den (programmier) technischen Fragen, danke für die zahllosen Gespräche, Ideen und all die Motivation, die mich durch die letzten vier Jahre getragen haben. Auf dich kann ich mich immer und überall, auch bei Sturm in der Steilwand, verlassen.

Last and the opposite of least, I would like to thank my family.
Danke Mama und Papa, ihr habt mir all das ermöglicht und mich in meinen Träumen unterstützt, auch wenn es mich dabei immer mehr in die große, weite Welt gezogen hat. Ich weiß, dass ihr mich mit jedem Loslassen fester im Herzen behaltet und dieses Wissen gibt mir den nötigen Mut. Außerdem komm ich ja zurück – versprochen!
Danke auch an Anna, David und Oma, ihr macht mein Leben ein Fest und Innsbruck mein Zuhause.

Table of Contents

Table of figures

List of tables

Abbreviations

%	percent
ADF	actin depolymerisation factor
ADP	Adenosine 5'-diphsphate
Arp	actin related protein
ATP	Adenosine 5'-triphsphate
AU	arbitrary unit
Borg	Binder of Rho GTPases
bp	base pairs
BSA	Bovine serum albumin
CB	cytoskeleton buffer
CCV	Clathrin-coated vesicle
CDC42	Cell division cycle 42
Cdc42EP	Cdc42 effector protein
CEV	cell-associated enveloped virion
CHC	Clathrin heavy chain
CK1	Casein kinase 1
CK2	Casein kinase 2
CLC	Clathrin light chain
cm	centimetre
CME	clathrin-mediated endocytosis
CPD	critical-point drying
CRIB	Cdc42- and Rac-interactive binding motif
CytoD	Cytochalasin
DAD	Dia auto-regulatory domain
DAPI	4',6 diamidino-2-phenylindole
DH	Dbl homology
DID	Dia inhibitory domain
DMEM	Dulbecco's modified eagle medium
DMSO	Dimethyl sulfoxide
DNA	deoxyribonucleic acid
dNTP	deoxynucleoside 5'-triphosphate
Drp1	dynamin-related protein
E.coli	Escherichia coli
EDTA	ethyl diamine N,N,N',N'-tetraacetic acid
EEV	extracellular enveloped virion
EFC	Eps15 homology
EGFR	Epidermal growth factor receptor
EGTA	Ethylene glycol tetraacetic acid

EH	Eps15 homology
EHEC	Enterohemorrhagic Escherichia coli
EM	Electron microscopy
EPEC	Enteropathogenic Escherichia coli
Eps15	Epidermal growth factor substrate 15
ER	endoplasmic reticulum
F-actin	filamentous actin
FCS	foetal calf serum
FH	formin homology
FRAP	fluorescence recovery after photo-bleaching
FSB	Final sample buffer
g-actin	monomeric actin
GAG	Glycosaminoglycan
GBD	GTP-binding domain
GED	GTPase effector domain
GEF	Guanine nucleotide exchange factor
GFP	green fluorescent protein
Grb2	Growth factor receptor-bound protein 2
GTP	Guanosine-5'-triphosphat
GTPase	Guanosine-5'-triphosphatase
HCV	hepatitis C virus
hpi	hours post infection
HPV-31	human papilloma virus type 31
hr	hour
HRP	horseradish peroxidase
HSV	herpes simplex virus
IAV	influenza A virus
IEV	intracellular enveloped virion
IF	immunofluorescence
IMV	intracellular mature virion
ITSN	Intersectin
JYM	junction-mediating regulatory protein
kb	kilo base
kDa	kilo Dalton
l	litre
LB	Luria Bertani
M	Molar
MCS	multiple cloning site
MEF	mouse embryo fibroblast
MEM	modified eagle medium
MES	2-(N-morpholino)-ethanesulphonic acid
mg	milligram

min	minute
ml	millilitre
mm	millimetre
mM	Millimolar
MOI	multiplicity of infection
ms	milliseconds
MT	Microtubule
MTOC	Microtubule organising centre
N-terminus	amino terminus
N-WASP	neural Wiskott Aldrich syndrome protein
Nck	Non-catalytic region of tyrosine kinase adaptor protein
ng	nanogram
nm	nanometre
NPF	Asparagine-Proline-Phenylalanine
ºC	degrees Celsius
OD	optical density
oligo	oligonucleotide
PAGE	Polyacrylamide gel electrophoresis
PBS	phosphate buffered saline
PCR	polymerase chain reaction
pE/L	early late promoter
Pen	penicillin
PFA	Paraformaldehyde
PFU	plaque forming units
PH	Pleckstrin homology
Pi	inorganic phosphate
PIP2	Phosphatidylinositol 4,5-bisphosphate
PRD	Polyproline-rich domain
Pt	platinum
PTM	Post-translational modifications
RFP	red fluorescent protein
RNAi	Ribonucleic acid interference
ROI	region of interest
rpm	Revolutions per minute
RT	room temperature
RTK	receptor tyrosine kinase
SD	standard deviation
SDS	sodium dodecyl sulphate
sec	seconds
SEM	Standard error of the mean
SEM	scanning electron microscopy

SH	Src homology domain
SIM	structured illumination microscopy
siRNA	small interfering ribonucleic acid
Src	Sarcoma
Strep	streptomycin
SV40	simian virus 40
t1/2	half time
T3SS	type III secretion system
TBE	Tris-borate-EDTA buffer
TEM	transmission electron microscopy
TGN	trans Golgi network
V	volts
VACV	Vaccinia virus
VSV	vesicular stomatitis virus
w/v	weight/volume
WASH	WASP and SCAR homologue
WASP	Wiskott-Aldrich-Syndrome protein
WAVE	WASP-family verprolin homologue
WCA	WASP homology 2, central and acidic region
WH2	WASP homology domain 2
WHAMM	WASP homologue associated with actin, membranes and microtubules
WHO	world health organization
WIP	WASP interacting protein
WT	Wild-type
YLDV	Yaba-like disease virus
Δ	delta
µl	microliter
µm	micrometre

Chapter 1. Introduction

1.1 Vaccinia virus

1.1.1 General

Viruses are obligate intracellular pathogens that cannot replicate outside their host. Vaccinia virus is a member of the poxvirus family, a group of large double-stranded DNA viruses which, for instance, includes variola, the causative agent of smallpox (Moss, 2007, Salzman, 1960). Vaccinia was successfully used as a vaccine against variola eventually leading to the eradication of smallpox (Newmark, 1980, 1972). Smallpox had a mortality rate of around 30% (Fenner et al., 1988, Henderson) and had endangered humanity since approximately 10.000 BC (Dixon, 1962). One of the first famous smallpox victims may have been the Egyptian Pharaoh Ramses V, as lesions found on the face of the mummy suggest this (Hopkins, 1985). In China, first attempts to protect people from the disease by intra-nasally administering dried, powdered smallpox scrabs are dated to the tenth century (Burnette, 1992, Gross and Sepkowitz, 1998). In a more Eurocentric world view Edward Jenner is often praised as the "father of immunology" who saved countless lives with his discovery (Smith, 2011). Jenner followed up on the observation that milkmaids, who often got infected with the less severe cowpox virus, seemed to be immune to smallpox. By inoculating a young boy (James Phipps) with cowpox pus, he successfully protected the child against a subsequent challenge with smallpox (Orr and McNeill, 1988, Radetsky, 1999). However, this practise had also been used by others even earlier in some parts of Europe and Jenner may have known about some of them (Hammarsten et al., 1979, Plett, 2006). Eventually, extensive vaccination programs and the fact that humans are the only host for smallpox allowed the world health organization (WHO) to eradicate this disastrous disease (1972, Barquet and Domingo, 1997).

The exact origin of vaccinia virus still remains a subject of speculation, since the strains used today are different to any other known poxvirus. However, some studies suggest that variola virus has evolved rather recently with the common ancestor emerging in the 16th century (Duggan et al., 2016, Babkin and Babkina, 2015).

Centuries of passaging the vaccinia in a variety of hosts probably allowed for the evolution of this artificial virus, which has no natural occurring host (Baxby, 1975, Baxby, 1977). One common hypothesis, however, is that it derived from cowpox, given that is was extracted from lesions caused by that disease.

Today vaccinia is still widely studied and new applications for the virus have arisen. In addition to bracing humanity against the threat that smallpox might be used as a bio-weapon, vaccinia is often used as a safe vaccine vector for a variety of diseases (Gómez et al., 2011, Grigg et al., 2013, Ramezanpour et al., 2016). Furthermore, modified vaccinia virus strains have great potential as oncolytic viruses (Deng et al., 2017, Fukuhara et al., 2016, Jefferson et al., 2015). Besides medical applications, vaccinia virus is also a great tool to study a range of cellular processes such as signalling pathways, microtubule transport, actin dynamics as well as the immune response to viral infection. (Miner and Hruby, 1990, Roberts and Smith, 2008, Iborra et al., 2012, Lousberg et al., 2011, Newsome and Marzook, 2015, Bonjardim, 2017, Leite and Way, 2015).

1.1.2 Viral entry

Vaccinia has a complex replication cycle in cells in culture that is depicted in Figure 1.1. Infectious vaccinia virus particles come in two states, the intracellular mature virion (IMV) and the extracellular enveloped virion (EEV). IMV are surrounded by a single membrane bilayer, whereas EEV are wrapped by a double membrane. Furthermore, the proteins integrated and associated with the viral membrane differ for the two virus populations (Moss, 2007). IMV represent the majority of virions in infected cells but are only released after host cell lysis. They are environmentally stable and particularly well-suited for long range host to host transmission (Smith et al., 2002). In contrast, EEV are responsible for local and rapid cell-to-cell spread (Law et al., 2002, Appleyard et al., 1971, Payne, 1980, Blasco and Moss, 1992, Doceul et al., 2010). Due to distinct morphology and protein composition it is not surprising that they utilize different cell entry mechanisms.

IMV entry is initiated by the binding of the virus to the plasma membrane through interactions between host cell surface glycosaminglycans (GAGs) (Carter et al.,

2005, Chiu et al., 2007, Chung et al., 1998, Hsiao et al., 1999, Lin et al., 2000). How exactly EEV attach to the host cell is not yet fully understood, but a current hypothesis suggests that upon interactions with host GAGs the outer membrane of EEV ruptures, revealing the proteins involved in IMV fusion (Law et al., 2006, Schmidt et al., 2012, Senkevich et al., 2004b). After binding, IMV can undergo lateral movement along filopodia towards the cell centre (Huang et al., 2008a, Mercer and Helenius, 2008). Thereupon the virus activates a signalling cascade that induces membrane blebbing, a process in which the plasma membrane detaches from the cortex and is retracted in an acto-myosin dependent manner (Charras, 2008, Mercer and Helenius, 2008). These membrane protrusions facilitate both EEV and IMV entry via micropinocytosis, a mechanism usually used to clear apoptotic bodies (Mercer and Helenius, 2008, Mercer and Helenius, 2009, Sandgren et al., 2010, Townsley et al., 2006, Mercer and Helenius, 2010, Mercer et al., 2010a, Schmidt et al., 2011, Hoffmann et al., 2001). The viral membrane is rich in phosphatidylserines (Ichihashi and Oie, 1983, Zwartouw, 1964), usually a hallmark for apoptotic cells and activates several kinases including PKC, Pak1 and PI(3)K and depends on Rac-mediated rearrangement of the actin cortex (Locker et al., 2000, Mercer and Helenius, 2008, Mercer et al., 2010a, Laliberte and Moss, 2009, Schmidt et al., 2011). Entering the cell via micropinocytosis allows the virus to easily cross the cell cortex, avoid recognition by the immune system and take advantage of spatio-temporally ordered endocytic cues, such as changing pH (Bidgood and Mercer, 2015, Moss, 2016, Amara and Mercer, 2015, Mercer, 2011). The acidification of endosomes is an essential trigger for the fusion of the viral and endosomal membranes (Townsley and Moss, 2007, Townsley et al., 2006). Membrane fusion is mediated by the entry-fusion complex (EFC), a multimeric structure composed of twelve viral proteins (Bisht et al., 2008, Brown et al., 2006, Izmailyan et al., 2006, Nichols et al., 2008, Ojeda et al., 2006a, Ojeda et al., 2006b, Senkevich et al., 2004a, Townsley et al., 2005, Wolfe et al., 2012). Two other viral proteins, A25 and A26, prevent premature fusion and negatively regulate EFC function (Chang et al., 2010). The A25:A26 dimer is inactivated by acidification, which can occur either by artificially lowering the pH of the media, or naturally during endosome maturation (Chang et al., 2010, Townsley et al., 2006). Subsequently viral and endosomal membranes fuse and the virus particle is released into the cytoplasm.

While there is clear evidence that vaccinia induced endocytosis is independent of clathrin and caveolae-mediated pathways, there are contradicting studies regarding the role of dynamin during vaccinia entry (Huang et al., 2008a, Schroeder et al., 2012, Mercer and Helenius, 2008, Laliberte et al., 2011). In the work of Mercer and Helenius, the dynamin inhibitor dynasore and the overexpression of the dominant-negative dynamin 2 had no significant impact on IMV entry (Mercer and Helenius, 2008, Mercer et al., 2010a). Yet others found that the same inhibitory treatments as well as siRNA-mediated knockdown of dynamin2 substantially decreased vaccinia virus entry into HeLa cells and mouse embryonic fibroblasts (MEFs) (Huang et al., 2008a, Schroeder et al., 2012, Laliberte et al., 2011).

While endocytosis represents the most common mechanism of vaccinia entry, there is also some limited evidence that the virus can also fuse directly with the plasma membrane to deposit its inner core into the cytoplasm (Carter et al., 2005, Law et al., 2006). An additional level of complexity is added as the mode of virus uptake and the requirements for entry vary between different cell types (Bengali et al., 2011, Bengali et al., 2009, Whitbeck et al., 2009, Mercer et al., 2010a) and virus strains (Chang et al., 2010, Mercer et al., 2010a).

Finally, there is evidence that in polarized epithelial cells the virus has a preference to enter through the basolateral surface (Rodriguez et al., 1991, Vermeer et al., 2007).

1.1.3 Virus replication and assembly

Once vaccinia has entered the cell and shed its membranes, the virus core is exposed to the cytoplasm (Dales, 1963, Moss, 2016). The virus core can reach the cell centre via microtubule-based transport (Carter et al., 2003). Vaccinia also induces cell blebbing soon after infection by modulating the cell cortex (Barry et al., 2015, Durkin et al., 2017, Schramm et al., 2006). The viral protein F11 alleviates the RhoD/Pak6-mediated inhibition of RhoC, which is then able to activate myosin-II via ROCK resulting in increased cortex contractility and bleb formation (Durkin et al., 2017). It is not clear what the purpose of this process is but one current hypothesis is that thereby cell organelles accumulate close to the nucleus allowing the virus to efficiently access the resources of the host cell.

One peculiarity of poxviruses is that their replication does not occur in the nucleus as seen with other large DNA viruses, such as herpes and adenovirus. Instead it takes place in so-called virus factories, which are infection-specific domains located in the host cytoplasm close to the microtubule-organizing centre (Moss, 2007, Ploubidou et al., 2000, Roberts and Smith, 2008, Tolonen et al., 2001). The genome of vaccinia encodes several replication machinery components including DNA polymerase, DNA ligase, topoisomerase and Helicase-primase, allowing for autonomous DNA replication (Moss, 2013). However, a recent study demonstrated that additional host proteins involved in the ATR dependent DNA damage response exit the nucleus and accumulate in the virus factories where they promote virus replication (Postigo et al., 2017). Once in the cytoplasm, the virus core is activated and undergoes morphological changes and viral proteins are released from proteinaceous structures flanking the DNA containing core called lateral bodies (Dales, 1963, Pedersen et al., 2000, Schmidt et al., 2013). Inside the virus core the viral RNA polymerase is already pre-bound to the early promoters enabling rapid transcription. The mRNA is released into the cytoplasm where it gets translated by host ribosomes, resulting in early viral protein production (Baldick and Moss, 1993, Yang and Moss, 2009). The viral AAA+ ATPase D5 is one of those early gene products and it helps to un-coat the vaccinia genome (Kilcher et al., 2014, Mercer et al., 2012). Simultaneously, vaccinia inhibits translation of host genes to maximize the available resources and to suppress the adaptive and innate immune responses (Moss, 1968, Person-Fernandez and Beaud, 1986, Strnadova et al., 2015). Approximately half of the 260 viral genes are transcribed early with most of them being involved in genome replication, immune evasion and preventing early host cell death (Broyles, 2003, Postigo and Ferrer, 2009, Postigo et al., 2009, Moss, 2007). A much smaller subset of intermediate genes is activated later and is largely responsible for initiating the translation of the late genes (Zhang et al., 1992, Assarsson et al., 2008, Yang et al., 2011). Late gene products are needed for the assembly of the next generation of virus particles (Kent, 1989, Rosel and Moss, 1985).

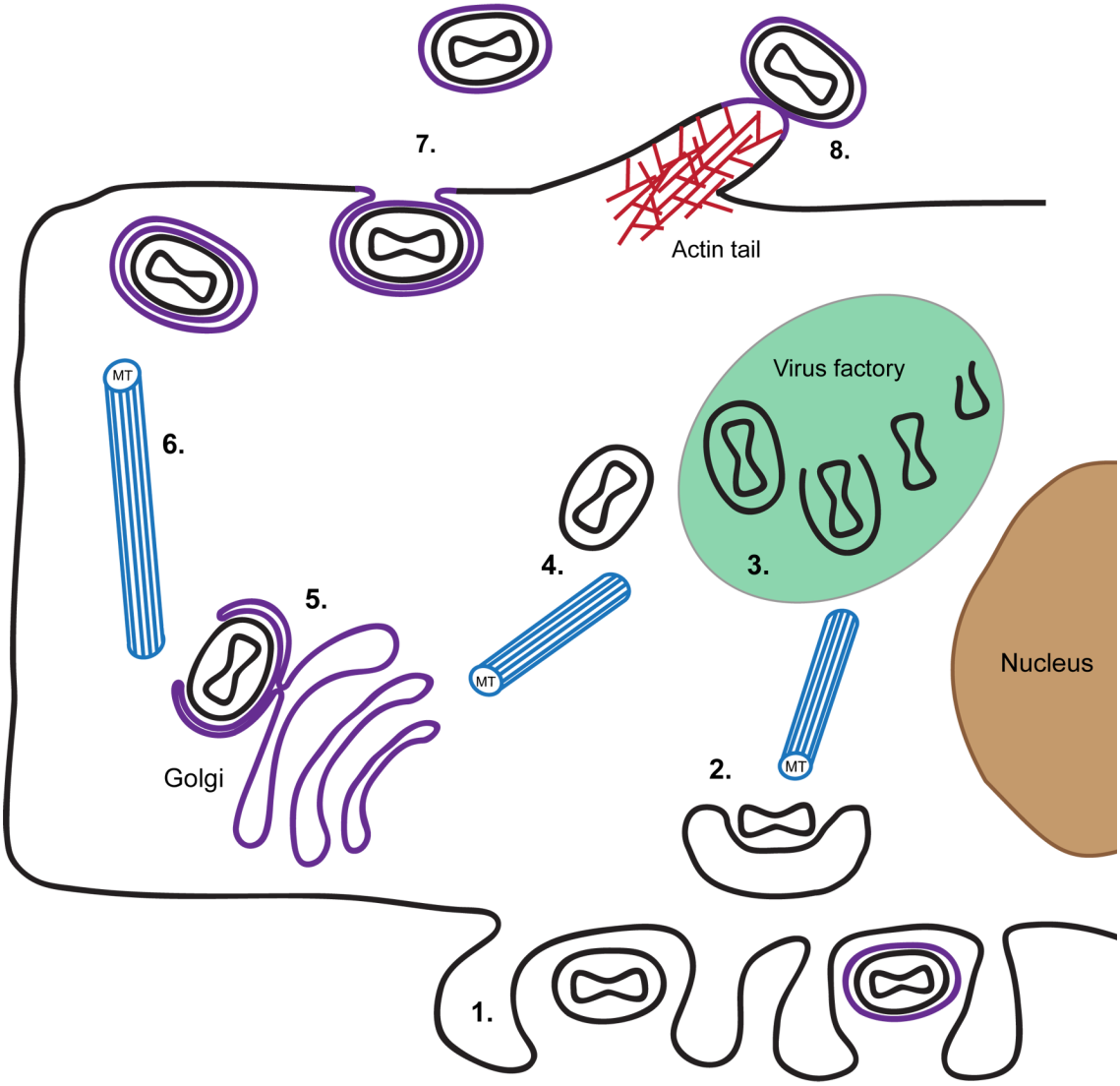

Figure 1.1 Replication cycle of vaccinia virus

1. IMV and EEV attach to the cell and stimulate micropinocytosis to induce its uptake. **2.** The viral core is released into the cytoplasm and viral cores are transported to the perinuclear region along microtubules. **3.** New virus particles are formed in the cytoplasmic virus factory. **4.** IMVs reach the TGN by microtubule-transport, **5.** where they are wrapped by a double membrane cisternae to become IEV. **6.** IEVs bind kinesin-1 to be transported to the cell periphery in a microtubule-dependent manner. **7.** IEVs cross the cortical actin and their outermost membrane fuses with the plasma membrane. Then they are either released into the surrounding or **8.** CEVs recruit Src/Abl family kinases to stimulate the formation of the actin tails (shown in red).

Crescent-shaped lipid membranes, derived from the endoplasmic reticulum (ER), are the first distinguishable structures of virus morphogenesis detectable by electron microscopy (Dales and Mosbach, 1968, Hollinshead et al., 1999, Husain et al., 2006, Risco et al., 2002). These membranes then surround the new viral core and the viral genome gets packaged into the core of these immature virions (IV) before the virion

membrane is sealed (Morgan, 1976, Cepeda and Esteban, 2014). Whilst some of the essential proteins for correct membrane wrapping are already well known, the mechanistic details remain rather obscure (Condit et al., 2006, Rodriguez et al., 1998, Sodeik et al., 1993, Sodeik and Krijnse-Locker, 2002, Zhang and Moss, 1992, Griffiths et al., 2001). Using advanced electron microscopy techniques, it became clear that a single de-novo derived membrane encloses the viral core (Heuser, 2005, Hollinshead et al., 1999). Proteolytic cleavage of capsid proteins and condensation of the core material results in substantial morphological changes leading to the formation of the typically barrel-shaped intracellular mature virion (IMV) (Condit et al., 2006, Moss and Rosenblum, 1973). This is where morphogenesis ends for most virions until IMVs are released from the host cell by cell lysis. A small subset of IMV undergo further adaptations to become intracellular enveloped virions (IEV). Microtubule-based transport facilitates the re-localization of some IMV from the virus factory to the trans-Golgi network (TGN) where an additional double membrane cisternae is wrapped around the IMV (Earley et al., 2008, Hiller and Weber, 1985, Payne and Kristenson, 1979, Sanderson et al., 2000, Schmelz et al., 1994, Tooze et al., 1993, Ward, 2005). The resulting intracellular enveloped virions (IEV) are now surrounded by three layers of lipid. Inserted to or associated with the two outermost membranes are several specific IEV proteins (A33, A34, A36, A56, B5, E2, F12 and F13). Some of them are involved in IEV formation (A27, B5 and F13) while others are implicated in the transport to the cell periphery (F12 and A36) (Roberts and Smith, 2008, Leite and Way, 2015).

The specific orientation of the viral proteins integrated or associated with the virus membrane is depicted in Figure 1.2. A36 and F12, for example, are only found in the outermost membrane and subsequently left behind in the plasma membrane when the virus exits the cell (van Eijl et al., 2002, van Eijl et al., 2000). B5 and F13, which are already inserted in the TGN and endosomal membrane, are essential for membrane wrapping. Together with other viral membrane proteins such as A33 and A36 they cycle between the plasma membrane and the TGN (Blasco and Moss, 1992, Engelstad and Smith, 1993, Wolffe et al., 1993, Husain and Moss, 2003, Husain and Moss, 2005, Ward and Moss, 2000).

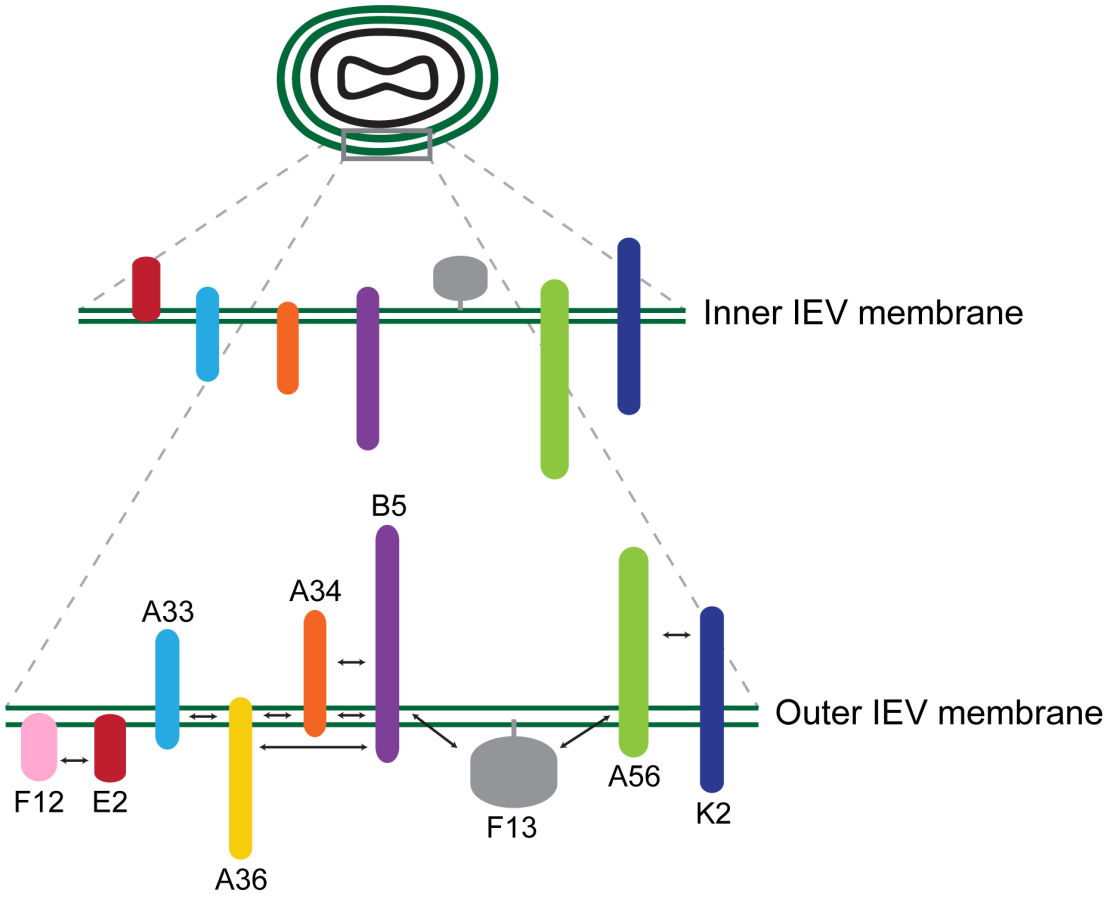

Figure 1.2 Viral proteins associated with the outer membranes of IEV

Schematic depicting the orientation of viral proteins that are integrated or associated with the two outermost membranes of IEV. Arrows indicate interactions between proteins.

Following the wrapping step IEV move along microtubules to the cell periphery (Geada et al., 2001, Hollinshead et al., 2001, Rietdorf et al., 2001, Ward, 2005, Ward and Moss, 2001a). F12 jointly recruited with E2 and A36 are implicated in microtubule-based motility and their deletion results in severe spreading defects (Herrero-Martinez et al., 2005, Rietdorf et al., 2001, Ward and Moss, 2001a, Parkinson and Smith, 1994, Morgan et al., 2010, Carpentier et al., 2015, Carpentier et al., 2017). IEV recruit kinesin1 via interactions of the bipartite tryptophan acidic motifs (WE WD) of A36 with the plus-end-directed microtubule motor (Dodding et al., 2011, Dodding et al., 2009, Ward and Moss, 2004, Pernigo et al., 2013). Bipartite tryptophan-acidic motifs are conserved kinesin1-binding motifs that are found in cellular kinesin-interacting proteins, such as calsyntenin-1 (Dodding et al., 2011, Dodding and Way, 2011, Morgan et al., 2010, Konecna et al., 2006, Araki et al., 2007).

Vaccinia not only hijacks the existing microtubules but actively regulates their dynamics leading to more microtubule tips reaching the cell periphery (Arakawa et al., 2007b). Therefore, F11 inhibits RhoA signalling to mDia1 leading to increased levels of tubulin acetylation (Arakawa et al., 2007b). In this way, the virus increases its transport to the plasma membrane. Once at the cell periphery, the dense meshwork of the actin cortex constitutes an obstacle to fusing with the plasma membrane. In order to cross this barrier vaccinia downregulates RhoA signalling to mDia via the viral protein F11(Arakawa et al., 2007a). Reduced mDia activity also changes the actin dynamics in the cortex and allows the virus to reach the plasma membrane (Arakawa et al., 2007a). In addition, regulation of RhoA via F11 also enhances cell migration and promotes viral spread in vivo and in vitro (Valderrama et al., 2006, Cordeiro et al., 2009).

1.1.4 Viral egress and cell-to-cell spread

When IEV reach the cell periphery and cross the cell cortex, their outermost membrane fuses with the plasma membrane thereby releasing the virion into the extracellular space (Smith and Law, 2004, Smith et al., 2002, Arakawa et al., 2007a, Blasco and Moss, 1992, Cudmore et al., 1995). The mechanistic details of how this membrane fusion occurs still remains to be established. The extracellular virions, referred to as extracellular enveloped virions (EEV), can be released from the cell and promote the long range spread of infection throughout an animal (Payne, 1980, Reeves et al., 2005). Alternatively, they can remain attached to the outer surface of the plasma membrane through interactions of viral membrane proteins spanning the plasma membrane and the virus membrane (Smith and Law, 2004, Smith et al., 2002). This sub-population of viruses is referred to as cell-associated enveloped virions (CEV). Upon fusion, the viral proteins A36 and F12, which were only located in the outer viral membrane, are left behind in the plasma membrane (Smith and Law, 2004, Smith et al., 2002). A36 accumulates underneath the CEV, as seen by immunofluorescence and electron microscopy (Ichihashi et al., 1971, van Eijl et al., 2000, Frischknecht et al., 1999b, Newsome et al., 2006). Subsequently, the cytoplasmic part of A36 gets phosphorylated by Src/Abl family kinases on two tyrosines. Thereby kinesin-1 dissociates and a receptor tyrosine-like signalling cascade locally induces Arp2/3-dependent actin polymerization (Blasco and Moss,

1992, Cudmore et al., 1995, Frischknecht et al., 1999b, Moreau et al., 2000, Newsome et al., 2004, Newsome et al., 2006, Scaplehorn et al., 2002, Stokes, 1976). Newly formed branched actin filaments underneath the virus assemble into a so-called actin tail. The pushing forces exerted by newly inserted actin monomers into the filaments propels vaccinia forward. Actin-based movement of the virus greatly enhances virus release and spread (Payne and Kristensson, 1982, Frischknecht et al., 1999b, Moreau et al., 2000, Rietdorf et al., 2001, Ward et al., 2003). Breaking the viral protein interactions that tether the virus to the cell surface are thought to be disrupted by the pushing forces of actin polymerization, allowing the virus to be released (Horsington et al., 2013). Under conditions where actin polymerization is prevented, virus release is significantly reduced and there is evidence that virus particles are stuck in membrane pits after fusion (Horsington et al., 2013). see Figure 1.3

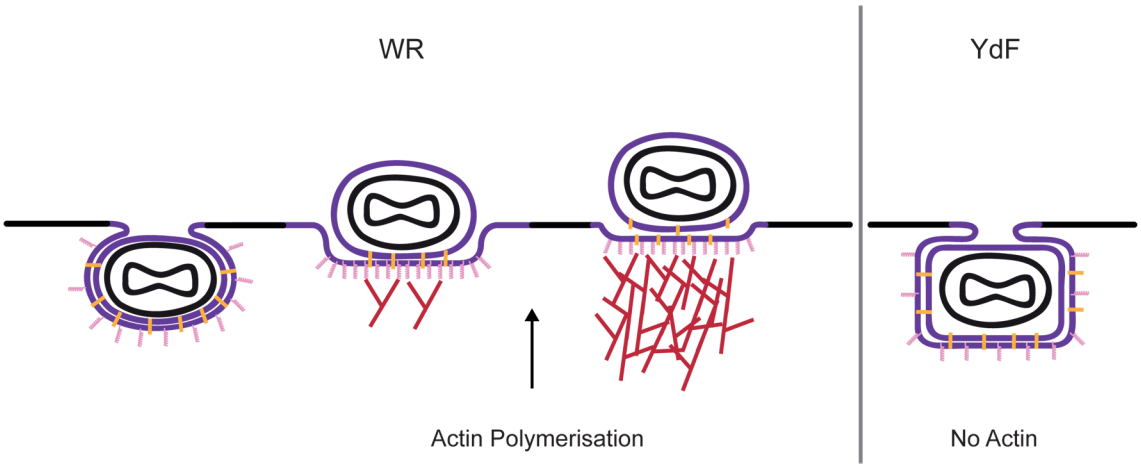

Figure 1.3 Actin promotes virus release

During egress the outermost membrane of vaccinia fuses with the plasma membrane. Transmembrane proteins anchor the virus particle to the surface of the host cell. Locally induce actin polymerization pushes the virus outwards. Without those pushing forces the virus particle remains trapped in the membrane pit.

1.2 Actin and its role during vaccinia egress

1.2.1 Actin

Actin is a highly conserved protein and is one of the most abundant proteins in the cell with concentrations up to several hundred micro-molar (Koestler et al., 2009,

Steinmetz et al., 1997). The 42 kDa-sized globular actin (G-actin) has the ability to polymerize into polar, helical filaments (F-actin) (Hanson and Lowy, 1964, Pollard, 1977, Dominguez and Holmes, 2011). By decorating actin filaments with the head group of the actin-motor myosin the orientation of the filament could be determined, see Figure 1.4A (Huxley, 1963)). Based on this labelling technique, the two ends of an actin filament are termed barbed and pointed end (Huxley, 1963, Woodrum et al., 1975). The rate-limiting step of actin polymerization is the assembly of the initial actin trimer, which forms the seed for subsequent filament elongation (Nishida and Sakai, 1983, Arisaka et al., 1975). The rate of actin polymerization in the presence of such seeds is directly proportional to the concentration of G-actin; however, a monomer is much more likely to be added to the barbed end than to the pointed end (Wegner, 1976, Pollard and Mooseker, 1981, Pollard, 1983). At a steady state concentration of G-actin, the filament length remains constant but due to the differential binding affinities of the two ends, monomers are integrated into the filament at the barbed end while at the same time the filament disassembles at the pointed end. This cycling process of actin is named treadmilling (Figure 1.4B) (Fujiwara et al., 2002, Pollard and Borisy, 2003).

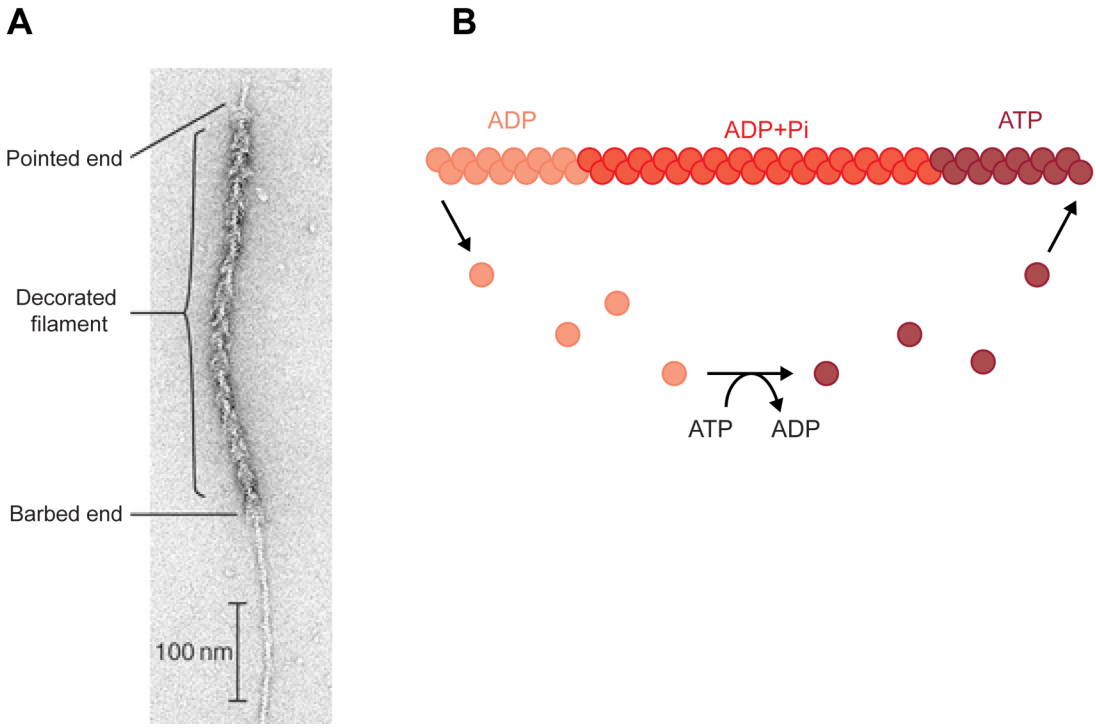

Figure 1.4 The actin filament

A Electron micrograph of a negatively stained actin filament partially decorated with myosin heads. © Adapted from Pollard and Borisy, 2003. Originally published in *Cell*

0092-8674 **B** Schematic depicting the process of simultaneous filament elongation and depolymerisation called actin treadmilling.

Actin is bound to an adenosine phosphate, which either comes as ATP, ADP or ADP-Pi. Monomeric actin bound to ATP can assemble into filaments, while polymerized actin can hydrolyse the nucleotide to ADP-Pi (Korn et al., 1987, Carlier and Pantaloni, 1986, Carlier et al., 1988). Over time the phosphate is lost and the remaining ADP allows a conformational change leading to decreased persistence length of the filament (Janmey et al., 1990, Orlova and Egelman, 1992). The transition from ATP-bound actin to the ADP-Pi-bound and subsequently the ADP-bound form in the filament acts as an intrinsic timer and is vital for actin treadmilling (Bugyi and Carlier, 2010, Carlier et al., 2011). In addition, the cell expresses several proteins, which locally regulate actin dynamics. For example, it was shown that actin depolymerizing factors (ADF) and cofilin bind ADP-bound actin and promote severing of F-actin by inducing additional torsion in the actin filament (Cao et al., 2006, Okreglak and Drubin, 2007, McGough et al., 1997). In addition, ADF and cofilin also bind to ADP-Pi-bound actin and accelerate the release of the phosphate thereby promoting subsequent actin depolymerisation (Blanchoin and Pollard, 1999). ADF and cofilin also promote actin polymerization at the barbed end, firstly by increasing the pool of monomeric actin and secondly by providing additional free barbed ends through severing of existing filaments (Shekhar et al., 2016, Bravo-Cordero et al., 2013).
In the cell, monomeric actin is mostly bound to profilin, a conserved 16 kDa actin binding protein (Carlsson et al., 1976, Carlsson et al., 1977, Yarmola and Bubb, 2006, Alkam et al., 2017, Courtemanche and Pollard, 2013). Binding of profilin to G-actin stimulates the exchange of bound ADP to ATP, which regenerates the pool of G-actin. Following the binding of profilin-actin to F-actin, profilin is released (Pollard and Cooper, 1984, Ding et al., Blanchoin and Pollard, 1998, Lu and Pollard, 2001, Porta and Borgstahl, 2012, Selden et al., 1999). Profilin-actin can only be incorporated into the barbed end of the filament and reinforces the underlying mechanism of actin treadmilling (Tilney et al., 1983, Pollard and Cooper, 1984). In addition, recent studies have shown that profilin inhibits the formation of branched actin and favours the formation of parallel actin bundles (Rotty and Bear, 2015, Suarez et al., 2015).
Another group of actin binding proteins are the capping proteins, which are widely found in all eukaryotes (Edwards et al., 2014, Shekhar et al., 2016). Originally

purified from ameoba (Isenberg et al., 1980), capping protein consists of a heterodimer of alpha and beta subunits that bind to the barbed end of actin filaments to prevent addition and dissociation of actin monomers (Cooper and Sept, 2008, Edwards et al., 2014, Wear et al., 2003). If all actin filament barbed ends were free and able to elongate, the cell would quickly run out of available G-actin (Pollard, 2016). Conversely, if all the capping proteins engaged with actin filaments, no barbed ends would be left. Since both scenarios are lethal, the cell tightly regulates the activity of capping proteins. Myothrophin sequesters a proportion of capping proteins away, while capping protein interactors (CPI) regulate the affinity of capping proteins to both the barbed ends and to myotrophin (Bhattacharya et al., 2006, Schafer et al., 1996, Edwards et al., 2014).

The regulation of actin is closely linked to motility. First, the contractile potential of muscles depends on myosin motors that walk along actin filaments (Geeves, 1991). Second, actin is an important component of the cytoskeleton and indispensable for cell migration (Rottner and Stradal, 2011, Lammermann and Sixt, 2009). Actin filaments can dynamically assemble and disassemble, and those filaments can either exert substantial pulling and pushing forces or, by being cross-linked provide rigidity (Fletcher and Mullins, 2010, Blanchoin et al., 2014). Balancing the ratio of filamentous and monomeric actin is crucial to allow rapid adaptations and dynamic changes in the actin cytoskeleton (Sept and McCammon, 2001, Pollard and Cooper, 2009, Shekhar et al., 2016). Furthermore, the number and length of actin filaments impacts on their ability to exert high pushing forces required for cell migration (Mogilner and Oster, 1996, Mogilner and Oster, 2003, Pollard and Borisy, 2003).

1.2.2 Actin filament nucleators

The initial rate limiting step to nucleate an actin filament is the binding of three actin monomers to form a stable, trimeric species that can elongate. While subsequent elongation of the seed occurs rapidly, the formation of the trimer is thermodynamically unfavourable (Pollard and Cooper, 1986, Pollard and Weeds, 1984, Gilbert and Frieden, 1983, Woodrum et al., 1975). Actin nucleators catalyse seed formation in order to promote actin filament formation (Figure 1.5). Examples of these different actin nucleators will be described below.

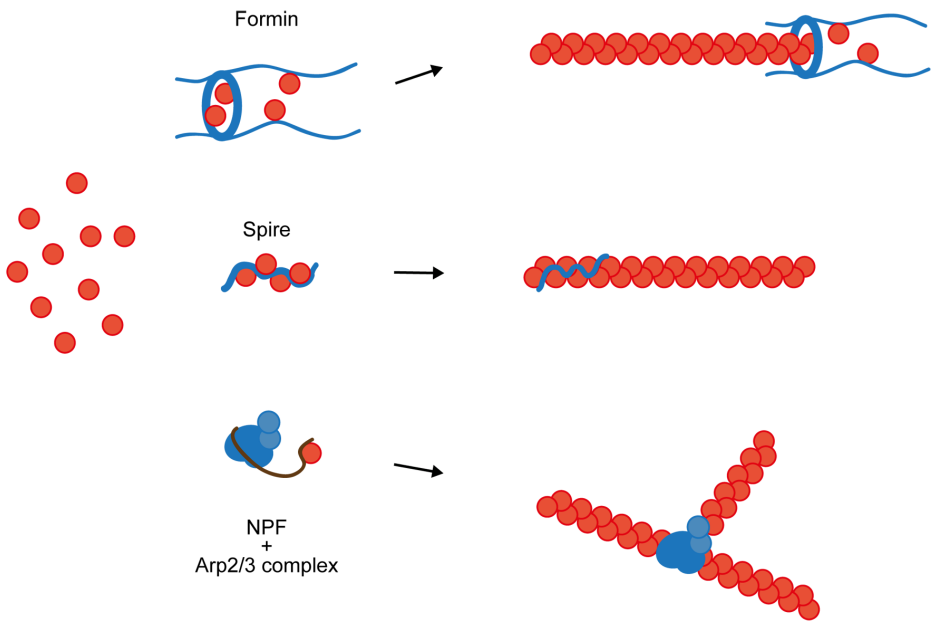

Figure 1.5 Actin nucleators

Schematic of actin nucleators and how they initiate a new actin filament. Formins remain attached to the growing barbed end further facilitating elongation. WH-2 containing proteins, such as Spire, promote filament nucleation by binding up to four actin monomers. The Arp2/3 complex, activated by a nucleation promoting factor, can branch a new daughter filament of a pre-existing mother filament.

Formins

Formins are unique amongst the actin nucleators in that they can facilitate both nucleation and elongation of unbranched actin filaments (Dominguez, 2016, Breitsprecher and Goode, 2013). Humans have 15 different formins, which are subdivided into 7 families. A conserved feature of all formins is the presence of formin homology domains 1 and 2 (FH1 and FH2) which play important roles in their ability to stimulate actin filament assembly (Chesarone et al., 2010, Schonichen and Geyer, 2010). A subgroup of formins was found to exist in the cytoplasm as auto-inhibited inactive monomers, or homo-dimers. The inactivation is mediated through the binding of the Dia inhibitory domain (DID) to the C-terminal Dia auto-regulatory domain (DAD) (Nezami et al., 2006, Kovar, 2006). Active Rho-GTPases, such as RhoA, Rac1 or Cdc42, release this inhibition and activate the formin (Maiti et al., 2012, Li and Higgs, 2003, Rose et al., 2005). The two FH2 domains of the dimer form a doughnut shaped ring, which can interact with either two actin monomers or the barbed end of the actin filament (Figure 1.6A). By staying attached to the fast-growing barbed end during elongation, the formin protects the filament from capping

proteins (Moser et al., 2003, Kovar et al., 2003, Pruyne et al., 2002, Xu et al., 2004). The FH1 domains bind and recruit the profilin-actin complexes in order to supply sufficient actin for rapid filament growth (Kovar et al., 2006, Paul and Pollard, 2008). Formins help to overcome the energy barrier of actin seed formation by stabilizing actin dimers and subsequent actin trimers (Kovar et al., 2003, Pring et al., 2003, Li and Higgs, 2003). However, *in vitro* the actin nucleation efficiency of formins is rather low compared to other nucleation promoting factors (Pring et al., 2003, Gould et al., 2011, Heimsath and Higgs, 2012). Several formins have an additional domain on the C-terminal site of the FH2 domain, which can either interact directly with actin monomers or recruit other actin binding proteins such as spire or APC that can also nucleate actin filaments (Quinlan et al., 2007, Breitsprecher et al., 2012, Pechlivanis et al., 2009, Montaville et al., 2016). Both mechanisms strongly increase the potential of formins to nucleate and elongate actin filaments (Blanchoin and Michelot, 2012, Paul and Pollard, 2008, Moseley et al., 2004, Schumacher et al., 2004, Dominguez, 2016).

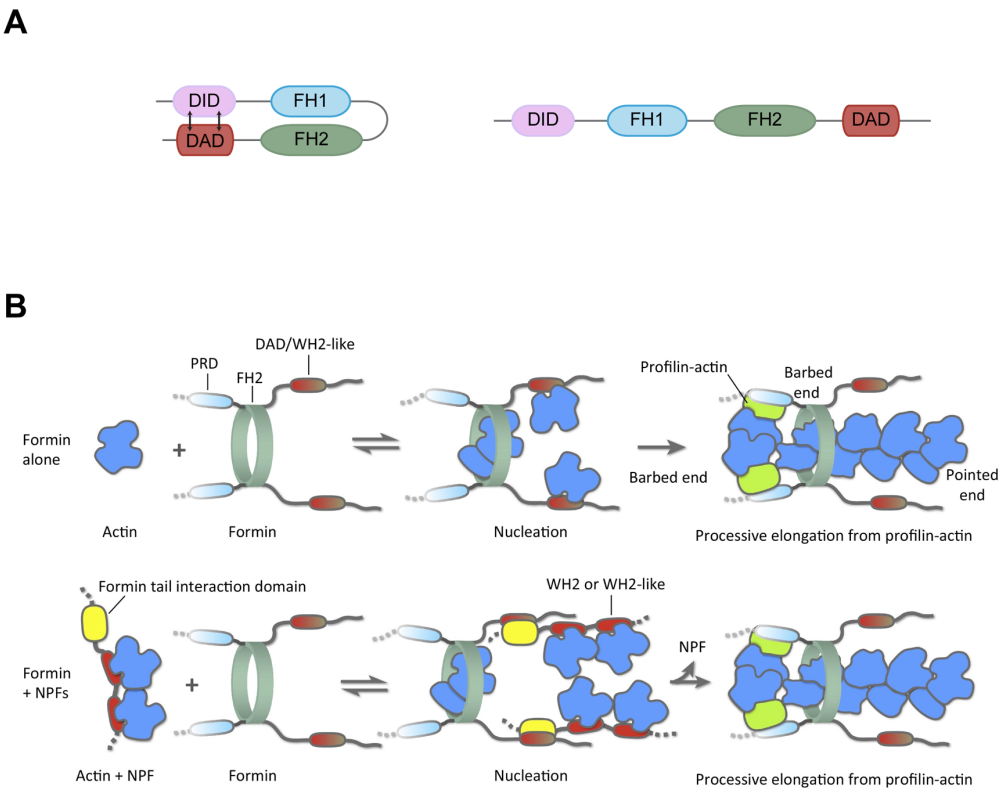

Figure 1.6 Formins can nucleate actin filaments

A Schematic showing the domain structure of formins. **B** Schematic of the nucleation mechanism by which formin can nucleate an actin filament either alone or in

cooperation with other actin binding proteins. © Dominguez, 2016. Originally published in *Trends Biochem Sci* 0968-0004.

WH2-domain containing proteins

The group of proteins containing a WASP homology 2 (WH2) domain is the most recently discovered family of actin nucleators and includes proteins such as Spire, Cobl and leiomodin (Dominguez, 2016, Quinlan et al., 2005, Qualmann and Kessels, 2009). The WH2 domain, initially found in Wiskott-Aldrich syndrome protein (WASP), is one of the most abundant G-actin binding domains (Symons et al., 1996, Carlier et al., 2011, Shekhar et al., 2016, Weiss and Schultz, 2015). WH2-domain containing proteins can have up to four repeats of this motif, with each one capable of binding one G-actin. It has been proposed that WH2 domains act by bringing three or four monomers in close proximity, thereby stabilizing the filament seed (Figure 1.5) (Ahuja et al., 2007, Campellone and Welch, 2010, Liverman et al., 2007, Quinlan et al., 2005, Tam et al., 2007). To optimize their nucleation efficiency, WH2-domain containing proteins can cooperate with other actin binding proteins such as formins (Dominguez, 2016). One such well-studied pair is Spire and Cappuccino, initially found in flies (Rosales-Nieves et al., 2006, Quinlan et al., 2007). Interesting, the bacterium Rickettsia expresses Sca2, which combines feature of a classical WH2-domain containing protein and has similarities to formins. Sca2 is able to polymerize the host actin into linear filaments (see 1.2.3) (Haglund et al., 2010, Choe and Welch, 2016, Reed et al., 2014).

Arp2/3 complex and its regulators

The Arp2/3 complex is the only actin nucleation factor that induces the formation of branched actin filaments (Machesky et al., 1994, Rotty et al., 2013, Goley and Welch, 2006). It is a complex of seven highly conserved subunits consisting of the actin related proteins 2 and 3 (Arp2 and Arp3), which have strong sequence and structural similarities to actin as well as five additional proteins (ArpC1 to ArpC5) (Goley and Welch, 2006, Kelleher et al., 1995, Machesky et al., 1994, Rouiller et al., 2008, Robinson et al., 2001, Welch et al., 1997a). Actin filament nucleation is achieved by binding one actin monomer, which, together with Arp2 and Arp3, mimics the first trimer of the filament (Goley and Welch, 2006, Pollard and Borisy, 2003, Mullins et al., 1998a, Mullins et al., 1998b). Initiating a new “daughter” filament while binding to

the side of a “mother” filament allows the Arp2/3 complex to form Y-shaped branches at an angle of approximately 74° (Figure 1.7) (Goley and Welch, 2006, Mullins et al., 1998a, Mullins et al., 1998b, Egile et al., 2005). The crystal structure of the Arp2/3 complex revealed an inactive conformation, in which Arp2 and Arp3 are rather distant from each other (Robinson et al., 2001). Up until now, it has not been possible to crystalize the active form of the Arp2/3 complex and a lower resolution cryo-electron tomography of branched actin provides the best resolved structure of the active form bound to actin filaments (Rouiller et al., 2008). Computational models have been used to simulate the necessary structural rearrangements that bring Arp2 and Arp3 together to allow growth of the daughter filament (Dalhaimer and Pollard, 2010). In order to adopt this active conformation, the Arp2/3 complex needs to be activated by additional proteins called nucleation promoting factors. Nucleation promoting factors are essential, since the isolated Arp2/3 complex has very poor actin nucleation activity (Goley and Welch, 2006, Mullins et al., 1998b, Welch et al., 1998, Welch and Mullins, 2002).

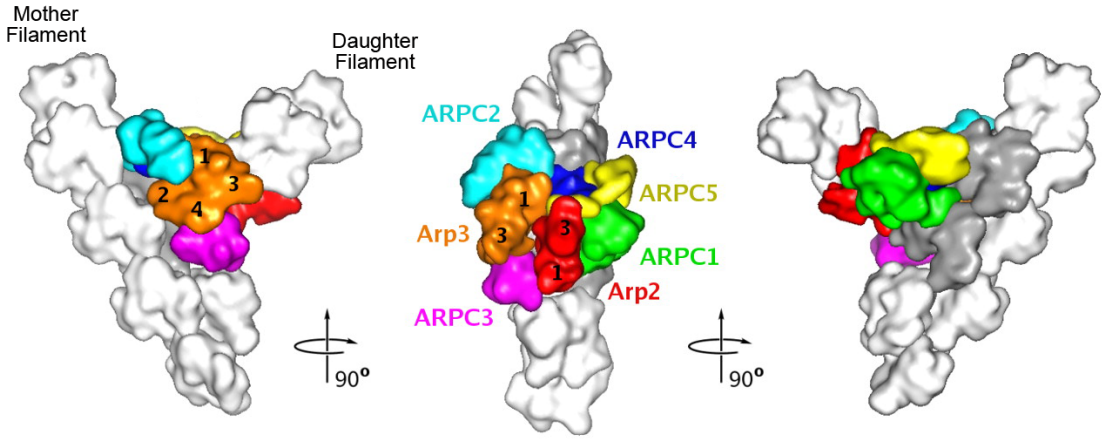

Figure 1.7 The Arp2/3 complex

Low resolution surface representation of the Arp2/3 complex at a branch point. Actin subunits are coloured in white or grey. © Roullier et al., 2008. Originally published in *Journal of cell biology*. 180:887-95.

Subsequent work over the years has subdivided nucleation promoting factors into two distinct classes. Class I nucleation promoting factors include WASP, neuronal WASP (N-WASP), WASP-family verprolin homologue (WAVE also known as SCAR), WASP and SCAR homologue (WASH), WASP homologue associated with actin, membranes and microtubules (WHAMM) and junction-mediating regulatory protein

(JMY). Class II nucleation promoting factors contain cortactin and hematopoietic-specific protein 1 (HS1) (Campellone and Welch, 2010). Members of the class I nucleation promoting factors each have a variable N-terminus, followed by a central proline rich domain of varying length and a conserved C-terminal WCA domain consisting of a WH2 domain (W), a connecting or central domain (C) and the acidic domain (A) (Tyler et al., 2016). Monomeric actin can bind to the WH2 domain, while the C and A domains interact with the Arp2/3 complex (Marchand et al., 2001, Chereau et al., 2005, Panchal et al., 2003). The current model of Arp2/3 activation is that while the acidic domain binds to the Arp2/3 complex, the central domain induces a conformational change that brings Arp2 and Arp3 closer together. Subsequently the W-domain delivers the first monomeric actin that forms together with Arp2 and Arp3 the trimer of the new daughter filament (Goley et al., 2004, Rodal et al., 2005b). Nucleation activity of pure Arp2/3 complex is rather poor but it is greatly enhanced by the addiction of a WCA domain, especially when the WCA domains can dimerise (Hufner et al., 2001, Padrick et al., 2008).

WASP and N-WASP are probably the best characterized nucleation promoting factors, partly because they were the first cellular nucleation promoting factors to be described (Miki et al., 1996, Yarar et al., 1999). Both proteins exist in an auto-inhibited state, in which the WCA domain binds intramolecularly to the GTPase binding domain (GBD) (Kim et al., 2000, Rohatgi et al., 2000, Miki et al., 1996, Prehoda et al., 2000 Yarar, 1999, Rohatgi et al., 1999). This inhibition can be overcome by several upstream signals including the binding of Cdc42 or phosphatidylinositol 4,5-bisphosphate (PIP_2) (Campellone and Welch, 2010, Prehoda et al., 2000). Furthermore, many adaptor proteins containing Src homology 3 (SH3) domains can bind to the proline rich domain (PRD) of WASP/N-WASP to activate the nucleation promoting factor. Examples are the non-catalytic kinase (Nck) and the growth factor receptor-bound protein 2 (Grb2) (Carlier et al., 2000, Rohatgi et al., 2001), both of which are recruited by Vaccinia virus (Donnelly et al., 2013, Frischknecht et al., 1999a, Scaplehorn et al., 2002, Moreau et al., 2000, Snapper et al., 2001). WASP interacting protein (WIP) can stabilize the auto-inhibited conformation of N-WASP and regulates its activation. Furthermore, WIP is also required for the recruitment of N-WASP to sides of actin polymerization (Anton et al., 2007, Martinez-Quiles et al., 2001, Stradal and Scita, 2006, Ho et al., 2004, Ramesh et al., 1997). Interestingly, WASP/N-WASP appear to always function in a complex

with WIP and WIP is also essential for the recruitment of N-WASP to vaccinia (Donnelly et al., 2013, Janssen et al., 2016, Weisswange et al., 2009, de la Fuente et al., 2007).

WAVE proteins are involved in plasma membrane protrusions and cell migration, where they are activated by the small GTPase, Rac1, and jointly with Ena/VASP proteins promote actin polymerization (Machesky et al., 1999, Chen et al., 2014, Miki et al., 1998b, Bear et al., 1998, Yamazaki et al., 2003). Ena/VASP proteins promote actin filament elongation by preventing filament capping (Krause et al., 2003).

WASH is found on early and recycling endosomes where the local branched actin network regulates the shape and content of endosomes (Carnell et al., 2011, Bartuzi et al., 2016, Derivery et al., 2009, Linardopoulou et al., 2007). WASH is also involved in receptor recycling (Piotrowski et al., 2013, Buckley et al., 2016, Zech et al., 2011)

JMY is found at the leading edge in migrating cells; however upon stress signals, such as DNA damage, JMY trans-locates into the nucleus where it facilitates p53-dependet transcription (Shikama et al., 1999, Zuchero et al., 2009, Zuchero et al., 2012). Interestingly, JMY can also promote Arp2/3 independent actin nucleation and is also involved in autophagosome formation (Coutts and La Thangue, 2015, Coutts et al., 2009, Zuchero et al., 2009).

WHAMM is found at the ER-Golgi intermediate compartment, where it is involved in the regulation of vesicle transport (Campellone et al., 2008). WHAMM can also bind to microtubules and this interaction simultaneously promotes membrane binding of WHAMM while inhibiting actin filament formation (Liu et al., 2017, Shen et al., 2012). Similar to JMY, WHAMM has also been shown to promote autophagosome formation during starvation (Kast et al., 2015).

The discovery of the first nucleation promoting factor is a prime example of how studying pathogens, which evolved to manipulate their host, provide valuable molecular insights into fundamental cellular processes. In 1998, Welch and co-workers found that ActA, a protein expressed by *Listeria monocytogenes*, can drastically increase the nucleation activity of Arp2/3 *in vitro* (Welch et al., 1998). Shortly after, nucleation promoting factors were identified in eukaryotes. WASP was already known to regulate actin dynamics in the cell, but it was only after the discovery of the Arp2/3 complex that the function of WASP as an Arp2/3 activator

was recognized (Symons et al., 1996, Machesky and Insall, 1998, Machesky et al., 1999, Winter et al., 1999, Yarar et al., 1999, Rohatgi et al., 1999).

1.2.3 Actin-based motility of pathogens

Pathogens have co-evolved with their unwilling hosts, which have developed various defence mechanisms against infection. Conversely, pathogens have established countless ways of manipulating the host cell machinery to counteract the hosts defences to enhance their replication and spread. Given the versatile functions of actin in a healthy cell, it is not surprising that many pathogens hijack this component of the cytoskeleton to promote their spread and movement (Figure 1.8). The first described example of a pathogen hijacking actin was the gram-positive bacterium *Listeria monocytogenes* (Tilney et al., 1990, Tilney and Portnoy, 1989), a food-borne pathogen, often causing food poisoning, sepsis and meningitis (Allerberger and Wagner, 2010, Farber and Peterkin, 1991). By analysing a bacterial mutant with a severe spreading defect, it was found that a bacterial surface protein, ActA, was disrupted and actin tails were no longer formed (Kocks et al., 1992). ActA contains conserved WH2 and CA domains, which enables it to directly bind and activate the Arp2/3 complex. Additional proline rich regions in ActA can recruit Ena/VASP proteins that further enhance actin polymerization (Welch et al., 1997b, Welch et al., 1998). Local induction of a branched actin network at one pole of the bacterium pushes the pathogen forward, while the formed actin network remains stationary and slowly disassembles (Carlsson and Brown, 2006, Tilney and Tilney, 1993).

The *in vitro* reconstitution of actin-based motility of *Listeria* with purified proteins allowed the determination of the minimal set of components required to support Arp2/3 dependent actin-based motility (Loisel et al., 1999). The minimal set of proteins, thus, consists of monomeric actin, Arp2/3, N-WASP, VASP, ADF and capping proteins (Loisel et al., 1999). *Listeria* actin tails have become a good model system to study the pushing forces exerted by Arp2/3-dependent actin polymerization, both *in vivo* and *in vitro* (Rolhion and Cossart, 2017, Small, 2015). Interestingly, it has been observed that in addition to Arp2/3-dependent actin tails, *Listeria* is able to switch to polymerising only parallel unbranched actin filaments, probably relying on VASP (Brieher et al., 2004). While Arp2/3 is needed for actin tail

initiation, actin bundling proteins, such as fascin, can trigger the transformation to unbranched, hollow actin tails (Brieher et al., 2004).

The baculovirus *Autographa californica*, commonly used as a protein expression system, is also propelled through the cytoplasm and into the nucleus by the power of actin polymerization (Goley et al., 2006, Ohkawa et al., 2010, Osz-Papai et al., 2015, van Oers et al., 2015, Lanier and Volkman, 1998, Wang et al., 2008). The capsid protein p78/83, found on one tip of the virus, like ActA, has similarity to the VCA domain of N-WASP family proteins. This enables it to activate the Arp2/3 complex, leading to a branched actin tail comprising of only four to five actin filaments, which are necessary to push the virus at a speed of 50 µm/min through the cytoplasm of the host cell (Goley et al., 2006, Machesky et al., 2001, Mueller et al., 2014).

Other pathogens have found alternative ways to locally stimulate Arp2/3-dependent actin polymerization. IscA (also called VirG) was found in a screen that identified pathogen proteins involved in promoting the spread of *Shigella flexneri* (Bernardini et al., 1989, Lett et al., 1989, Makino et al., 1986). IscA is polarized on the bacterium and recruits N-WASP, but not the closely related WASP, to one pole of the pathogen (Robbins et al., 2001, Suzuki et al., 1998, Suzuki et al., 2002). Upon binding to IscA, N-WASP adopts its active open conformation, enabling it to interact with the Arp2/3 complex (Mauricio et al., 2017, Egile et al., 1999). WIP and Nck are also found at *Shigella* tails, however, they are not required for formation of actin tails (Loisel et al., 1999, Moreau et al., 2000). While Cdc42 is involved in the uptake of *Shigella,* it is dispensable for actin tail formation (Shibata et al., 2002).

Mycobacterium marinum belongs also to a group of pathogens which optimizes their spread by actin-based motility. *Mycobacterium* also induces branched actin networks and relies on nucleation promoting factors, in particular WASP or N-WASP, but it does not require Nck, WIP or Cdc42 (Stamm et al., 2003, Stamm et al., 2005). Further work will be needed to identify the bacterial factor involved in N-WASP recruitment.

Instead of forming a classical actin tail as described above, the virulent forms of *E.coli* Enteropathogenic Escherichia coli (EPEC) and Enterohemorrhagic

Escherichia coli (EHEC) induce the formation of so called actin pedestals to promote their cell-to-cell spread (Hayward et al., 2006, Velle and Campellone, 2017). The bacteria express a protein called Tir (translocated intimin receptor), which is inserted into the host plasma membrane by weakly adhering bacteria (Kenny et al., 1997). Upon binding of the bacterial surface-protein intimin to Tir, the pathogen becomes tightly attached to the host cell (Lai et al., 2013). Binding of intimin induces Tir clustering and phosphorylation of tyrosine 474 of EPEC Tir (Swimm et al., 2004, Kenny, 1999). In the case of EPEC, phosphorylated tyrosine 474 is a docking site for the SH2 domain of Nck (Gruenheid et al., 2001). Nck in turn recruits N-WASP, which locally activates the Arp2/3 complex (Campellone et al., 2004a, Frese et al., 2006, Swimm et al., 2004, Bommarius et al., 2007, Gruenheid et al., 2001). In contrast, EHEC Tir does not get phosphorylated but the bacterial effector $EspF_U$ gets injected into the host cell, which binds to Tir via the host protein IRSp53 (Weiss et al., 2009). $EspF_U$ then recruits and activates N-WASP, leading to Arp2/3 driven actin polymerization (Garmendia et al., 2004, Campellone et al., 2004b). In either case, these resulting pedestal-like actin structures allow the bacteria still sitting on the outside of the host plasma membrane to surf on the cell surface and reach neighbouring cells (Velle and Campellone, 2017).

Intracellular movement of *Rickettsia rickettsii* was first observed in 1957 (Schaechter et al., 1957). *Rickettsia* can exploit both Arp2/3 dependent and independent actin polymerization. Early during infection, the pathogen uses the bacterial nucleation promoting factor, RickA, to activate the Arp2/3 complex and induce shorter, curved actin tails (Gouin et al., 2004, Jeng et al., 2004, Reed et al., 2014). Hours later, the formin-like bacterial protein, Sca2, directly polymerizes unbranched actin filaments at one pole of the bacterium (Haglund et al., 2010, Kleba et al., 2010, Reed et al., 2014, Serio et al., 2010). Furthermore, *Rickettsia* also reduces intracellular tension by secretion of an effector protein, Sca4, which disrupts the binding between vinculin and α-catenin (Lamason et al., 2016). Reduced intracellular tension promotes cell-to-cell spread of the bacterium and consequently relies less on the pushing force of actin polymerisation (Lamason et al., 2016).

Burkholderia sps express a protein BimA, which, depending on the strain, either activates Arp2/3 or mimics Ena/VASP proteins to directly nucleate and elongate actin

filaments (Breitbach et al., 2003, Stevens et al., 2005, Sitthidet et al., 2010, Benanti et al., 2015). It is interesting that BimA from different species initiate either branched or unbranched actin tails. The efficiency to form these tails varies, but once they are formed, the speed of the propelled bacteria is the same, regardless of the different underlying actin network (Benanti et al., 2015).

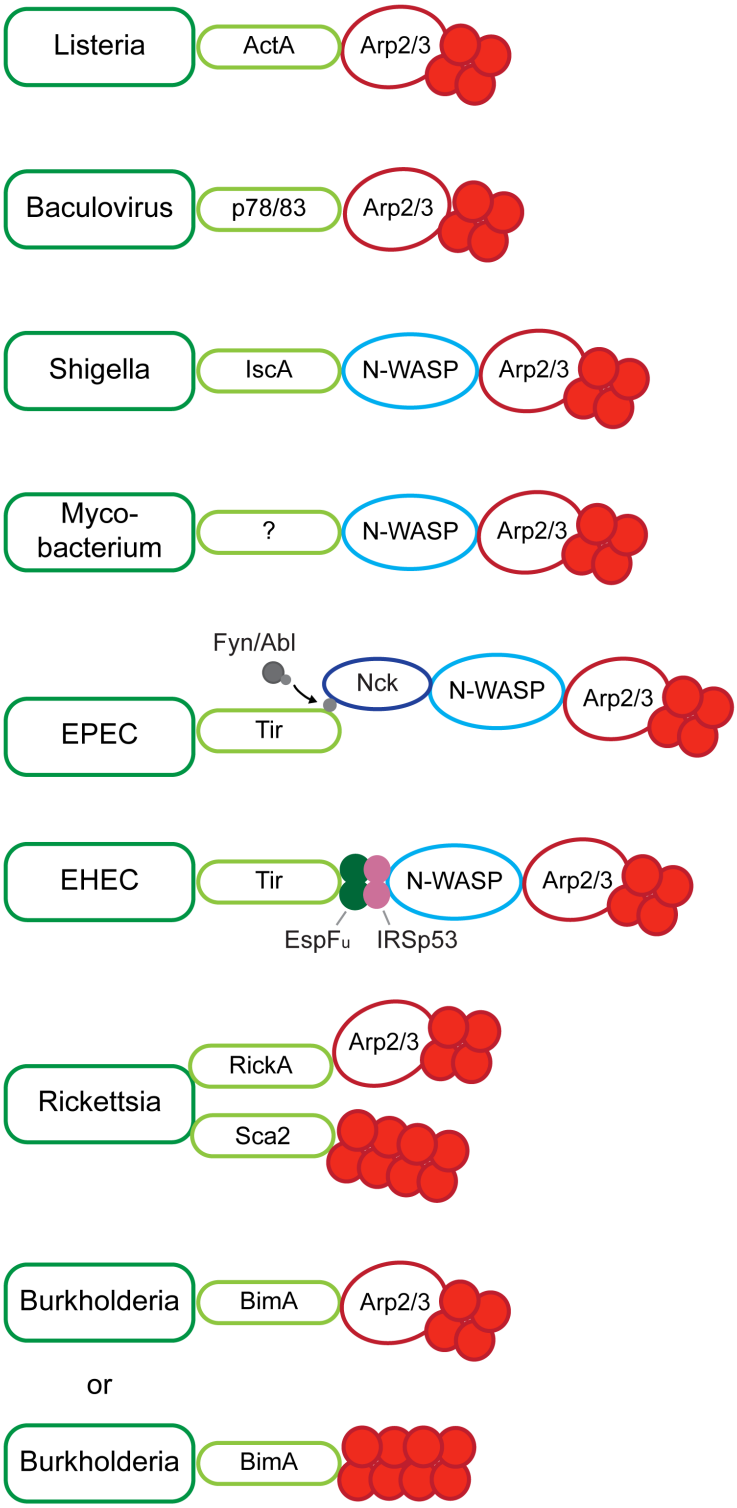

Figure 1.8 Various pathogens can induce polymerization of host-cell actin

Schematic of various strategies to locally induce actin polymerization exploited by different intracellular pathogens. Microbes and their proteins are depicted in green.

1.2.4 How vaccinia virus can induce actin tails

In 1976, it was noticed that some vaccinia particles are found at the tips of microvilli during viral release (Stokes, 1976). These viral tipped microvilli were actin-rich structures containing actin cross-linkers such as α-actinin, fimbrin and filamin but not myosin or tropomyosin (Hiller et al., 1981, Hiller et al., 1979, Krempien et al., 1981). However, it took another 15 years to show that rapid actin polymerization could propel the virus forward (Cudmore et al., 1995, Cudmore et al., 1996). Since then, a significant effort has been put into elucidating the nature of these actin tails and deducing the mechanism by which they are formed.

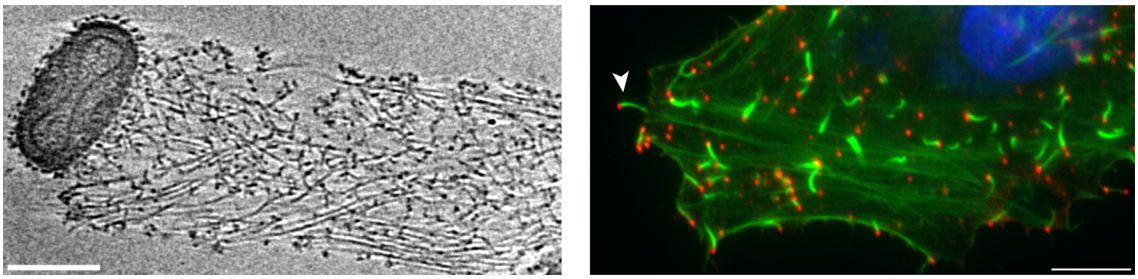

Figure 1.9 Vaccinia can induce actin tails

A A z-section through a cryo-electron tomogram of vaccinia associated with an actin tail (Pfanzelter, 2013). Scale bar = 200nm. **B** Immunofluorescence image of a Hela cell infected with WR. Actin stained with phalloidin is shown in green, virus in red and DAPI in blue. The white arrow highlights a virus tipped actin tail. Scale bar = 10µm.

After fusion with the plasma membrane, CEV can initiate these actin protrusions by locally recruiting and activating members of the Src and Abl family kinases, which in turn phosphorylate tyrosines 112 and 132 on the cytoplasmic domain of the viral protein A36 (Frischknecht et al., 1999a, Newsome et al., 2006, Reeves et al., 2005, Scaplehorn et al., 2002). Arg, Abl, Src, Fyn and Yes kinases are capable of phosphorylating A36 and thereby allow actin tail formation. Furthermore, Arg and Abl are additionally involved in virus release, although the underlying mechanism remains unclear (Newsome et al., 2006, Reeves et al., 2005). Inhibition of Abl/Arg by Imatinib reduces the release of extracellular enveloped viruses (EEV) by 60-70% and promotes survival of infected mice (Reeves et al., 2005). The fourth short consensus repeat (SCR4) of B5 is required for the recruitment and activation of Src/Abl family kinases underneath the virus/CEV at the plasma membrane (Newsome et al., 2004). Phosphorylation of A36 also triggers the release of kinesin-

1 from the virion at the plasma membrane (Newsome et al., 2004). The signalling cascade following A36 phosphorylation is very similar to phospho-tyrosine receptors (Figure 1.10).

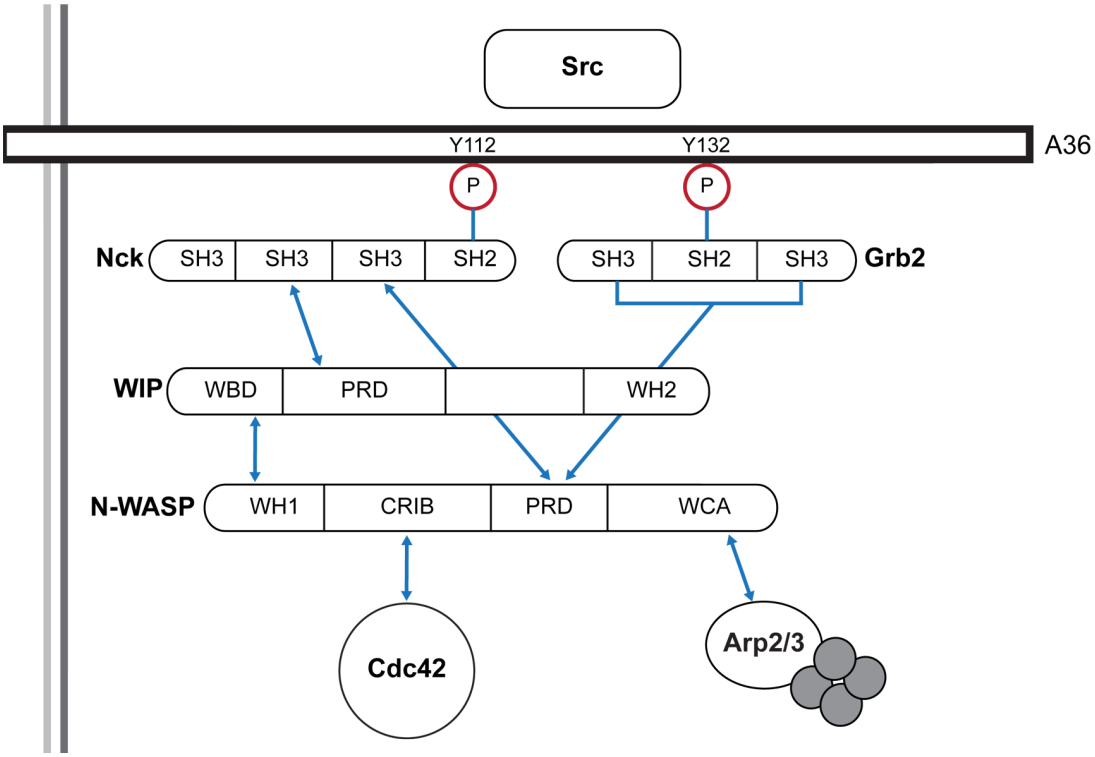

Figure 1.10 Signalling cascade leading to vaccinia-induced actin tails

Schematic depicting the signalling cascade downstream of the two phospho-tyrosines in the viral protein A36 leading to local actin polymerization. Domains are annotated: (P) phospho-tyrosine, SH2 (Src homology 2), SH3 (Src homology 3), WBD (WASP binding domain), PRD (Polyproline-rich domain), WH1/2 (WASP homology 1/2), GBD (GTPase binding domain), WCA (WH2, central and acidic region), CRIB (Cdc42- and Rac-interactive binding motif).

The residues around phosphorylated tyrosine Y112 in A36 conform to a consensus for a Nck SH2 binding site (Frese et al., 2006, Songyang et al., 1993) and are responsible for recruiting Nck to the virus (Donnelly et al., 2013, Frischknecht et al., 1999a, Scaplehorn et al., 2002). Nck is a SH2/SH3 adaptor protein that links signalling receptors with downstream effector proteins (Li et al., 2001, Buday et al., 2002). It contains one SH2 domain which binds to the phospho-tyrosine motif, and three Src homology-3 (SH3) domains that interact with PxxP motifs in a variety of binding partners (Lehmann et al., 1990, Li et al., 2001, Buday et al., 2002). Nck is involved in various processes such as cell migration, invadopodia formation, and

axon guidance (Chaki and Rivera, 2013, Li et al., 2001, McCarty, 1998). While some PxxP containing proteins show preferential binding to specific Nck SH3 domains, others have no specificity and can interact with all three domains (Buday et al., 2002, Antoku et al., 2008, Ger et al., 2011). During vaccinia egress, N-WASP and WIP are recruited as a complex to the CEV (Donnelly et al., 2013, Moreau et al., 2000, Weisswange et al., 2009). The second SH3 domain of Nck interacts with the polyproline region in WIP, while the third SH3 domain of Nck binds to the polyproline region in N-WASP (Donnelly et al., 2013). The first interaction is important for the recruitment of the complex, whereas the second interaction helps to activate N-WASP and allows subsequent Arp2/3-based actin polymerization. Because of the role of Nck in the formation of this complex, it was found to be essential for actin tail formation (Donnelly et al., 2013, Frischknecht et al., 1999a, Moreau et al., 2000, Newsome et al., 2004, Scaplehorn et al., 2002, Snapper et al., 2001, Weisswange et al., 2009, Zettl and Way, 2002).

In addition, the adaptor protein Grb2 is recruited to the phospho-Y132 in A36 (Donnelly et al., 2013, Scaplehorn et al., 2002). Grb2 is one of the best characterized SH2/SH3 adaptor proteins that links the epidermal growth factor receptor tyrosine kinase (EGFR) to the Ras-Raf-MEK-ERK pathway (Buday, 1999, Lowenstein et al., 1992, Giubellino et al., 2008, Wee and Wang, 2017). During vaccinia infection, Grb2 helps to stabilize the WIP:N-WASP complex and enhances actin tail formation (Donnelly et al., 2013, Scaplehorn et al., 2002). In contrast to tyrosine 112, phosphorylation of Y132 in A36 is not essential for actin tail formation (Donnelly et al., 2013, Scaplehorn et al., 2002, Ward and Moss, 2001b, Weisswange et al., 2009).

The list of proteins influencing vaccinia induced actin tails continues. For example, Casein kinase 2 was shown to enhance actin tail formation by stimulating recruitment of active Src (Alvarez and Agaisse, 2012). Alvarez and Agaisse also found that FHOD1, a formin, is recruited throughout the actin tail in a Rac1 and N-WASP dependent manner (Alvarez and Agaisse, 2013). Furthermore, knockdown of either Rac1, FHOD or profilin, significantly reduced the percentage of CEV associated with an actin tail (Alvarez and Agaisse, 2013). It was proposed that FHOD1 initially nucleates new actin filaments from which Arp2/3 can generate new daughter filaments. However, FHOD1 had no nucleation activity *in vitro* and acted as a

capping protein instead (Schonichen et al., 2013). While the interpretation of these data is currently under debate, it is clear that FHOD1 impacts on vaccinia virus spread.

Vaccinia virus is not the only poxvirus hijacking the actin cytoskeleton. Orthologues of A36 are found in many other orthopox viruses, such as the YL126 protein from the Yaba-like disease virus (YLDV) (Dodding and Way, 2009). Phosphorylation of YL126 similarly leads to branched actin tails downstream of Nck, Grb2 and N-WASP (Dodding and Way, 2009).

1.3 Endocytic machinery impacts on vaccinia egress and spread

1.3.1 Clathrin-mediated endocytosis

Endocytosis refers to the active uptake of liquid or solid substances into a cell by membrane engulfment (Kumari et al., 2010). Caveolae-mediated endocytosis, micropinocytosis, phagocytosis and pinocytosis are clathrin-independent ways of internalization, whereas receptor-mediated endocytosis relies on the formation of clathrin-coated vesicles (Kirchhausen et al., 2014). Clathrin-mediated endocytosis (CME) is used to internalize and recycle lipids and proteins but it can also be hijacked by invading pathogens (McMahon and Boucrot, 2011, Robinson, 2015, Yamauchi and Helenius, 2013). Clathrin-mediated endocytosis (CME) is a stepwise and tightly regulated process that can be divided into nucleation, cargo selection, coat assembly, invagination and finally vesicle scission and subsequent uncoating (Figure 1.11) (Geli and Riezman, 1998, Engqvist-Goldstein and Drubin, 2003, Lu et al., 2016, Goode et al., 2015).

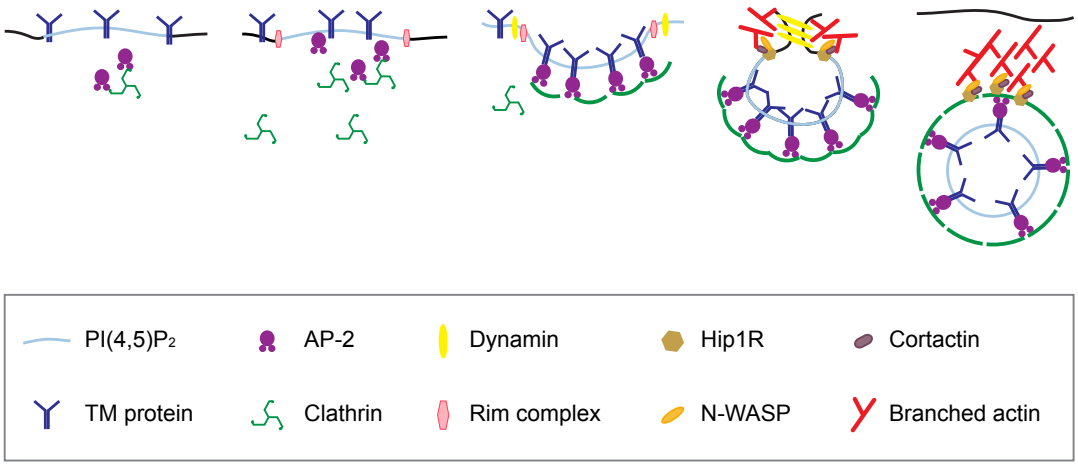

Figure 1.11 Stages of mammalian clathrin-mediated endocytosis

Schematic showing the steps leading to the formation of clathrin-coated vesicles. Following the coordinated arrival of two AP-2 molecules and one clathrin triskelion to a PIP_2-rich area at the plasma membrane, additional accessory proteins promote vesicle progression and cargo incorporation. Restriction of dynamin facilitates scission of the vesicle neck.

Clathrin

In the early 1970s Barbara Pearse started her postdoc project with the aim of purifying tubulin from pig brain. In failing to do so, she discovered intriguing vesicular structures reminiscent of a sliced tomato and similar to the “vesicle in a basket” described before by Kanaseki and Kadota (Pearse, 1975, Kanaseki and Kadota, 1969). What Pearse purified were clathrin-coated vesicles and her pioneering work has led to decades of studying clathrin and its role in endocytosis (Robinson, 2015, Pearse, 1975). Clathrin, highly conserved in all eukaryotes, plays an important role in many cellular events including vesicular trafficking, chemical neurotransmission, neuronal development, cell division and immunity (Wakeham et al., 2005, Spiro et al., 2014, Ybe, 2014, Brodsky et al., 2014, Seto et al., 2002, Kzhyshkowska and Krusell, 2009, Royle et al., 2005). The typical clathrin triskelion is formed by three 180 kDa clathrin heavy chains (CHC) and three clathrin light chains (CLC, 33-36kDa), see Figure 1.12A. The CHC form the three legs of the triskelion, while the CLC bind to the proximal leg domain of CHC. Clathrin triskelia have the tendency to self-assemble into a lattice of hexagons and pentagons, that can easily be visualised in electron microscopy Figure 1.12B (Ungewickell and Branton, 1981, Kirchhausen and Harrison, 1981, Roth and Porter, 1964, Liu et al., 1995, Kirchhausen et al., 1987b,

Kirchhausen et al., 1987a). CLC regulate the assembly of clathrin triskelia and the curvature of the resulting lattice varies depending on the ratio of hexa- and pentagons (Kirchhausen, 2009, McMahon and Boucrot, 2011, Brodsky, 1988, Greene et al., 2000, Wilbur et al., 2010).

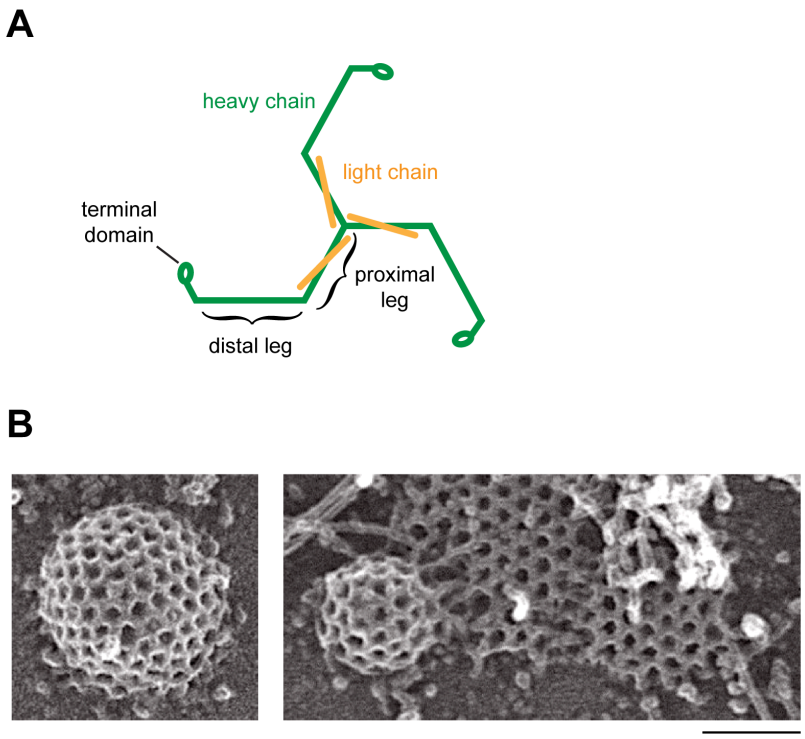

Figure 1.12 Structure of clathrin

A Schematic showing the structure of the clathrin triskelion composed of three heavy and three light chains. **B** Platinum replicas of clathrin lattices in flat patches and on forming endocytic vesicles. © Sochacki et al., 2017. Originally published in *Nature Cell Biology* 1465-7392.

Clathrin adaptor proteins

While clathrin forms the structural backbone of the vesicle coat, it relies on adaptor proteins to bind to the plasma membrane and to sort the cargo that is to be placed in the vesicle. Over twenty clathrin adaptor proteins are currently known. The most abundant and well-studied example is the adaptor protein 2 (AP-2), which, in its active form is exclusively found at the plasma membrane (Brodsky et al., 2001, Pearse and Robinson, 1984, Robinson, 1987, Collins et al., 2002, Jackson et al., 2010, Rapoport et al., 1997, Popova et al., 2013). AP-2 interacts directly with PIP_2 in the plasma membrane, clathrin heavy chain and with its cargo via a common cargo internalisation motif (Beck and Keen, 1991b, Beck and Keen, 1991a, Ohno et al.,

1995, Owen and Evans, 1998, Padron et al., 2003, Shih et al., 1995, Edeling et al., 2006, Kelly et al., 2014)

Eps15 homology family members, such as the epidermal growth factor receptor substrate 15 (Eps15) and intersectin, are involved in endocytosis as well as endosome trafficking to the TGN (Fazioli et al., 1993, Chen et al., 1998, Fernandez-Chacon et al., 2000, Benmerah et al., 1998, van Delft et al., 1997, Chi et al., 2008, Sengar et al., 1999, Yamabhai et al., 1998). The Epsin15 homology (EH) domain, the defining feature of this class of proteins, is roughly 100 amino acids long. The EH domains in Eps15 and intersectin specifically bind to the NPF (Asn-Pro-Phe) motif found cargos (Paoluzi et al., 1998, Salcini et al., 1997, Wong et al., 1994, Wong et al., 1995).
Eps15, which forms homo-dimers and tetramers, binds directly to NPF cargo and adaptor proteins but not clathrin or membranes (Coda et al., 1998, Cupers et al., 1997, Sengar et al., 1999, Suzuki et al., 2012, Wang et al., 2016). During vesicle formation Eps15 specifically localizes to the rim of the growing clathrin pit (Ehrlich et al., 2004, Saffarian et al., 2009, Sochacki et al., 2017, Tebar et al., 1996).

Humans have two intersectin (1 and 2) isoforms, which can form homo- and heterodimers with themselves and Eps15 (Sengar et al., 1999, Wong et al., 1994, Yamabhai et al., 1998). Eps15 and intersectin associate with FCHo1/2, an accessory protein, participate in vesicle initiation and are found at the rim of the clathrin pit (Cocucci et al., 2012, Henne et al., 2010, Ma et al., 2016, Sochacki et al., 2017). Intersectin-1 has also been shown to directly bind AP-2 (Pechstein et al., 2010) and, like Eps15, interacts with cargo via the conserved NPF motif (Yamabhai et al., 1998). In addition, intersectin has the ability to link the endocytic machinery to actin polymerization (O'Bryan, 2010). Intersectin contains a Pleckstrin homology (PH) and a Dbl homology (DH) domain and five SH3 domains, making it an ideal scaffold protein (Hussain et al., 1999, Guipponi et al., 1998, Zamanian and Kelly, 2003, Hussain et al., 2001). Intersectin is a guanine exchange factor (GEF) for Cdc42, capable of activating the GTPase. The binding between the GTPase and intersectin requires the DH-PH domains of the GEF (Novokhatska et al., 2011, McGavin et al., 2001, Pruitt et al., 2003). This interaction is believed to promote the binding of intersectin to N-WASP. Once activated by intersectin, Cdc42 can in turn bind to and

activate N-WASP to locally stimulate Arp2/3-dependent actin polymerization (Novokhatska et al., 2011, McGavin et al., 2001, Hussain et al., 2001, Pruitt et al., 2003, Zamanian and Kelly, 2003). Intersectin-dependent activation of Cdc42 occurs during endocytosis, vaccinia actin tail formation, exocytosis and phagocytosis (Gasman et al., 2004, Humphries et al., 2014, Moreau et al., 2000).

Formation of clathrin-coated vesicles

Clathrin-mediated endocytosis (CME) is a sequence of tightly regulated events and latest advances in imaging techniques have allowed to visualize these steps with great precision (Picco et al., 2015, Sochacki et al., 2017, Cocucci et al., 2012 Lu, 2016, Maib et al., 2017). PIP_2 enrichment is the start signal for the formation of clathrin-coated vesicle (CCV). The phospholipid determines the size and stability of the clathrin lattice (Antonescu et al., 2011).

Initially, one clathrin triskelion, together with two AP-2 molecules, arrive at the plasma membrane (Cocucci et al., 2012). Assembly and growth of the clathrin pit is subsequently promoted by the RIM complex, consisting of F-BAR proteins, FCHo1/2 proteins, Eps15 and intersectin (Tebar et al., 1996, Saffarian et al., 2009, Reider et al., 2009, Henne et al., 2010). As the clathrin coat grows the associated membrane bends inwards and the membrane invagination becomes deeper. There was a long-standing debate as to how clathrin assembly induces such membrane curvature. One hypothesis was that the clathrin lattice has an intrinsic curvature and that as more clathrin triskelia attach, a dome-like structure is formed that transforms into a sphere (Kirchhausen, 2009, Saffarian et al., 2009). Alternatively, it was proposed that clathrin assembles into a flat lattice, which is remodelled to induce the required curvature while maintaining a constant size. Initial electron images supported the latter hypothesis (Heuser, 1980, Larkin et al., 1986), however, the widely accepted model was the one with constant intrinsic curvature (Lampe et al., 2016). Recent correlative light and electron microscopy analysis has now revealed very strong evidence supporting Heuser's initial suggestion and contradict the constant curvature model (Avinoam et al., 2015, Sochacki et al., 2017). Avinoam et al., 2015 found that within one cell, there are clathrin-coated pits with a wide range of sizes, curvatures and degrees of invagination. Furthermore, they could correlate flat clathrin pits with earlier time points (no cargo attached yet) and highly curved clathrin coats with later stages of endocytosis (dynamin located to the rim of the coat)

(Avinoam et al., 2015). A more recent study was able to correlate the arrival and rearrangement of endocytic proteins with various degrees of clathrin coat curvature and progress of vesicle formation (Sochacki et al., 2017). It has also been proposed that large patches of clathrin lattice act as hotspots for CME (Nunez et al., 2011, Leyton-Puig et al., 2017). In addition, theoretical models confirm that actin can exert the forces required to bend the membrane and present a mechanism where internal stress can lead to rearrangements inside the clathrin coat to transform a flat lattice into a curved coat (den Otter and Briels, 2011, Tweten et al., 2017).

Once clathrin and the underlying membrane adopt a spherical conformation, dynamin wraps around the membrane neck and induces scission (Sundborger and Hinshaw, 2014, Baba et al., 1995). Forces exerted by actin polymerization also contribute to membrane fission during CME (Goode et al., 2015, Idrissi and Geli, 2014). The formed vesicle is released into the cytoplasm where auxillin and HSC70 induce disassembly of the clathrin coat (Ungewickell et al., 1995, Schlossman et al., 1984).

Actin and the formation of clathrin-coated vesicles

The importance of actin during endocytosis was first reported in yeast (Ayscough et al., 1997, Wendland and Emr, 1998, Ayscough, 2000, Lu et al., 2016). Genetic screens identified proteins involved in actin polymerization as essential components for endocytosis (Ayscough et al., 1997, Wendland and Emr, 1998, Ayscough, 2000, Lu et al., 2016). Following early coat formation on the plasma membrane, a mobile phase of the vesicle is initiated, during which actin polymerization pushes the invaginated membrane inwards (Sun et al., 2015, Kaksonen et al., 2005, Kaksonen et al., 2003, Goode et al., 2015). This transient burst of actin, which lasts only 15-20 seconds, is triggered by a switch like activation of Arp2/3 via WASP and WIP, where the total process of endocytosis can range between one and four minutes (Sun et al., 2017). The barbed ends of the newly polymerized actin filaments are oriented towards the membrane forming an actin-rich collar around the neck of the vesicle (Collins et al., 2011). Thereby actin contributes to the constriction of the neck and subsequently pushes the vesicle inwards. In contrast to yeast cells, actin polymerization is not essential for endocytosis in mammalian cells (Gottlieb et al., 1993, Lamaze et al., 1997). Recent experimental and theoretical findings have clarified the role of actin during CME (Mooren et al., 2012). In cells where membrane

tension is high, for example due to turgor pressure in yeast, actin is required to exert force for vesicle internalization (Aghamohammadzadeh and Ayscough, 2009). In cells with lower membrane tension (such as mammalian cells) actin is no longer essential and only plays a supportive role. Artificially lowering or increasing membrane tension in yeast or mammalian cells respectively inverted the requirement for actin during CME (Boulant et al., 2011, Batchelder and Yarar, 2010, Liu et al., 2009). Theoretical models have elaborated on how force generated by actin contributes to membrane bending prior to vesicle scission (Tweten et al., 2017, Hassinger et al., 2017). In mammalian cells, N-WASP is thought to be recruited and activated by dynamin, leading to the formation of branched actin filaments (Benesch et al., 2005, Innocenti et al., 2005, Merrifield et al., 2004, Taylor et al., 2011). Actin helps to bend and constrict the membrane and it pushes the vesicle further towards the cell centre (Mooren et al., 2012, Goode et al., 2015, Qualmann et al., 2000, Taunton et al., 2000).

1.3.2 Dynamin

Dynamin was first discovered in 1989 as a binding partner of microtubules that influences their dynamic instability (Shpetner and Vallee, 1989, Shpetner and Vallee, 1992, Scaife and Margolis, 1990, Tanabe and Takei, 2009). More recently, dynamin is recognized for its involvement in clathrin-mediated endocytosis (Sundborger and Hinshaw, 2014, Antonny et al., 2016). There are three dynamins (1, 2, and 3) in humans, in addition to several dynamin-related proteins including Drp1, which plays a role in mitochondria fission (Kraus and Ryan, 2017, Pagliuso et al., 2017, Ramachandran, 2017). Dynamin 1 expression is mostly restricted to neurons, dynamin 3 is predominantly found in testis, whereas dynamin 2 is ubiquitous (Cao et al., 1998, Cook et al., 1996, Nakata et al., 1993). Dyn II is a 98kDa protein with an N-terminal GTP hydrolysis domain, a middle domain, a pleckstrin homology (PH) domain, a GTPase effector domain (GED), and a C-terminal proline-rich domain (PRD) (Figure 1.13A) (Heymann and Hinshaw, 2009). Dynamin has the remarkable capability to assemble into dimers and tetramers, which can oligomerize around membranes into contractile helices or rings (Hinshaw and Schmid, 1995). This feature allows dynamin to promote membrane tubulation and also gives it a binding preference for highly curved membranes, microtubules and lipid nanorods (Stowell

et al., 1999, Marks et al., 2001, Roux et al., 2010, Takei et al., 1999, Sweitzer and Hinshaw, 1998, Shpetner and Vallee, 1989).

The GTPase activity of dynamin, promoted by G domain dimerization, allows the protein to use the released energy to induce structural changes in the assembled oligomers (Chappie et al., 2010, Damke et al., 1994, Roux, 2014). In the GTP-bound state, dynamin forms non-restricted ("open") rings with an outer diameter of 50nm that can enclose a membrane tube with 20 nm diameter. Upon GTP hydrolysis dynamin changes its conformation leading to a restriction of the helix, resulting in an inner membrane diameter of less than 4 nm, see Figure 1.13B (Danino et al., 2004, Mears et al., 2007, Chen et al., 2004, Takei et al., 1999, Sweitzer and Hinshaw, 1998, Liu et al., 2013, Sundborger et al., 2014 , Marks et al., 2001). The conversion of the highly constricted membrane state to a hemi-fusion state can occur stochastically and is reversible. From a thermodynamic point of view, the elastic energy of the membrane is influenced by its tension and rigidity so membranes under tension should have reduced fission rates. Experimentally it was confirmed that both tension and rigidity impact on fission rates (Mattila et al., 2015, Danino et al., 2004, Shnyrova et al., 2013, Morlot et al., 2012, Pinot et al., 2014, Roux et al., 2006, Hassinger et al., 2017). In addition to hydrolysis driven constriction, dynamin has additional ways to promote membrane fission. The constriction of dynamin causes the spiral to twist and the induced torque can destabilize the membrane and promote fission (Morlot et al., 2012). In addition, the PH domain of dynamin inserts into the outer leaflet of the membrane and helps to overcome the fusion energy barrier (Shnyrova et al., 2013, Ramachandran et al., 2009).

In order to study the function of dynamin, two dynamin mutants have been instructive. The Dyn II K44A clone has a point mutation in the GTPase domain resulting in a dominant negative, kinase-dead version of dynamin (van der Bliek et al., 1993). The second dynamin mutant lacks the PRD domain so the protein is unable to interact with most of its binding partners, which leads to severe recruitment defects (McNiven et al., 2000).

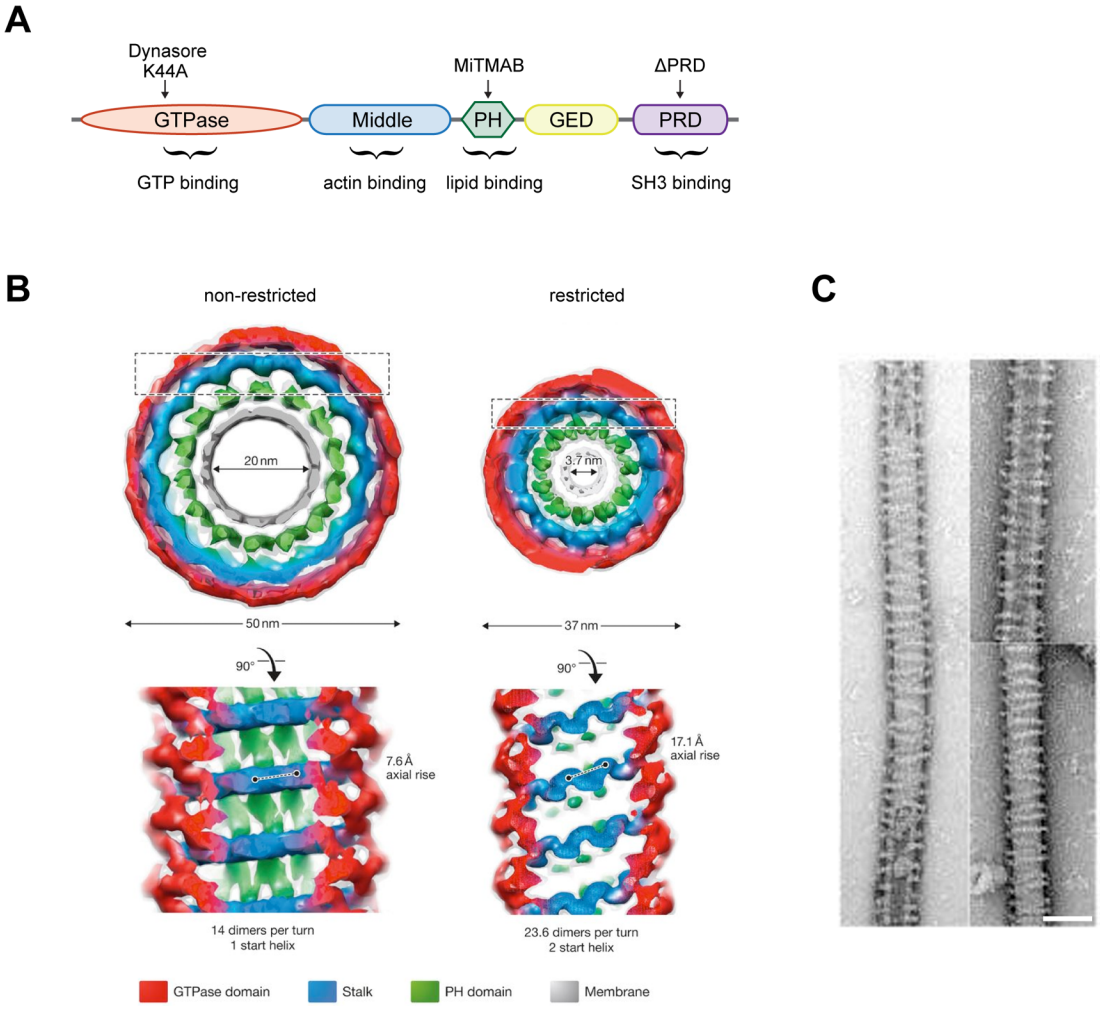

Figure 1.13 The structure of dynamin

A Schematic depicting the domain organisation of dynamin. **B** Three-dimensional reconstruction of the dynamin structure surrounding a lipid tube. Adapted from © Sundborger et al., 2014. Originally published in *Cell Reports* 2211-1247. **C** Purified dynamin wrapped around lipid tubes visualized by negative staining and transmission electron microscopy. © Marks et al., 2001 Originally published in *Nature* 0028-0836. Scale bar = 40nm.

Vesicle formation at the plasma membrane is facilitated by dynamin 1-3, whereas other internal membrane fission events are promoted by dynamin-related proteins (Antonny et al., 2016). Vps1, for example, is involved in endosomal membrane fission (Chi et al., 2014). Dynamin-related protein 1 (Drp-1) together with Dyn2 and its yeast homolog DNM1 induce the fission of mitochondria (Ramachandran, 2017, Chi et al., 2014, Legesse-Miller et al., 2003, Ingerman et al., 2005, Koirala et al., 2013, Mears et al., 2011). Interestingly, other dynamin-related proteins such as

mitofusin 1 and 2 can catalyse the conceptually opposite event, namely membrane fusion (Guttman et al., 2010). Vsp1 is even believed to be bifunctional as it can promote both fission and fusion (Peters et al., 2004, Praefcke and McMahon, 2004).

Besides membrane fission, dynamin is implicated in many actin-dependent processes and structures such as neuronal growth cones, lamellipodia, dorsal membrane ruffles, podosomes and invadopodia (Schlunck et al., 2004, Baldassarre et al., 2003, Krueger et al., 2003, Ochoa et al., 2000, Yamada et al., 2013). Dynamin regulates actin dependent processes through its PRD domain which interacts with a variety of proteins, that are linked to the actin cytoskeleton, including Cortactin, Profilin, Src, Intersectin, Grb2 and Nck (Foster-Barber and Bishop, 1998, Gout et al., 1993, McNiven et al., 2000, Miki et al., 1994, Okamoto et al., 1999a, Seedorf et al., 1994, Wigge et al., 1997, Witke et al., 1998, Wunderlich et al., 1999).
Dynamin impacts directly and indirectly on actin polymerisation *in vivo* and *in vitro* (Schafer et al., 2002, Gu et al., 2010). Adding low levels of Dyn II to purified Arp2/3 and cortactin increases filament formation, whereas high levels of Dyn II have an inhibitory effect (Schafer et al., 2002). Furthermore, through its middle domain, dynamin can directly bind actin to regulate stress fibre formation and induce actin bundling. Dyn II is also able to remove gelsolin from the barbed end of actin filaments to allow actin polymerisation to occur (Gu et al., 2010). In most cases, dynamin is linked to branched Arp2/3-dependent actin networks. More recently, however, it was reported that dynamin 1 and 2 can promote filopodia formation (Chou et al., 2014, Yamada et al., 2016). Interestingly, it is not only dynamin, which influences actin but actin can also impact on dynamin. Inhibiting actin polymerization with the drug Latrunculin B significantly decreases dynamin recruitment to endocytic sites (Taylor et al., 2012).

1.3.3 Endocytic machinery promotes infection

Since viruses are between 30nm - 440 nm in size, (Arslan et al., 2011, Cheng et al., 2007) and clathrin-coated vesicles range between 60-200nm (Crowther et al., 1976, Pearse, 1982) it is not surprising that some viruses hijack various endocytic pathways to enter the host cell (Mercer et al., 2010b, Yamauchi and Helenius, 2013, Humphries and Way, 2013). Smaller viruses, such as dengue virus for example, can

enter pre-formed clathrin-coated pits, while other viruses like the vesicular stomatitis virus (VSV), influenza A virus (IAV) and reoviruses induce the formation of clathrin-coated vesicles when they bind the plasma membrane (Johannsdottir et al., 2009, Rust et al., 2004, Ehrlich et al., 2004, van der Schaar et al., 2008). Some of the larger VSV mutants need additional force generated by actin to form exceptionally large elongated vesicles containing the virus (Cureton et al., 2010). In all cases, dynamin is recruited to facilitate vesicle scission.

Dynamin is also involved in clathrin-independent uptake of viruses. Caveolin-1 mediated endocytosis of human papilloma virus type 31(HPV-31), and simian virus 40 (SV40), as well as uptake of rotaviruses depend on dynamin (Pelkmans et al., 2002, Li et al., 2017, Smith et al., 2007). Large viruses such as herpes simplex virus (HSV) or members of the mimivirus family exploit phagocytosis as their way into the host cell. Again, Dyn II is involved in their uptake (Ghigo et al., 2008, Clement et al., 2006).

As with viral infection, many bacterial pathogens also use the endocytic machinery to enter their host. Yersinia pseudotuberculosis depends on clathrin and AP2 to enter the host cell (Van Nhieu et al., 1996). There is also evidence that other bacteria such as *Staphylococcus aureus, Streptococcus Ehrlichia risticii, Brucella abortus* and *Klebsiella pneumoniae* utilize clathrin dependent endocytosis (Veiga and Cossart, 2006)

Listeria monocytogenes is another bacterial pathogen that utilizes the host endocytic machinery to enter the cell. The bacterial surface proteins InIA or InIB engage with E-cadherin or Met receptors respectively (Pizarro-Cerda et al., 2012). Clustering of the receptors triggers their post-translational modification and downstream signalling phosphorylates and recruits clathrin to the invading bacterium (Bonazzi et al., 2012). In the absence of clathrin, fewer bacteria are internalized (Bonazzi et al., 2011, Veiga et al., 2007, Veiga and Cossart, 2005). Dynamin is also present at *Listeria* entry sites and its depletion also impairs bacterial uptake (Veiga and Cossart, 2005). The mechanistic details still remain to be established but it is possible that dynamin promotes scission at the neck of the phagosome or it can induce actin assembly to facilitate bacterial entry. It is also believed that dynamin locally activates Arp2/3 via

cortactin (González-Jamett et al., 2013). Furthermore, dynamin also plays a role in *Listeria* induced actin tail formation (Lee and De Camilli, 2002, Henmi et al., 2011). Dynamin localizes all along the actin tail but is enriched at the tip close to the pathogen (Lee and De Camilli, 2002). Although dynamin is not essential for actin tail formation *in vitro*, it has enhancing effects *in vivo* (Henmi et al., 2011, Loisel et al., 1999, Orth et al., 2002). Knockdown of dynamin also leads to shorter and slower actin tails. Interestingly, the depolymerisation of the microtubule network with colchicine can revert these phenotypes (Henmi et al., 2011). This led to the speculation that dynamin helps to locally destabilize the microtubule network reducing the resistance that actin driven *Listeria* experiences (Henmi et al., 2011). Overexpression of the kinase dead K44A mutant results in fewer, shorter and less persistent actin tails induced by PIP5KIα (Orth et al., 2002).

Dynamin is also involved in the cell-to-cell spread of *Shigella flexneri* (Fukumatsu et al., 2012). Actin tails propel the pathogen through the cytoplasm and push it, preferentially at tricellular junctions into neighbouring cells (Fukumatsu et al., 2012). The subsequent uptake into the uninfected cells relies on a non-canonical clathrin-dependent endocytic pathway in which dynamin is involved (Fukumatsu et al., 2012).

Interestingly, EPEC and EHEC also hijack parts of the endocytic machinery but these components do not induce uptake of the bacteria. Clathrin, Eps15 and Epsin1 are recruited to actin pedestals downstream of Tir phosphorylation (Guttman et al., 2010, Lin et al., 2011). Clathrin facilitates local actin polymerization, while Eps15 and Epsin1 play more essential role (Lin et al., 2011, Veiga et al., 2007). Furthermore, dynamin 2 is also recruited to roughly 80% of EPEC or EHEC in a Nck and N-WASP dependent manner (Unsworth et al., 2007). Those bacteria can induce actin pedestals, as described in section 1.2.4, but knockdown of Dyn II or expression of Dyn K44A and Dyn ΔPRD largely inhibits actin polymerization. Overexpression of the dynamin mutants significantly reduces the recruitment of N-WASP, cortactin, Arp2/3 and actin to the pathogen, explaining the defect in actin pedestal formation. The same study also showed that the overexpression of the dynamin mutants does not change the percentage of vaccinia infected cells with one or more virus-induced actin tails (Unsworth et al., 2007). However, while effects of dynamin depletion on EPEC pedestals and *Listeria* actin tails were observed, the underlying mechanism is

not clear. How dynamin facilitates the formation of these actin structures remains to be established.

1.3.4 How vaccinia hijacks the endocytic machinery

In addition to the core components Nck, Grb2, WIP and N-WASP involved or required for vaccinia actin tail formation, CEV also recruit the small GTPase Cdc42, an activator of N-WASP (Carlier et al., 1999, Humphries et al., 2014, Moreau et al., 2000, Snetkov et al., 2016). Although not essential, Cdc42 collaborates with Nck to help activate and stabilize the WIP:N-WASP complex during actin tail formation (Humphries et al., 2014, Moreau et al., 2000, Snetkov et al., 2016). N-WASP can only interact with the active GTP-bound form of Cdc42 (Miki et al., 1998a). Intersectin-1 was subsequently identified as the Rho GEF responsible for activating Cdc42 at the virus (Humphries et al., 2014, Snetkov et al., 2016). Intersectin-1, is recruited by three NPF motifs near the C-terminus of A36, which interact directly with the EH domain of the RhoGEF, see Figure 1.14 (Snetkov et al., 2016). Mutating the three NPF motifs in A36 abolishes recruitment of Eps15 and intersectin to the virus leading to loss of Cdc42 activation. This leads to reduced virus spread and release, as well as fewer but longer actin tails (Snetkov et al., 2016). Interestingly, activation of Cdc42 is not the sole function for intersectin downstream of the A36 NPF motifs. Intersectin together with Eps15 is also responsible for recruiting AP-2 and clathrin beneath CEV (Snetkov et al., 2016). Electron micrographs of CEV on the plasma membrane reveal a structure reminiscent of the clathrin coat around endocytic vesicles (Humphries et al., 2012). This structure is apparent in earlier studies but had been missed. Subsequent analysis revealed that clathrin and AP-2 are transiently recruited to the CEV prior to actin tail formation but are left behind as the virus is propelled away. Structured illumination imaging revealed that the recruitment of clathrin underneath CEV helps to cluster A36 and N-WASP, increasing the local density of the signalling network making it easier to promote actin tail formation. Conversely, the lack of clathrin and AP-2 recruitment results in faster turnover of N-WASP, and slower rate of actin tail disassembly (Humphries et al., 2012). Depleting clathrin:AP-2 or mutating the NPF motifs, delays initiation of actin tails and their life-time is significantly shorter (Humphries et al., 2012, Snetkov et al., 2016), but the average actin tail length was substantially increased and actin-based motility of the

virus was accelerated (Humphries et al., 2012, Snetkov et al., 2016). Though virus spread through a confluent monolayer of cells was impeded in the absence of AP-2 / clathrin / intersectin (Humphries et al., 2012, Snetkov et al., 2016), this spreading defect is most likely due to reduced levels of virus release mediated through Cdc42 activation downstream of intersectin (Snetkov et al., 2016).

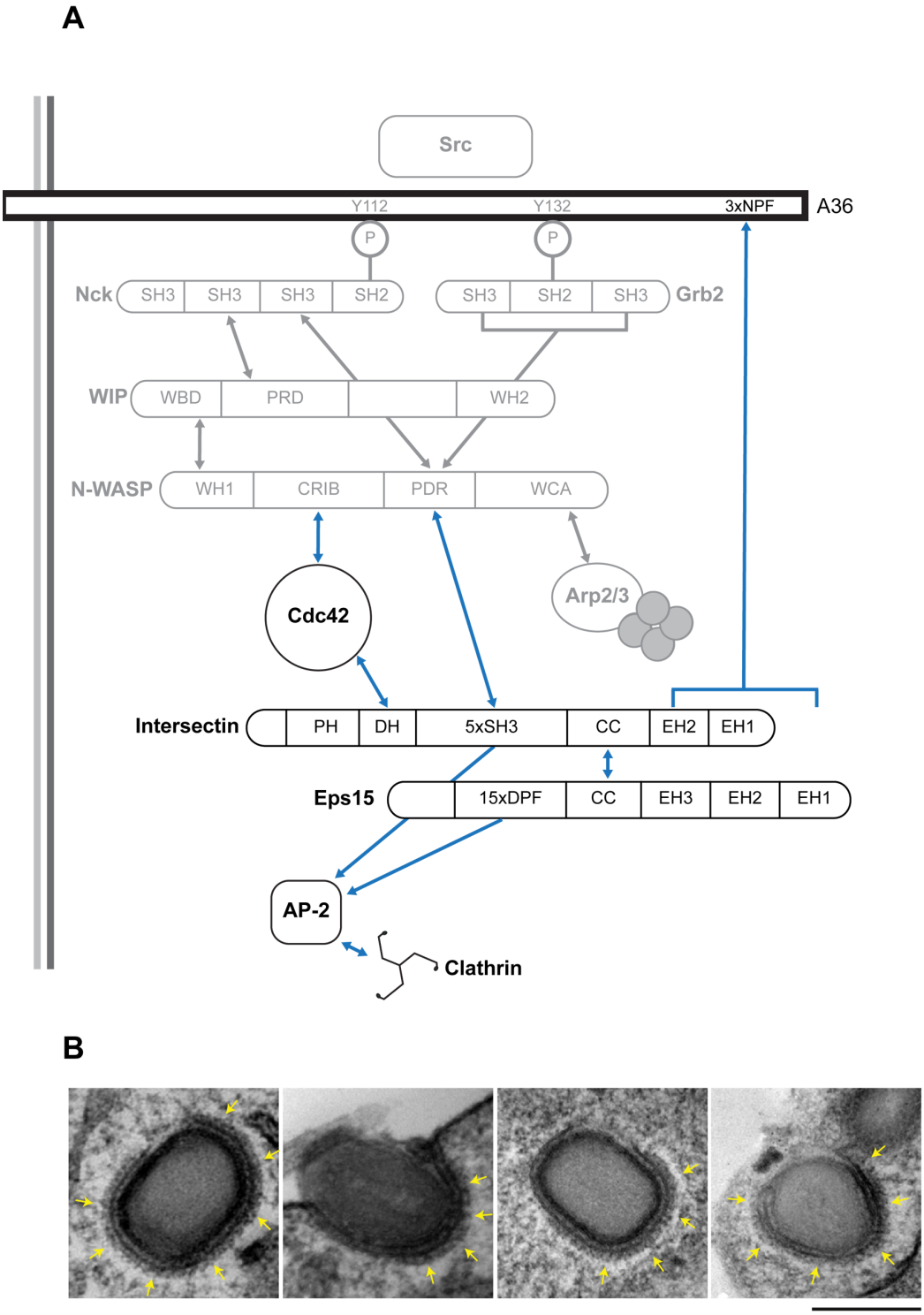

Figure 1.14 NPF motifs in A36 recruit clathrin and promote virus spread

A Schematic of the signalling cascade downstream of the NPF motifs in A36, which supports actin tail formation and results in the recruitment of clathrin to the CEV. New domains are annotated: EH (Eps15-homologydomain), DH (Dbl-homology domain), PH (Pleckstrin-homology domain), CC (Coiled coil). **B** Electron micrographs depicting the clathrin coat recruited to vaccinia virus. Scale bar = 250nm. © Humphries et al., 2012. Originally published in *Cell Host & Microbe* 1934-6069.

1.4 Septins

1.4.1 General

In 1971, Hartwell published his study which screened for proteins essential for yeast septation (Hartwell, 1971). Among the hits was a family of GTPases, which were later observed to localize to the septating bud neck and therefore named septins (Haarer and Pringle, 1987, Kim et al., 1991). Septins are found in animals and fungi but are absent in plants (Pan et al., 2007, Cao et al., 2007). The number of different septins in a species can vary between two in *C.elegans* and 13 in humans (Pan et al., 2007). Human septins are divided into four sub-groups based on sequence similarity, namely SEPT2 (containing SEPT1, 2, 4, 5), SEPT3 (containing SEPT3, 9, 12), SEPT6 (containing SEPT6, 8, 10, 11, 14) and SEPT7 (containing only SEPT7) (Table 1). SEPT13, also referred to as SEPT7P2, is classified as a pseudogene. Septins are 30-65kDa proteins that share several structural domains (Figure 1.15). They have a variable N-terminal domain followed by a poly-basic region that allows direct binding to phosphoinositides (Zhang et al., 1999, Casamayor and Snyder, 2003). Adjacent is a GTP-binding domain that contains a highly conserved P-loop, responsible for nucleotide binding, and is closely related to the P-loop in Ras GTPases. The 53 most C-terminal amino acids of the GTPase domain are highly conserved and unique to septins, and referred to as the septin unique element (SUE) (Versele et al., 2004, Pan et al., 2007). After the GTPase domain, all septins, except for members of the SEPT3 sub-group, contain a coiled-coiled domain followed by a flexible C-terminus (Figure 1.15).

Table 1 Human septins

Subgroup	Name	Amino acids	Expression
SEPT2			
	Septin 1	367	Lymphocytes and cells of the CNS
	Septin 2	361	Ubiquitous
	Septin 4	478	Lymphocytes, cells of the CNS, eyes and testes
	Septin 5	369	Ubiquitous
SEPT3			
	Septin 3	358	Cells of the CNS
	Septin 9	586	Ubiquitous
	Septin 12	358	Lymphocytes and testes
SEPT6			
	Septin 6	434	Ubiquitous
	Septin 8	483	Lymphocytes, cells of the CNS, eyes, intestinal track and placenta
	Septin 10	454	Ubiquitous
	Septin 11	429	Ubiquitous
	Septin 14	432	Cells of the CNS and testes
SEPT7			
	Septin 7	437	Ubiquitous

Adapted from (Mostowy and Cossart, 2012).

Additional studies also showed that this hexamer can be extended by one SEPT9 binding to SEPT7 on each site to form SEPT9-SEPT7-SEPT6-SEPT2-SEPT2-SEPT6-SEPT7-SEPT9 octamers (Kim et al., 2011, Sandrock et al., 2011, Sellin et al., 2011b). These hexamers and octamers can assemble into filaments and higher-order structures such as bundles, rings or gauzes (Bertin et al., 2008, Kinoshita et al., 2002, Rodal et al., 2005a). Due to the palindromic nature of the hexamer and octamer, resulting filaments are non-polar along their polymerization axis. The coiled-coiled ends of the septins, which were not detected in the initial crystal structure, presumably all extend perpendicularly from the same side of the filament

(Sirajuddin et al., 2007). Coiled-coiled domains of SEPT6 and SEPT7 were shown to interact with each other for oligomer formation, and were suggested to prevent SEPT7 aggregation (Sheffield et al., 2003). It is viewed that the coiled-coiled domains extending perpendicular to the octamer give the filament and subsequent higher-order structures a lateral asymmetry, creating two distinct sides that allow for differential binding. In this case, a sheet formed of septin filaments can interact with membrane using one surface whilst enabling the opposite side to recruit binding partners (Barral and Kinoshita, 2008).

All septins contain a GTPase domain, however, their hydrolysis rates vary substantially *in vitro* and are slow in comparison to other GTPases (Field et al., 1996, Mendoza et al., 2002, Sheffield et al., 2003, Versele and Thorner, 2004). Moreover, some septins are unable to hydrolyse GTP *in vitro* (Zent and Wittinghofer, 2014). Elucidating the precise function of septin GTPase activity is the subject of intense investigation. Several studies indicate that depending on whether GTP or GDP is bound, septins adopt different configurations which influences their ability to oligomerize (Johnson et al., 2015a, Nagaraj et al., 2008, Sirajuddin et al., 2009, Weems et al., 2014, Zent and Wittinghofer, 2014). The state of the bound nucleotide impacts on the G interface, and also dictates the binding ability of the NC interface (Johnson et al., 2015a, Nagaraj et al., 2008, Sirajuddin et al., 2009, Weems et al., 2014, Zent and Wittinghofer, 2014). This led to the hypothesis that, similar to actin and microtubules, the hydrolysis cycle could influence the assembly and disassembly of septin filaments. However, there is also evidence contradicting this hypothesis. Septin assembly is relatively fast and free septin monomers are rarely detected *in vivo* but septin-mediated GTP hydrolysis is comparatively slow inside the cell (Sellin et al., 2011b, Johnson et al., 2015a, Field et al., 1996, Frazier et al., 1998, Farkasovsky et al., 2005). Recently, Weems and McMurray discovered a step-wise assembly pathway for the assembly of septin octamers (Weems and McMurray, 2017). They suggest that only some septin interactions are sensitive to the nucleotide state while others are not. Therefore, regulation of the hydrolysis rate impacts septin filament assembly as well as composition of the resulting oligomers (Weems and McMurray, 2017). Clearly more work is needed to understand the precise role of septin GTPase activity during filament assembly and homoeostasis.

A

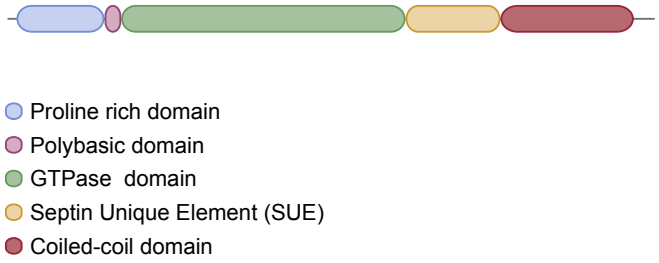

B

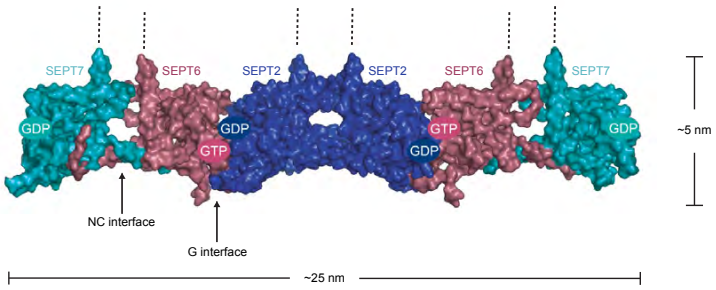

Figure 1.15 Structure of septin monomer and hexamer

A Schematic depicting the domain structure of septins**. B** Crystal structure of septin hexamer; dotted lines indicate the predicted orientation of coiled-coil regions not resolved in this structure. © Sirajuddin et al., 2007. Originally published in Journal of cell biology. 180:887-95.

Post-translational modifications (PTM) are a common way to regulate the behaviour of proteins in cells (Walsh, 2006). Septins can be phosphorylated, acetylated and SUMOylated (Johnson and Blobel, 1999, Sinha et al., 2007, Mortensen et al., 2002, Tang and Reed, 2002, Mitchell et al., 2011, Dobbelaere et al., 2003). SUMOylation of septin was first identified in *S. cerevisiae* where it appears to regulate filament disassembly (Hernandez-Rodriguez and Momany, 2012). When SUMOylation sites are mutated, the septin ring formed during cell division remains intact and does not disassemble after cytokinesis (Johnson and Blobel, 1999, Ho et al., 2011, Takahashi et al., 2003, Takahashi et al., 1999).

Acetylation of septins has been reported in *S. cerevisiae* and *Candida albicans*, where its role is not yet clear, but again filament dynamics and septin ring formation are influenced by this PTM (Sinha et al., 2007, Mitchell et al., 2011).

Slightly more is known about the effects of septin phosphorylation (Hernandez-Rodriguez and Momany, 2012). In yeast, the responsible kinases are Cdc28, Cla4 and Gin4, while in mammals PKG-I, GSK3, casein kinase2, Cdk5 and PKA have been identified to phosphorylate septins (Xue et al., 2004, Xue et al., 2000, Koch et al., 2015, Shen et al., 2017, DeMay et al., 2009, Hernandez-Rodriguez and Momany, 2012, Yu et al., 2009, She et al., 2004). Phosphorylation regulates the dynamics of septins as well as their ability to assemble into higher order structures. In neurons, for example, phosphorylation of serine residue number 327 of SEPT5 by Cdk5 decreases the binding between syntaxin and SEPT5 to regulate exocytosis (Amin et al., 2008). Septin phosphorylation also regulates dynamic changes during the cell cycle such as cell division and proliferation (Longtine et al., 1998, Sinha et al., 2007, Tang and Reed, 2002, Dobbelaere et al., 2003, Garcia et al., 2011, Egelhofer et al., 2008, Yu et al., 2009, Gonzalez-Novo et al., 2008, Meseroll et al., 2012, Meseroll et al., 2013, Cvrcková et al., 1995). Recent work indicates that phospho-mimetic mutations in different areas of the yeast septin Shs1 can either impair the bundling of septin filaments or induce the formation of septin gauzes (Garcia et al., 2011). Hence post translational modification might be a key mechanism for regulating septin structures in the cell.

1.4.2 Septins and actin/microtubule

Co-localization of septin filaments with both actin and microtubule networks has been reported in a variety of different cell types (Spiliotis et al., 2016). Actin filaments were shown to act as a template for septin filament assembly, with anillin mediating the association between septin and actin filaments (Kinoshita et al., 2002). A separate study has reported that septins have the ability to directly bind, bundle and bend actin filaments into rings by cross linking them (Mavrakis et al., 2014). The interdependence of septin and actin filaments is well documented. Chemical disruption of the actin cytoskeleton (using CytoD for example) severely alters the organization of septin filaments, leading to the formation of septin rings in the cytoplasm (Kinoshita et al., 1997, Kinoshita et al., 2002, Schmidt and Nichols, 2004).

On the other hand, the depletion of septins changes the architecture of the actin cytoskeleton (Dolat et al., 2014, Kinoshita et al., 2002, Kremer et al., 2007, Schmidt and Nichols, 2004). In addition to anillin, which recruits septins to the acto-myosin ring during cytokinesis, myosin II is another protein that has been reported to link actin and septins (Oegema et al., 2000, Joo et al., 2007). SEPT2 was shown to directly bind the myosin heavy chain and act as a scaffold that brings myosin and its kinases to acto-myosin structures, to ensure full activation of myosin (Joo et al., 2007). The scaffolding function of septins is also observed during DNA damage response (Kremer et al., 2007). In this case, septin filaments sequester SOCS7 and its binding partner Nck away from the nucleus into the cytoplasm. Upon damage or septin depletion, Nck accumulates in the nucleus where it activates p53, and downstream signals rearrange the actin cytoskeleton (Kremer et al., 2007). In yeast, septins were found to bind to the formin Bnr1p and co-localize with them at the bud neck (Kikyo et al., 1999, Gao et al., 2010). Recruitment of actin nucleation factors is one method that septins could use to influence the actin cytoskeleton. Furthermore, by stabilizing actin stress fibres and nascent focal adhesions septins have a direct impact on cell migration (Dolat et al., 2014). In amoeboid T cells, knockdown of SEPT7 decreases the efficiency of two-dimensional random migration of cells, however it strongly increases transmigration through very small pores (Tooley et al., 2009). The ability of cells to squeeze through narrow holes correlates with their cortical rigidity. Consistent with this, depletion of septins impacts cell cortex stiffness and elasticity (Gilden et al., 2012, Mostowy et al., 2011, Tooley et al., 2009). Septins can contribute to cortex stiffness, their depletion leads to membrane blebbing and reduced retractions of membrane protrusions (Gilden et al., 2012, Tooley et al., 2009). A variety of studies have also reported that cell migration and directionality is influenced by septin depletion in mouse embryonic fibroblasts (MEFs), cardiac endothelial, and breast cancer cells (Liu et al., 2014, Chacko et al., 2005, Fuchtbauer et al., 2011).

In addition to actin, septins can also align with microtubules (MT) in diverse cells such as neurons, platelets and epithelial cells (Hanai et al., 2004, Martinez et al., 2006, Moon et al., 2013, Nagata et al., 2003, Spiliotis et al., 2008, Surka et al., 2002). SEPT9 was reported to directly bind and bundle MTs *in vitro* (Bai et al., 2013). Moreover, in *Drosophila* septins co-purify with MTs, indicating that they stably

associate with each other (Sisson et al., 2000). Septins were shown to facilitate resistance to the cancer chemo therapeutic agent Taxol by enhance MT stability and regulating polyglutamylation of MTs (Froidevaux-Klipfel et al., 2015). Furthermore, it was found that loss of SEPT7 in neurons reduces MT elongation and impairs dendrite growth due to increased acetylation of MT (Ageta-Ishihara et al., 2013a). By competing with the MT binding protein MAP4, septins destabilize MTs (Kremer et al., 2005, Spiliotis et al., 2005, Spiliotis et al., 2008). Conversely, stabilizing or depolymerizing MT protects or disassembles septin filaments, respectively (Bowen et al., 2011, Nagata et al., 2003, Sellin et al., 2011a, Surka et al., 2002). Septins can also impact on the cargo binding to the microtubule motor KIF17 by directly binding to the C-terminal tail of kinesin (Bai et al., 2016).

1.4.3 Septins and membranes

In 1976 scientists first described a ring of membrane-associated filaments in yeast, and these structures were later identified as septins (Byers and Goetsch, 1976, Rodal et al., 2005a, Ong et al., 2014). Septins preferentially bind to PIP_2 via their poly-basic region (Casamayor and Snyder, 2003, Zhang et al., 1999). Moreover, septin assembly is promoted by PIP_2 lipids (Bertin et al., 2010). Visualizing septin filament assembly at the plasma membrane as well as on supported lipid bilayers reveals that septin rods can associate with membrane, then collide through lateral diffusion and anneal end-to-end to form longer filaments and bundles (Bridges et al., 2014).

In cells, septins are often enriched in regions of highly curved membranes, such as the cleavage furrow, the base of dendritic spines, cilia, phagocytic cups or at the annulus of sperm (Hu et al., 2010, Huang et al., 2008b, Ihara et al., 2005, Kim et al., 2010, Kissel et al., 2005, Kwitny et al., 2010, Maddox et al., 2007, Tada et al., 2007). These observations led to the hypothesis that septins sense and/or induce membrane curvature.

Evidence for the latter was provided by Tanaka-Takiguchi et al., when purified septins and large liposomes were combined. Septins assembled at the lipid surface and induced the growth of long tubular lipid extensions protruding from the vesicle (Tanaka-Takiguchi et al., 2009). These tubules (with a mean diameter of 430nm) were surrounded by tightly packed septin rings (Tanaka-Takiguchi et al., 2009).

These experiments also showed for the first time that septin assembly is greatly accelerated in the presence of lipids compared to the self-assembly rate of purified septins in solution.
More recently, it was discovered that purified yeast and human septins hexamers can distinguish different sized lipid-coated beads, and preferentially assemble on beads with a diameter of 1-3 μm (Bridges et al., 2016). This makes septins unique in sensing micron scale membrane curvature, while BAR proteins and endocytic proteins (such as dynamin, ESCRT and clathrin) are associated with curvature in the nanometre range.

Once bound to a lipid membrane, septins can also act as a diffusion barrier (Fung et al., 2014). This has been shown in cilia, where diffusion of membrane proteins out of the cilia is highly restricted by septins, while non-membrane-bound proteins can freely exchange with the cytoplasmic pool (Hu et al., 2010). Knock-down of septins in murine inner medullary collecting duct cells decreases cilia number and length, and significantly increases the lateral diffusion of membrane proteins in and out of the cilia (Hu et al., 2010). Similar results were seen in cilia of septin-depleted *Xenopus* cells (Kim et al., 2010). Septins also prevent mixing of membrane bound proteins from the axon with the rest of the neuron.

During spermatogenesis septins act as diffusion barrier between the sperm head and the tail region making septins vital for sperm maturation. Dysregulation or depletion of SEPT4 and SEPT12 prevents functional sperm tail formation and leads to male infertility in mice (Koch et al., 2015, Shen et al., 2017).

Restricting lateral diffusion through the membrane is also a key function of the septin ring during asymmetric yeast budding/division (Caudron and Barral, 2009). In order to determine a different fate for the mother and the daughter cell, certain proteins, such as IST2, are deposited in the daughter bud (Takizawa et al., 2000). Other factors such as extrachromosomal ribosomal DNA circles are retained in the mother cell and are responsible for its aging (Sinclair and Guarente, 1997). Septins at the neck directly and indirectly prevent diffusion at the plasma membrane, the ER and at the nuclear membrane and thereby maintain cell polarity (Barral et al., 2000, Luedeke et al., 2005, Takizawa et al., 2000).

Septins are also involved in membrane fusion during exocytosis (Hsu et al., 1998, Beites et al., 1999, Tokhtaeva et al., 2015). They were shown to bind to members of the exocyst complex, guiding vesicles to the correct location for exocytosis (Hsu et al., 1998, Vega and Hsu, 2003, Gupta et al., 2015, Nakahira et al., 2010). In addition, septins directly interact with syntaxin, allowing it to regulate the fusion step of exosomes (Beites et al., 1999). In neurons, septins play an important role in controlling the release of neurotransmitters (Amin et al., 2008, Beites et al., 2005, Beites et al., 1999, Ihara et al., 2005, Tokhtaeva et al., 2015). Elucidating the precise role of membranes during septin assembly and function is of great interest, considering that septins can associate with a wide variety of membrane structures such as the plasma membrane, mitochondria, endosomes or the endoplasmic reticulum (Chao et al., 2014, Luedeke et al., 2005, Pagliuso et al., 2017, Beise and Trimble, 2011, Song et al., 2016).

Furthermore, septins were also shown to facilitate mitochondrial fission (Pagliuso et al., 2016, Sirianni et al., 2016). The number and length of mitochondria is regulated by constant fission and fusion events. Drp-1, the dynamin-related protein 1 described in chapter 1.3.2, is responsible for mitochondrial fission. Recent studies reveal that septins facilitate Drp-1-mediated fission, since septin depletion results in extended mitochondria.

1.4.4 Borgs

Borgs (binder of Rho GTPases), also called CDC42 effector proteins (CDC42EP), were discovered by two labs independently (Burbelo et al., 1999, Hirsch et al., 2001, Joberty et al., 1999). Borg5 was first identified as a binding partner of Cdc42 that promoted the formation of actin rich protrusions (Burbelo et al., 1999). Based on sequence homology, Borg1-4 were subsequently identified as additional family members equally capable of interacting with Cdc42 and rearranging the actin cytoskeleton (Hirsch et al., 2001). Simultaneously, a yeast-two-hybrid screen uncovered the family of Borgs as effectors of Cdc42 (Joberty et al., 1999). Overexpression of Borgs in 3T3 fibroblast leads to an elongated cell shape, and overexpression of Borg1 or Borg3 delays cell spreading (Joberty et al., 1999). Borgs

are between 150 and 409 amino acids long and contain several conserved domains. At the N-terminus a basic region is followed by the Cdc42- and Rac-interactive binding motif (CRIB) responsible for binding to Cdc42 and a borg homology domain (BH) 1 (Figure 1.16A). Borgs can contain a BH 2 as well as pro-rich regions, heptad repeats and actin binding domains (Farrugia and Calvo, 2016a). BH3 is a ~20 amino acid long domain found in all Borgs responsible for binding to septins (Joberty et al., 2001). Borg3 binds to oligomeric septins and not to monomers, and can recognize the interface between SEPT6 and SEPT7 (Sheffield et al., 2003). Due to their binding properties, Borgs can align with septin and actin filaments (Liu et al., 2014, Zhao and Rotenberg, 2014). Borg3 and 5 have been implicated in lamellipodia formation, while Borg4 was reported to induce filopodia (Burbelo et al., 1995, Burbelo et al., 1999, Joberty et al., 1999, Zhao and Rotenberg, 2014). In cancer associated fibroblasts (CAFs), Borg2 expression is significantly increased and required for mechano-transduction and subsequent transformation to a cancer-associated fibroblast (Calvo et al., 2013, Calvo et al., 2015). Borg2 can bind both actin and septin filaments, acting as a glue that enhances the stability of both filamentous networks. Cdc42 regulates Borg2 by directly binding to it, and disruption of the Cdc42 binding site of Borg2 results in a dominant negative Borg mutant (Farrugia and Calvo, 2016b).

Interestingly, Borgs are only found in vertebrates, suggesting their recent emergence during evolution. Nevertheless, functional homologs have been discovered in yeast (Gic1 and Gic2) (Brown et al., 1997, Chen et al., 1997, Gandhi et al., 2006, Sadian et al., 2013). Work using cryo-electron tomography revealed that Gic1 bridges two septin filaments by binding specifically to the yeast septin Cdc10 to act as a septin cross-linker, see Figure 1.16B (Sadian et al., 2013). Having the ability to regulate actin and septin downstream of Cdc42 suggests that Borgs fulfil many important functions, but clearly more work is needed to fully understand the role of Borgs in septin biology.

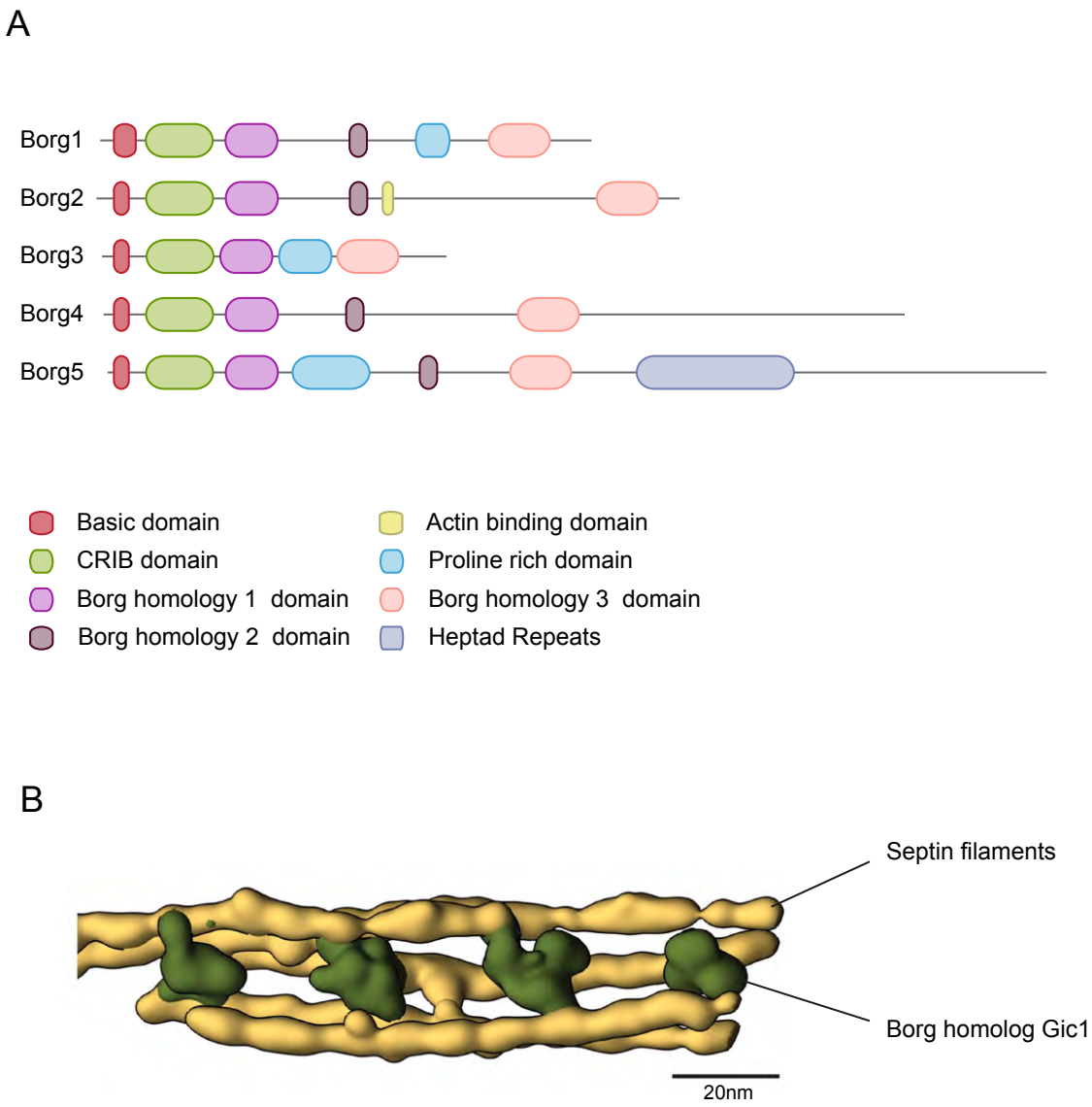

Figure 1.16 The family of Borg proteins

A Schematic showing the domain structure of Borgs. **B** Three-dimensional reconstruction of septin filaments linked by Gic1, a yeast homolog of Borgs © Sadian et al.,2013, originally published in *eLife* 2050-084X.

1.4.5 Septins and pathogens

Investigation of the cytoskeleton has led to key discoveries in both infection and cell biology (Colonne et al., 2016, Naghavi and Walsh, 2017, Welch, 2015, Welch and Way, 2013) . As with the other cytoskeletal proteins, septins are also involved in bacterial infection (Torraca and Mostowy, 2016). In some cases, septins have the ability to restrict the spread of pathogens. On the other hand, septins can be hijacked

by some pathogens to promote the spread of infection. There are examples where pathogens interact with septins both at the plasma membrane and in the cytoplasm.

Listeria monocytogenes induces its uptake via binding of bacterial InIA or InlB to the host cell receptors E-cadherin or Met, respectively (see section 1.3.3.) SEPT9 was initially found to be recruited to latex beads coated with InlB, which were endocytosed by colorectal cancer cells (Pizarro-Cerda et al., 2002). Subsequent work showed that septins are also present at the entry site of *Listeria* and *Shigella*, forming 0.6µm rings around the invading bacteria (Mostowy et al., 2009b). Septin recruitment is prevented by treatment with the actin polymerization inhibitor Cytochalasin D. Studies have shown that depletion of SEPT2 significantly reduces the uptake of *Listera*, *Shigella* and InlB-coated latex beads (Pizarro-Cerda et al., 2002). In contrast, depletion of SEPT11 increases the relative invasion of *Listeria* into HeLa cells (Mostowy et al., 2009a). Investigating the changes caused by septin depletion using atomic force microscopy revealed that septins anchor the Met receptor to the cytoskeleton (Mostowy et al., 2011). Knockdown of SEPT2 decreases the total amount of Met receptor, thus reducing its binding levels to InlB. This could account for the decreased uptake of bacteria and InlB-coated beads as well as reduced response to InlB stimulation in SEPT2-depleted cells (Mostowy et al., 2009a). Furthermore, overall cell elasticity and viscosity is also altered in uninfected cells (Mostowy et al., 2011). The mechanism by which septins mediate bacterial entry is still unclear. Given their function in compartmentalizing plasma membrane (Kusumi et al., 2012; Bridges and Gladfelter, 2015), septins may enrich certain phospholipids in the membrane and recruit host cell receptors together with signalling molecules to aid phagocytic cup formation (Barral et al., 2000; Caudron and Barral, 2009; Mostowy and Cossart, 2011; Ostrowski et al., 2016). A previous study provided evidence that PIP_2 enrichment at the phagocytic cup is maintained by diffusion barriers “fencing” the phospholipids and limiting their diffusion (Golebiewska et al., 2011). While the nature of this fence is not known, it is tempting to speculate that septins might form this diffusion barrier.

In addition to bacterial entry, septins are involved in later stages of *Listeria* and *Shigella* infection (Torraca and Mostowy, 2016). Septin recruitment was observed in cases of *Shigella* and *Listeria* being propelled by actin tails through the host

cytoplasm (Mostowy et al., 2010). Septin rings also form around immobile *Shigella*, entrapping the bacteria in a cage-like structure. In all cases, actin polymerization is essential for septin recruitment. Entrapment of *Shigella* was found to restrict actin tail formation and cell-to-cell spread of the pathogen (Mostowy et al., 2010). Septin cages also reduced the replication of bacteria by triggering autophagy, a process during which intracellular components, including invading pathogens, are degraded (Sirianni et al., 2016 , Yu et al., 2017). Septin-caged *Shigella* associate with autophagy markers such as p62 and Atg8. The pathogen, however, developed a way to escape destruction. Mitochondria may provide a membrane template that facilitates septin cage assembly since longer and shorter mitochondria increase and decrease the percentage of entrapped *Shigella* respectively (Sirianni et al., 2016). In order to counteract septin entrapment and subsequent degradation, *Shigella* induces mitochondria fragmentation by increasing mitochondrial fission (Sirianni et al., 2016). Interestingly, septin cages around *Shigella* were also observed in live zebra fish larvae and septins were found to regulate inflammation (Mazon-Moya et al., 2017).

EPEC uses a type III secretion system (T3SS) to inject virulent factors into the host cell, which manipulate the cell and allow successful infection (Gaytan et al., 2016, Zhuang et al., 2017, Wong et al., 2011). Scholz and colleagues performed a screen to identify changes in host protein phosphorylation upon EPEC infection (Scholz et al., 2015). Among the hits were several cytoskeletal proteins such as cofilin, and microtubule-associated protein 1B, as well as clathrin light chain. Furthermore, phosphorylation of SEPT9 increases in a T3SS-dependent fashion, while total level of SEPT9 remain constant (Scholz et al., 2015). RNAi-mediated knockdown of SEPT9 results in reduced EPEC adherence and cytotoxicity. Moreover, expression of a non-phosphorylatable SEPT9 resulted in the same phenotype, while a phosphomimetic version increased bacterial adherence and cytotoxicity. The mechanistic basis for these septin-mediated effects on EPEC remain to be established. Notably, a previous study found that overexpression of EPEC effector proteins (EspF and Map) induce septin rearrangements, yet whether this is a direct effect or mediated through actin and MTs remains to be established (Rodriguez-Escudero et al., 2005). Interestingly, altered septin phosphorylation levels are also induced by *Salmonella* and *Shigella* infection (Rogers et al., 2011, Schmutz et al., 2013).

Chlamydia trachomatis replicates inside the host cell using a protective replicative niche called an inclusion (Hammerschlag, 2002). These membrane compartments are surrounded by septins, which also recruit actin filaments (Volceanov et al., 2014). Knockdown of septins reduces the extrusion of these inclusion from the cell and results in a ~4-fold reduction of bacterial release (Volceanov et al., 2014). Actin has already been shown to be required for the successful release of chlamydia inclusions (Chin et al., 2012).

The spore-forming bacterium *Clostridium difficile* can cause severe diarrhoea and sepsis (Bartlett, 2017). *C. difficile* expresses a toxin that depolymerizes actin and also induces the protrusion of MT-filled finger-like structures (Schwan and Aktories, 2017). Those protrusions wrap around external bacteria and facilitate their adherence (Schwan et al., 2014). More recently it has been shown that septins, together with Borgs, are recruited to the base of MT protrusions (Nölke et al., 2016). Here, septins guide MTs to the site where the future protrusion forms by binding to the microtubule tip tracking protein EB1 (Nölke et al., 2016). Perturbation of septins significantly affects the number and length of these protrusions, indicating that septins regulate the initiation and elongation of these MT-based protrusions.

Similar to bacterial invasion, septins are also involved in the uptake of the pathogenic fungi *Candida albicans* (Phan et al., 2013). Upon binding to N-cadherin, actin-driven pseudopods form around the pathogen and allow it to be endocytosed in a clathrin-dependent fashion (Moreno-Ruiz et al., 2009). An additional study found that SEPT7 and N-cadherin are interdependently recruited to the pathogen in an actin-dependent manner. Knockdown of SEPT7 impairs the endocytosis of *C. albicans,* indicating that fungi (like bacteria) can also hijack septins to facilitate their uptake (Phan et al., 2013).

There are also a number of studies indicating that septins are important during viral infection. A truncated variant of SEPT4 was shown to interact in a phage display cDNA library screen with the tumorigenic protein Kaposin A of human herpes virus 8 (Stevens et al., 2005). Kaposin A is the most abundant protein in herpes virus 8 and induces tumorigenic transformation by activating nuclear receptors and cellular serine-threonine kinases (Tomkowicz et al., 2005, Muralidhar et al., 2000, Muralidhar

et al., 1998). It remains to be established whether full length SEPT4 also binds to the viral protein, and what the physiological consequences for this interaction entail.

More is known about the role of septins during the replication of hepatitis C virus (HCV). SEPT6 requires its GTP-binding domain as well as the poly-basic region to bind to the viral RNA polymerase NS5b (Kim et al., 2007). Simultaneously SEPT6 binds to the host RNA binding protein hnRNP A1. Depletion or overexpression of SEPT6 or hnRNP A1 mutants significantly reduces HCV replication (Kim et al., 2007). More recently, it has been shown that in HCV-induced cirrhosis septin expression is upregulated (Akil et al., 2016). At later time points of HCV infection, septin filaments form around the cluster of virus cores. SEPT9 was found to stabilize MTs and enhance lipid droplet growth by binding to the lipid component PtdIns5P (Akil et al., 2016). Accumulation of lipid droplets promotes HCV replication, which is reduced upon SEPT9 knockdown. Taken together, septins appear to create a beneficial environment for herpes virus replication.

Septins also influence vaccinia virus (VACV) replication and/or spread (Beard et al., 2014, Sivan et al., 2013). In the work from the Moss lab a whole genome siRNA screen was performed on HeLa cells, which were subsequently infected with the recombinant VACV IHD-J/GFP strain at a ratio of one infectious virus per five cells (Sivan et al., 2013). The percentage of GFP-positive cells was used as a read-out for viral replication after 18 hours of infection. In this case, SEPT11 was found to have an anti-viral role, while SEPT3 and SEPT10 appear to promote virus replication and/or spread. In the study by Beard et al, a RNAi screen of the druggable host genome was performed on HeLa cells. Cells were infected with a WR virus expressing a GFP-tagged virus core protein at a low multiplicity of infection of 0.05 and fixed 48 hours later (Beard et al., 2014). Total level of fluorescence was used as a read-out to assess viral replication. Knockdown of SEPT1 and SEPT9 significantly increased GFP signal suggesting increased viral replication and/or spread. Furthermore SEPT2, SEPT3 and SEPT11 had a similar (but milder) effect. Vaccinia virus can replicate, exit and re-infect several times during the course of the experiments performed in those screens. Therefore, the data only indicate that septins play a role during vaccinia infection but they could not distinguish between effects on entry, replication or egress. Furthermore, some of the septins that were

found as hits, such as SEPT1 and SEPT3 are not thought to be expressed in HeLa cells (Mostowy and Cossart, 2012). Overall it becomes clear that more work is needed to define the role of septins during vaccinia infection.

1.5 Aims of this thesis

Studies over the past twenty years have provided detailed insights into how vaccinia virus hijacks both the actin and the microtubule cytoskeleton to promote its spread (Leite and Way, 2015, Newsome and Marzook, 2015, Smith and Law, 2004). Septins, the fourth component of the cytoskeleton, have a close relationship with actin and microtubules (Fung et al., 2014, Mostowy and Cossart, 2012, Spiliotis and Nelson, 2006). Given this and the fact that septins have been implicated in regulating vaccinia replication and spread (Beard et al., 2014, Sivan et al., 2013), I set out to elucidate the precise role of septins during vaccinia virus infection.

Chapter 2. Materials & Methods

2.1 General buffers and solutions

The in-house media kitchen at London Research Institute and at the Francis Crick Institute provided many of the general buffers and culture media, with details listed below. Specific reagents will be described in the relevant section.

2.1.1 General buffers

Phosphate Buffered Saline A (PBSA)

8.00 g	Sodium chloride, NaCl
0.25 g	Potassium chloride, KCl
1.43 g	Sodium phosphate dibasic, Na_2HPO_4, pH 7.2
0.25 g	Potassium phosphate monobasic, KH_2PO_4, pH 7.2

2.1.2 Cell Culture Media

Versene Solution

8.00 g	NaCl
0.20 g	KCl
1.15 g	Na_2HPO_4, pH 7.2
0.20 g	KH_2PO_4, pH 7.2
0.20 g	EDTA
1.50 mL	1% (w/v) Phenol red solution

The above reagents were dissolved in distilled water, the pH was adjusted to 7.2 with HCl and the solution was autoclaved to sterilise.

Trypsin

The trypsin-EDTA Solution (Sigma) was diluted 1:5 in versene solution and filtered through a 0.22 µm filter.

Minimal Essential Medium (MEM)

9.68 g MEM powder

3.70 g $NaHCO_3$

The reagents were dissolved in 10 L of distilled water and the pH adjusted to 7.0. MEM was then sterilized using a 0.22 µm filter and stored at 4°C.

2.1.3 Bacteriological Media

Lysogeny broth (LB) Medium

10 g Bacto-tryptone

5 g Bacto-yeast extract

10 g NaCl

LB Agar

15 g of Bacto-agar was dissolved in 1 L of LB medium and autoclaved.

2.2 Cell culture

All cell lines and their culture conditions used in this thesis are listed in Table 2.

Table 2 Cell lines and culture conditions

Cell Line	Species	Medium	Source
A549	Human	MEM, 10% FCS, Pen/Strep, 2 mM Glutamine	ATCC
BSC-I	Monkey	MEM, 10% FCS, Pen/Strep, 2 mM Glutamine	ATCC
Dyn -/- MEFs	Mouse	DMEM, 10% FCS, Pen/Strep, 2 mM Glutamine	P. De Camilli (Yale school of medicine)
HeLa	Human	MEM, 10% FCS, Pen/Strep, 2 mM Glutamine	G.Griffiths (EMBL)
HeLa GFP	Human	MEM, 10% FCS, Pen/Strep,	J.V.Abella

		2 mM Glutamine, 1 µg/mL puromycin	(Crick)
HeLa GFP-Cortactin	Human	MEM, 10% FCS, Pen/Strep, 2 mM Glutamine, 1 µg/mL puromycin	J.V.Abella (Crick)
Nck -/- MEFs	Mouse	DMEM, 10% FCS, Pen/Strep, 2 mM Glutamine	T. Pawson (SLRI)
N-WASP -/- MEFs	Mouse	DMEM, 10% FCS, Pen/Strep, 2 mM Glutamine	S. Snapper (MGH)
SYF	Mouse	DMEM, 10% FCS, Pen/Strep, 2 mM Glutamine	P. Soriano (Fred Hutchinson Cancer Research Center, Seattle)
HEK293FT	Human	DMEM, 10% FCS, Pen/Strep, 2 mM Glutamine	Invitrogen

2.2.1 Culturing stocks

Cells were cultured at 37°C in 5% CO_2 and maintained at a confluency of ~50-80% by passaging every 3 days. To passage cells, the media was removed and cells were washed twice with PBSA. Using 10-cm dishes 1 mL of 0.05% trypsin was added to the cells. After incubation for 5-10 min at 37°C, detached cells were re-suspended in warm complete media and passaged to the desired confluency. When required, cells were counted using the Scepter 2.0 Cell Counter (Merck Millipore). To seed cells on glass cover slips or Matek dishes the surface was coated with fibronectin. Therefore, the cell culture dish was incubated with 1:200 diluted fibronectin in PBSA for 30 min. Before plating the cells, the dish was washed twice with PBSA.

2.2.2 Freezing stocks

In order to store aliquots of cells in liquid nitrogen, 80% confluent cells were washed twice in PBSA and trypsinised as described above. Once completely detached, cells were resuspended in complete media and transferred in a falcon tube. After 5 min

centrifugation at 700 rpm at 4°C, the supernatant was aspirated and the pelleted cells were resuspended in 1 mL FCS with 10% DMSO or 0.5ml BamBanker (Wako Chemicals, USA) for long term storage at -80°C. Cells were then aliquoted in cryogenic vials and stored at -80°C or moved to liquid nitrogen. Frozen cells were recovered by quickly thawing an aliquot in the 37°C water bath and transferring the cells to a 10-cm dish containing complete media. Once the cells had adhered, the media was changed.

2.2.3 Transient transfection

HiPerFect

HiPerFect (Qiagen) was used for RNAi (RNA interference) transfection of HeLa and A549 cells. For one well of a 6-well dish, 4 µL siRNA of interest (20 nM) and 10 µL of HiPerFect were added to 100 µL Opti-MEM (Thermo Fisher Scientific). After 20 min, the transfection mix was added to 2 mL of freshly seeded cells (1×10^5 per mL). 24 hrs later, 2 mL of fresh media was added to the cells, which were analysed 72 hrs post transfection. Pools of 4 siRNAs were used in all the experiments.

Fugene

Fugene 6 (Roche) was used to transfect transient expression plasmids into HeLa cells. For a 6 well plate, cells were plated to a confluency of 70% prior to transfection. 1 µg of DNA and 4.5 µl Fugene 6 was added to 100 µl Opti-MEM, after 15 min incubation at room temperature the mixture was added to the cells. Experiments were performed after 24 hrs to allow for adequate expression.

Lipofectamine 2000

Lipofectamine 2000 (Qiagen) was used to transfect HEK293FT cells to generate lentiviruses that contain a gene of interest. HEK293FT were plated to 80% confluency in 10-cm plates. After 24 hrs 10 µg of DNA, 7 µg pPax, and 3 µg MD.2G vectors were added to 500 µL of Opti-MEM. In a second eppendorf tube, 40 µL of Lipofectamine 2000 were added to 500 µL Opti-MEM and incubated for 5 min at room temperature. Both solutions were mixed together the final solution was incubated for further 30 min. The mixture was added dropwise to the cells after changing the media.

Table 3 siRNA target sequences

Gene	Target sequence	Catalogue number
Borg2	GAUGAGGUGCUGAAUGUAA CCAAUAACAAGAAAGGAAA GCUCUCAUGUUGCCCUUAU CGAUGUCUUUGGAGAUAUU	D-017358-01 D-017358-02 D-017358-03 D-017358-04
DIP	GUGGCAACUGGUACAACCUUU AGGUUGUACCAGUUGCCAC AAGUGGCAACUGGUACAACCUUU UUGACAUUGGCGUGUUUGCUCUU	Sigma
Dyn I	GAAAGAAAUUCACCGACUU GAGCUAAUCAGCACCGUUA CCACUUGGCUGACCGUAUG GAGAAUCUGUCCUGGUACA	D-003940-01 D-003940-02 D-003940-03 D-003940-04
Dyn II	CCGAAUCAAUCGCAUCUUC GACAUGAUCCUGCAGUUCA CCUCCGAGCUGGCGUCUAC AGUCCUACAUCAACACGAA	D-004007-01 D-004007-02 D-004007-04 D-004007-18
SEPT7	UUGCAGCUGUGACUUAUAA UGAAUUCACGCUUAUGGUA UAUGAGAACUACAGAAGCA GCUGAGGAGAGGAGCGUCA	D-011607-02 D-011607-03 D-011607-04 D-011607-17
Non-targeting	Allstar negative control	Qiagen

2.2.4 Stable cell lines

Stable cell lines were generated using the pLVX-puromycin and pLVX-IRES-hygromicin vectors (Clontech). These vectors, contain a constitutively active human cytomegalovirus immediate early promoter, located just upstream of the multiple cloning site (MCS). Furthermore, the plasmids have a puromycin/hygromicin resistance cassette that allows selection of stably transfected cells. Constant selection reduces the risk of spontaneous loss of the gene of interest. All the genes,

except for LifeAct, contain the fluorescent tag that the N-terminus. HEK293FT cells were seeded to 80% confluency in 10-cm dishes and after 24 hrs transfected with the construct of interest inserted in the pLVX vector using Lipofectamine 2000 and the protocol above. The following day, the medium was replaced with 10 mL of complete DMEM and lentiviruses were collected at the consecutive two days. Therefore, the medium was collected and passed through a 0.45 µm Millex HV filter (Millipore SLV033RB). The cells were carefully covered with fresh media. HeLa cells were plated at 70% confluence in a 6-well plate and 2 mL of the lentivirus solution was added to the cells. The cells were incubated for two days allowing the lentivirus to infect the cells and integrate the gene stably into the cell's genome. After 72 hrs, the cells were passaged and 1 µg/mL puromycin or 400 µg/mL hygromycin B selected the cells containing the gene of interest. The cell lines generated by this method and the constructs used are listed in Table 4.

Table 4 Stable cell lines generated

Cell Line	Introduced protein	Selection	Species of introduced protein
HeLa	GFP-SEPT6	Puromycin	Human
HeLa	mCherry-SEPT6	Puromycin	Human
HeLa	GFP-SEPT6, LifeAct-iRFP	Puromycin, hygromycin	Human
HeLa	mCherry-SEPT6, LifeAct-iRFP	Puromycin, hygromycin	Human
HeLa	GFP-SEPT6, iRFP-Dyn II	Puromycin, hygromycin	Human
HeLa	GFP-SEPT6, mCherry-Dyn II, LifeAct-iRFP	Puromycin, hygromycin	Human
HeLa	GFP-Dyn II	Puromycin	Human
HeLa	LifeAct-iRFP	Puromycin	Human

2.3 Vaccinia Virus

The Western Reserve (WR) strain of vaccinia was used as wild type virus throughout the thesis. Recombinant viruses used for this work are listed in Table 5.

Table 5 Recombinant viruses used in the thesis

Virus	Source
ΔA36R	G. Smith (Parkinson and Smith, 1994)
ΔA36R + CSTN	M. Dodding (Dodding et al., 2011b)
ΔA36R + YL126	M. Dodding (Dodding et al., 2009)
ΔA36R + YL126 Y6F	M. Dodding (Dodding et al., 2009)
A36 Y112F	A. Holmström
A36 Y132F	N.Scaplehorn (Scaplehorn et al, 2002)
A36 YdF	A. Holmström (Rietdörf et al., 2001)
A36 YdF + RFP A3L	S. Schleich
A36 YdF-ΔNPF	X. Snetkov (LRI)
A36 ΔNPF	X. Snetkov (Snetkov et al., 2016)
A36 ΔNPF + RFP-A3L	X. Snetkov (Snetkov et al., 2016)
WR + RFP-A3L	S. Schleich

2.3.1 General buffers for virology

Tris buffer

10mM Tris-HCl pH 9

2mM MgCl2

Made up in distilled water and filter sterilised using a 0.22μm filter.

Sucrose cushion: 35% sucrose (w/v) in Tris buffer

Crystal violet

0.1% Crystal violet (w/v)

20% Ethanol in distilled water

Viral lysis buffer

10mM Tris-HCl pH 9

10mM KCl

3mM Mg(CH3COO)2

Made up in distilled water and filter sterilised using a 0.22 µm filter.

2.3.2 Infection

The multiplicity of infection (MOI) was calculated from the plaque forming units (PFU) of the viral stock and the number of cells to infect. A MOI of 5 was used to infect cells for immunofluorescence and live-cell imaging. The day of the experiment, the viral aliquot was briefly sonicated in a water bath for 30 secs. The appropriate volume of virus was added to the cells in serum free MEM. After 1 hr, the serum free MEM was removed and replaced with complete MEM. Cells were incubated at 37°C and fixed or imaged after 8 hr post infection.

2.3.3 Sucrose Purification of vaccinia virus

HeLa cells were grown in 15-cm culture dishes to a confluency of 90%. Cells were infected with vaccinia virus at a multiplicity of infection (MOI) = 0.05-0.2 for 72 hrs. Media was removed and cells were scraped in 5 ml of PBSA and harvested cells were centrifuged for 5 min at 1,700rpm at 4°C. The pellet was washed once in PBSA and after another centrifugation step resuspended in 7 ml of Tris buffer. The infected cells were lysed by 15 strokes with a 7 ml Dounce homogenizer (Wheaton). The resulting solution was centrifuged at 1,700rpm at 4°C for 5 min and the viral supernatant was stored at -20°C, while the pellet containing cell nuclei and cell debris was discarded. Next, the viral supernatant was thawed, the precise volume was noted and everything was carefully added on top of an 8 ml 35% sucrose cushion in Beckman SV40 ultracentrifuge tubes. Tris buffer was added to make up a total volume of 30 ml. The viral supernatant was centrifuged at 24,000 rpm for 30 min at 4°C in a Beckman Optima L-100 XP ultracentrifuge and the pellet containing the virus was resuspended in Tris buffer and stored in 20 µl aliquots at -80°C.

2.3.4 Plaque Assay

Plaque assays can be used to determine the titer of a virus or to measure virus spread. For titer determination BSC-1 cells were plated at 2 x 10^5 in 6-well dishes,

forming a confluent monolayer after 24 hrs. Viral preparations were sonicated and serially diluted 1:10 in 1ml of serum free MEM. The culture media was removed from the BS-C-1 cells and replaced with 200µl of the serial dilutions of virus. After 1 hr of viral uptake, the media was replaced with a semi-solid overlay of 1 x MEM, 2% FCS and 1.5% carboxy-methyl cellulose. After 48-72 hrs, the overlay was removed and the cells were fixed with 3.8% formaldehyde for 1 hr. Plaques were visualized with crystal violet staining for 1 hr. The plaque forming unit per ml (PFU/ml) was determined by counting the number of cell cleared viral plaques per dilution, where plaques are both discernible and isolated.

The plaque formation as a measure for viral spread was performed using A549 and Dynamin KO cells. A549 cells were transfected with siRNA as described before. After 24 hrs 2 ml of complete media was added and after 48 hrs cells were again transfected with siRNA after being split into a 12-well dish forming a confluent monolayer. Dynamin parental and KO cells were also plated into 12-well dishes at 100% confluency. Cells were infected with roughly 100 PFU per well and after 1 hr over-laid as described above. After 72 hrs, the overlay was removed and cells fixed in 4% paraformaldehyde (PFA) in PBSA. After 1 hr of fixation cells were washed twice with PBSA and permeabilized with 0.1% triton in PBSA for 5 min. After another washing step with PBSA cells were incubated with the rat antibody against B5 diluted 1:2000 in PBSA plus 3% FCS for 2 hrs gently rocking. After washing twice for 2 min with PBSA cells were incubated with the secondary anti-rat HRP diluted 1:3000 in PBSA with 3%FCS for 1 hr. After another two washing steps the cells were exposed to 250µl of TMB peroxidase substrate for 15min. Finally, cells were washed with distilled water and the 12-well plate was scanned using the Epson V500 scanner. The diameter of the blue plaques formed was measured using the line tool in ImageJ.

2.3.5 Virus release assays

To quantify EEV release, cells were infected with a MOI = 0.1. At 1 hr post infection the inoculum was removed, cells were washed with serum free medium and 0.5 ml of complete medium was added. After 18 hrs of infection, complete MEM was carefully harvested, detached cells were spun down at 13 000 rpm and the supernatant was kept. The viral titer was immediately determined in duplicates by plaque assay on confluent BSC-1 cells as described above.

2.3.6 Single step growth curve

Single step growth curves were carried out to determine the replication dynamics of the viruses under different conditions. A549 cells were transfected with siRNA at 0 and 48 hrs and plated into 12 well plates. Dyn KO cells were plated directly forming confluent monolayers. Cells were infected in duplicate at an MOI = 5. The inoculum was removed 1 hr post infection, cells were washed and 0.5ml of complete media was added. At 5, 9, 18 and 24 hpi, the supernatant was aspirated off and the infected cells were removed from the dish by incubating in 0.5 ml of trypsin at 37°C. Cells were then collected in 1ml of virus lysis buffer. The samples were freeze/thawed three times in liquid nitrogen and 37°C water bath to ensure complete lysis of the cells. Following sonication of the samples each time point was titrated in duplicate by plaque assay as in 2.3.4.

2.3.7 Drug treatments during infection

Infected cells HeLa cells were treated with the indicated concentrations for the indicated time interval are listed below.

Table 6 Drug treatments during infection

Drug	Concentration	Incubation time	Source
CK666	100μM	1 hr prior to fixation	Sigma
Cytochalasin D	1μg/ml	30 min prior to fixation	Torcis
D4476	100μM	1 hr prior to fixation	Calbiochem
Imatinib	25mM	1 hr prior to fixation	Sigma
MitMAB	30μM	30 min prior to fixation	Abcam
PP1	12.5μM	4 hrs prior to fixation	Cayman Chemical
SMIFH2	20μM	30 min prior to fixation	Torcis
TBB	20μM	1 hr prior to fixation	Cayman Chemical

2.4 Molecular Biology

2.4.1 General buffers

10x DNA Loading Buffer

0.25% (w/v)	Bromophenol Blue
30% (v/v)	Glycerol

Everything was diluted in 5x TBE.

5x TBE

445 mM	Tris Base
445 mM	Boric Acid
10 mM	EDTA

Made up to 1 L final volume with distilled water.

RF1

12 g	Rubidium chloride
9 g	Manganese chloride
2.94 g	Potassium acetate
1.5 g	Calcium chloride
150 g	Glycerol

The reagents were dissolved in 900 mL distilled water, the pH was adjusted to 5.8 with acetic acid before topping up to 1 L with distilled water. The solution was filtered using a 0.22 µm filter and stored at 4°C.

RF2

2.09 g	MOPS
1.2 g	Rubidium chloride
11 g	Calcium chloride
150 g	Glycerol

The reagents were dissolved in 900 mL of distilled water, the pH was adjusted to 6.8 with sodium hydroxide before adding distilled water to reach the final volume of 1 L. The solution was passed through a 0.22 µm filter and stored at 4°C.

2.4.2 Expression vectors

A number of different expression vectors were used in this thesis, however, pLVX and pE/L were used in the majority of cases. The pLVX system is described in 2.2.4, and was used to make stable cell lines and for expression outside the context of infection. Borg2 and Src-GFP was expressed under a CB6 promoter. Expression vectors used during the course of infection were pE/L driven. This vector contains a synthetic early/late vaccinia promoter to promote expression during the course of infection in mammalian cells (Chakrabarti et al., 1997). The expression constructs used in this thesis are listed in Table 7.

Table 7 Expression vectors

Vector	Source
pEGFP-Borg2	F. Calvo (Calvo et al., 2013)
pLVX GFP-SEPT6	J Pfanzelter
pLVX mCherry-SEPT6	J Pfanzelter
pE/L mCherry-CLC	A Humphries
pLVX iRFP-Dyn II	J Pfanzelter
pLVX LifeAct-iRFP	J Pfanzelter
pLVX mCherry-Dyn II	J Pfanzelter
pLVX GFP-Dyn II	J Pfanzelter
pLVX iRFP-Dyn II	J Pfanzelter
CB6 Src-GFP	G Linker

2.4.3 Polymerase chain reaction (PCR)

To generate suitable restriction sites for sub-cloning, the genes of interest were amplified using PCR reactions. A standard of 50 µL of PCR mixture contained the reagents listed in Table 8 was prepared.

Table 8 Reagents for PCR

DNA template (50 ng)	1 µL
Primer Forward (10 µM)	1 µL

Primer Reverse (10 µM)	1 µL
dNTPs mix (25 mM)	1 µL
DMSO	1.5 µL
5x Phusion HF buffer	10 µL
Phusion high fidelity DNA polymerase (NEB)	0.5 µL
dH_2O	34 µL

The PCR reaction was performed with an Applied Biosystems GeneAmp PCR machine, using the following standard conditions:

1. 98°C 5 min

2. 98°C 30 sec
   55°C 30 sec
   72°C 30 sec/kb of gene length 30 cycles

3. 72°C 10 min

The PCR product was run through a 0.8% (w/v) agarose gel in 1xTBE containing 8 µL of SYBR safe DNA gel stain (Invitrogen) at 100 Volt for 30 min. The amplified DNA was detected using a Safe Imager (Invitrogen), cut out of the gel and purified using Qiagen QIAquick gel extraction kit. The DNA was eluted in 35 µL of distilled water and used for further sub-cloning.

2.4.4 Sub-cloning

The purified PCR product as well as 2 ng of pre-existing vectors were digested using 0.3 µL of restriction enzymes (NEB) in 20 µl of the appropriate NEB buffer. After 1 hr of incubation at 37°C 1 µl of CIP was added to the mixture containing the vector. After further incubation of 30 min at 37°C the DNA was run through a 1% (w/v) agarose gel at 100 Volt for 30 min. The products of interest were purified using the Qiagen QIAquick gel extraction kit and eluted in 35 µL of distilled water. The insert and vector were mixed at a ratio of 5:1 and 2 µL of 10x T4 ligase buffer and 1 µL of

T4 ligase (NEB) were added to the total mixture of 20 µl. The ligation reaction was incubated for 1 hr at room temperature prior to transforming it into bacteria.

Table 9 Primers used for cloning

Primer	Sequence
iRFP C-tag	For GATGGCGGCCGCGCCCGCAAGGTGGACCTGACCTCCTG Rev GATGGATCCTTATCTCTGGTGGTGGGCGGCGGTGAAGT
iRFP N-tag	For AGATCTGGTACCACCATGGCCCGCAAGGTGGACCTGACCT Rev GCGGCCGCCTCTCTGGTGGTGGGCGGCGGTGAAGT
Dyn II	For GATGCGGCCGCATGGGCAACCGCGGGATGG Rev GATGAATTCCTAGTCGAGCAGGGACGGCTCGGCT

2.4.5 Preparation of chemically competent bacteria

To prepare chemically competent *E.coli* XL-10 cells 500 mL of LB media was inoculated with 2 mL of a 5 mL culture grown overnight. The bacteria were incubated for 3-4 hrs with shaking at 37°C until the exponential growth phase at an OD_{600} of 0.5 was reached. The culture was placed on ice for 30 min and centrifuged at 2,500 rpm for 12 min. After removing the supernatant, the pellet was resuspended in RF1 buffer and placed on ice for 15 min. The bacterial culture was centrifuged again at 2,500 rpm for 10 min and the pellet was resuspended in 7 mL of RF2 buffer whilst keeping it on ice. The bacteria were snap frozen in 100 µL aliquots and stored at -80°C.

2.4.6 Plasmid DNA transformation of bacteria

To transform a plasmid of interest into *E.coli* bacteria, 5 µL of ligation reaction was added to 25 µL of chemically competent XL-10 cells (2.4.5) and placed on ice for 5 min. Next, the bacteria were heat shocked for 45 sec at 42°C, and incubated on ice for 2 min. 100 µL of LB media was added and the mixture was incubated at 37°C for 15 min under constant shaking. The bacteria were then spread on LB-agar plates containing the selection antibiotics (usually 100 µg/mL ampicillin) and left in the 37°C incubator overnight.

2.4.7 Colony screen PCR

Colony PCR was performed to confirm XL-10 colonies, which contain the plasmid of interest. Single bacterial colonies were picked and dissolved in 25 µl of the following PCR reaction (Table 10).
The PCR product was resolved in a 0.8% (w/v) agarose gel.

Table 10 Reagents for colony PCR

Primer Forward (10µM)	1 µL
Primer Reverse (10µM)	1 µL
dNTPs (25 mM)	0.25 µL
10x PCR reaction Buffer	2.5 µL
$MgCl_2$	0.75 µL
Taq polymerase (5U/µL) Invitrogen	0.25 µL
dH_2O	19.25 µL

1. 94°C 10 min

2. 94°C 30 sec
   55°C 30 sec
   72°C 60 sec/kilobase 25 cycles

3. 72°C 10 min

2.4.8 Plasmid DNA preparation

Plasmid DNA was amplified using XL-10 cultures inoculated with the positive colonies containing the DNA insert of interest. Overnight cultures were grown in 7 mL of LB containing antibiotic (usually 100 µg/mL ampicillin) at 37°C with shaking. Plasmid DNA was purified using the Miniprep kit (Monarch) and eluted in 35 Ml of distilled water.

2.4.9 DNA sequencing

To confirm the sequence of a plasmid DNA, sequencing primers were ordered flanking the region of interest as well as every 700 bp. The sequencing PCR reaction was performed using 200ng of DNA, 3.2 pmol primer and 8 µl BDTv3.1 reaction mix (Big Dye Terminator Cycle sequencing kit) under the following conditions:

1.	95°C	1 min	
2.	95°C	10 sec	
	55°C	5 sec	
	60°C	4 min	25 cycles

2.5 Biochemistry

2.5.1 Whole cell lysate

Cells were washed once with PBSA before adding 50-70 µl of final sample buffer (FSB) containing 0.5 µl of benzonase (Novagen) to each well of a 6 well dish. The lysates were transferred into eppendorf tubes and incubated at 95°C for 10 min before loading into a SDS-PAGE.

2x Final Sample Buffer (FSB)

125 mM	Tris.HCl, pH 7.5
4%	SDS
20%	Glycerol
2%	Beta-mercaptoethanol
Bromophenol blue	

The final volume was reached by adding distilled water.

2.5.2 Immunoblot Analysis

Table 11 Antibodies used for Western blot analysis

Antigen	Species	Dilution	Source
A36R	Rabbit	1:5000	S.Cudmore (Way Lab)
Borg2	Rabbit	1:1000	Proteintech
Drp1	Mouse	1:1000	Abcam
Dyn II for Western	Rabbit	1:1000	Bethyl
GAPDH	Mouse	1:5000	Abcam
GFP	Mouse	1:5000	CRUCK
Grb2	Mouse	1:1000	Cell Signalling
4G10	Mouse	1:1000	Merck
SEPT2	Mouse	1:1000	ProteinTech
SEPT7	Rabbit	1:1000	IBL
PY20	Mouse	1:1000	Santa Cruz
PY99	Mouse	1:1000	Santa Cruz

For immunoblot analysis pre-cast NuPAGE 4-12% Bis-Tris gels (Invitrogen) were used according to the manufacturer's instructions. Gels were run in MES running buffer (Invitrogen) for 80 min at 150 V and SeeBluePlus2 protein standard (Invitrogen) was used as reference.

Next, proteins were transferred from the gel onto nitrocellulose membranes using the iBlot gel transfer kit (Invitrogen). The membrane was stained for a few min with Ponceau S solution (Sigma) to visualize the protein lanes before being blocked in 5% milk in PBSA with 0.1% Tween20 (Sigma) (PBS-T) for 15 min at room temperature. Primary antibodies (Table 11) were diluted in 5% milk in PBS-T and the membrane was incubated on a shaker at 4°C overnight. Next day the membrane was washed 3x 10 min using PBS-T before incubating with HRP conjugated secondary antibody diluted in 5% milk in PBS-T for 30 min at room temperature. The membrane was again washed 3x in PBS-T for 10 min, and incubated with ECL solution (Amersham Biosciences) for 1 min before being analysed using the Amersham Imager 600.

2.5.3 GFP-Trap

HeLa cells stably expressing GFP or a GFP-tagged protein of interest were plated at 80% confluency in 10-cm dishes and where indicated infected with vaccinia. The next morning cells were washed twice with PBSA on ice, scraped into 600µl lysis buffer and transferred to an eppendorf tube. Subsequently, the lysates were centrifuged at 10,000 rpm at 4°C for 5 min and the supernatant was transferred into a new tube and the volume adjusted to 1 ml. Therefrom 25 µl were kept as input sample. The remaining lysates were incubated with 15 µl of GFP-trap beads (Chromotek), which were previously equilibrated by washing 3x with ice-cold wash buffer. The samples were incubated for 1 hr at 4°C under constant rotation. Subsequently, the beads were washed 3x with 500 µl of ice-cold wash buffer. After the last wash, the beads were resuspended in 50 µl of FSB. The same amount of FSB was also added to the input samples. The samples were incubated at 95°C for 10 min and centrifuged for 30 sec at maximum speed before resolving by SDS-PAGE.

Lysis buffer

10 mM	Tris/Cl, pH 7.5
150 mM	NaCl
1%	Triton X100
0.5 mM	EDTA

Freshly added protease inhibitor (1 tablet in 50 mL Lysis buffer) (Roche).
The final volume was reached by adding distilled water.

Wash buffer

10 mM	Tris/Cl, pH 7.5
150 mM	NaCl
0.5 mM	EDTA

The final volume was reached by adding distilled water.

2.5.4 Blue immunoprecipitation

Hela cells were plated at 80% confluency in 15-cm dishes and infected for 16hrs with an MOI of 5. Where indicated cells were incubated with PP1 for 1hr at 12µM. Cells

were washed twice with PBSAand lysed in 50µl 2x sample buffer supplemented with 1 µl benzonase, 200µM orthovanadate, 1mM PMSF and protease inhibitor (Roche). Cell lysates were scraped into an Eppendorf and passed 3x through a 30G needle. After boiling the lysates for 5 min Buffer 3 was added until a total volume of 1ml was reached and 15µl were set aside as input control. Lysates were incubated with 1 µg of primary antibody for 2 hrs at 4°C. Protein A beads were washed 3x with Buffer 3 and 20µl of 50% bead slurry was added to the lysate. After 30 min incubation beads were washed 3x with Buffer 3, resuspended in 30µl 2x sample buffer and boiled for 5 min before resolving by SDS-PAGE. Subsequent antibody incubations were all performed in the presence of orthovanadate.

Buffer 3

50 mM	HEPES, pH 7.5
150 mM	NaCl
10%	Glycerol
1%	Triton X100
1 mM	EGTA pH 8.0
1.5 mM	$MgCl_2$

The final volume was reached by adding distilled water and supplemented with 200µM orthovanadate, 1mM PMSF, 100µM NaF and protein inhibitor (Roche).

2.6 Imaging

2.6.1 General reagents

1x Cytoskeletal buffer (CB)

10mM	MES, pH 6.1
150mM	NaCl
5mM	EGTA
5mM	$MgCl_2$
5mM	Glucose

The reagents were dissolved in distilled water.

Blocking buffer

1% BSA

2% FCS

The reagents were dissolved in 1x CB, and filtered through a 0.45 µm filter and stored at -20°C.

Mowiol

2.4 g Mowiol

6 g Glycerol

12 mL 200 mM Tris/HCl, pH 8.5

Mowiol and glycerol were added to 6 mL of distilled water. The mixture was stirred for 2 hrs at room temperature, before the addition of Tris/HCl. The final solution was stirred for additional 10 min at 60°C and centrifuged at 5,000 rpm for 5 min. The solution was aliquoted and stored at -20°C.

Paraformaldehyde (PFA)

50 g of PFA was added to 500 mL of warm PBSA, and under constant stirring 1 M NaOH tablets were added until the PFA had completely dissolved. After cooling at room temperature, the pH was adjusted to 7.5, and the solution was passed through a 0.45 µm filter before 12 ml aliquots were stored. Prior to use, 10% PFA aliquots were thawed in the water bath and diluted to 4% in PBSA.

2.6.2 Fixation

Cells plated on coverslips were unless otherwise stated incubated with 4% PFA for 10 min at room temperature. Alternatively, 4% PFA was supplemented with 0.1% TX. For methanol fixation coverslips were transferred into ice cold methanol and incubated for 20 min at -20°C. Cells were washed three times with PBSAafter fixation.

Table 12 Antibodies used for immunofluorescence

Antigen	Species	Dilution	Source
AP-2	Mouse	1:500	Abcam
Borg2	Rabbit	1:1000	ProteinTech

B5	Rat	1:500	Gerhardt Hiller
CHC	Rabbit	1:1000	Abcam
Dyn II	Rabbit	1:300	Mark McNiven
SEPT2	Mouse	1:300	ProteinTech
SEPT7	Rabbit	1:500	IBL
SEPT9	Rabbit	1:300	ProteinTech
Src PY418	Rabbit	1:500	Life Technology

2.6.3 Immunofluorescence

Drops of 50µl blocking buffer were placed on a parafilm and the cover slip was placed on top incubating for 20min. In order to label extracellular virus (CEV) cells were incubated with B5 for 30min prior to permeabilization. After three washes cells were incubated with secondary antibody for 30 min. Subsequently, cells were permeabilized for 1 min using 0.1% Triton-X100 in cytoskeleton buffer and washed 3x with PBS. After 1 hr incubation with the second set of primary antibodies as described in Table 12, cells were washed 3 x with PBSA and incubated with secondary antibody for 30 min together with phalloidin diluted 1:100 in blocking buffer to label F-actin. DAPI (300 nM in PBS) was added for 1 min followed by three more washes with PBSA and one rinse in distilled water before mounting the coverslip on a microscopy slide using 2 µl Mowoil.

2.6.4 Sample preparation for EM

Buffer A

30mM HEPES, pH 7.5
70mM KCl
3mM EGTA
5mM $MgCl_2$

1/3 Buffer A

One part Buffer A is mixed with two parts water.

Poly-L-lysine

0.5mg/ml poly-L-lysine diluted in Buffer A.

Cells were grown on fibronectin coated coverslips as described in 2.2.1. After eight hrs of infection cells were incubated for 5 sec in poly-L-lysine to enhance their attachment to the cover slip. After washing once in Buffer A, cells were incubated 3 x 10 sec in hypotonic 1/3 Buffer A to induce swelling. Subsequently the upper half of the cells was removed leaving the basal membrane attached to the cover slip, which is also termed “unroofing”. This was achieved by two different methods. Either the coverslip was placed in 0.5% PFA diluted in Buffer A and the same solution was manually squirted onto the cells using a 0.3 µm needle and syringe. Alternatively, cells were placed at a 45° angle propped against a small insert in a 10-cm dish containing 0.5% PFA diluted in Buffer A. Next, a 1/8-inch microprobe from a sonicator was placed a few mm above the cells. A blast of buffer unroofing the cells was generated by switching the sonicator on for 0.5 sec at 2-3 mAmp. After cells were unroofed they were immediately fixed for 15 min in 4% PFA diluted in Buffer A. In case of gold labelling immunostaining was performed as described in 2.x using 2% FCS and 1% BSA for blocking and diluting antibodies. Secondary antibodies were coupled to gold spheres with a diameter of 5 nm. Following incubation with the secondary antibody, cells were fixed in 2% glutaraldehyde diluted in Buffer A for 2min. Subsequently cells were either dehydrated by incubating 2 x 5 min in 70% 90% and absolute ethanol and subsequently air dried. Alternatively, critical point drying (CPD) can be used to optimize sample conservation. CPD was performed on a Leica EM CPD300 where the water contained in the sample is replaced by acetone, which in turn is replaced by liquid CO_2. Next the sample is brought to the critical point of CO_2 (31°C and 74 bar), where CO_2 can convert from liquid to gas phase without causing any damage associated with evaporation.

Following dehydration, samples were mounted on metal studs and coated with 2 nm of platinum (Pt) using the Q150R S Sputter coater.

2.6.5 Microscopes

Zeiss Axioplan Upright

Fixed samples were imaged on a Zeiss Axioplan2 epifluorescent microscope equipped with a Photometrics Cool Snap HQ cooled CCD camera, external Prior Scientific filter wheels (DAPI; FITC; Texas Red; Cy5) and a 63x / 1.4 Plan Achromat objective. The system was purchased from Zeiss and Universal Imaging Corporation Limited and was controlled with MetaMorph 7.8.13.0 software. Images were analyzed using Fiji and processed with the Adobe software package.

Spinning-disk confocal

Live-cell imaging experiments were performed on a Zeiss Axio Observer microscope equipped with a Plan Achromat 63x / 1.4 Ph3 M27 oil lens, an Evolve 512 camera and a Yokagawa CSUX spinning disk. The system was purchased from 3i Intelligent Imaging Innovations and was controlled by Slidebook 6.0 (Intelligent imaging). Movies were analyzed using either Fiji or MATLAB.

Structured Illumination microscopy (SIM)

Structured Illumination microscopy was performed on an Elyra PS.1 microscope (Zeiss) using 488 nm and 561 nm laser excitation and a 63x/1.40 plan apochromat oil-immersion objective (Zeiss). Imaging was started 20 min after placing the coverslip on the microscope to minimize sample drift. Two-color alignment was performed by using a multi-color bead sample (Zeiss) and the channel alignment function in the Zen software (Zeiss). Images were reconstructed in the Zen software using a theoretical point-spread function.

Scanning electron microscope

The scanning electron microscope was a Quanta 250 FEG SEM (FEI Company, Eindhoven) using the FEI Quanta 250 Everhart-Thorneley backscatter detector for normal samples, as well as the FEI Quanta 250 low-voltage high-contrast vCD detector at a working distance of 6 mm, and inverted contrast images were acquired in high vacuum (5 kV, spot size 2.5 and dwell time of 4-10 µs). The xT microscope control v6.2.4 from FEI was used to operate the microscope.

2.6.6 Quantification of virus speed

To measure the speed of actin-based motility of HeLa cells stably expressing LifeAct-GFP were infected with WR RFP-A3L virus at a MOI of 5. After eight hrs cells were imaged at 37°C, in phenol red free MEM containing 40 mM HEPES on the spinning disk confocal microscope for 5 min with 1 frame/second and exposure times varying between 50 and 200ns. Virus speed and directionality were determined using the particle tracker plugin for Fiji as described before (Abella et al., 2015).

2.6.7 Fluorescence Recovery after Photo-Bleaching (FRAP)

FRAP experiments were performed using HeLa cells stably expressing GFP-SEPT6 infected with WR RFP-A3L. After eight hrs cells were treated with 100μM CK666 in phenol red free MEM containing 40 mM HEPES and images were acquired every second on the spinning disc confocal microscope. The fluorescence was bleached using the 488 laser at 100% power while the size of the bleached area as well as the time interval of bleaching was kept consistent throughout all experiments. The mean fluorescence intensity of the bleached area was analysed over time using Fiji. The intensity values were normalized and an exponential function was used to extract the recovery plateau and the time of half maximal recovery using Prism 7.

2.6.8 Analysis of protein arrival prior to actin tails

In order to analyse the dynamics of septin replacement from the virus cells stably expressing LifeAct-iRFP, mCherry-Dyn II and GFP-SEPT6 were infected. Alternatively cells stably expressing LifeAct-iRFP and GFP-SEPT6 were infected with WR and after 4 hrs transiently transfected with pEL mCherry CLC. From eight hrs post infection onwards cells were imaged every 2 sec for 5 min. Subsequently images were opened in Fiji and an area of roughly 2.5μm^2 around the virus was selected and cropped. Cropped videos were loaded into MATLAB (R2017A) where the mean fluorescence intensity of the area for each time point was determined and normalized. A Savitzky-Golay filter of order 5 and frame length 11 was applied to the intensity profile of dynamin and subsequently the maximum of the smoothed dynamin data was determined. The unfiltered intensity values of all proteins were

temporally aligned with respect to the peak of dynamin intensity. The mean and s.d. of all the unfiltered movies were plotted using Prism 7.

2.6.9 Analysing super resolution data

Cells were infected either with YdF or YdF A3L and stained with SEPT7 and B5 or only SEPT7 respectively after eight hrs of infection. Images were acquired on the SIM, processed using the Zen program and image stacks were opened in Fiji. To measure the diameter of septin rings a straight line through the septin ring was drawn. In order to determine the dimensions of CEV two perpendicular lines (one along the short and one along the long axis) were drawn through the ex.B5 label. The intensity profile along those lines was determined and loaded into MATLAB (R2017A). Subsequently, a sum of two Gaussian peaks was fit to the intensity profile using the built-in fitting function. To ensure robustness of the fit the starting parameters were determined using MATLAB's findpeaks function. The distance between the two means of the double Gaussian functions was taken as the diameter of the ring.

2.7 Statistical Analysis

Data in all graphs are presented as the standard error of the mean, unless otherwise stated. Prism 7.0 (GraphPad) was used to perform standard statistical analysis of data sets. A Student's T-test was performed to compare two data sets. To compare multiple data sets a One Way Anova analysis was performed, followed by a Tukey Multiple Comparison to compare all pairs of samples. A p value of <0.05, <0.01, <0.001 and <0.0001 is represented as *, **, *** and **** respectively. A p-value > 0.05 was not considered statistically significant, and in this event the data was labeled, n.s. for not significant.

Chapter 3. Septins are recruited to vaccinia during its egress

3.1 Introduction

In two recent studies genome-wide RNAi screens were utilized to look for proteins impacting on the replication and spread of vaccinia virus (Sivan et al., 2013, Beard et al., 2014). In both cases HeLa cells were infected at low multiplicity of infection (MOI) and the amount of fluorescent virus or the number of infected cells was measured 18h or 48h post infection. Septins were found as hits with some having anti-viral (SEPT1, SEPT2, SEPT9 and SEPT11) or pro-viral (SEPT10) effects. Unfortunately, none of these hits were validated and nobody looked into how or where septins influence the replication and/or spread of vaccinia.

In contrast, there is some knowledge about the role of septins during bacterial infection. Septins support the uptake or adherence of EPEC, *Listeria, Shigella* as well as the fungi *Candida albicans* (Mostowy et al., 2009b, Phan et al., 2013, Scholz et al., 2015). Later in infection septins are found to form septin rings around *Listeria* and *Shigella* and restrict their intracellular movement (Mostowy et al., 2010). Moreover, in the case of *Shigella* it was shown that these septin cages trigger autophagy and thereby limit the proliferation of the bacterium (Sirianni et al., 2016).

Given their anti-bacterial role I set out to investigate where and how septins impact on vaccinia replication or spread.

3.2 Results

3.2.1 Septins are recruited to cell-associated extracellular virus particles

Both siRNA screens measured virus levels after several replication cycles. These data indicated that septins could play many roles such as virus entry, replication, or spread of vaccinia virus. As an initial experiment, I infected HeLa cells with the Western Reserve (WR) strain of vaccinia virus containing a RFP-tagged core protein, A3. Cells were fixed following 15min, 3hrs, 6hrs and 8hrs of infection and immunostained using an antibody against SEPT7. Since SEPT7 is found in all functional septin structures and cannot be replaced by another septin family member,

it is the perfect marker to label septins in the cell (Kinoshita et al., 1997, Zent et al., 2011).

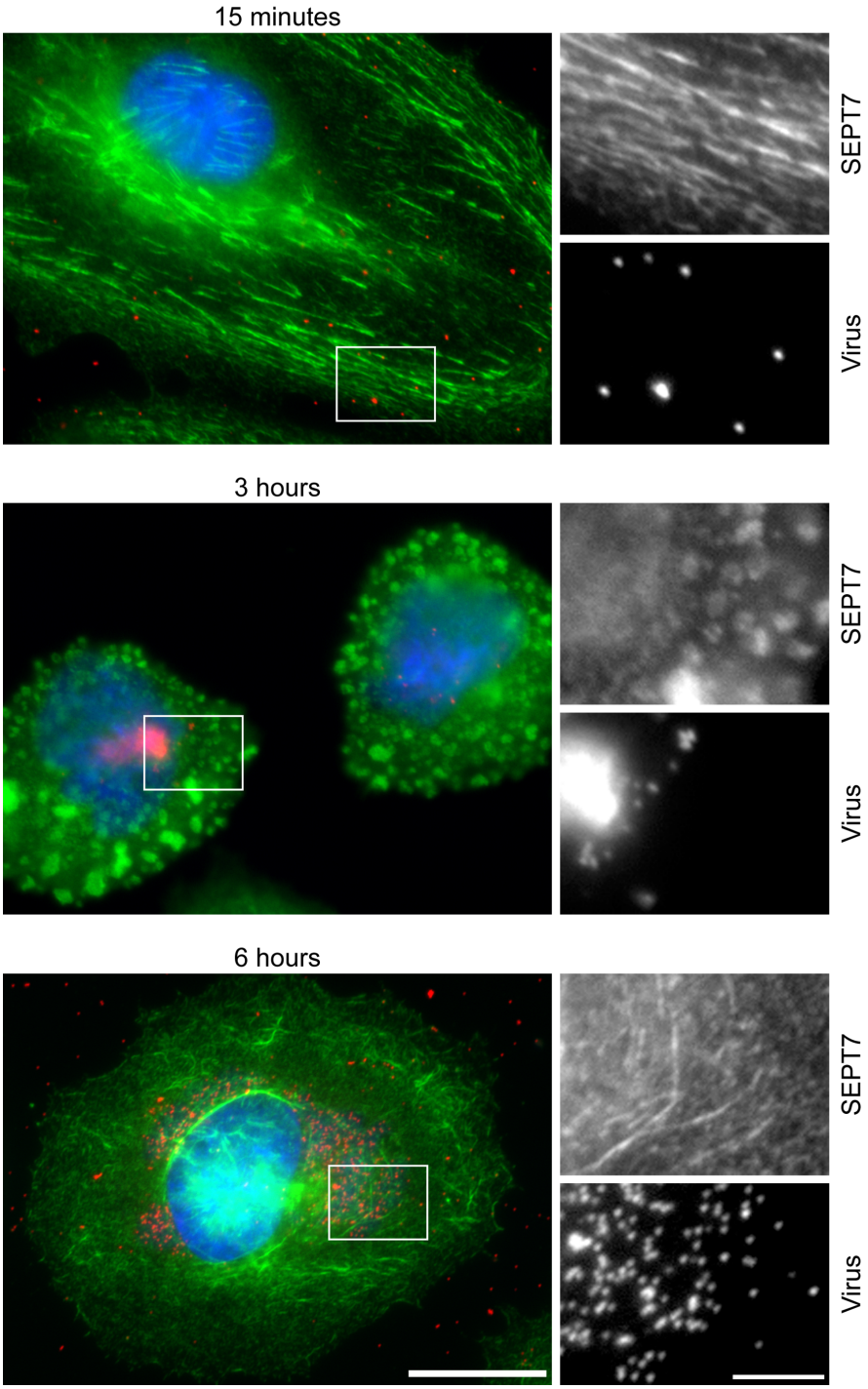

Figure 3.1 Septin during early stages of vaccinia infection

Representative immunofluorescence images showing SEPT7 (green) in HeLa cells infected with RFP-A3 WR virus (red) for the indicated time. Scale bar = 10 μm and in the insert 5 μm.

At the first time-point of 15 min, representing virus entry, I did not observe any obvious changes in septin organization (Figure 3.1A). Septins still formed filamentous structures like in uninfected cells and also the characteristic enrichment of septins around the nucleus could be seen. No relationship between virus particles attached to the cell and septins was found. After three hours infection, the morphology of the cells was severely changed as cells started to contract and bleb (Bablanian et al., 1978, Durkin et al., 2017). During this stage, septins seemed to localize to the plasma membrane and appeared enriched in some blebs, however, there was no co-localization between the virus and septins (Figure 3.1). After six hours of infection the cells started to respread and adopt their usual flat morphology. The virus factory was easily recognized in the cytoplasm, but again there was no virus-specific alteration of septins localization around the virus (Fig3.1C).

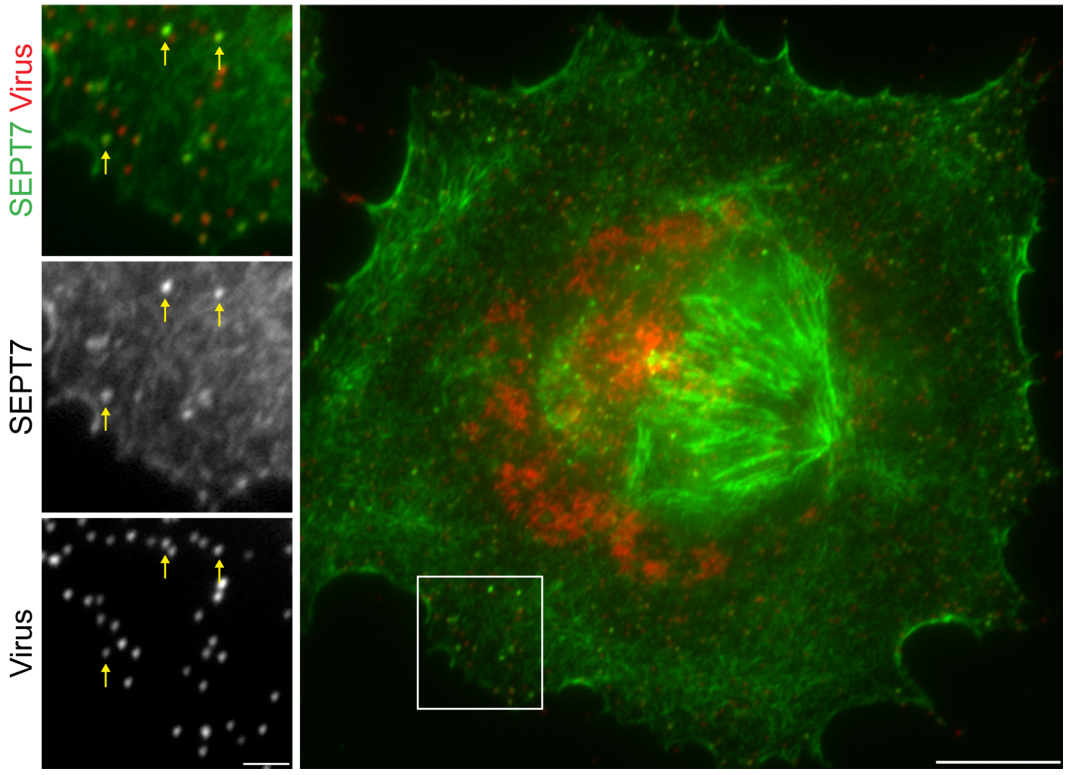

Figure 3.2 Vaccinia can recruit septins during its egress

Representative immunofluorescence image showing the association of SEPT7 (green) with RFP-A3 WR virus (red) in HeLa cells infected for eight hours. Scale bar = 5 μm and in the insert 1 μm.

At eight hours post infection (hpi), newly formed virus particles started to leave the cell. During this point of infection, some of the virus particles in the cell periphery co-localize with SEPT7 (Figure 3.2). In addition, I found that SEPT2 and SEPT9 were

also recruited to virus particles in the cell periphery (Figure 3.3). Based on the results from this time course, I analysed cells at eight hpi and used the SEPT7 antibody for all my future experiments unless otherwise stated.

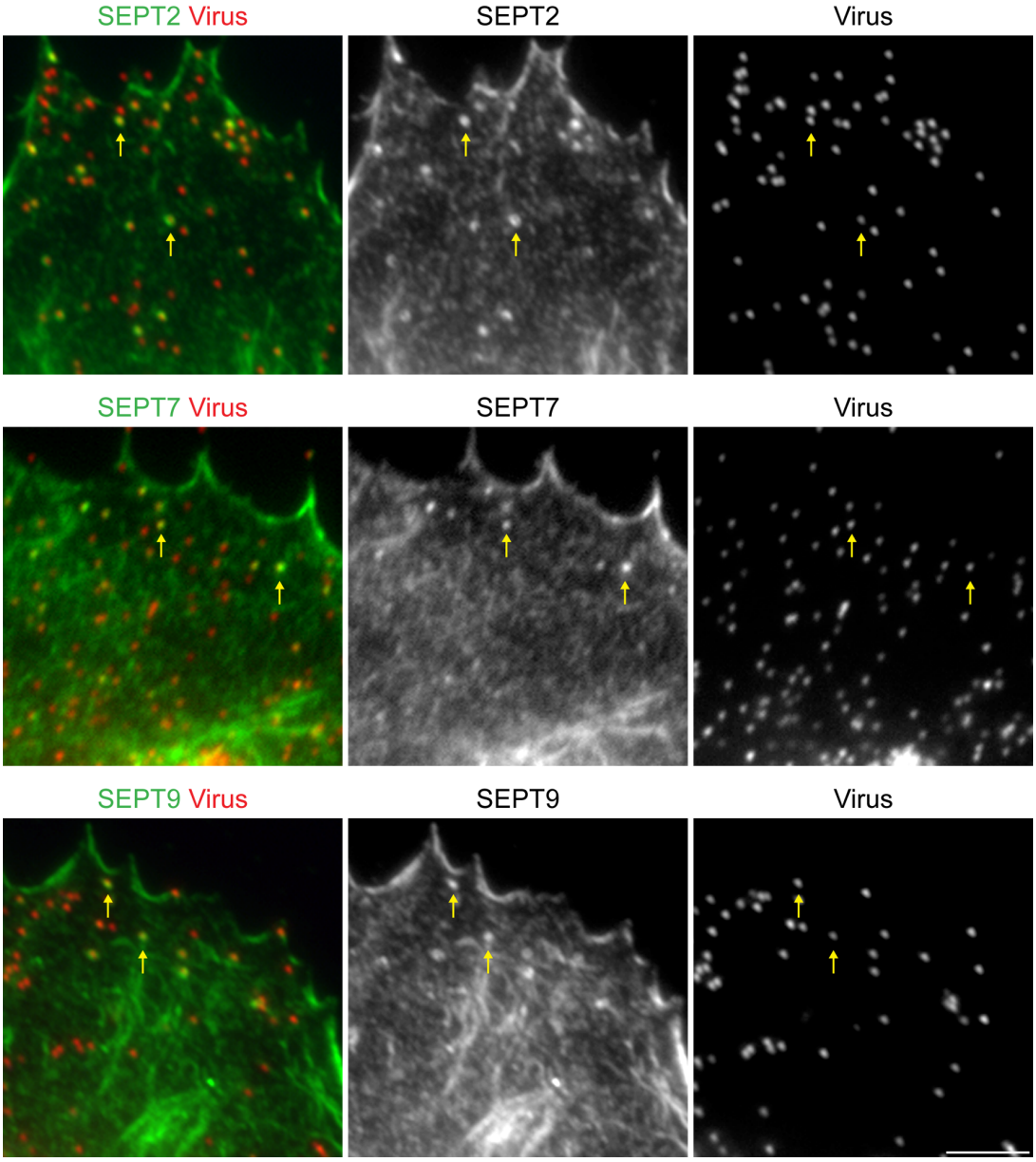

Figure 3.3 SEPT2, SEPT7 and SEPT9 co-localize with a subset of viruses

Representative immunofluorescence images showing the association (highlighted by yellow arrows) of SEPT2, SEPT7 and SEPT9 (green) with RFP-A3 WR virus (red) in HeLa cells infected for eight hours. Scale bar = 2 μm.

During viral egress, vaccinia hijacks the host cytoskeleton to facilitate its spread. The schematic in Figure 3.4 summarises the key events that we know so far. First, vaccinia reaches the cell periphery via microtubule-based transport by binding to

kinesin-1 from six to seven hours post infection onwards (Dodding and Way, 2011, Geada et al., 2001, Hollinshead et al., 2001, Newsome et al., 2006, Rietdorf et al., 2001, Ward and Moss, 2001a). After the outermost membrane of the IEV fuses with the plasma membrane, the virus is now on the outside of the cells and can diffuse away (Smith and Law, 2004). Some virus particles remain attached to the cell and Src/Abl kinases are recruited to the virus to phosphorylate two tyrosines on the transmembrane viral protein, A36 (Frischknecht et al., 1999b, Newsome et al., 2004, Newsome et al., 2006, Reeves et al., 2005). Thereby kinesin-1 is released from the virus (Newsome et al., 2006). Clathrin is recruited to the CEV and promotes the subsequent formation of an actin tail by clustering A36 beneath the virus (Humphries et al., 2012, Snetkov et al., 2016). Arp2/3 complex-dependent actin polymerisation is induced by the recruitment of N-WASP and WIP via the adaptor proteins, Nck and Grb2 (Newsome et al., 2006, Scaplehorn et al., 2002, Donnelly et al., 2013, Frischknecht et al., 1999b, Moreau et al., 2000). These actin tails propel the virus onto neighbouring cells and promote cell-to-cell spread (Doceul et al., 2012, Doceul et al., 2010, Horsington et al., 2013, Ward et al., 2003).

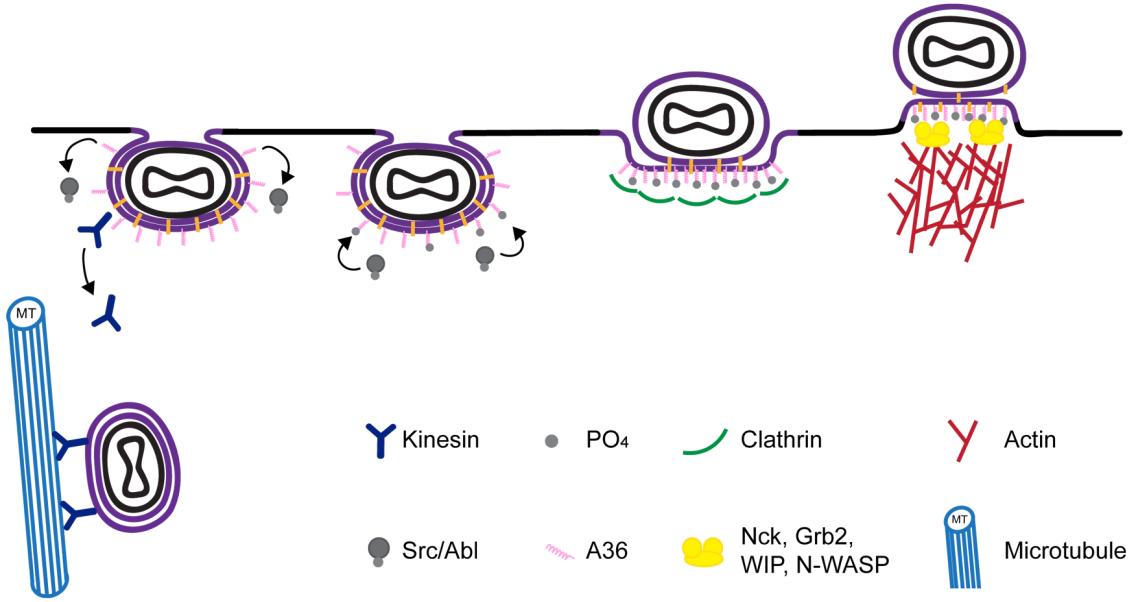

Figure 3.4 Key events during vaccinia egress

Schematic depicting the transition from microtubule-based to actin-based motility of vaccinia during its egress. Following fusion, phosphorylation of A36 by Src leads to the loss of kinesin-1 and recruitment of Nck, Grb2 and WIP:N-WASP, which activate Arp2/3. NPF motifs in A36 recruit clathrin which clusters A36 and enhances thereby actin tail formation.

The question for me now was when do septins arrive at the virus in regard to these well studied processes. Given these characterized steps, my aim was to determine at which point septins associated with the virus in order to understand the role of septins during viral spread. To accomplish this goal, I examined immunostaining of infected cells with an antibody against the integral virus protein B5. Using this antibody prior to permeabilization allows us to detect only extracellular virus particles, specifically those that have already fused with the plasma membrane but have stayed attached. These virus particles are referred to as cell-associated enveloped viruses (CEV). Co-staining infected cells with extracellular B5 and SEPT7 (post permeabilization) revealed that septins are recruited to vaccinia after its fusion with the plasma membrane, since all the virus particles positive for septins are also labelled with exB5 (Fig.3.5).

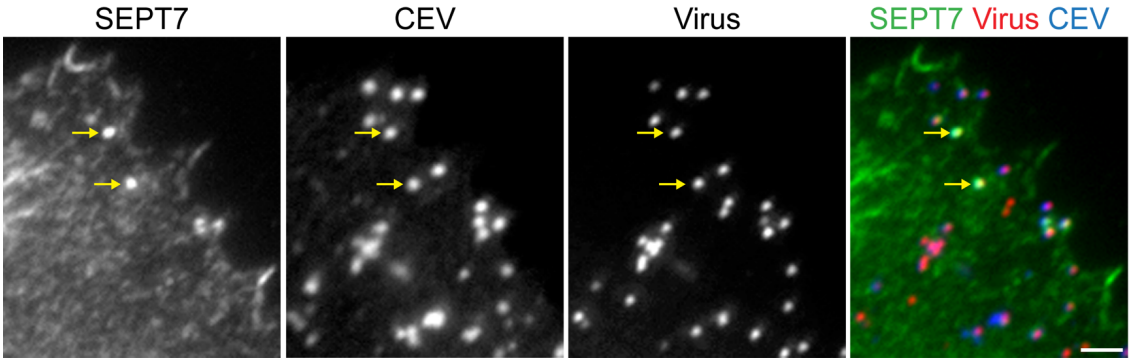

Figure 3.5 Vaccinia recruits septins after its fusion with the plasma membrane

Representative immunofluorescence images of a HeLa cell infected for eight hours. Yellow arrows highlight the co-localization of SEPT7 (green) with RFP-A3 WR virus (red) that has already fused and remained attached to the membrane (CEV in blue). Scale bar = 2 μm.

3.2.2 Septin recruitment precedes actin tail formation

To further investigate the recruitment of septins, infected cells were immunostained with exB5, SEPT7 and phalloidin to label filamentous actin at eight hours post-infection. Approximately 13.2 ± 1.9% of the CEVs co-localized with septins, while 23.4 ± 2.6% of the CEVs induced an actin tail. Interestingly, septin recruitment and actin tail formation were mutually exclusive (Figure 3.6). These data indicate that there are either two subpopulations of virions, one that makes tails and another one

that recruits septins. Alternatively, septin recruitment and actin tail formation are temporally distinct events.

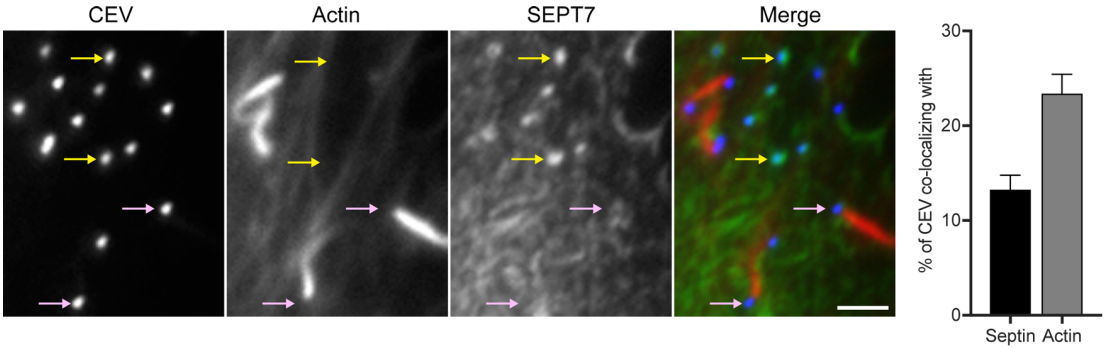

Figure 3.6 Septin recruitment and actin tails are mutually exclusive

Representative immunofluorescence images of a HeLa cell infected for eight hours showing SEPT7 in green, CEV in blue and actin labelled with phalloidin in red. CEV can either recruit septins (yellow arrows) or induce an actin tail (pink arrows). Quantification of the % of CEV co-localizing with SEPT7 or inducing an actin tail. Error bars represent SEM from three independent experiments in which over 900 virions from 30 cells were analysed. Scale bar = 2 μm.

To address this question, I generated a HeLa cell line stably expressing GFP-SEPT6. Overexpression of proteins can potentially alter the behaviour of the cell. One advantage of stable cell lines is that they usually find an expression level that is well tolerated. The expression of SEPT2, SEPT7 and SEPT9 was comparable in control and GFP-SEPT6 HeLa cells as assessed by immunoblot analysis (Figure 3.7A). In my GFP-SEPT6 cell line I could not detect any obvious morphological or proliferative changes (Figure 3.7B). The percentage of CEVs recruiting septins was also the same in wildtype (11.6 ± 1.6%) and GFP-SEPT6 HeLa cells (11.5 ± 1.6) see Figure 3.7C. I was therefore confident that the stable cell line shows representative behaviour.

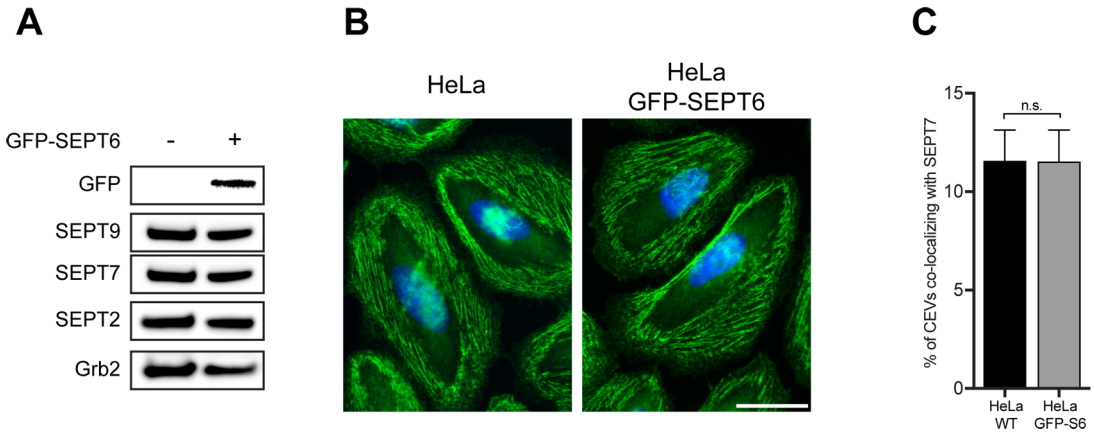

Figure 3.7 Characterisation of HeLa cells stably expressing GFP-SEPT6

A Western blot analysis showing the levels of SEPT2, SEPT7 and SEPT9 in control and GFP-SEPT6 HeLa cells. Grb2 was included as loading control. **B** Immunofluorescence images depicting control and GFP-SEPT6 HeLa cells. SEPT7 is shown in green and DAPI in blue. **C** Quantification of the % of CEV co-localizing with SEPT7 in the indicated cell line after eight hours of infection. Scale bar = 5 µm.

Performing live cell imaging using HeLa cells infected with RFP-A3 WR and stably expressing GFP-SEPT6 as well as LifeAct-iRFP, a marker for filamentous actin, revealed that septins are recruited to the virus prior to actin tail formation (Figure 3.8). As shown in the movie stills, the virus reaches the periphery after rapid directed movements, typical for microtubule-based transport. From 64 to 142 sec the virus in this movie is stationary and SEPT6 is recruited until actin starts to polymerize underneath the virus and the fluorescence intensity of SEPT6 decreases. As the actin tail is built up and the virus is being pushed forward, septins are lost from the virus.

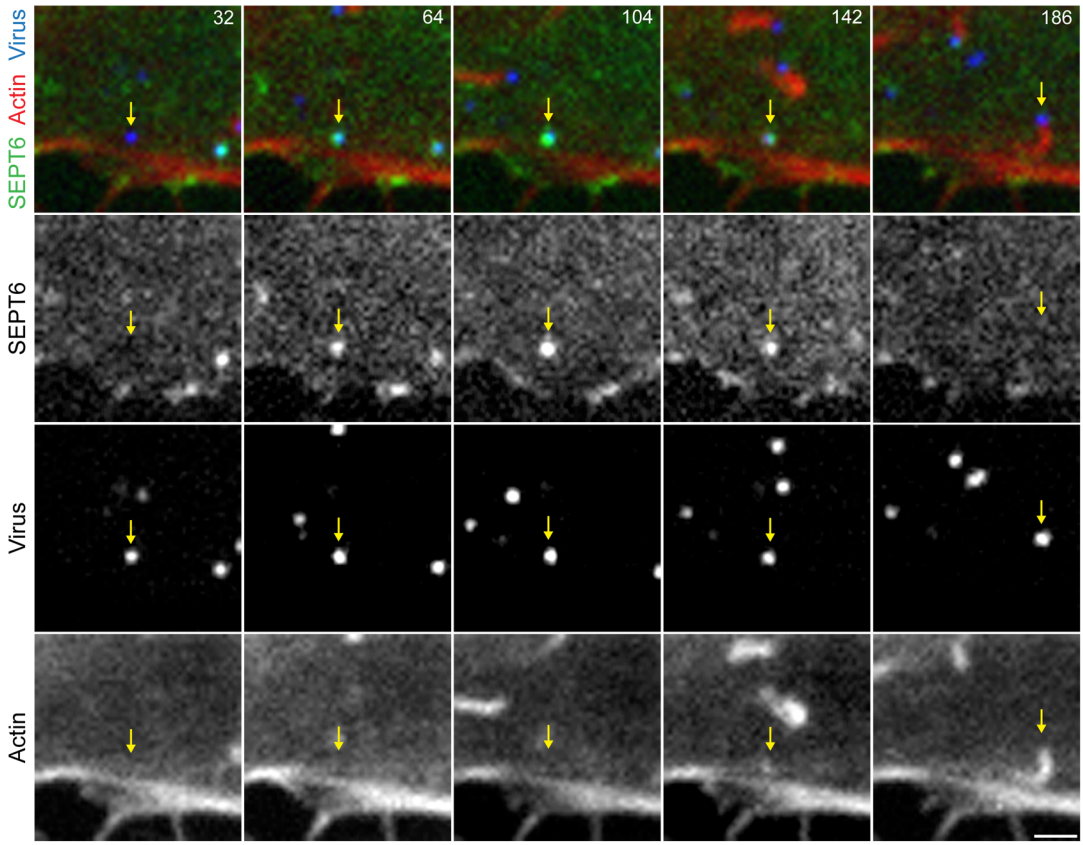

Figure 3.8 Septins are recruited prior to actin tail formation

Movie stills from live cell imaging of HeLa cells stably expressing LifeAct-iRFP (actin) and GFP-SEPT6 that were infected with RFP-A3 WR (virus) for eight hours. Septin is recruited to CEV but lost as the actin polymerization starts (yellow arrow). The time in seconds is indicated. Scale bar = 2µm.

3.2.3 Clathrin and septins are recruited independently from each other

Clathrin and AP-2 are also transiently recruited to vaccinia just before actin tail initiation (Humphries et al., 2012, Snetkov et al., 2016). To compare the loss of clathrin and AP-2 with the loss of septins from the virus, I immunostained infected HeLa cells for SEPT7 and AP-2. When staining for these components, 13.1 ± 1.6% of CEVs co-localize with septins (Figure 3.9A, green arrow), 25.6 ± 2.3% recruit AP-2 (Figure 3.9A, pink arrow) and 5.2 ± 0.5% are positive for SEPT6 and AP-2 (Figure 3.9A, yellow arrow). This indicates that septin and AP-2/clathrin recruitment partially overlap at the virus.

To determine the temporal order of events of clathrin and septin recruitment to the virus, cells transiently expressing mCherry-Clathrin Light Chain in the GFP-SEPT6

LifeAct-iRFP cells were imaged after eight hours of infection (Figure 3.9B). Septins are being recruited approximately 4 minutes prior to actin tail formation. Clathrin was detected 2 minutes before actin polymerization. As the actin tail is formed and the virus is pushed away, both proteins stayed behind and disassembled, with septins disappearing approximately 3 seconds earlier than clathrin. In addition, it is also worth mentioning that there were a few occasions in which clathrin was not recruited prior to actin tail formation.

The overlapping presence and timings of septin and clathrin at the virus raises the question if septin and clathrin/AP-2 influence the recruitment of each other. To investigate this subject, I took advantage of the A36 ΔNPF1-3 virus (ΔNPF), which is unable to recruit AP-2 and clathrin (Snetkov et al., 2016). The level of CEVs co-localizing with SEPT7 was unchanged in the absence or presence of clathrin (WR 13.8 ± 1.6% and ΔNPF 15.46 ± 1.5%; see Figure 3.9C).

Conversely, I performed a siRNA knockdown of SEPT7 (with a pool of four siRNA oligos) prior to infection with WR. The efficiency of SEPT7 knockdown was assessed by immunoblot analysis, which showed substantial depletion of SEPT7 at 72 hours after siRNA treatment (Figure 3.9E). As described before (Kremer et al., 2005, Kinoshita et al., 2002), SEPT7 is essential as its knockdown leads to the loss of functional septin structures and a reduction of other septin levels (Figure 3.9E). Depletion of septins led to no significant change in the number of CEVs recruiting clathrin (Allstar 22.9 ± 4.1% and SEPT7-depleted 22.3 ± 2.9%, Figure 3.9D). Based on these results, septins and clathrin, although temporally overlapping, are recruited independently of each other to the virus.

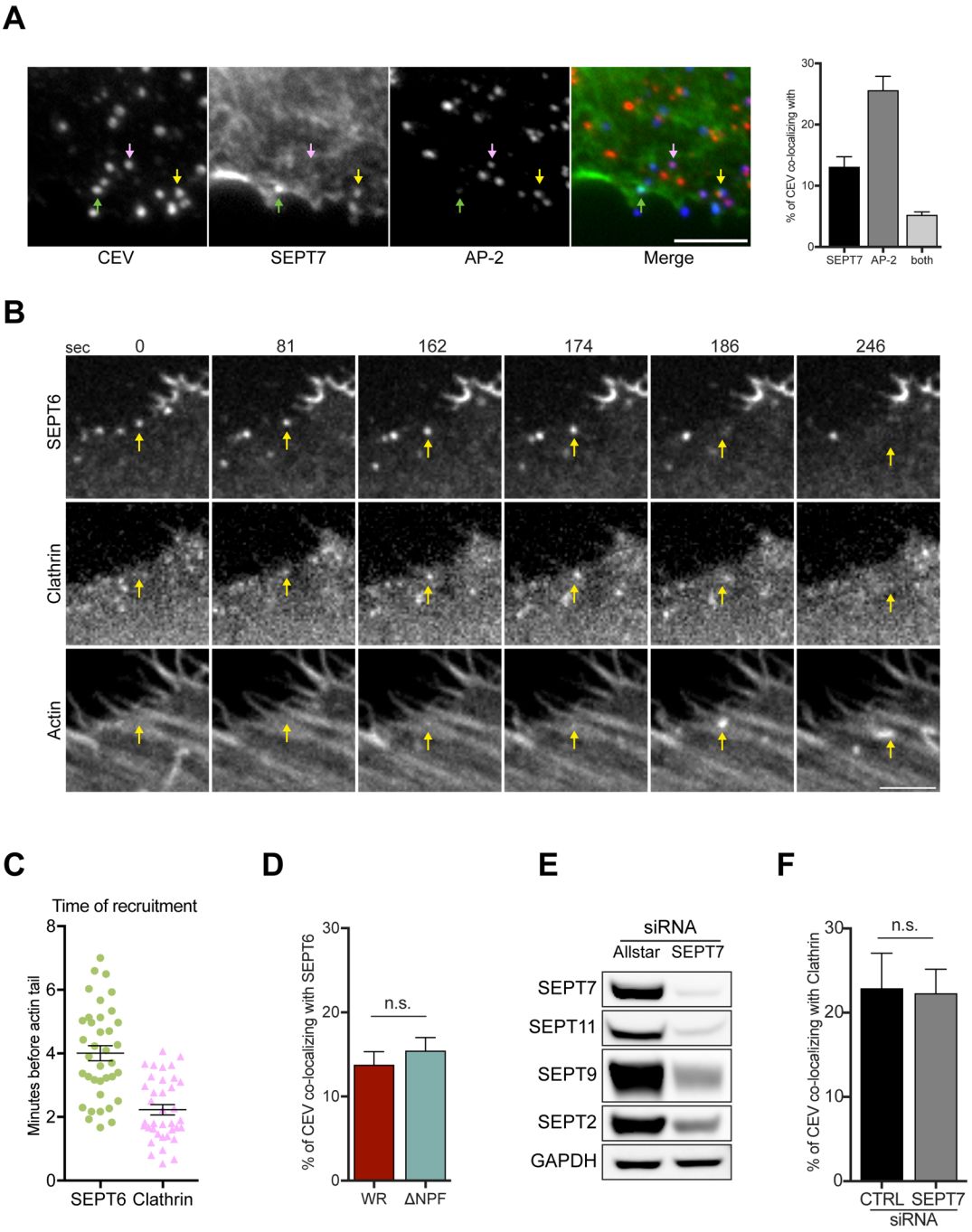

Figure 3.9 Clathrin and septins are recruited independently of each other to CEV

A Immunofluorescence image showing the association of SEPT7 (green arrows), AP-2 (pink arrows) or both proteins (yellow arrows) with CEV in HeLa cells infected with WR for eight hours. The graph shows the percentage of CEV co-localizing with SEPT7, AP-2 or both proteins. **B** Movie stills taken from live cell imaging of WR infected HeLa cells that express GFP-SEPT6, mCherry-clathrin light chain (Clathrin) and LifeAct-iRFP (Actin). SEPT6 is recruited to CEV before clathrin, but both proteins are lost when actin polymerization starts. The time in seconds is indicated. **C** The graph shows the time of SEPT6 and clathrin arrival prior to actin tail formation. **D** The graph shows the % of CEV recruiting septin in the presence (WR) or absence (ΔNPF)

of clathrin. **E** Western blot analysis confirming the knockdown of SEPT7. Other septin levels are subsequently also reduced. GADPH was included as a loading control. **F** The % of CEV recruiting clathrin in the presence or absence of SEPT7. Scale bars = 2 µm; n.s. indicates a p-value > 0.05. Error bars represent SEM from three independent experiments. For protein timings over 37 virus particles were analysed and for each of the other conditions over 900 virus particles were analysed in 30 cells.

3.2.4 Structural arrangement of septins at the virus

Next, I tried to resolve the spacial arrangement of septins at the virus. In some of the immunofluorescence images acquired with our Zeiss AxioPlan2 epifluorescence microscope, septins associated with the virus appear as a ring. The same septin arrangement is sometimes observed with the exB5 staining. B5 is known to be inserted in the viral membrane, hence outlining the brick-shaped virion (Fig 3.9 A and B, purple lines). Depending on the focal plane, septins can look like a ring or a disc (Figure 3.3). Since it has been established according to my data that the virus is already attached to the outside of the cell after fusion and host septins are located inside the cell, seeing a ring can be caused by two scenarios. Assuming the virus is still invaginated, like an endocytic vesicle shortly before scission, septins could either form a cup underneath the virus (Figure 3.10A), or they could form a collar around the neck of the invagination (Figure 3.10B), or any intermediate mix of both. In order to distinguish between those two options, I performed structured illumination microscopy using the Elyra PS.1 microscope. HeLa cells were infected with the mutant virus A36 YdF virus (YdF), which is deficient in actin tail formation and has increased levels of septin recruitment (see chapter 4.2.1, Figure 4.1). In addition, the vaccinia core protein A3L was fused to RFP (Figure 3.10 red core) and the cell was immunostained against SEPT7 (Figure 3.10, green). In the obtained images, most virus associated septins appeared as rings. Plotting the orthogonal views of the z-stack revealed that septins and the virus core appear to be in the same z-plane and have a comparable expansion in the z-direction (Figure 3.10C), which would argue for the cup like scenario in Figure 3.10A. In some cases, dimmer intensities of SEPT7 staining above or below the virus core were detected. Due to the limited resolution in z, it is difficult to distinguish whether these intensities indicated the presence of septin or whether they were mere imaging artefacts.

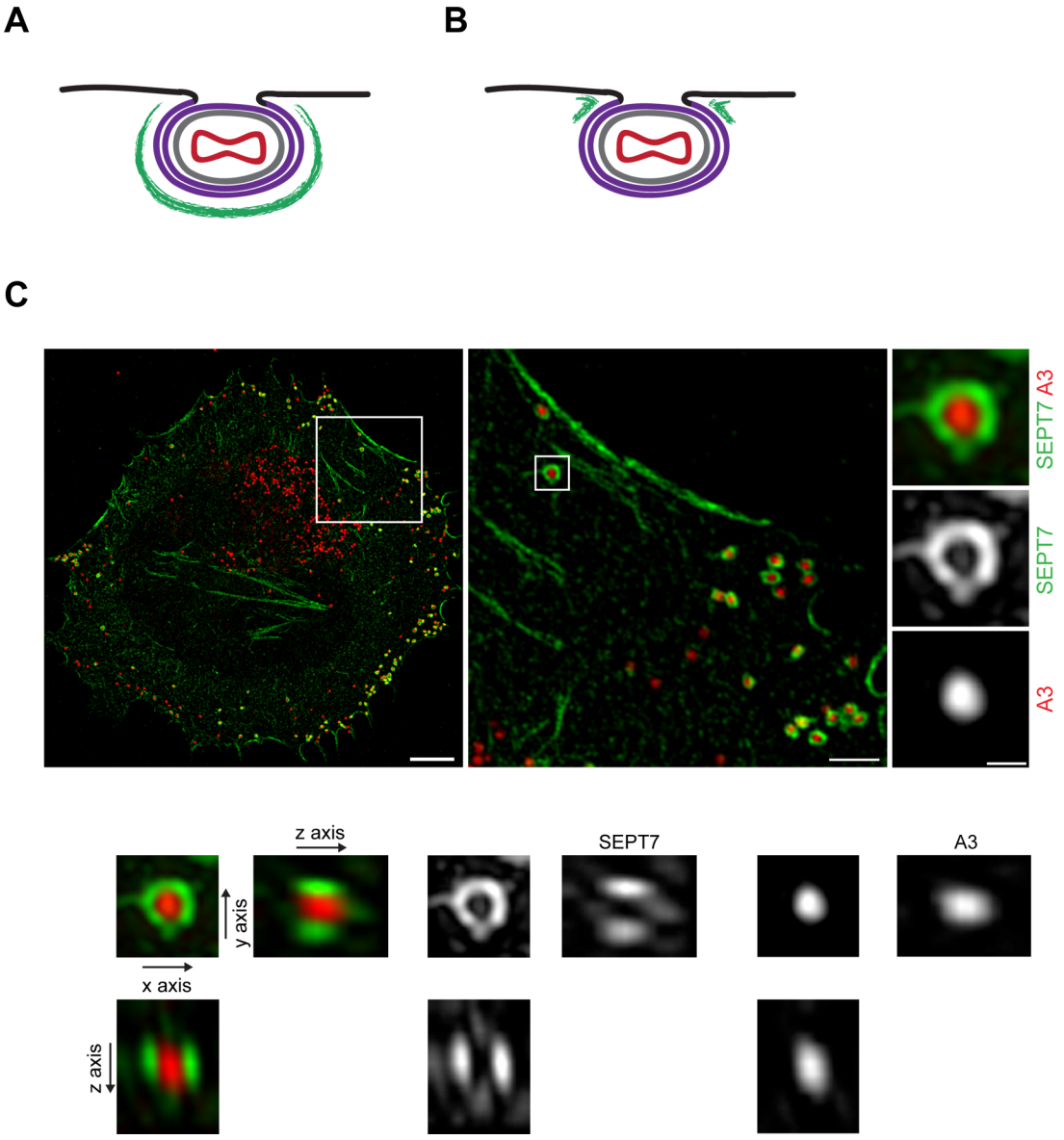

Figure 3.10 Septins form a ring around the virus

A and **B** Schematic of how septins (green) might be arranged at the virus on the plasma membrane (black). Virus core is depicted in red and B5 containing viral membrane in purple. **C** Structured illumination micrographs of SEPT7 (green) associated with YdF virus expressing RFP-A3 in infected HeLa cells. Maximum intensity projection and orthogonal views of the z-stack acquired. Scale bars going from right to left represent 5µm, 500nm and 100nm.

Taking advantage of the high resolution in x and y, I measured the diameter of the septin rings. Through this approach, the intensity profile along a straight line through the centre of the ring was determined. A double Gaussian curve (Figure 3.11A red line) was fitted to the measured intensity values (Figure 3.11A blue dots) and the distance between the two means of the Gaussian represented the diameter of the

ring. The average diameter of septin rings surrounding vaccinia virus is 343 ± 4 nm (Figure 3.11). I measured in one z-plane and any structure that was tilted in respect to this plane will appear shorter than it is. Therefore, it is likely that the measurements in average slightly underestimate the real dimensions of the septin ring.

To further examine the location between extracellular virus and septins, I immunolabelled exB5 and SEPT7. In contrast to septins, which appeared relatively circular, B5 had an elongated appearance. The staining of B5 agrees with previous electron microscopy (EM) data, which reported the virion to be brick-shaped with dimensions of 360x270x250nm (Cyrklaff et al., 2005). Hence, I measured the dimensions of B5 as a control, using two perpendicular lines to determine the long and the short axis of the virus particle. Along the long axis, the virus appeared 283 ± 5 nm and 234 ± 4 nm along the shorter axis (Figure 3.11B). Again, the slightly smaller dimensions might be due to imperfect alignment of the virus particles along the acquired x-y plane. Importantly, the septin ring displayed on average a larger diameter than the B5 staining, confirming the idea that septins surround the virus.

Comparing the orthogonal views of SEPT7 and B5 revealed that the two proteins had a similar expansion in the z-direction (Figure 3.11B). Although B5 is located all around the virus particle, there is no clear signal at the top or at the bottom of the virus, revealing the limitations of this imaging technique.

Taken together, septins are found at the virus particle surrounding it, which indicates that the CEV needs to be at least partially invaginated. Unfortunately, I was not able to confirm or exclude the existence of septins underneath the virus particle due to resolution limitations.

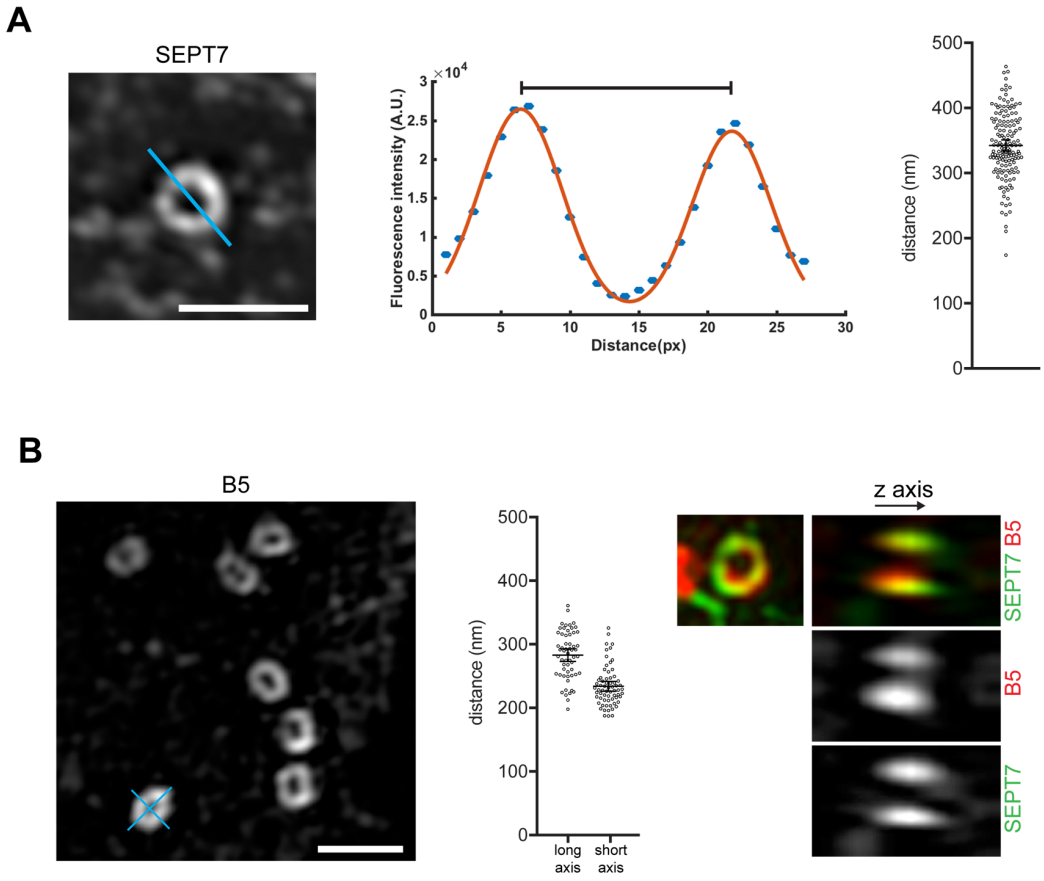

Figure 3.11 Septins surround the outer membrane of CEV

A Maximum intensity projection of the z-stack acquired with a structured illumination microscope of infected HeLa cells labelled with SEPT7. The diameter of the septin ring surrounding the virus was measured by fitting the sum of two Gaussian peaks (red) to the fluorescence intensity profile (blue dots) along a line crossing the virus ring (blue line). Quantification of septin ring diameter. **B** Infected cells were stained with exB5 and the dimensions along the long and short axis of the virus was measured. Maximum intensity projection and orthogonal views of the z-stack acquired. Error bars represent SEM from two independent experiments in which over 150 septin rings and over 60 B5 stained viruses from over 10 cells were analysed. Scale bars = 500nm.

To gain the desired resolution to examine if septins are accumulated beneath the virus, I utilized electron microscopy (EM). As an initial trial, YdF infected HeLa cells were embedded in resin, cut into thin sections and imaged using a transmission electron microscope (TEM) with help from the EM facility. Virus particles and a few actin bundles (yellow arrow heads) as well as microtubules (orange arrow heads) in

the cell periphery were identified, but we did not find any structure associated with invaginated viruses that could be identified as septins (Figure 3.12).

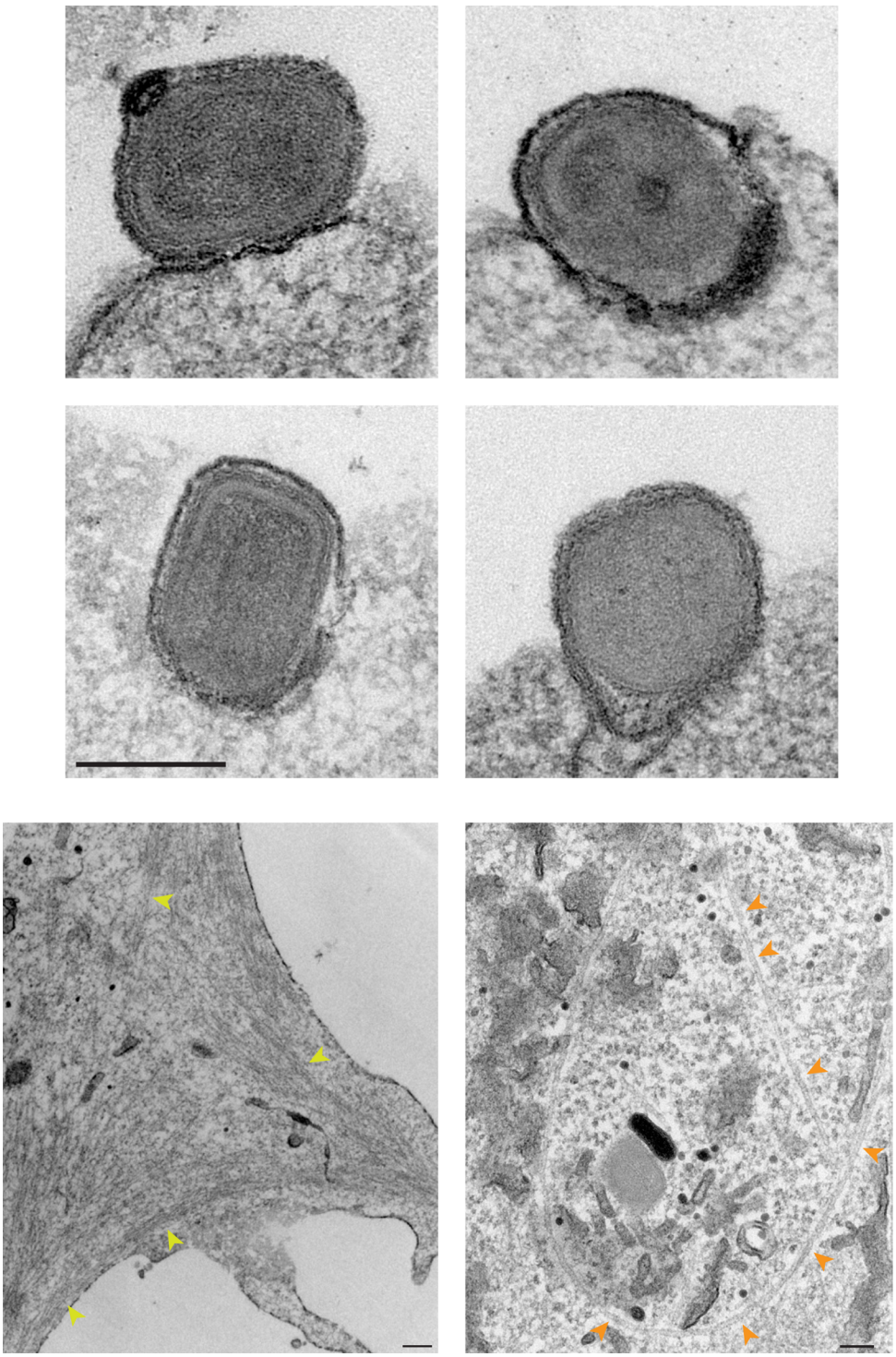

Figure 3.12 Sections of infected HeLa cells examined with TEM

Infected HeLa cells were embedded in resin and cut in sections that were examined using a TEM. Actin filaments (yellow arrow heads) and microtubules (orange arrow heads) were partially preserved but no septin structure was identified. Scale bars = 200 nm.

Potentially septins are not suited to maintain a striking feature throughout the embedding process. We therefore decided to try another method for sample preparation developed by Heuser (Heuser, 2000). This method allows for “unroofing” of the cell by removing the upper half of adherent cells. This leaves the interior of the cell exposed and the nucleus as well as the cytoplasmic content is washed away while the basal membrane remains attached.

Therefore, I grew cells on fibronectin-coated coverslips and after eight hours of infection cells were “glued” down to the cover slip by incubating them for ten seconds in 0.5 mg/ml poly-L-lysine. Subsequently, cells were exposed to a hypotonic buffer causing them to swell. Cells were then “unroofed”, by a blast of buffer while the basal membrane remains attached to the coverslip. The plasma membrane together with associated proteins was fixed in PFA. I tested two different methods to generate the “unroofing” blast of buffer. First, I generated the blast by squirting media through a 0.3 µm needle. Alternatively, I placed the tip of a sonicator in a 45-degree angle closely above the cover slip and the cells were “unroofed” by a gentle, brief sonication step. However, no significant qualitative difference was observed (Figure 3.14).

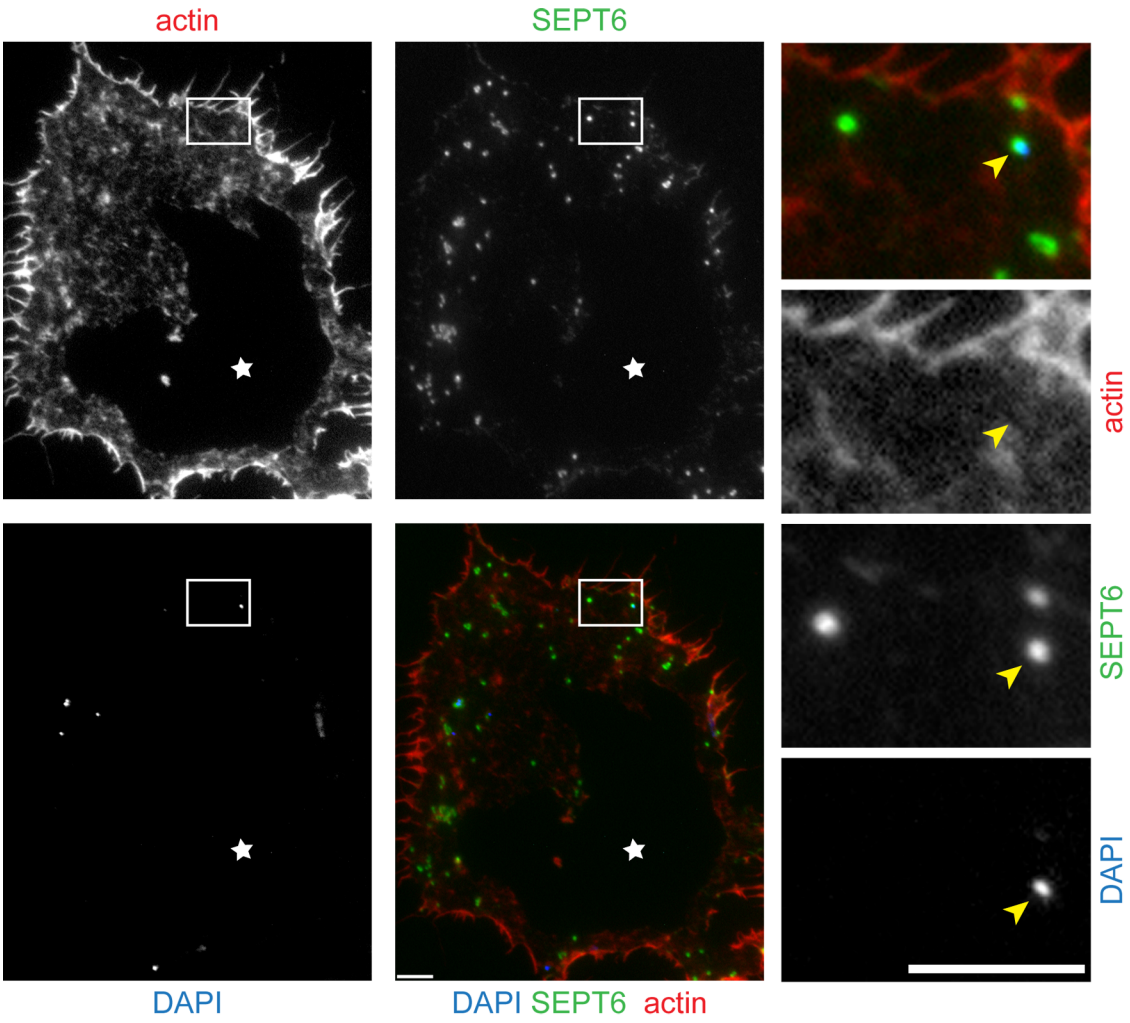

Figure 3.13 Immunofluorescence images of unroofed infected HeLa cells

Immunofluorescence image of infected HeLa stably expressing GFP-SEPT6 (green) cells after "unroofing" process using a 0.3µm syringe. Actin stained with phalloidin (red) and DNA stained with DAPI (blue). The apical part including the nucleus are removed but septin associated with viruses remained intact (yellow arrow head). The star indicates an area where the basal membrane was also removed. Scale bar = 5µm.

Following fixation, cells were either stained with phalloidin and DAPI or dehydrated, coated with 2 nm of platinum (Pt) and then imaged using a scanning electron microscope (Quanta 250 FEG SEM). Immunofluorescence confirmed that the upper half of the cell including the nucleus was removed (Figure 3.13). Most parts of the basal membrane remained intact and septins associated with viruses were still visible (see yellow arrow heads in Figure 3.13.).

Virus particles as well as actin filaments could also be identified under the scanning electron microscope (Figure 3.14). However, there was no typical clathrin lattice on

virus particles found, unlike previously seen when performing transmission electron microscopy on resin-embedded sections (Humphries et al., 2012). Furthermore, comparing the two different techniques of “unroofing” the cell (syringe versus sonicator) there was no qualitative difference observed.

To aid in distinguishing septins under these conditions for EM, I immunolabelled with the SEPT7 antibody together with a gold conjugated secondary antibody. The 2 nm gold particles appear as bright dots in the electron micrograph. Figure 3.15 shows CEVs with gold particles not only on the lateral side of the virus (where the ring would be found) but also at the top of the virus (which is the side of the virus particle that is still exposed to the cytoplasm). Given the location of septins with respect to the virus, my data supports the idea that septins form a cup around the virus as they are found both at the lateral sides and underneath the virus particle.

Current work aims to improve the sample preparation to better preserve the ultra-structure of septins, clathrin and the virus. Using critical-point drying instead of air drying showed promising improvements. Actin tails are now easily recognized (blue star in Figure 3.16) and more material at the cortex is preserved. Interestingly, now two subsets of virus particles are distinguishable. Some viruses have a smooth surface (yellow arrow heads in Figure 3.16), while others have a rough appearance (red arrow heads in Figure 3.16). One explanation is that the smooth viruses are still inside the cell, whereas the rougher ones have already fused and now the cortex and potentially septins covers the particle. Performing immunogold labelling on critical-point dried samples will confirm whether those rough viruses are associated with septins.

Syringe

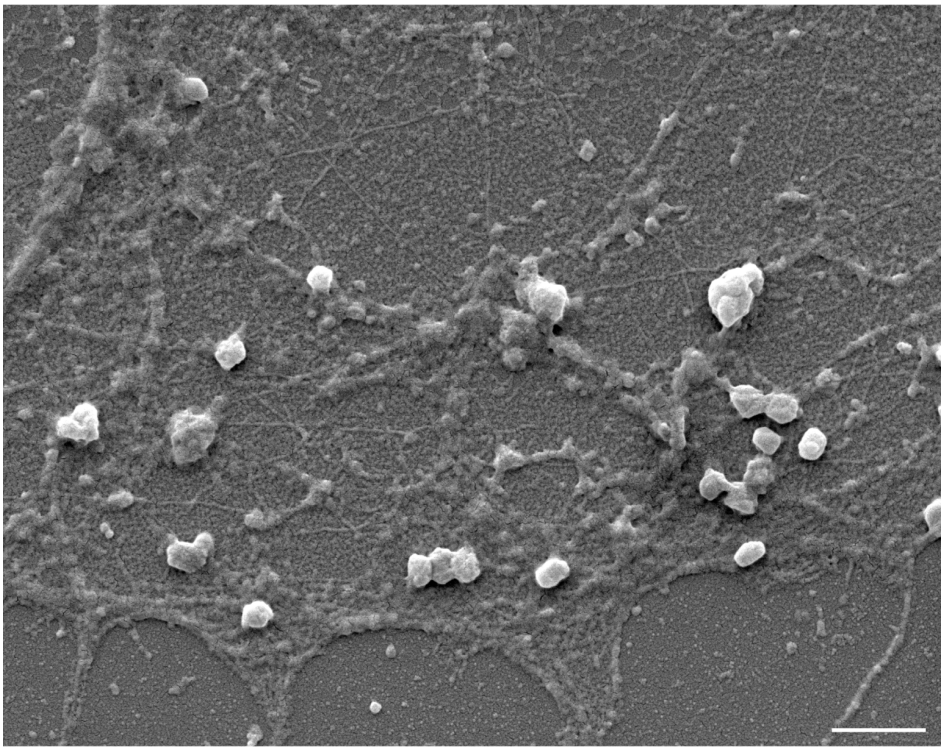

Sonicator

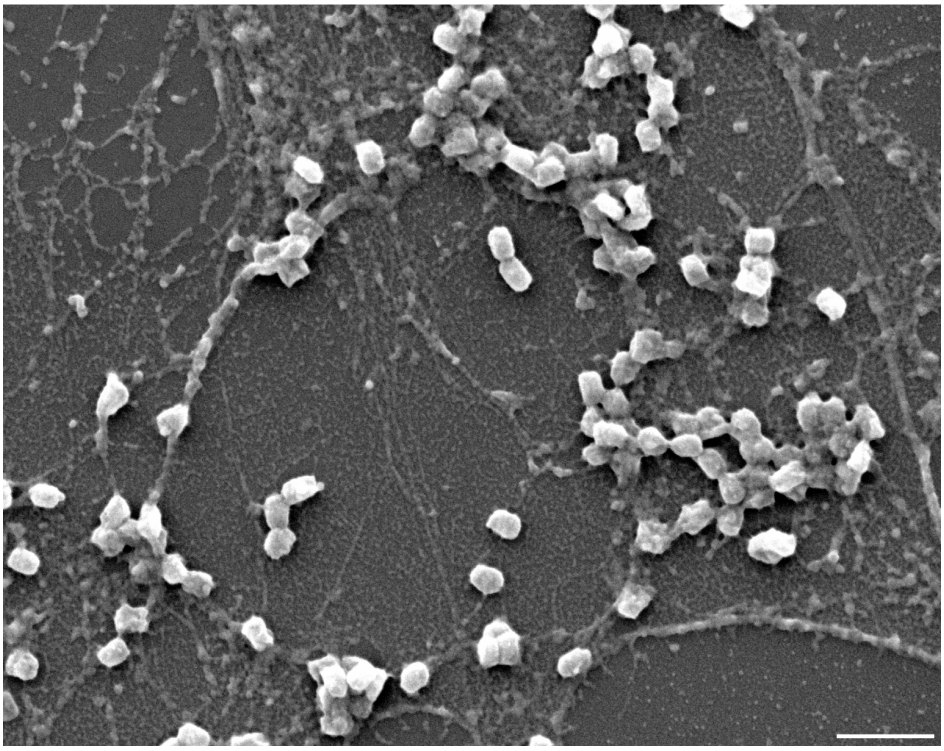

Figure 3.14 Scanning Electron-micrographs of "unroofed" cells

Infected HeLa cells were unroofed with the indicated method after eight hours of infection. Scale bare = 1µm.

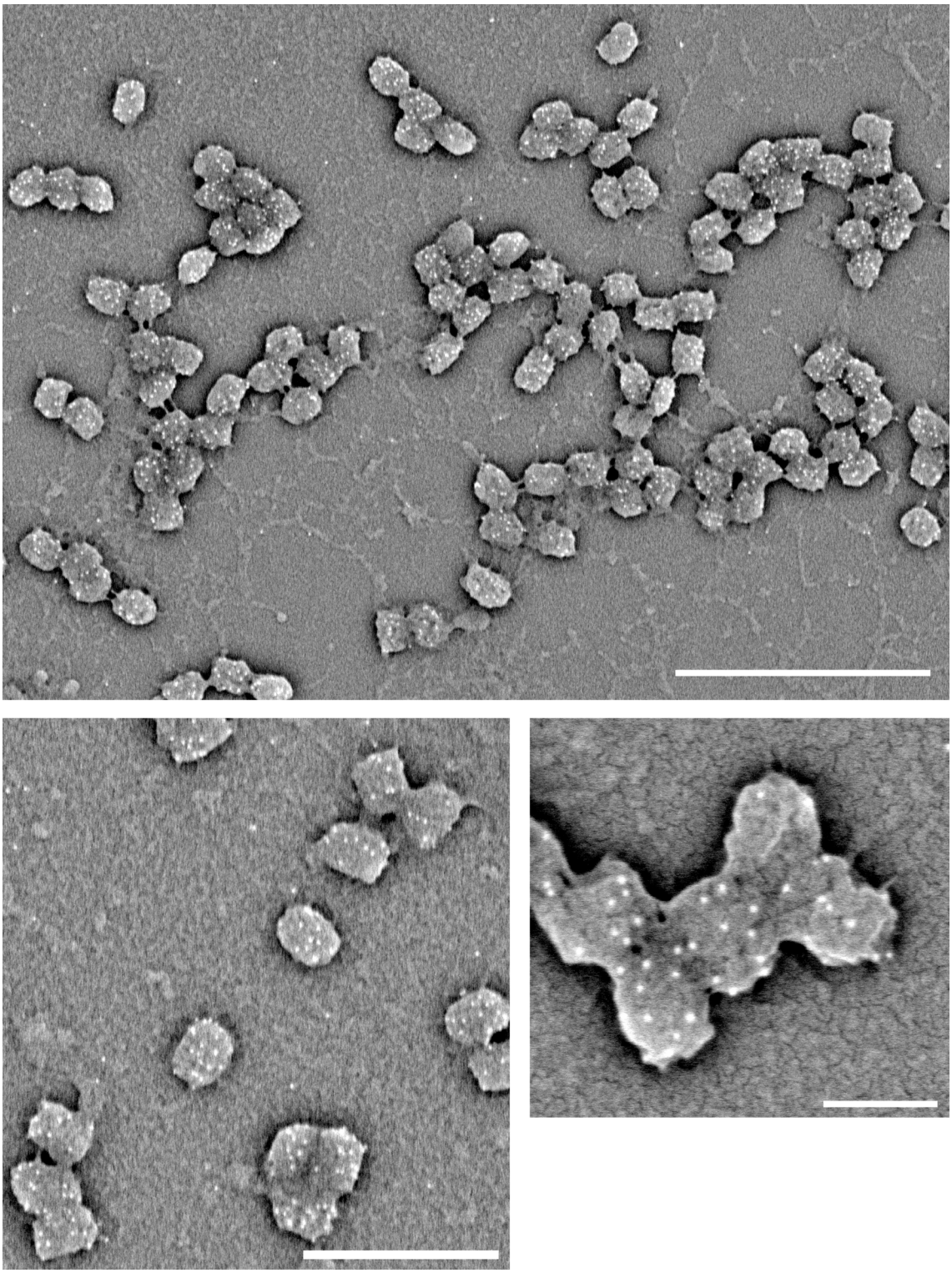

Figure 3.15 Immunogold labelled septins surrounding the virus

Scanning electron-micrographs of „unroofed" HeLa cells infected with YdF virus for eight hours and immunogold labelled for SEPT7. Scale bars are 2 µm, 1 µm and 300 nm in images with increasing magnification.

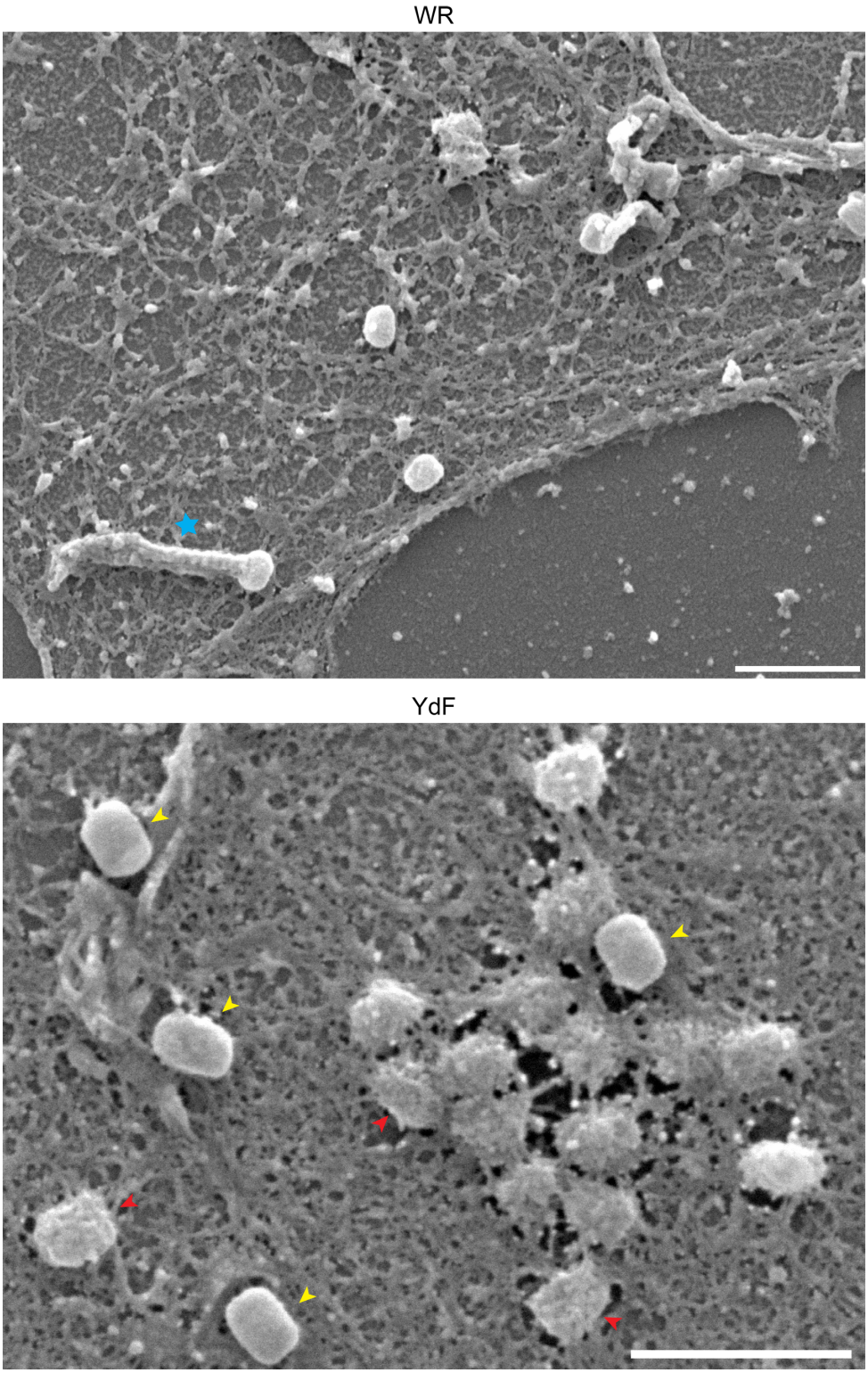

Figure 3.16 Critical-point drying improves the preservation of ultra-structure

Infected cells were “unroofed” and critical-point dried and examined with SEM. The blue star highlights a WR virus associated with an actin tail. Some viruses have a smooth appearance (yellow arrow heads), while others have a rougher texture (red arrow heads). Scale bars = 1μm.

3.3 Summary

The work presented in this chapter shows that septins are recruited to vaccinia virus during egress. Septins arrive at the virus after its fusion with the plasma membrane and prior to actin tail formation. As the actin tail is formed, septins are lost from the virus, similar to the clathrin coat (Humphries et al., 2012, Snetkov et al., 2016). Septin and clathrin partially co-localize at the virus, but septins are recruited approximately 2 minutes earlier. Both septins and clathrin are recruited independently of each other, as the absence of one does not influence the behaviour of the other. Data from structured resolution microscopy and scanning electron microscopy support the hypothesis that septins form a cup around the virus covering the whole area exposed to the cytoplasm. Subsequent work will shed light on the functional role of septins during vaccinia infection and its relationship to actin tail formation.

Chapter 4. Investigating how septins are displaced from the virus

4.1 Introduction

In the previous chapter I established that septins are recruited to a subset of vaccinia virus particles during viral egress. The formation of virus induced actin tails leads to the loss of septins from the virus. A similar situation is seen with clathrin, which is also recruited to vaccinia CEV after fusion with the plasma membrane (Humphries et al., 2012, Snetkov et al., 2016). I therefore set out to investigate the relationship between septin recruitment to CEV and subsequent actin tail formation.

4.2 Results

4.2.1 Inhibition of actin tails does not change the percentage of CEV co-localizing with septins

After initial analysis of live-cell imaging data in Figure 3.8, one hypothesis was that actin polymerization leads to the displacement of septins from the virus. To test this theory, I used a recombinant virus that is deficient in actin tail formation (Frischknecht et al., 1999b, Rietdorf et al., 2001, Ward et al., 2003, Moreau et al., 2000). In the A36 YdF virus (here referred to as YdF) the two tyrosines in position 112 and 132, which are usually phosphorylated by Src and Abl family kinases, are mutated to phenylalanines (Rietdorf et al., 2001). Consequently, the whole downstream signalling cascade is missing, no actin tails are formed and the virus has severe spreading defects (Frischknecht et al., 1999b, Moreau et al., 2000, Rietdorf et al., 2001, Ward et al., 2003). Infecting HeLa cells with the YdF virus and examining the amount of CEVs co-localizing with septins revealed a striking result. In the case of the YdF virus, 84.1 ± 1.1% of all CEV recruit septin compared to 13.8 ± 1.6% for WR (Figure 4.1). Furthermore, it is noticeable that the YdF CEV accumulate at the cell periphery, as they were not propelled away by actin tails. These data suggest that the lack of actin polymerization leads to an accumulation of septins on CEV. In order to test whether the recruitment of clathrin and AP-2 impact on the observed increase in septin recruitment I used the double mutant virus A36 YdF ΔNPF1-3 (YdF NPF),

which cannot recruit AP-2/clathrin or induce actin tails (Snetkov, 2015). Again, a strong increase in the number of CEV co-localizing with septins was observed (86.0 ± 1.5%; Figure 4.1), confirming that clathrin and AP-2 do not impact on septin recruitment. Taken together, these experiments provided further evidence that newly formed actin tails displace septins from the virus as the inability of stimulating actin polymerization leads to a drastic increase in the number of CEV co-localizing with septins.

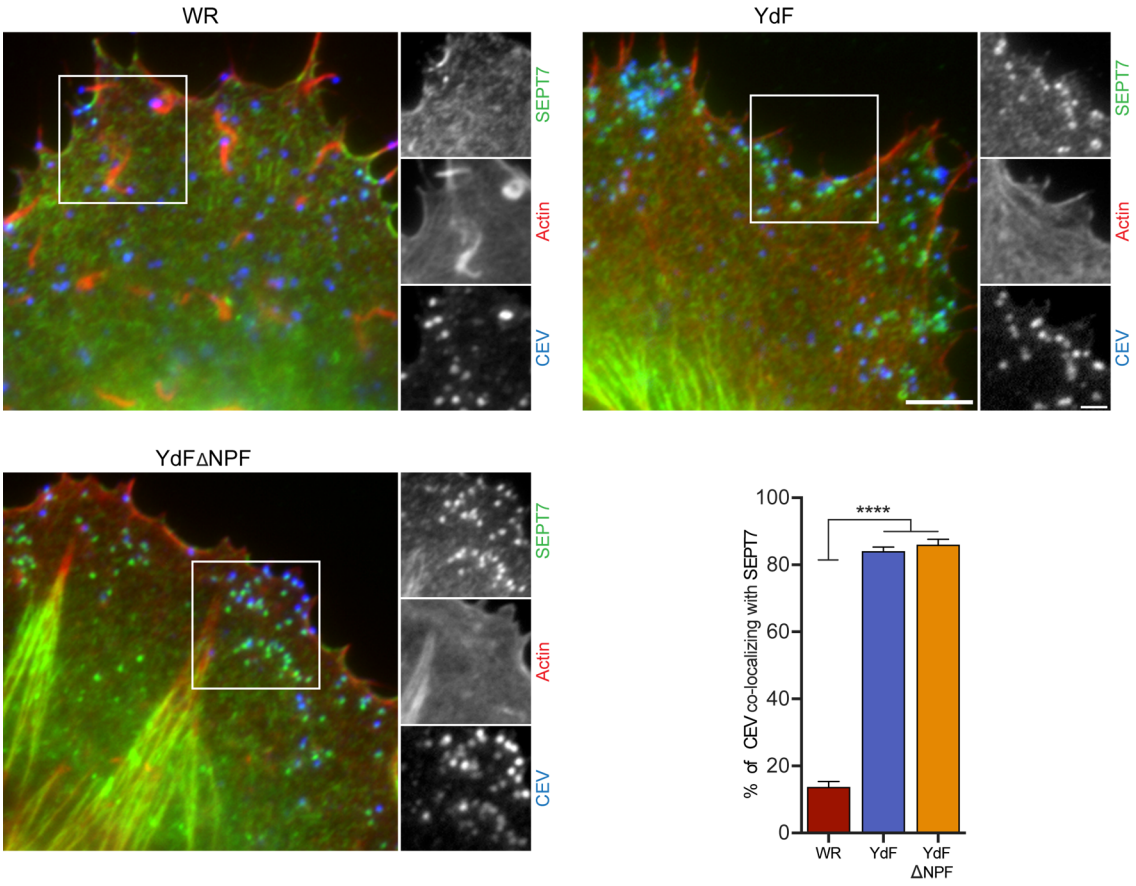

Figure 4.1 Mutation of Y112 and Y132 in A36 strongly increases the recruitment of septins to CEV

Representative immunofluorescence images of HeLa cells infected for eight hours with the indicated virus showing SEPT7 in green, CEV in blue, and actin labelled with phalloidin in red. Quantification of the % of CEV co-localizing with SEPT7. Error bars represent SEM from three independent experiments in which over 900 virions from 30 cells were analysed. A p-value of < 0.0001 is indicated by ****. Scale bar = 5 μm and in inset 1 μm.

It is possible to inhibit actin tail formation using chemical inhibitors (Hollinshead et al., 2001, Weisswange et al., 2009). Since the vaccinia actin tail is an Arp2/3 complex dependent structure (Welch and Way, 2013) treatment with the Arp2/3 inhibitor

CK666 should block its formation. CK666, a small molecule inhibitor, acts as an allosteric effector that stabilizes the inactive form of the Arp 2/3 complex, thereby preventing the formation of new branched actin networks (Nolen et al., 2009, Hetrick et al., 2013). Infected cells were treated with 100μM CK666 for one hour prior to fixation. As expected, actin tails were abolished, yet, surprisingly, the number of CEV co-localizing with septins was unchanged (CTRL 10.8 ± 1.5% and CK666 treated 7.3 ± 2.2%, see Figure 4.2A). This could mean that it is not the actin tail itself that replaces the septins. Alternatively, it could be that the drug has off-target effects on septins and they can no longer accumulate as seen in YdF infected cells. I therefore also treated cells infected with the YdF virus with the Arp2/3 inhibitor. Yet the number of CEVs co-localizing with septins was still high (CTRL 76.8 ± 4.4% and CK-666 treated 79.1 ± 2.7%, see Figure 4.2A) indicating that CK666 does not inhibit septin accumulation. In summary, these results suggest that it is not the Arp2/3-dependent actin polymerisation itself that displaces septins from the virus.

Another way of blocking actin tail formation is to remove the activator of Arp2/3, in this case N-WASP. As previously described, vaccinia virus is unable to form actin tails in N-WASP knockout MEFs (Snapper et al., 2001, Weisswange et al., 2009). I therefore infected N-WASP parental and KO cells with WR and the YdF virus. In this cell line the replication cycle of vaccinia is slightly delayed so I fixed cells after ten hours of infection instead of the usual eight hours in HeLa. In the parental cell line, WR induces actin tails and I found that 13.2 ± 7.3% of CEVs co-localize with septin. As seen in HeLa cells, the YdF virus had increased numbers of CEV with septin, namely 74.4 ± 7.4% (Figure 4.2B). In the N-WASP knockout cells WR still had low levels of septin recruitment (22.9 ± 3.6%) and YdF levels were still high (86.0 ± 2.2%). Hence, the absence or presence of N-WASP did not significantly change septin recruitment to either WR or the YdF virus. N-WASP is recruited as a complex together with WIP to the virus (Moreau et al., 2000, Zettl and Way, 2002, Donnelly et al., 2013). I can therefore conclude that neither the recruitment of N-WASP:WIP nor the subsequent activation of the Arp2/3 complex and the actin tail formation impact on the levels of CEVs recruiting septins.

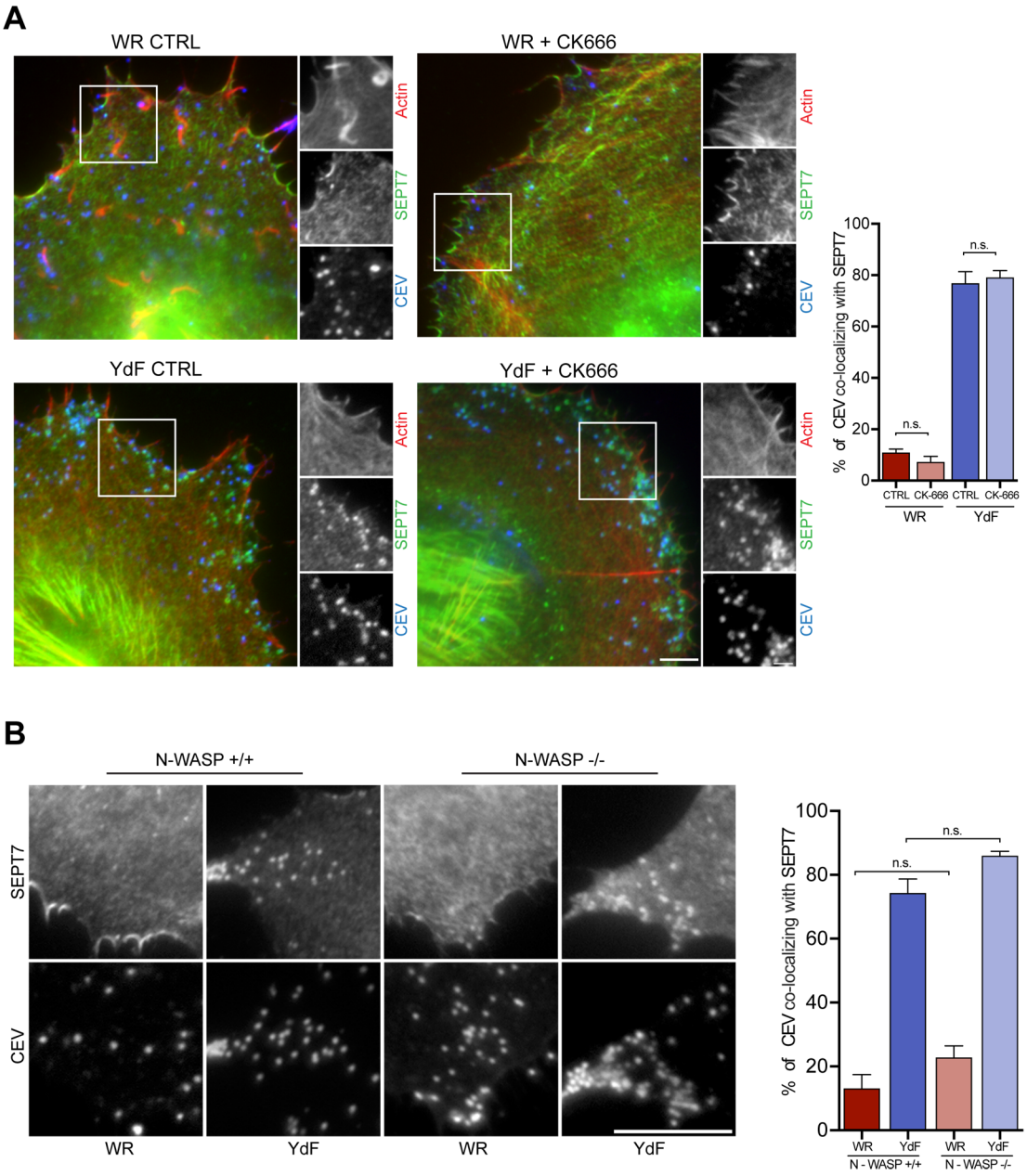

Figure 4.2 Inhibition of actin tail formation does not impact on septin recruitment

A Representative immunofluorescence images of HeLa cells infected for eight hours with the indicated virus in the absence or presence of CK666 showing SEPT7 in green, CEV in blue and actin labelled with phalloidin in red. Quantification of the % of CEV co-localizing with SEPT7. Scale bar = 5 µm and in inset 1 µm. **B** Representative images showing the association of SEPT7 with CEV in N-WASP parental and knockout cells infected with WR and YdF for 10 hours. The graph shows the % of CEV co-localizing with SEPT7 for the indicated viruses in the presence (+/+) or absence (-/-) of N-WASP. Error bars represent SEM from three independent experiments in which over 900 virions from 30 cells were analysed. A p-value of > 0.05 is indicated by n.s. ; scale bar = 5 µm.

4.2.2 Phosphorylation of A36 influences septin recruitment to CEV

My previous observations led me to question what causes the difference between WR and YdF in terms of the ability of the two different viruses to recruit septins. As described previously, at the top of the signalling cascade inducing actin tails is the activation of Src and Abl family kinases (Welch and Way, 2013). Src is recruited to the virus once it reaches the plasma membrane where it mediates the switch between microtubule-based transport and actin tail formation (Frischknecht et al., 1999b, Newsome et al., 2004). Immunostaining for active Src required fixation in the presence of permeabilizing Triton X-100, hence I could not distinguish extracellular and intracellular EV. Using DAPI as a marker for virus particles, I could confirm the recruitment of active Src to the virus (Figure 4.3A). In the case of WR infected cells 31.8 ± 4.2% of the virus in the cell periphery co-localized with active Src (Figure 4.3 B). Even though A36 YdF does not get phosphorylated itself, it still recruits and activates Src (22.9 ± 6.7%) as seen before (Newsome et al., 2004). Co-staining for septin and active Src reveals that 18.6 ± 8.1% of septin dots associated with WR virus also co-localize with active Src (yellow arrow in Figure 4.3A and Figure 4.3C) whereas the majority of virus-associated septins did not overlap with Src (pink arrows in Figure 4.3A). In contrast to WR, only 8.8 ± 3.6% of the septin puncta associated with YdF virus co-localized with active Src (Figure 4.3C).

These findings led me to ask whether Src and septins are independently recruited to the virus or if the presence of one induces or prevents the recruitment of the other? In order to determine the temporal order of protein arrival at the CEV I decided to perform live-cell imaging. I transiently over-expressed GFP-Src in the mCherry-SEPT6 HeLa cell line. Surprisingly, when infected with WR, I hardly found any septin recruited to the virus. Over-expression of Src appeared to negatively impact on septin recruitment to the virus. When cells were infected with YdF virus, I observed that septins were lost from the virus the moment Src was recruited and once Src was lost, septins returned to the virus (Figure 4.3D).

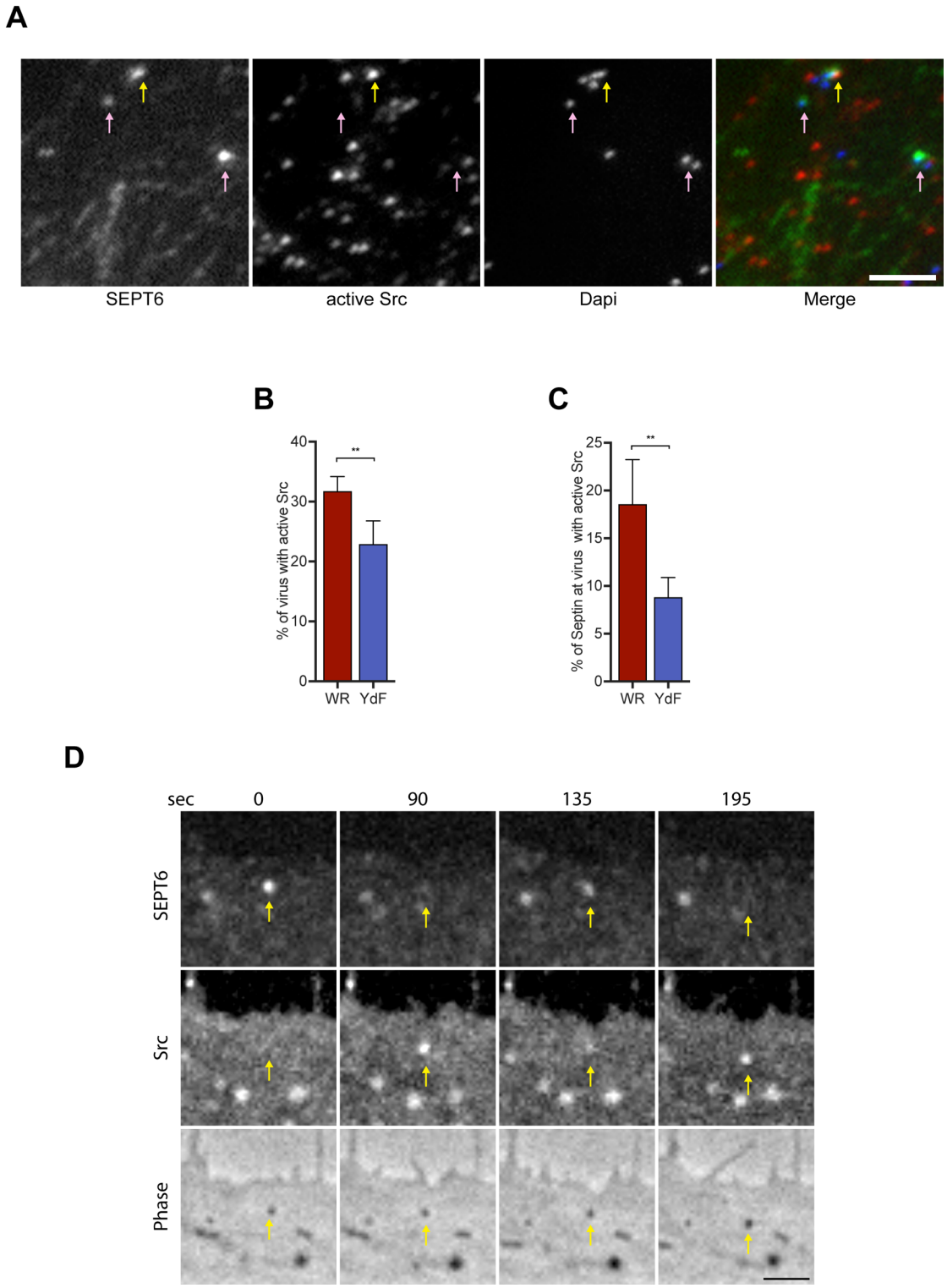

Figure 4.3 Src and septins temporally overlap at the CEV

A Representative immunofluorescence images of HeLa cells infected for eight hours with WR showing SEPT7 in green, DAPI in blue and active Src in red. Septin and Src can co-localize at the virus (yellow arrow) but most viruses recruiting septin do not stain for active Src (pink arrows). **B** The graph shows the % of CEV co-localizing with active Src. **C** Quantification of septin associated CEV co-localising with active

Src. **D** Movie stills taken from live cell imaging of YdF infected HeLa cells that express mCherry-SEPT6 and GFP-Src (Src). Yellow arrow indicates a virus on which SEPT6 and Src alternate. The time in seconds is indicated. Scale bars = 3 μm. Error bars represent SEM from three independent experiments in which over 900 virions from 30 cells were analysed. A p-value of < 0.01 is indicated by **.

The alternating presence of Src and septins at the virus could be explained by mutual antagonism or competition for the same binding site. When looking at Src and septin in uninfected cells I noticed that the two proteins never overlapped (Figure 4.4A). A good example for this are stress fibres. As seen before septins and actin tend to co-localize with stress fibres (Dolat et al., 2014). Yet at the tips where stress fibres are anchored to focal adhesions and where Src is present, septins are absent (Figure 4.4A).

In order to quantify the effects of Src over-expression I performed immunostaining on fixed cells. As already seen in live-cell imaging the number of CEV in WR infected cells recruiting septin is decreased to 2.9 ± 0.4% when expressing GFP-Src compared to 12.5 ± 1.1% in cells expressing GFP alone. A similar trend was observed in YdF infected cells, where 71.2 ± 2.7% of CEV recruit septins in GFP control cells, whereas only 16.4 ± 1.9% of virus co-localized with septins in GFP-Src over-expressing cells (Figure 4.4B). These data suggest that Src negatively regulates the ability of CEV to recruit septin.

One way of testing this hypothesis was to inhibit Src activity and see if this induced an opposite effect to its over-expression. I therefore took advantage of the well-characterized ATP-competitive Src inhibitor, PP1, which blocks the kinase activity of Src and Abl kinases (Hanke et al., 1996). It is already established that treating infected cells with PP1 blocks vaccinia induced actin tail formation (Frischknecht et al., 1999b). When cells infected for four hours were treated with 12.5 μM PP1 for additional four hours before fixation, I found that WR no longer induced actin tails. More importantly, there was a strong increase in the number of CEV recruiting septins to the levels seen with the YdF virus (CTRL 11.1 ± 0.8% and PP1 treated cells 81.5 ± 2.4%) (Figure 4.4C). In YdF infected cells, inhibiting Src did not significantly increase the levels of septin recruitment to the virus (CTRL 76.9 ± 4.4% PP1 treated cells 81.1+/- ± 3.0%).

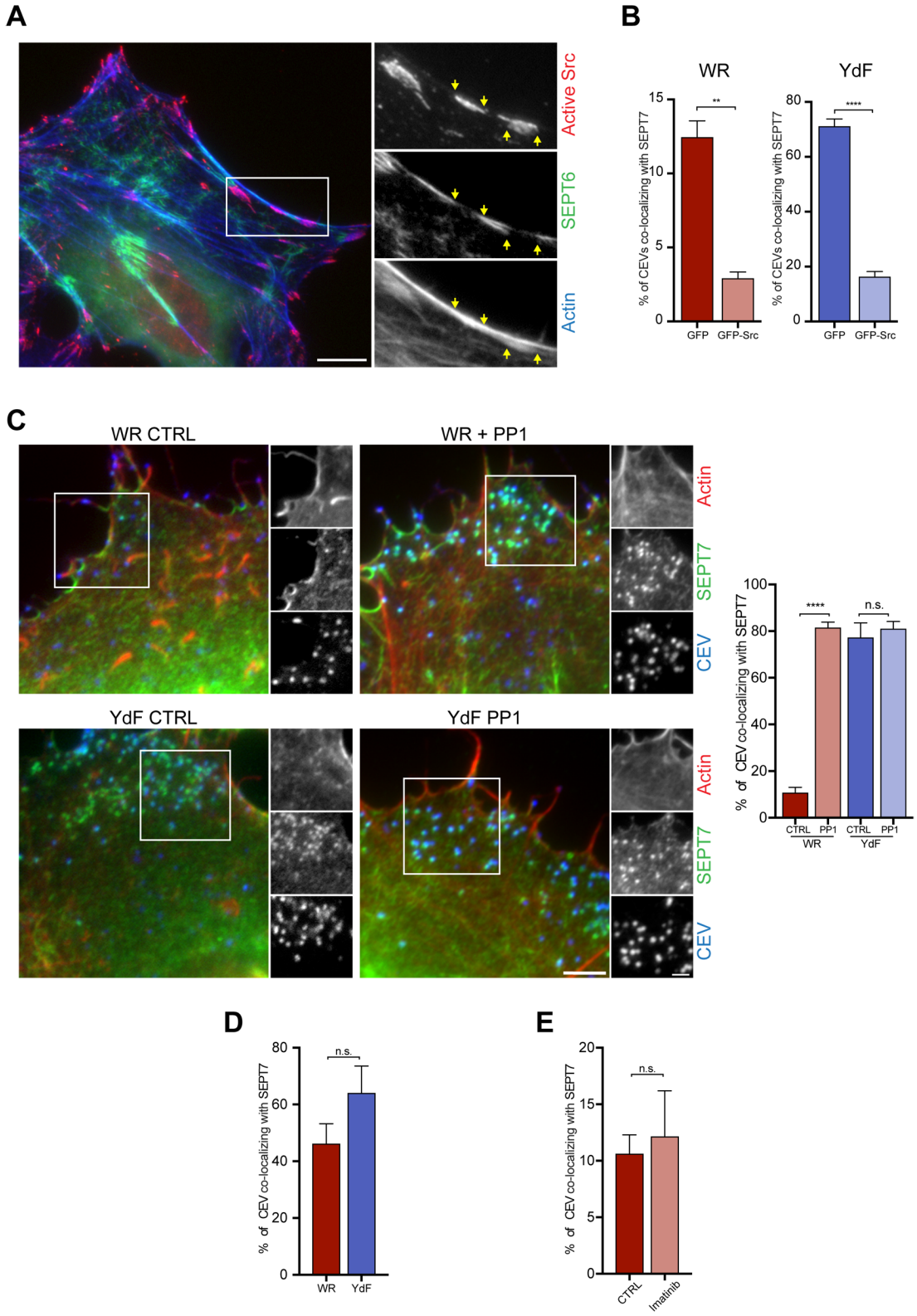

Figure 4.4 Inhibition of Src increases septin recruitment

A Representative immunofluorescence images of an uninfected HeLa cell showing SEPT7 in green, actin stained with phalloidin in blue and active Src in red. Yellow arrows highlight the spatial exclusion of Src and septin along an actin bundle. **B** The

graph shows the % of WR and YdF CEV co-localizing with SEPT7 in cells overexpressing GFP or GFP-Src. **C** Representative immunofluorescence images of HeLa cells infected for eight hours with WR or YdF in the absence or presence of PP1 showing SEPT7 in green, CEV in blue and actin stained with phalloidin in red. Quantification of the % of CEV co-localizing with SEPT7. **D** The graph shows the % of WR and YdF CEV co-localizing with SEPT7 in SYF cells. **E** The graph shows the % of WR CEV co-localizing with SEPT7 in cells in the absence or presence of Imatinib. Scale bar = 5 μm and in inset 1 μm. Error bars represent SEM from three independent experiments in which over 900 virions from 30 cells were analysed; n.s. p-value > 0.05; ** p-value < 0.01; **** p-value < 0.0001.

Next, I used Src, Yes, and Fyn knockout (SYF) cells to investigate whether other kinase could take over the role of Src in displacing septins from the virus. These mouse fibroblasts lacking Src, Yes, and Fyn showed an intermediate result. For WR, 46.25 ± 12.1% of CEVs co-localized with septins whereas in YdF infected cells 64 ± 16.4% of CEVs were septin positive (Figure 4.4D). Without Src, Yes and Fyn there was no longer a significant difference in septin co-localization between WR and YdF virus, although WR could still induce some actin tails. It has been previously reported that besides Src, actin tails can also be initiated by Arg, Yes and Fyn, but Arg is notably less efficient in phosphorylating A36 in vitro and in SYF cells the number of cells forming actin tails is reduced by roughly 50% (Newsome et al., 2006, Reeves et al., 2005). Hence it is probably Arg, which can partially compensate for the lack of the other kinases in terms of actin tail formation but less so in respect to replacing septins.

Moreover, when I inhibit Abl and Arg using the drug Imatinib / Gleevec (Wisniewski et al., 2002, Dorsey et al., 2000, Kraker et al., 2000) I see no significant change in septin recruitment to CEV in WR infected cells (10.6 ± 1.7% in control cells; 12.1 ± 4.0% in Imatinib treated cells, see Figure 4.4E), indicating that Src is sufficient to trigger the displacement of septins from vaccinia.

In summary, these experiments suggest that Src, Yes and Fyn kinases are required for displacing septins from the virus. This leads to the question of how these kinases modulate septin recruitment or displacement.

One possibility would be that septins are a Src substrate and that upon phosphorylation septins are lost from the virus. In yeast, it has already been shown that septin assembly and stability is regulated by phosphorylation, mediated by kinases such as GIN4 and Cla4 (Cvrcková et al., 1995, Longtine et al., 1998, Versele

and Thorner, 2004, Dobbelaere et al., 2003 Garcia, Garcia et al.). While in mammalians phosphorylation of SEPT4 or SEPT12 regulates the stability of septins at the sperm annulus (Koch et al., 2015, Shen et al., 2017).

In order to test this hypothesis, I set out to see if I could detect Src-dependent phosphorylation of septins by performing pull-down experiments. Since Src can only phosphorylate tyrosines (Collett et al., 1980, Songyang and Cantley, 1995), I used phospho-tyrosine (pY) antibodies to detect any potential tyrosine phosphorylation. Initially, I tested the phospho-tyrosine antibodies available in our lab. Vaccinia infection is known to increase phosphorylation of several host proteins, including the EGF-receptor (200kD; marked with *) and cortactin (80/85kDa; marked with ←), as well as A36 (40kDa; marked with <) as seen in Figure 4.5A (Frischknecht et al., 1999b). Using cell lysates from WR and non-infected cells, I was able to observe these increases in phosphorylation (Figure 4.5A). When comparing control and PP1 treated cells, it became clear that the PY99 and 4G10 antibodies detected differences in phosphorylation patterns, whereas the PY20 antibody was not sensitive to Src inhibition (Figure 4.5B). The band marked with < in Figure 4.4 is only present in WR infected control cells but absent in PP1 treated or YdF infected cell, indicating that the band corresponds to phosphorylated A36.

To detect potential phosphorylated septins, I performed a GFP trap. In this assay, GFP-tagged proteins are coupled to beads allowing precipitation of the labelled protein and its binding partners. GFP-SEPT6 cells were treated with 12.5μM PP1 for two hours before lysis and subsequent pull-down of septins. Together with GFP-SEPT6 I was also able to precipitate SEPT7 and SEPT2 but not the loading control Grb2, indicating that the buffer conditions conserved protein-protein interactions but washing was stringent enough to remove non-binding partners. Staining with the 4G10 antibody revealed a very faint band corresponding to the molecular weight of SEPT2 marked with ← in Figure 4.5C). However, PP1 treatment did not noticeably change the levels of phosphorylated protein the seize of SEPT2. This would suggest that SEPT2 might be phosphorylated at a tyrosine but insensitivity to PP2 would exclude Src and Abl family kinases as the responsible enzyme.

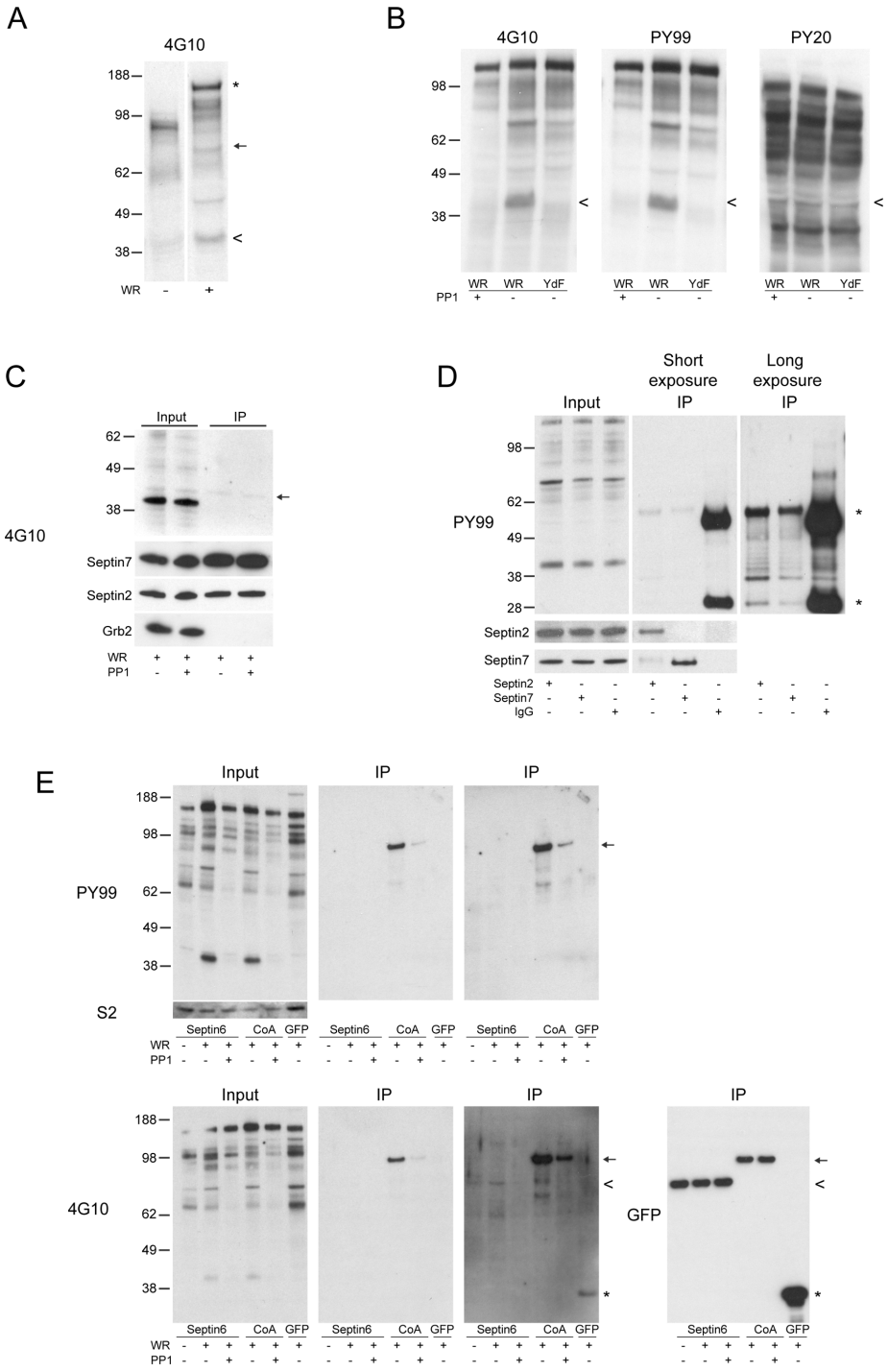

Figure 4.5 Phosphorylation of septins is not clearly detectable by Western blot analysis

A,B Whole-cell extract of infected and uninfected HeLa cells treated with the Src inhibitor PP1 where indicated, using the indicated phospho-tyrosine antibodies. **C** GFP-trap pull-down lysates of infected GFP-SEPT6 HeLa cells treated with PP1 where indicated. Arrow indicates a faint paint using the phospho-antibody 4G10. **D** Lysates from immunoprecipitation using the indicated antibodies showed no phospho-tyrosine signal. **E** GFP-trap pull-down lysates using the indicated cell lines infected with WR and treated with PP1 where indicated.

To further analyse the potential phosphorylation status of septins, I performed an immunoprecipitation that aimed to disrupt protein-protein interactions and inactivate phosphatases in order to preserve phosphorylation changes. To accomplish this, HeLa cells were infected with WR for 16 hours before being lysed directly into 2x sample buffer and briefly boiled before being resuspended in 1 mL lysis buffer followed by incubation with primary antibodies against SEPT2, SEPT7 and control IgG and precipitated with protein A beads. Blotting with antibodies against SEPT2 and SEPT7 confirmed that the pulldown was specific for each individual septin. Phospho-tyrosine antibodies did not detect any phosphorylation at the corresponding molecular weight for SEPT2 (41kDa) or SEPT7 (50kDa) using either short or longer exposures (Figure 4.5D). There were two prominent bands correlating to the light and heavy chain of IgG (marked with * Figure 4.5D).

These data suggest that neither SEPT2 nor SEPT7 had detectable tyrosine phosphorylation using the described antibodies and pull-down methods. The faint band observed in the GFP-pulldown experiments (Figure 4.5C) is likely to be unspecific. To verify this hypothesis, I repeated the GFP-trap pull-down experiments using WR infected cells expressing either GFP-SEPT6, GFP-cortactin or GFP alone. GFP-Cortactin was used as a positive control, because it has been previously described as a target of Src during infection (Frischknecht et al., 1999b). Using an antibody against GFP confirmed that the respective proteins were pulled down and levels did not change upon infection or PP1 treatment. However, the amount of precipitated GFP was significantly larger than precipitated GFP-SEPT6 or GFP-Cortactin. The PY99 antibody only detected phosphorylation of GFP-cortactin, which was strongly reduced upon PP1 treatment. Using a 4G10 antibody with short exposure times, I could also only see PP1 sensitive phosphorylation of GFP-cortactin (marked with ← in Figure 4.5E). Longer exposures revealed an additional band that corresponded to GFP alone (see < in Figure 4.5E). This suggested that the phospho-tyrosine antibody can start to non-specifically recognized proteins if they are present at very high concentrations. Alternatively, it might be possible that GFP gets tyrosine phosphorylated during vaccinia infection.

There is also a faint band at the size of GFP-SEPT6 in WR infected cells. Interestingly this band is even more faint in uninfected and almost absent in PP1 treated cells. Overall, I could find no clear evidence that septin is phosphorylated by

Src/Abl. However, phosphorylation is often a transient event and therefore it can be hard to detect it. In addition, assuming that septins are only phosphorylated by Src once, they are both recruited to the virus, the phosphorylated pool of septins would represent only a fraction of the total amount of septins in the cell. Furthermore, if septins disassemble upon phosphorylation, they might not co-precipitate with one another anymore. Even if septins are not directly phosphorylated by Src, the kinase could still indirectly influence the stability of septins at the virus.

Trying to better understand how septins are regulated at the virus I took another approach. I used fluorescence recovery after photo bleaching (FRAP) to investigate whether the differences in septin recruitment to WR and YdF virus are caused by distinct assembly and disassembly rates. To do so GFP-SEPT6 cells were infected for eight hours and treated with 100 µM CK666 during image acquisition to inhibit actin tail formation. Thereby, events, in which septin turnover cannot occur because the virus is propelled away by actin polymerization, should be prevented. From pervious experiments, I concluded that CK666 itself had no impact on the number of CEV recruiting septins (Figure 4.2A). Individual septin puncta associated with virus particles were bleached and fluorescent recovery by exchange of septins from outside the bleached area was monitored by acquiring images every second for 3min. Analysis was performed as described in the methods, briefly a non-linear function was used to fit the normalized mean fluorescence intensities (Figure 4.6A). From this function, the required time for half maximal recovery, as well as the plateau fluorescence value representing maximal recovery, were determined. Septins associated with WR virus required 24.4 ± 1.4 sec to reach half of the maximum (Figure 4.6B). The recovered fluorescence intensities plateaued at 54.2 ± 1.5% of the maximal fluorescence before bleaching (Figure 4.6C). These values agree with previously observed FRAP experiments performed on SEPT2 in septin filaments and rings induced by Cytochalasin D (Schmidt and Nichols, 2004). In yeast cells, however, the septin ring at the division neck can adopt a fluid state with recovery times of around 150 seconds or change to a frozen state were hardly any exchange is observed (Dobbelaere et al., 2003). Furthermore, FRAP experiments performed on septin rings entrapping *Shigella* showed no exchange of septins (Mostowy, personal communication).

Comparing the dynamics of septins associated with WR or YdF virus revealed no significant differences. Fluorescence of GFP-SEPT6 recruited to YdF viruses recovered up to 55.0 ± 1.4% after bleaching and the half maximal recovery was accomplished after 29.7 ± 1.8 sec (Figure 4.6A,B). Taken together these experiments show that septins recruited to the virus turn over and the speed of septin exchange is comparable between septins co-localizing with WR and YdF viruses.

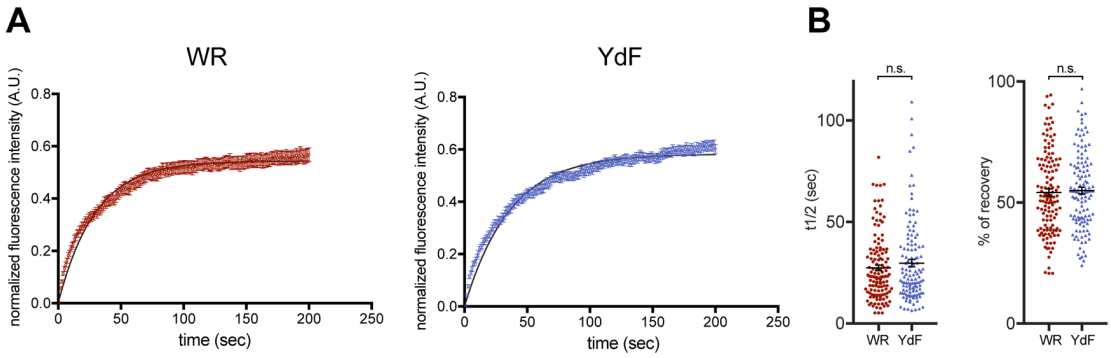

Figure 4.6 Septins turn over with the same rate on WR and YdF viruses

Graph showing the quantification of GFP-SEPT6 fluorescence after photo-bleaching. The average recovery curves are shown for WR and YdF infected cells. Intensity values were normalized to the pre-bleach intensity. **B**
Values for half-life of recovery and percentage recovery. Over 120 events measured from three independent experiments; n.s. indicates a p-value of > 0.05.

Next, I returned to the question of how Src/Abl kinases might regulate septin recruitment and what causes so many YdF virus particles to accumulate septins. One relevant substrate of Src in the context of vaccinia infection is the viral protein A36 (Frischknecht et al., 1999b). I therefore infected cells with a recombinant virus lacking A36. If the phosphorylation of A36 is the trigger to reduce septin recruitment to the virus, I should see high levels of CEV with septin when A36 is absent. Alternatively, if septins are recruited to unphosphorylated A36, I will see no co-localization of CEV and septins. As mentioned before, A36 is not only needed for actin tail formation but is also essential for microtubule-based transport, since it binds to kinesin (Herrero-Martinez et al., 2005, Rietdorf et al., 2001, Ward and Moss, 2001a, Parkinson and Smith, 1994, Morgan et al., 2010, Dodding, 2011, Dodding et al., 2009, Ward and Moss, 2004). Consequently, the egress of the ΔA36R virus is very inefficient as hardly any virions reach the plasma membrane. To compensate for the delayed movement to the cell periphery I fixed cells after 10 hours when sufficient virus particles had reached the plasma membrane. However, most virions

were found above or below the virus factory / cell centre and hardly any reached the distant cell periphery. Analysing those ΔA36R particles I found that 15.6 ± 3.2% of CEV recruit septins, very similar to WR infected cells (Figure 4.7A). This would indicate that septins are not recruited by A36 and in addition the phosphorylation of A36 is not responsible for the displacement of the septins. Furthermore, it implies that there is a different substrate of Src that triggers the loss of septins. Therefore, PP1 treatment of cells infected with ΔA36R should result in high levels of CEV recruiting SEPT7. I tested this hypothesis and found no dramatic increase in CEV co-localising with septins (25.2 ± 2.7%). Data from five independent experiments revealed no significant difference between control and PP1 treated cells infected with ΔA36R (Figure 4.7A). Taken together these results were rather puzzling. On one hand A36 neither seem to be involved in septin recruitment nor in its displacement, since the absence of A36 results in wild-type levels of septins at the CEV. On the other hand, without A36 PP1 treatment is no longer efficiently increasing septin recruitment to an extent that would be comparable to YdF infected cells or WR infected PP1 treated cells. A possible explanation would be that A36 is involved in septin recruitment and displacement. By removing A36, assembly and disassembly of septins at the virus are impaired to the same extent, resulting in wild-type levels of CEV recruiting septins. Furthermore, it could be that high levels of septin recruitment preferentially occur when the virus accumulates in the cell periphery.

One way to overcome the trafficking defect of the ΔA36 virus is to substitute the cytoplasmic part of A36 containing the kinesin binding motifs with the one found in calsyntenin-1 (CSTN). A hybrid protein was constructed containing the transmembrane domain of A36 attached to the amino acids 879-971 from CSTN (Dodding et al., 2011). A virus expressing this protein in place of A36 is able to reach the cell periphery using microtubule-based transport and fuse with the plasma membrane but is unable to induce actin tails (Dodding et al., 2011). When quantifying the septin levels on the CEVs of the ΔA36R CSTN virus they were high (82.0 ± 4.2%) compared to those at the YdF virus (Figure 4.7B). This experiment suggests that prevention of phosphorylation of A36 after the virus reaches the cell periphery permits septin accumulation underneath the virus.

Previous studies found that the Yaba-like disease virus (YLDV) contains a divergent functional orthologue of A36, called YL126. Although their amino acid similarity is less than 15% YL126 was shown to restore both microtubule transport and actin tail

formation (Dodding and Way, 2009). Instead of two tyrosines in A36, YL126 has six tyrosines, which are phosphorylated by Src, recruit Nck and N-WASP and thereby activate the Arp2/3 complex. Mutating all of them abolishes virus induced actin polymerization (Dodding and Way, 2009).

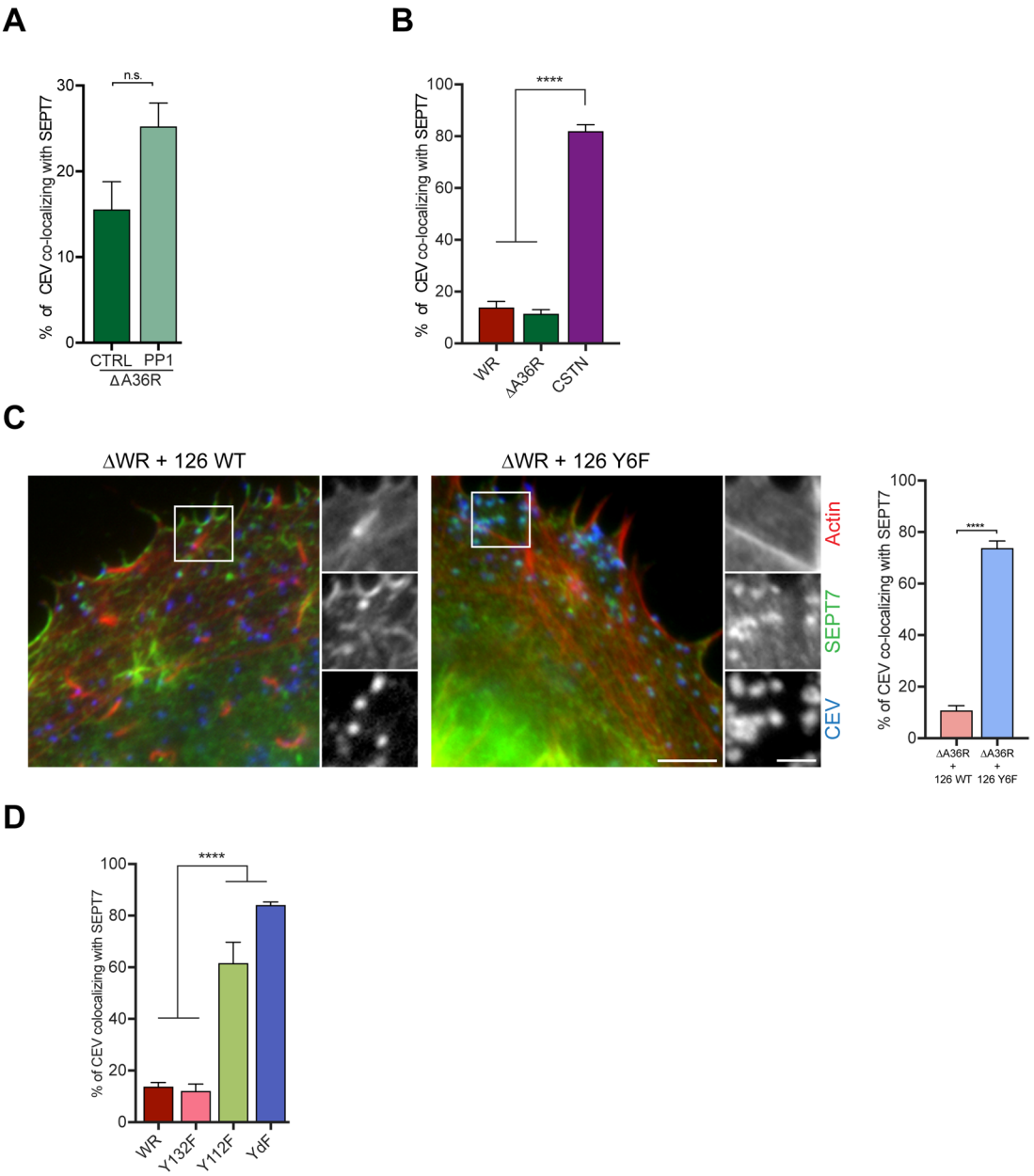

Figure 4.7 Phosphorylation of Y112 triggers the loss of septins from CEV

A Quantification of the % of CEV co-localizing with SEPT7 in HeLa cells infected with ΔA36 virus in the absence or presence of PP1. **B** The graph shows the % of CEV co-localizing with SEPT7 in cells infected for eight hours with the indicated viruses. **C** Representative immunofluorescence images of HeLa cells infected with the indicated virus. The graph shows the % of CEV co-localizing with SEPT7 in cells

infected for eight hours with the indicated virus. The graph shows the % of WR and YdF CEV co-localizing with SEPT7 in SYF cells. **D** Quantification of the % of CEV co-localizing with SEPT7 in HeLa cells infected for eight hours with the indicated virus. Scale bar = 5µm and in inset 2 µm. Error bars represent SEM from three independent experiments in which over 900 virions from 30 cells were analysed. A p-value of > 0.05 and < 0.0001 is indicated by n.s. and **** respectively.

I therefore decided to use those two viruses to further investigate the role of A36 and its phosphorylation by Src.
ΔA36R expressing YL126 wild type (WT) was able to induce actin tails and 10.8 ± 1.8% of the CEV co-localized with SEPT7, whereas in the YL126 Y6F situation no actin tails were formed but 73.8 ± 2.7% of the CEV recruited septin (Figure 4.7C).
Overall, these experiments show that A36 is not needed to recruit septins but in the absence of phosphorylated A36 or YL126 septins can accumulate at the CEV.

This raised the question of whether the phosphorylation of both tyrosines is needed or whether one is sufficient. To investigate this matter, I took advantage of the existing single mutant viruses A36 Y112F and Y132F (Scaplehorn et al., 2002). It has been shown that Nck is recruited to phospho-Y112, while Grb2 only binds to phospho-Y132 (Donnelly et al., 2013, Frischknecht et al., 1999a, Moreau et al., 2000, Scaplehorn et al., 2002, Snapper et al., 2001, Zettl and Way, 2002). The Y112F virus, deficient in Nck recruitment and actin tail formation, recruited septins to 61.6 ± 8.7% of the CEV. In contrast, in cells infected with the Y132F virus, deficient in Grb2 recruitment, only 12.0 ± 2.7% of the CEV recruited SEPT7 (Figure 4.7D). This indicates that phosphorylation of Y112 alone has the potential to strongly increase septin recruitment, although not to the same extend as the YdF virus. In contrast, mutation of Y132 alone does not affect the number of CEV co-localising with septins and might only act in concert with mutated Y112.

4.2.3 Nck recruitment antagonises septin localisation to CEV

Finding that phosphorylation of Y112 but not Y132 in A36 impacts on septin recruitment raised the possibility that binding of Nck to phospho-Y112 might displace septins from the virus. This would agree with the observation that Nck is recruited to WT YL126, where only few CEV co-localize with SEPT7, but Nck is absent in Y6F YL126 and CSTN viruses, which have high levels of septin recruitment. To

investigate this hypothesis, I took advantage of Nck double knock-out MEFs (Bladt et al., 2003). The vaccinia replication cycle is a bit delayed in both the parental and the knockout MEFs compared to HeLa cells, so I examined the ability of CEV to recruit septin at 20 hrs post infection. In Nck parental and knockout cells infected with YdF virus the majority of CEV co-localised with SEPT7 (Nck +/+ 61.1 ± 1.7% and Nck -/- 70.1 ± 8.2%, see Figure 4.8A). In WR infected cells the percentage of CEVs co-localizing with septins dramatically increased from 15.5 ± 1.8% to 62.0 ± 2.5% in the absence of Nck. This strongly suggests that Nck is required to displace septins from the virus. This could either happen directly, for example through steric hindrance between Nck and septins. Alternatively, Nck could regulate septin levels indirectly by recruiting an additional protein, which in turn displaces septins.

Nck is an SH2/SH3 domain containing adaptor protein that directly binds to phospho-Y112 in A36 via its SH2 domain (Scaplehorn et al., 2002). Subsequently Nck recruits and interacts with WIP:N-WASP via its second and third SH3 domain leading to local activation of the Arp2/3 complex (Donnelly et al., 2013, Frischknecht et al., 1999a, Moreau et al., 2000, Newsome et al., 2004, Scaplehorn et al., 2002, Snapper et al., 2001, Zettl and Way, 2002). Mutating the SH2 domain abolishes the recruitment of Nck to vaccinia and prevents actin tail formation. Conversely, mutating the SH3 domains allows recruitment of Nck to the virus but prevents any additional interactions with downstream binding partners (Donnelly et al., 2013, Scaplehorn et al., 2002). In order to test whether Nck induces the loss of septins directly or indirectly, I infected Nck knock-out MEFs that stably expressing different GFP-tagged Nck mutants, see Figure 4.8B (Donnelly et al., 2013).

The expression of GFP-Nck in Nck -/- MEFs infected with WR rescued actin tail formation and led to low levels of septin recruitment (22.4 ± 0.7%). In contrast, when each of the three SH3 domains was disrupted by mutating the essential tryptophan to a lysine (Donnelly et al., 2013, Tanaka et al., 1995), the number of CEV co-localizing with septin was increased (73.5 ± 0.6%). This demonstrates that a binding partner downstream of Nck, but not Nck directly, influences septin levels on vaccinia. To gain further insight, single SH3 mutants of Nck were also analysed. Only the third SH3 domain of Nck was required to restrict septin recruitment to CEVs, while mutating the first or second SH3 domain had no effect on septin levels (Figure 4.8B).

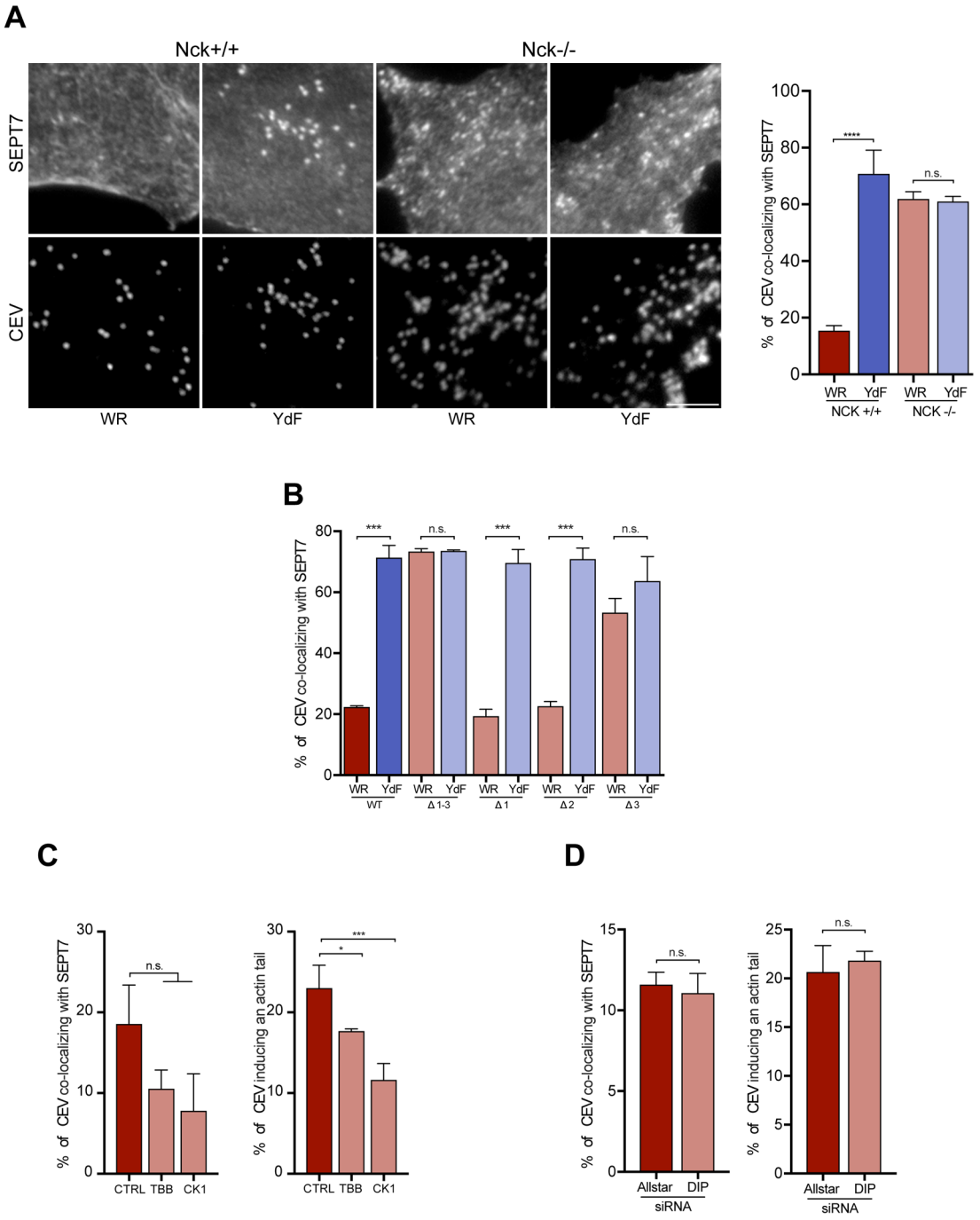

Figure 4.8 The third SH3 domain of Nck is required to displace septins from CEV

A Representative immunofluorescence images showing the recruitment of SEPT7 to CEV in Nck parental and knockout cells infected with WR or YdF virus for 20 hours. The graph shows the % of CEV co-localizing with SEPT7. **B** Quantification of CEV co-localizing with SEPT7 in Nck knockout cells stably expressing the indicated Nck construct. **C** The graph shows the % of CEV co-localizing with SEPT7 or inducing an actin tail in the absence or presence of TBB or D4476 (CK1). **D** The graph shows the % of CEV co-localizing with SEPT7 or inducing an actin tail in control cells or DIP-depleted cells. Error bars represent SEM from three independent

experiments in which over 900 virions from 30 cells were analysed. n.s. p-value > 0.05; * p-value < 0.05; *** p-value < 0.001; **** p-value < 0.0001.

4.2.4 Dynamin II displaces septins from CEV

The data so far indicate that Nck may influence septins indirectly through an interactor of its third SH3 domain. SH3 domains bind proline-rich regions containing a core consensus of PxxP (Zarrinpar et al., 2003). For Nck, over thirty different SH3 binding partners have been reported (Buday et al., 2002). After excluding proteins that specifically bind to the first or second SH3 domain I had a candidate list of 13 proteins. Five of these proteins, casein kinase 1, dynamin, PINCH, Sos and WASP, were reported to only bind the third SH3 domain of Nck (Hu et al., 1995, Lussier and Larose, 1997, Rivero-Lezcano et al., 1995, Tu et al., 1998, Wunderlich et al., 1999). Additionally, unpublished data from the Innocenti lab suggested DIP/WISH/SPIN90 (Lim et al., 2001) as potential binding partner of Nck.

The serine/threonine casein kinase 1 has been reported to regulate septin organization in yeast (Robinson et al., 1999). In humans, casein kinase 2 phosphorylates SEPT2 and in the context of vaccinia infection, casein kinase 2 is proposed to promote virus induced actin tail formation (Alvarez and Agaisse, 2012, Huang et al., 2006). I took advantage of the chemical inhibitors D4476 and TBB, which specifically target casein kinase 1 and 2 respectively (Sarno et al., 2001, Rena et al., 2004). Treating infected cells with either drug at 7 hpi for 1 h to block the activity of casein kinase I and II did not significantly change the number of CEVs co-localizing with septins (Figure 4.8C). In fact, there was a slight reduction in septin recruitment to CEV (CTRL 18.6 ± 4.8% CK1 7.8 ± 4.6% and CK2 10.54 ± 2.3%). As previously reported for TBB (Alvarez and Agaisse, 2012), I observed a mild inhibitory effect on actin tail formation for both casein kinase 1 and 2 (CTRL 25.3 ± 1.5% CK1 13.6 ± 0.7% and CK2 10.54 ± 2.3%). This suggests that the drugs are effective but neither casein kinase 1 nor 2 appear to affect septin dynamics at the virus.

In parallel, I investigated the potential involvement of DIP during septin recruitment by vaccinia. Using a pool of four different siRNA oligos against DIP 72 h before infecting with WR did not induce a significant change in septin levels at CEV (Allstar 11.6 ± 0.8% versus 11.1 ± 1.2% siRNA against DIP). Equally, the number of CEV

inducing actin tails was also unchanged (Allstar 20.7 ± 2.7% versus 21.8 ± 0.6% DIP KD; see Figure 4.8D). Therefore, I also decided to exclude DIP as responsible factor in septin displacement.

Next, I examined dynamin, which not only selectively binds the third SH3 domain of Nck (Wunderlich et al., 1999) but was also reported to be recruited to EPEC, where it promotes actin pedestal formation (Unsworth et al., 2007) and can directly bind septins in neurons (Maimaitiyiming et al., 2013). Moreover, in a collaboration with the lab of Serge Mostowy we discovered a link between the dynamin-related protein Drp-1 and septin cages around *Shigella* (Sirianni et al., 2016). In this study, I demonstrated an interaction between Drp-1 and septins by performing a GFP-trap pulldown on the GFP-SEPT6 cell line (Figure 4.8 A). In the case of *Shigella* infection, Drp-1 is recruited to the septin cage where it facilitates mitochondria fission. Fragmentation of mitochondria in turn helps the bacteria to evade the septin cage.

Previously, it was reported that dynamin II, when overexpressed, is not recruited to vaccinia viruses that induce actin tails (Scaplehorn et al., 2002). In addition, overexpression of dominant negative mutants of dynamin had no impact on actin-based motility of vaccinia (Unsworth et al., 2007).
To investigate the role of endogenous dynamin, I used a Dyn II antibody kindly provided by Mark McNiven (Mayo Clinic, Rochester, USA) and found that a small proportion (12.53 ± 0.5%) of the CEVs co-localized with dynamin II (Figure 4.8 B). Interestingly, in the case of YdF infected cells where no Nck is recruited, the number of CEVs co-localizing with dynamin is reduced (3.1 ± 0.2%).

To test if Nck is responsible for recruiting dynamin, I infected the Nck parental and KO cells and stained for dynamin II. Parental Nck +/+ MEFs resembled HeLa cells, with WR co-localizing in 7.5 ± 2.5% with dynamin whereas only 1.8 ± 0.4% of YdF CEVs recruited dynamin II. In the absence of Nck, WR and YdF recruited similar amounts of dynamin (2.0 ± 0.4% WR and 1.9 ± 0.4% YdF) (Figure 4.8 C). These results show a previously missed recruitment of dynamin to vaccinia CEV. Reduced levels of dynamin at YdF could indicate that in the absence of Nck, less dynamin is recruited.

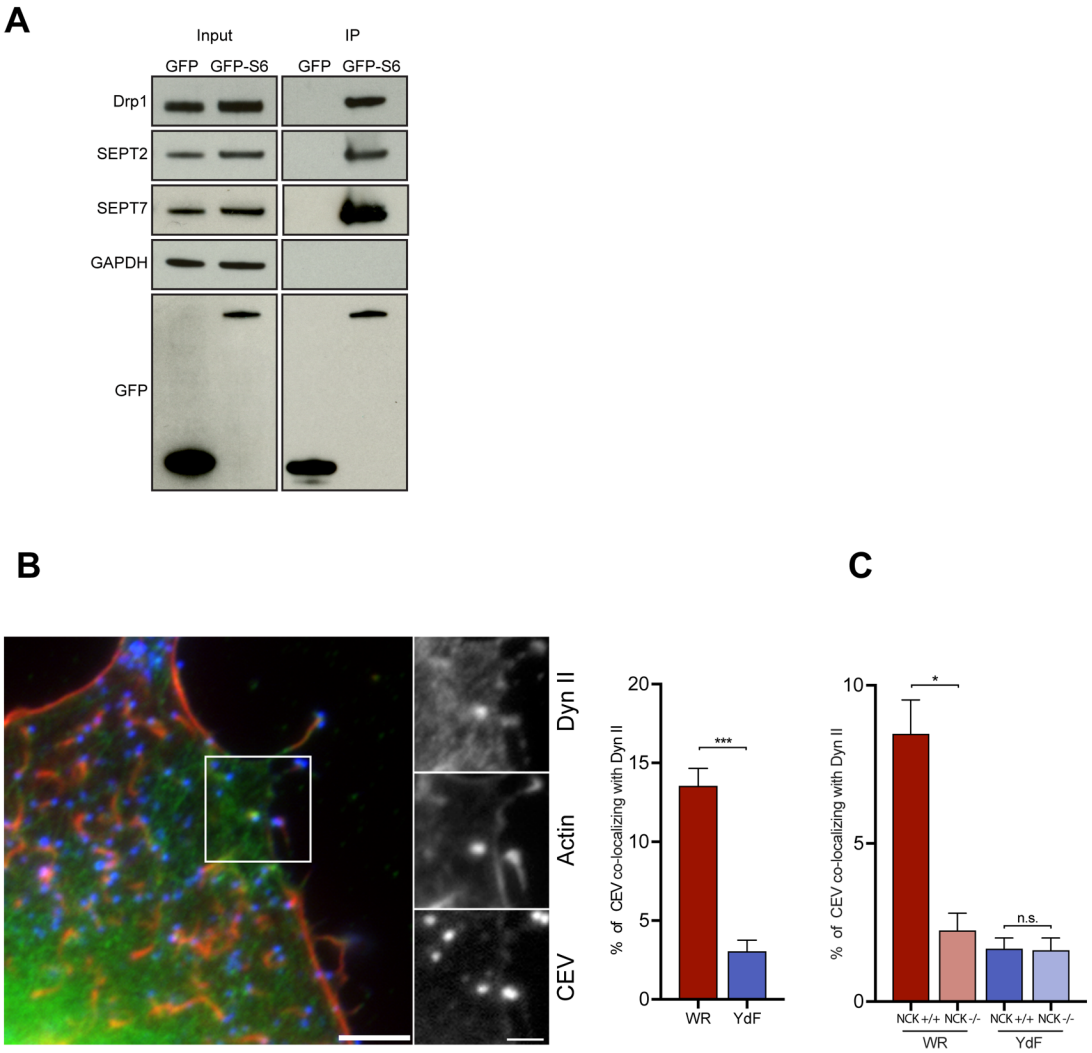

Figure 4.9 Nck facilitates the recruitment of dynamin II to CEV

A Western blot analysis showing that Drp-1 co-precipitates together with GFP-SEPT6 and other septins during a GFP-trap pull-down experiment. GAPDH is shown as a loading control. **B** Representative immunofluorescence images of HeLa cells infected with WR for eight hours. Dyn II is shown in green, actin stained with phalloidin in red and CEV in blue. The graph shows the % of WR and YdF CEV co-localizing with Dyn II. Scale bar = 5µm and in insert 1µm. **C** Quantification of CEV co-localizing with Dyn II in Nck parental and knockout cells infected with WR or YdF virus. Error bars represent SEM from three independent experiments in which over 900 virions from 30 cells were analysed. n.s. p-value > 0.05; * p-value < 0.05; *** p-value < 0.001.

In order to investigate dynamin recruitment by live-cell imaging, I generated HeLa cells stably expressing iRFP-Dyn II as well as GFP-SEPT6. Infecting these cells with the WR RFP-A3L virus I found that dynamin is transiently recruited to the virus (Figure 4.9A). Strikingly, whenever dynamin was recruited to a virus co-localizing

with GFP-SEPT6 the latter was lost. The stills from a representative movie in Figure 4.9A show how dynamin transiently localises as septins are lost from the virus particle. Live-cell imaging was also repeated using a cell line stably expressing GFP-SEPT6, iRFP-LifeAct and mCherry-dynamin. I found that the brief recruitment of dynamin also coincided with a transient burst of actin polymerization on the virus (Figure 4.9 B). To precisely determine the chronology of events on the virus I performed automated image analysis. Briefly, a small area around the virus (roughly 2.5μm^2) was cropped and the three channels representing the three different proteins were saved separately. I wrote a MATLAB script that measured and normalized the mean fluorescence for each time point. When plotting the mean intensities over time there was always a very prominent, transient peak in dynamin. The maximum peak for dynamin was therefore set as a reference time point and all the movies were aligned relative to it. Then the mean and SD of all the movies was determined and plotted (Figure 4.9 C). This procedure was performed on movies showing dynamin, septin and actin and on another set with dynamin, septin and clathrin (Figure 4.9 D,E). This quantitative analysis confirmed that the intensity of dynamin negatively correlates with septin intensity. As apparent in the movie stills, together with the recruitment of dynamin there was also a transient burst of actin. The peak of actin was delayed by approximately five seconds in relation to dynamin. In most cases, the initial actin burst is followed by the formation of a typical actin tail. However, as the intensities are monitored locally, actin intensities decrease while the virus is propelled away by the tail.

Septin levels remain relatively constant before dynamin recruitment, whereas clathrin intensities continue to increase until dynamin peaks. In addition, loss of clathrin occurs approximately ten seconds after loss of septin, although the rates of disassembly, inferred from the steepness of the declining intensities, seem very similar. Taken together, live-cell imaging indicates that dynamin displaces septin and clathrin from the virus.

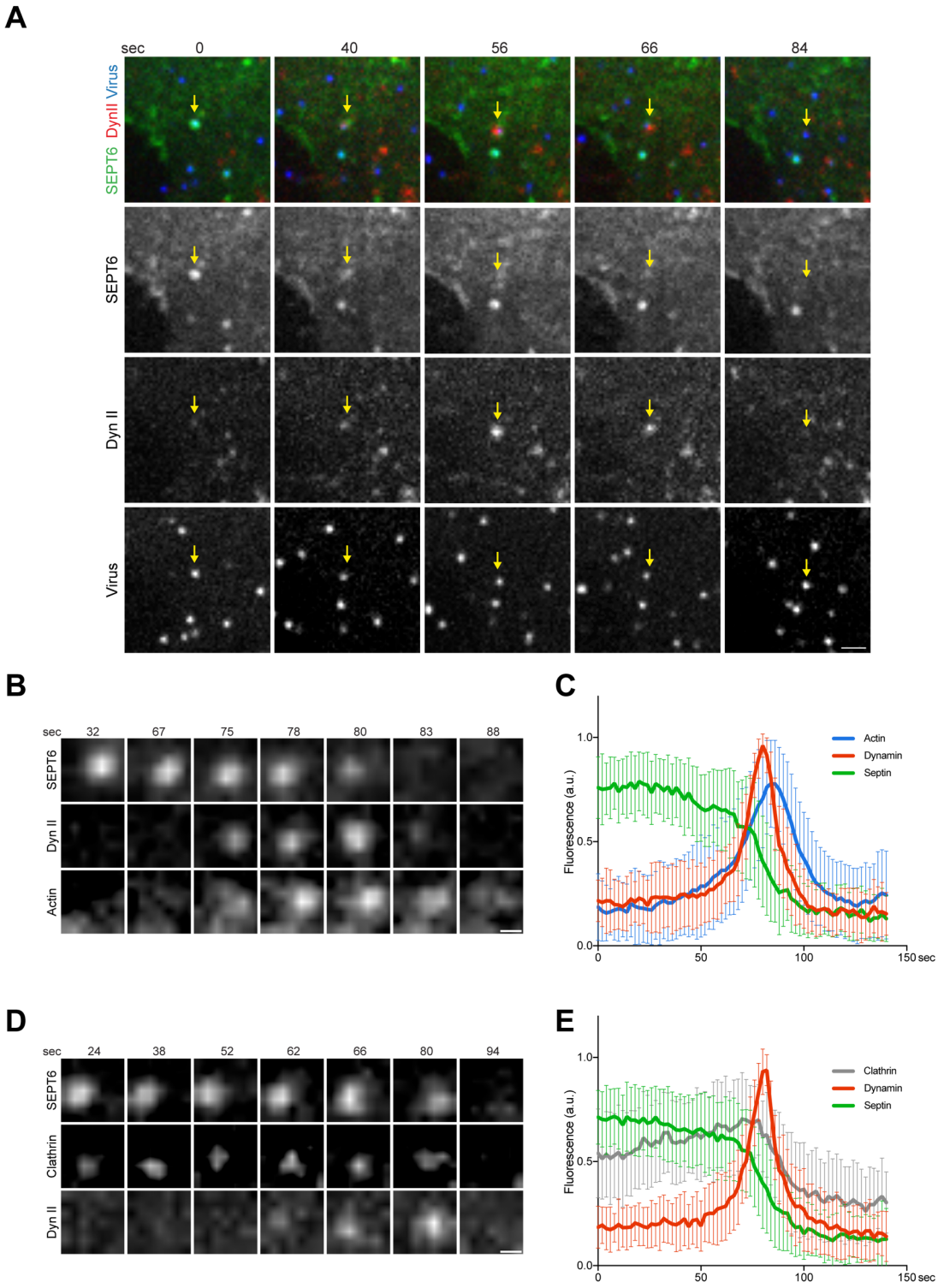

Figure 4.10 The transient recruitment of dynamin marks the loss of septins from the virus

A Movie stills of the association of GFP-SEPT6 and iRFP-Dyn II with RFP-A3 WR in a HeLa cell after eight hours of infection. **B** Movie stills of the association of GFP-SEPT6, mCherry-Dyn II and LifeAct-iRFP (actin) with WR. **C** The graph shows the mean normalized fluorescence intensity of each protein on the virus over time. Loss

of septin coincides with the recruitment of dynamin and actin polymerization prior to virus movement. **D** Images showing the presence of GFP-SEPT6, mCherry-clathrin light chain (clathrin) and iRFP-Dyn II on CEV in WR infected HeLa cells over time. **E** The graph shows the mean normalized fluorescence intensity of each protein on the virus prior to actin-based motility. Loss of septin and delayed loss of clathrin coincides with the recruitment of dynamin. The error bars represent SD from three independent experiments in which a total of over 70 virus particles were analysed. Scale bars = 2 µm in **A** and 500 nm in **B** and **D**.

To test whether these correlated observations were also functionally linked, I set out to inhibit dynamin function. Dynosore is a chemical compound that inhibits the GTPase activity of dynamin and thereby prevents clathrin-dependent endocytosis (Macia et al., 2006). More recently it has become clear that this drug has severe off-target effects (Park et al., 2013, Preta et al., 2015). Therefore, other drugs have been developed (McCluskey et al., 2013). MiTMAB, for example, inhibits the localization of dynamin to the membrane and thereby efficiently blocks endocytosis without any known off-target effects (Hill et al., 2004, Quan et al., 2007). When infected cells were treated with MiTMAB for half an hour prior to fixation a significant increase in septin recruitment to WR CEVs was observed (42.3 ± 3.3% treated versus 13.3 ± 1.4% control; Figure 4.11A). Suboptimal efficiency of the inhibitor might explain why septin recruitment to CEV was not as high as that seen in YdF cells. In addition to increased septin levels, blocking dynamin led to a decreased proportion of CEV inducing actin tails (MiTMAB 5.8 ± 1.0% versus CTRL 22.9 ± 2.3%; see Figure 4.11A). In summary, these data suggest that dynamin displaces septins from the virus and furthermore directly or indirectly promotes actin tail formation.

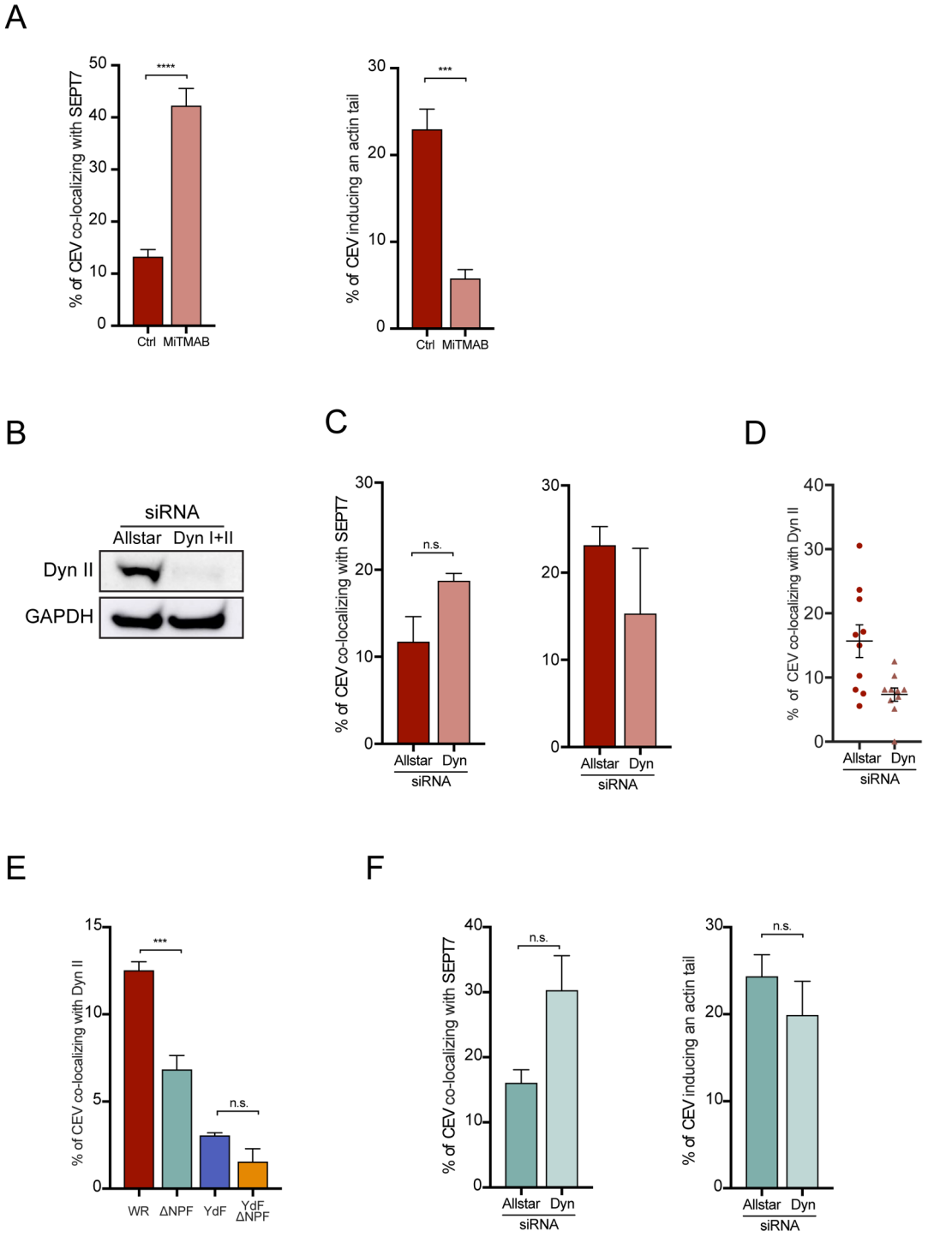

Figure 4.11 Chemical inhibition of dynamin affects septin recruitment and actin tail formation

A Quantification of the % of WR CEV recruiting SEPT7 and inducing actin tails in HeLa cells treated with the dynamin inhibitor MiTMAB. **B** Western blot analysis of dynamin knockdown. GAPDH was included as a loading control. **C** Quantification of the % of WR CEV recruiting SEPT7 and inducing actin tails in HeLa cells treated with dynamin and control siRNA. **D** The graph shows the % of WR CEV co-localizing with Dyn II in control and dynamin-depleted cells. **E** The graph shows the % of CEV

co-localizing with Dyn II in HeLa cells infected with the indicated virus. **F** Quantification of the % of ΔNPF CEV recruiting SEPT7 and inducing actin tails. In graphs A, B, C and F the error bars represent SEM from three independent experiments in which over 900 virus particles were analysed across 30 cells. In graph A, over 1500 virus particles from five independent experiments were analysed across 50 cells, while in graph D only 30 viruses from 10 cells were analysed. n.s. p-value > 0.05; *** p-value < 0.001; **** p-value < 0.0001.

In order to confirm these findings, I performed siRNA-mediated knockdown of dynamin I and II. Dynamin III is mainly found in testis, brain and lungs (Cao et al., 1998, Nakata et al., 1993, Urrutia et al., 1997) and dynamin II is the predominant dynamin found in HeLa cells (Kulak et al., 2014). The level of dynamin II depletion was confirmed by immunoblot analysis on whole cell lysates (Figure 4.11B). Under these conditions, only a mild increase in the number of CEV recruiting septins was observed (Allstar 11.7 ± 2.9% versus Dyn I+II 18.7 ± 0.8%). Actin tails were also indistinguishable from control cells in the absence of dynamin, see Figure 4.11C. Viruses have mastered the art of manipulating host cells and vaccinia can be very efficient in recruiting proteins of interest. I therefore tested if some of the remaining dynamin was still recruited to the virus particles and found that still 7.4 ± 1.0% of the CEV co-localized with dynamin II. This meant that the substantial global reduction of dynamin resulted only in a 50% reduction of dynamin recruitment to the virus (Figure 4.11D). This could explain why there is no dramatic increase in septin recruitment levels on the virus.

Dynamin can also bind intersectin (Okamoto et al., 1999b, Roos and Kelly, 1998, Sengar et al., 1999, Yamabhai et al., 1998), which is recruited to the virus by the NPF motifs in A36 (Humphries et al., 2012, Snetkov et al., 2016). Upon analysing cells infected with ΔNPF and YdF ΔNPF viruses, I observed a reduction in dynamin recruitment to CEV compared with the WR and YdF viruses (ΔNPF 6.8 ± 0.8 and YdF ΔNPF 1.6 ± 0.7) (Figure 4.11E). This suggests that intersectin also helps to recruit and/or stabilize dynamin in addition to Nck.

I therefore tested whether the mild effect of knocking down dynamin would be exaggerated by removing intersectin from the virus and thereby preventing this potential secondary mode of dynamin recruitment. Indeed, depleting dynamin in ΔNPF infected cells increased the levels of CEV with septin from 16.1 ± 2.0% to 30.3 ± 5.3%. Performing the student's t test resulted in a non-significant p-value of 0.06.

Thus, chemical inhibition and knockdown of dynamin by siRNA yielded inconclusive results.

To circumvent the concern of off-target and partial effects of the approaches above, we used dynamin knockout cells (tamoxifen inducible dynamin triple knockout fibroblasts generously gifted by Dr. Pietro De Camilli (Yale school of medicine, USA) (Ferguson et al., 2009, Park et al., 2013). The efficiency of tamoxifen treatment was confirmed by Western blot analysis using whole cell lysates (Figure 4.12A). I infected non-treated control and dynamin knockout cells with WR and YdF viruses. In the presence of dynamin, WR CEV had low levels of septin recruitment (15.5 ± 2.5%) and YdF CEV had high levels (75.1 ± 4.2%) as expected. Strikingly, in the dynamin triple knockout cells, WR had equally high levels of CEVs co-localizing with septins as the YdF virus (WR 57.0 ± 8.1% and YdF 63.4 ± 4%, Figure 4.12B). These data clearly demonstrate that dynamin restricts the extent to which septins are retained at the virus.

As seen with MiTMAB treatment, knockout of dynamin decreased the number of CEV inducing an actin tail (25.9 ± 3.0 % in the parental cells and 9.6 ± 1.1% in the triple KO cells). However, actin tail length was not affected in the absence of dynamin (2.3 ± 0.1µm in Dyn+/+ cells versus 2.4 ± 0.2 µm in Dyn-/- cells, see Figure 4.12C), which is in contrast with the situation in MiTMAB-treated cells. This could suggest that the drug has off-target effects on the actin cytoskeleton. However, MiTMAB only prevents the recruitment of dynamin to the membrane (Hill et al., 2004, Quan et al., 2007), which still allows the cytoplasmic pool of dynamin to influence actin tail formation, whereas in the knockout cells no dynamin is present.

As dynamin displaces septins from the virus, I tested whether reciprocally, septin levels regulate dynamin recruitment to the virus. Knockdown of SEPT7 was performed in WR infected HeLa cells and the amount of CEV recruiting dynamin was quantified. In control cells 14.4 ± 1.6% of CEV co-localize with dynamin II. In contrast, when septin was depleted the number of CEV recruiting dynamin II doubled to 30.0 ± 1.6% (Figure 4.12D). This supports the notion that septins and dynamin may compete for localisation at CEV.

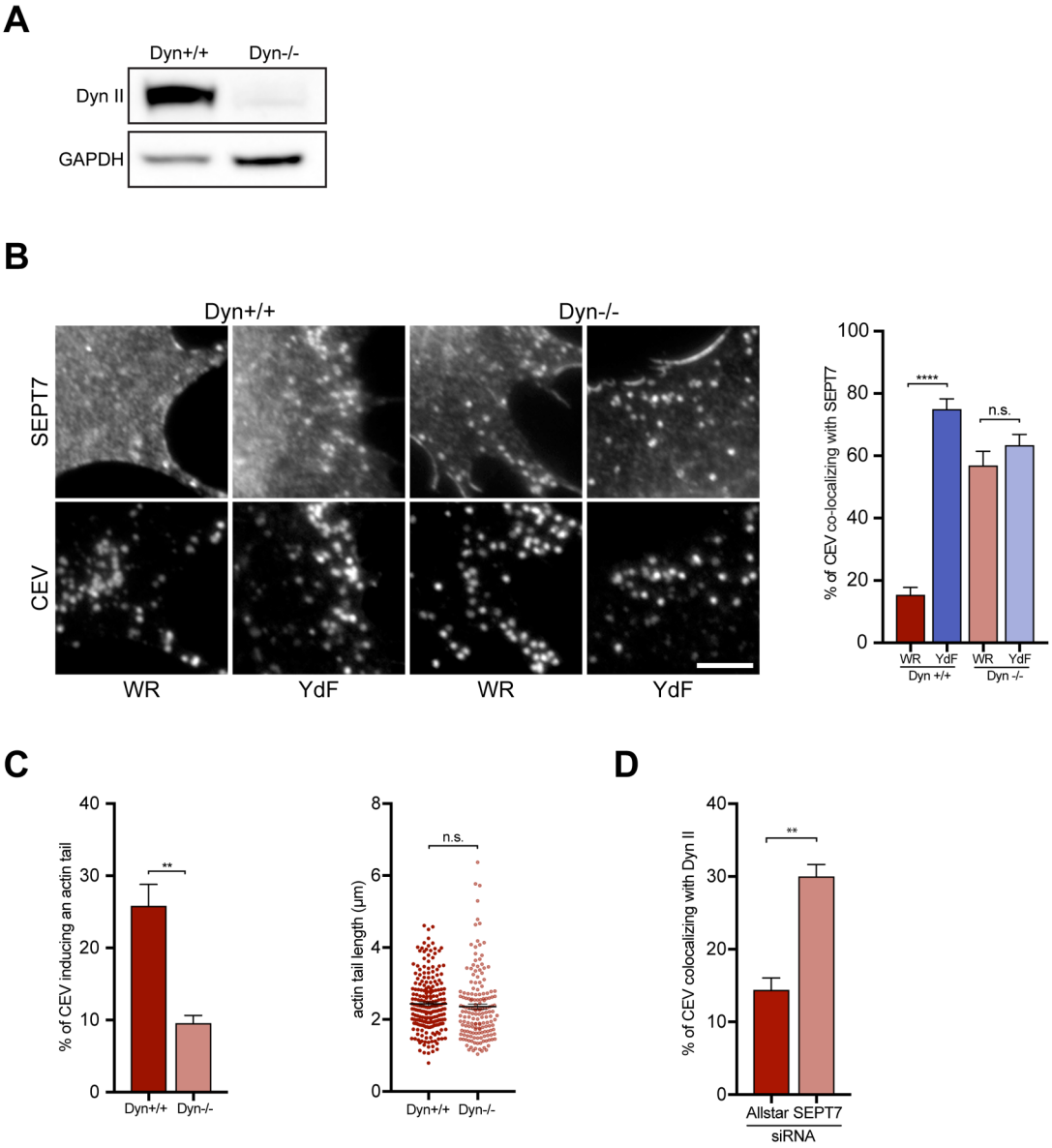

Figure 4.12 Dynamin facilitates septin displacement and actin tail formation

A Western blot analysis confirming the loss of Dyn II upon tamoxifen treatment. GAPDH was included as a loading control. **B** Representative immunofluorescence images showing the recruitment of SEPT7 to CEV in dynamin control and knockout cells infected with WR and YdF for 16 hours. Quantification of the % of CEV co-localizing with SEPT7. **C** The graphs show the percentage of CEV inducing an actin tail as well as the tail length. **D** Quantification of the % of CEV co-localizing Dyn II in control and SEPT7-depleted HeLa cells infected with WR for eight hours. Error bars represent SEM from three independent experiments in which a total of over 900 virus particles or 170 actin tails from 30 cells were analysed. Scale bars = 5 µm; ns. p-value > 0.05; ** p-value < 0.01; **** p-value < 0.0001.

4.2.5 A potential role for formins in displacing septins from vaccinia

Live-cell imaging revealed that dynamin-mediated displacement of septins coincides with a burst of actin polymerisation at the virus (Figure 4.10B). Dynamin is known to induce local N-WASP-dependent actin polymerization during endocytosis (Ayscough, Ayscough et al., 1997, Benesch et al., 2005, da Costa et al., 2003, Innocenti et al., 2005). However, inhibiting formation of branched actin using an Arp2/3 inhibitor did not influence septin recruitment to vaccinia (Figure 4.2). However, dynamin can interact with actin directly and enhance actin polymerization independent of Arp2/3 (Gu et al., 2010). To fully disrupt actin polymerization independent of the nature of nucleating proteins, I used the general actin inhibitor Cytochalasin D (CytoD), a toxin that disrupts and depolymerizes the actin cytoskeleton (Schliwa, 1982, Urbanik and Ware, 1989). Treatment of WR-infected cells with CytoD for 30 min abolished vaccinia-induced actin tails, as expected. In addition, the number of CEV co-localizing with septins was significantly increased (10.9 ± 1.3% CTRL versus 36.0 ± 3.5% CytoD, Figure 4.12 A). Since blocking actin polymerization in general impacts on septin displacement yet inhibition of the Arp2/3 complex did not, another mode of actin nucleation might be involved. To investigate the possible involvement of formins in septin displacement, cells were treated with the formin inhibitor SMIFH2 (Rizvi et al., 2009). Indeed, a significant increase in septin recruitment, similar to MiTMAB and CytoD treatment, was observed (40.6 ± 4.7%, Figure 4.12 A). The previous results observed with Arp2/3 inhibition were reproducible (12.5 ± 2.2%, Figure 4.12 A). While treatment with CK666 and CytoD abolished actin tails, formin inhibition did not significantly change the number of CEVs inducing an actin tail (CTRL 24.1 ± 4.4% versus SMIFH2 15.7 ± 1.9%, Figure 4.12 B). This indicates that while actin tail formation depends on the Arp2/3 complex, the displacement of septins relies at least partially on formin-driven actin polymerization.

To see whether formin-dependent actin polymerization was acting in the same pathway or in parallel with dynamin recruitment, cells were treated with both inhibitors (MiTMAB and SMIFH2) simultaneously. There was no additive effect seen. The double treatment resulted in similar levels of CEV co-localising with SEPT7 as the single treatments (CTRL 13.2 ± 0.5% MiTMAB 45.5 ± 1.1% SMIFH2 45.0 ± 2.6%

and MiTMAB + SMIFH2 43.7 ± 6.1%, see Figure 4.12 C). This suggests that formin and dynamin act in the same pathway.

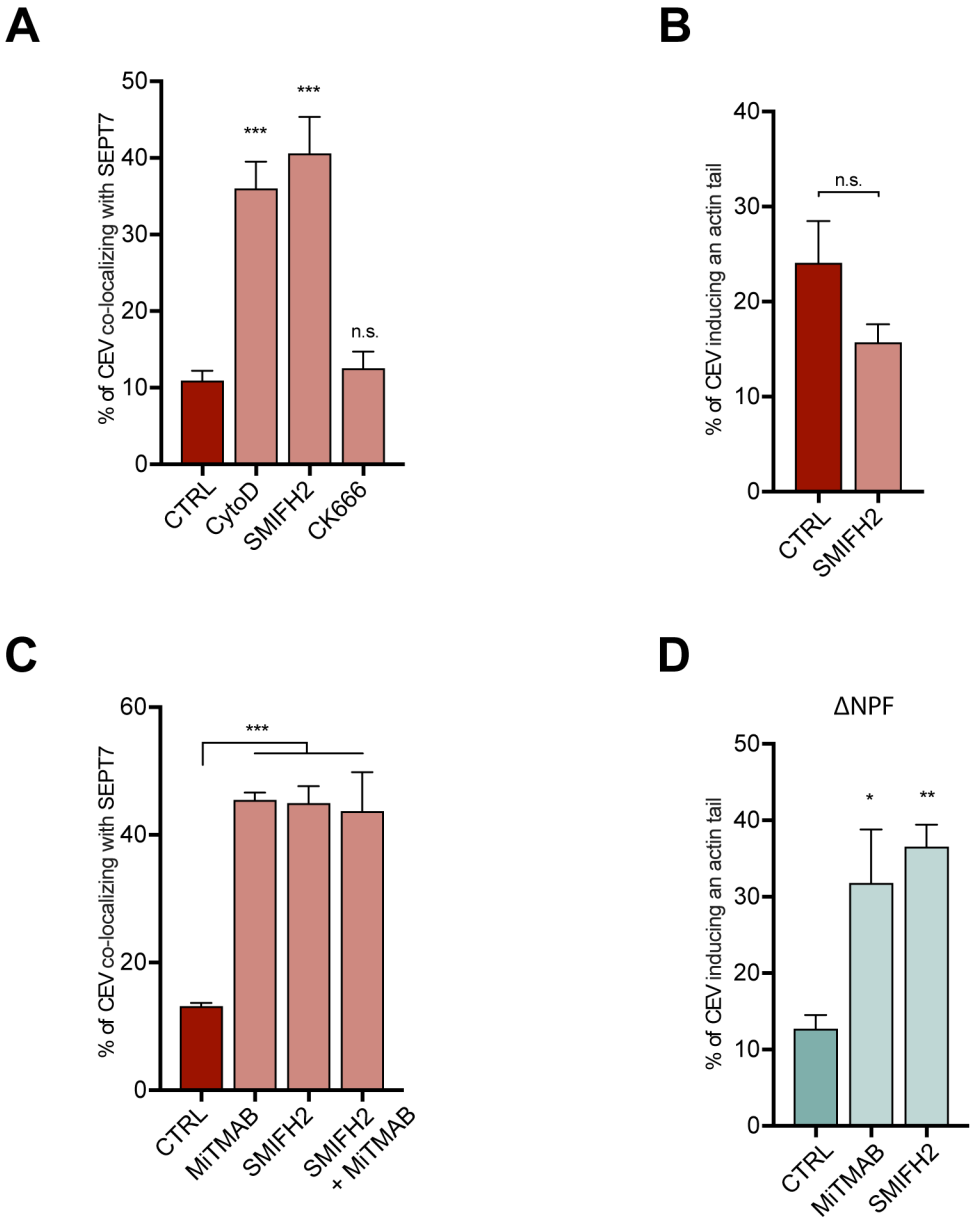

Figure 4.13 Chemical formin inhibition increases co-localization of septins and CEV

A, B Quantification of the % of CEV recruiting SEPT7 and inducing actin tails in HeLa cells infected with WR for eight hours and treated with CytoD, SMIFH2 or CK666. **C** The graph shows the % of CEV recruiting SEPT7 when dynamin (MiTMAB), formin (SMIFH2) or both were chemically inhibited. **D** Quantification of the % of CEV recruiting SEPT7 and inducing actin tails in HeLa cells infected with NPF for eight hours and treated with MiTMAB or SMIFH2. Error bars represent SEM from three independent experiments in which over 900 virus particles were analysed across 30 cells; n.s. p-value > 0.05; * p-value < 0.05; ** p-value < 0.01; *** p-value < 0.001.

Dynamin and formin inhibition in ΔNPF infected HeLa cells revealed an interesting phenotype. While septin recruitment to CEV was increased in both cases as seen during WR infection (CTRL 11.5 ± 1.8% MiTMAB 31.8 ± 7.0% and SMIFH2 36.4 ± 4.1%, Figure 4.14), actin tail formation showed important differences. While in WR-infected cells MiTMAB treatment decreased the number of CEV associated with actin tails, chemical inhibition of dynamin had no significant effect on actin tails induced by ΔNPF viruses. In addition, actin tail length was increased upon MiTMAB treatment in WR infected cells (CTRL 2.9 ± 0.1 μm and MiTMAB 4.7 ± 0.1 μm) but was unchanged in cells infected with the ΔNPF virus (CTRL 4.9 ± 0.2 μm and MiTMAB 4.6 ± 0.3μm) (Figure 4.14). SMIFH2 treatment showed a more striking difference. WR infected cells formed longer tails in the presence of the inhibitor (3.8 ± 0.1 μm) but the percentage of CEV being propelled by actin tails was comparable to the untreated cells. The opposite was observed during ΔNPF infection. SMIFH2 treatment led to many more (46.7 ± 1.9%) and much shorter actin tails (1.0 ± 0.2 μm). Taken together these data suggests that actin tails that are formed in the absence of clathrin and its adaptor proteins are more reliant on formin-mediated actin assembly. In contrast, dynamin inhibition has more impact on actin tails formed by the WR virus. It remains to be determined what exactly causes these striking differences. It could be the clustering effect of clathrin, the presence of one of the adaptor proteins or the local activation of Cdc42. Further experiments, including knockdown of clathrin and the adaptor proteins and infection of Cdc42 knockout cells, are needed to distinguish these possibilities.

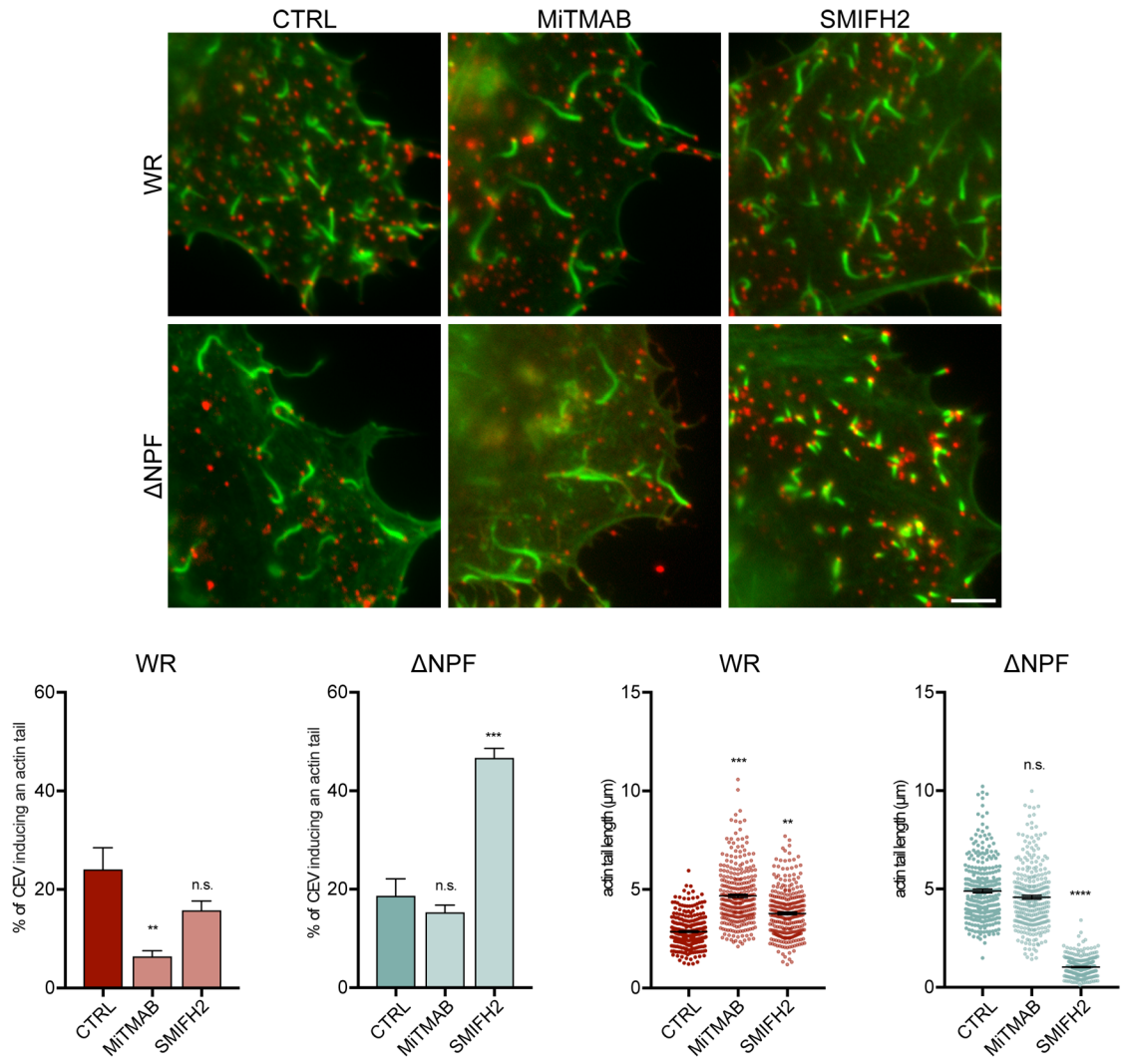

Figure 4.14 Effects of formin inhibitor vary between actin tails induced by WR and NPF virus

Representative immunofluorescence images showing actin stained with phalloidin in green and CEV in red. HeLa cells were infected for eight hours with the indicated virus and treated with the indicated inhibitor for 30 min. The graphs show the % of CEV inducing an actin tail as well as the tail length under the indicated conditions. Error bars represent SEM from three independent experiments in which a total of over 900 virus particles or 300 actin tails from 30 cells were analysed. Scale bar = 5 µm; ns. p-value > 0.05; ** p-value < 0.01; *** p-value < 0.001; **** p-value < 0.0001.

4.3 Summary

Septins are recruited to CEV, as demonstrated in the previous chapter. Data presented here show that mutating the two tyrosines Y112 and Y132 in the virus protein A36, which are phosphorylated by Src, dramatically increases the levels of CEV that recruit septins. This YdF virus is deficient in actin tail formation and spread (Frischknecht et al., 1999b, Moreau et al., 2000, Rietdorf, 2001, Ward et al., 2003), suggesting that actin tail formation displaces septins from the virus. However, neither recruitment of N-WASP:WIP nor the formation of branched actin tails influence the levels of septin recruitment. The dramatic difference in septin co-localizing with WR and YdF virus is Src-dependent, since overexpression of Src reduces septin levels at the virus and inhibition of Src increases them. There was no strong evidence that Src directly phosphorylates septins in order to regulate their presence at the virus particle. Moreover, the dynamics of septins at WR and YdF viruses measured by FRAP are comparable. Increased accumulation of septins at the YdF virus is due to the lack of phosphorylation of the Y112 in A36 and subsequent recruitment of Nck. More specifically, Nck requires its third SH3 domain in order to reduce septin levels at vaccinia. Dynamin is one of the binding partners of Nck that specifically bind to this SH3 domain (Wunderlich et al., 1999). I found that dynamin is transiently recruited to CEV and displaces septins from the virus. Loss or inhibition of dynamin II leads to an increased accumulation of septins at CEV. Furthermore, in the absence of dynamin fewer actin tails are formed. Live-cell imaging revealed that dynamin recruitment coincides with a burst of actin polymerisation at the virus. This local actin polymerisation appears to be formin driven and helps displace septins from the virus. Identifying the involved formin in the process is an important goal for future experiments. Surprisingly, actin tails formed by WR and ΔNPF viruses respond differently to formin inhibition. Clarifying the underlying mechanism for this distinct behaviour is another aim among my future plans.

Chapter 5. Septins suppress virus release and spread

5.1 Introduction

All viruses rely on several steps to successfully infect, replicate and spread in cultured cells.

Following virus entry, genome replication and translation of viral proteins, new virus particles are assembled. In some cases, this is directly coupled to the budding process by which the virus leaves the cell. These new viral progenies need to exit the cell and reach neighbouring uninfected cells, where the next round of infection can occur. Proteins that either increase or decrease the efficiency of one or several of the above steps are referred to as pro or anti-viral factors. Identifying pro and anti-viral host proteins in the context of vaccinia infection was the aim of two genome wide RNAi screens (Beard et al., 2014, Sivan et al., 2013). The screens were performed in a way that at least two rounds of infection would occur. Namely entry, replication, egress and second round of infection, summarized as spread, were measured. In order to clarify the role of septins during vaccinia infection I examined their impact on those individual steps.

As it became clear that septins supress virus release and spread I investigated whether dynamin, which was shown to replace septins in the previous chapter, promotes virus release and spread. In addition, I decided to also examine whether Borgs, a group of proteins known to regulate septins (Joberty et al., 2001) (see 1.4.4), are also involved in regulating Vaccinia egress. Investigating their role during vaccinia infection could potentially widen our understanding of how septins exert their anti-viral effect.

5.2 Results

5.2.1 Septins suppress actin tail formation

Actin-based motility is a common strategy used by a number of pathogens to accelerate their cell-to-cell spread (Bugalhão et al., 2015, Ireton, 2013, Welch and Way, 2013). In the previous chapter, I found that without dynamin septins are not

displaced from the virus and fewer actin tails are formed. This raises the question whether the absence of septins at the virus enhances actin tail formation. To test this hypothesis, I performed siRNA knockdown of SEPT7 in HeLa cells and infected them with WR expressing A3-RFP. Visualisation of actin with fluorescently labelled phalloidin revealed that the percentage of CEV inducing an actin tail was significantly increased (Allstar 23.9 ± 0.5% versus SEPT7 35.5 ± 1.7%, Figure 5.1A). Furthermore, the average actin tail was significantly longer (Allstar 2.5 ± 0.1μm and SEPT7 3.9 ± 0.1μm; see Figure 5.1B). Humphries and Snetkov previously demonstrated that the absence of clathrin also increases actin tail length (Humphries et al., 2012, Snetkov et al., 2016). Knockdown of septins in HeLa cells infected with the A36 ΔNPF1-3 virus, which is deficient in clathrin recruitment, further increased actin tail length (Allstar 3.3 ± 0.1 μm versus SEPT7 4.8 ± 0.1μm, Figure 5.1B). This is additional evidence that clathrin and septin act independently of each other at the virus. Actin tail length is influenced by actin polymerisation and depolymerisation rates beneath the virus and in the actin tail respectively. Given this, it is possible that longer actin tails are induced by an increase actin polymerization rate, which would be reflected by an increase in virus speed. To test whether this was the case, I performed live-cell imaging on HeLa cells treated with Allstar and SEPT7 siRNA. I then automatically determined the speed and directionality of viruses being propelled by actin tails using a Fiji plug-in particle tracker (Abella et al., 2015). There was no detectable difference in the speed of actin-based virus movement between control cells (185.8 ± 2.4 nm/sec) and septin-depleted cells (188.5 ± 2.1 nm/sec). Equally there was no difference in the directionality of the virus (Figure 5.1C). This data suggests that decreased depolymerisation, rather than increased polymerization, leads to longer actin tails in the absence of septins. Assuming that the actin depolymerisation machinery itself is unchanged in the absence of septin, it is more likely that the architecture of the tail is different. Lack of septins might result in the formation of a denser actin tail potentially with a higher density of Arp2/3 branches, making the actin structure more resistant to depolymerisation. Detailed analysis of the actin structure as well as photo-activation experiments of polymerized actin will be needed to dissect the underlying mechanisms.

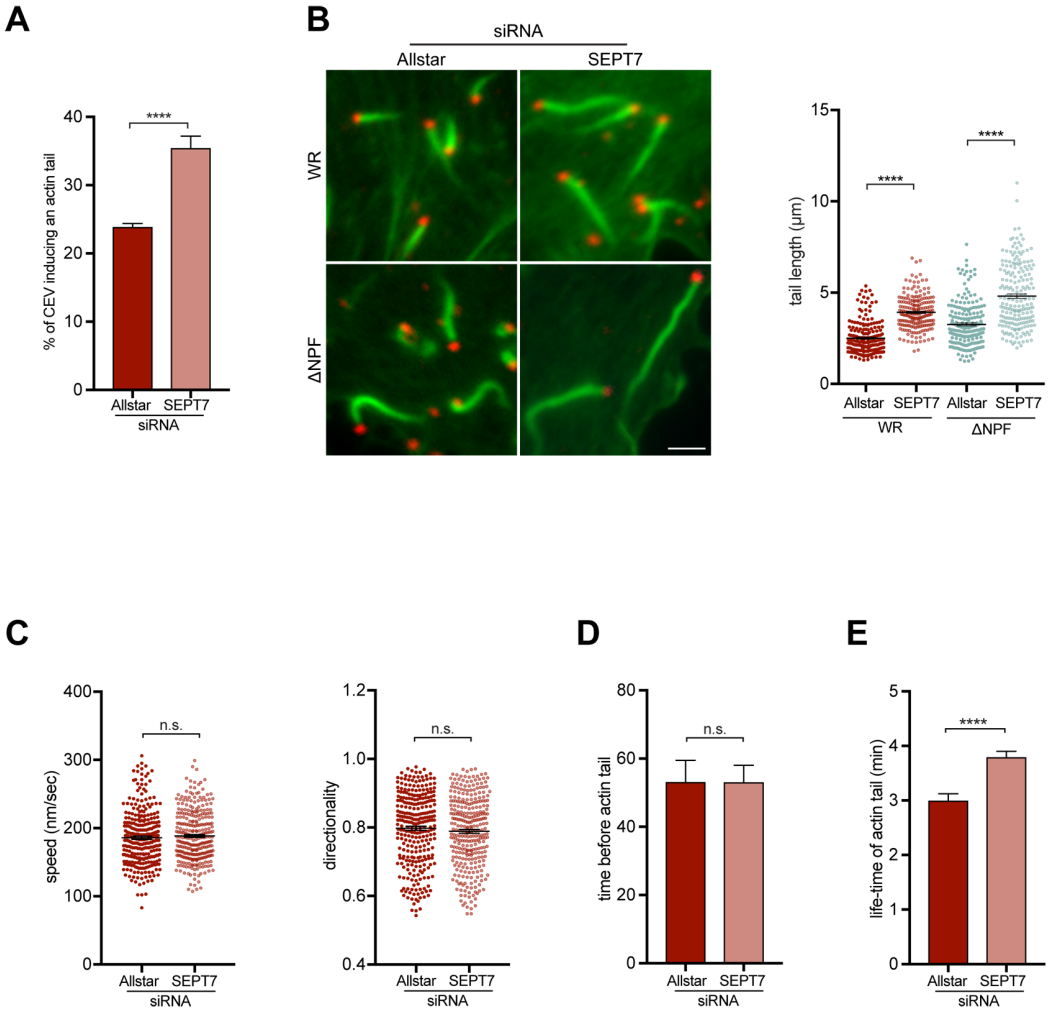

Figure 5.1 Depletion of SEPT7 impairs actin tail formation

A Quantification of WR CEV inducing an actin tail in control and SEPT7-depleted cells. **B** Representative immunofluorescence images showing actin stained with phalloidin in green and CEV in red in HeLa cells infected with WR and ΔNPF virus for eight hours. Scale bar = 2 μm. The graph shows actin tail length in control and SEPT7-depleted cells. **C** Quantification of speed and directionality of actin-dependent movement of vaccinia. **D** Quantification of time to induce an actin tail. **E** Quantification of life-time of actin tails. Error bars represent SEM from three independent experiments; for **A**, **B**, **C** and **E** over 100 events and for **D** over 30 events were analysed; n.s. p-value > 0.05; **** p < 0.0001.

Given that septins are recruited after fusion and prior to actin tail formation one idea was that septins could impede and slow down the initiation of local actin polymerization without affecting the steady state velocity of the tail. In the case of clathrin it was shown that its absence increases the time between delivery of the virus to the cell periphery and actin tail initiation (Humphries et al., 2012, Snetkov et al., 2016). To test whether septin depletion has a similar effect on tail formation, I

determined the time between the end of microtubule-based movement and the onset of actin-based motility of the virus in the absence of SEPT7. Comparing cells transfected with Allstar and SEPT7 siRNA no significant difference in time to form an actin tail was observed (Figure 5.1D).

However, when I determined the life-time of actin tails in control and septin-depleted cells, I found that actin tails existed for 3.0 ± 0.1 minutes in the presence of septins, whereas without septins the average life-time of an actin tail was 3.8 ± 0.1 minutes (Figure 5.1E). This data shows that actin tails formed in the absence of septin are more robust with an increased life-time. A denser actin network would not only impede depolymerisation leading to longer tails but also better ensures that plenty of mother filaments are available from which new daughter filaments can be branched off, making the tail less susceptible to perturbations.

5.2.2 Septins inhibit virus release and spread

From the siRNA screens, it is known that knockdown of septins results in more infected cell and more total amount of virus. This could either be due to an increase or acceleration in virus entry and replication or due to an increase in virus release or spread independent of more virus progeny. Therefore, I performed a single-step growth analysis. This technique allows to study one single replication cycle, covering virus entry and production of new virus particles. Septins were depleted in A549 cells using SEPT7 siRNA. The knockdown was confirmed by immunoblot analysis at 72 hours after transfection (Figure 5.2A). Cells were infected with a high multiplicity of infection (MOI =10) to ensure that each cell is infected and will start producing new progeny virus. Cells were then harvested at 5, 9, 18 and 24 hours post-infection and the total amount of intracellular and cell-associated virus was determined by plaque assays performed on confluent monolayers of BS-C-1 cells. There was no significant difference in the virus titer between control and septin-depleted cells at any of the measured time points (Figure 5.2B). These data indicate that septins do not play a role during virus entry and replication.

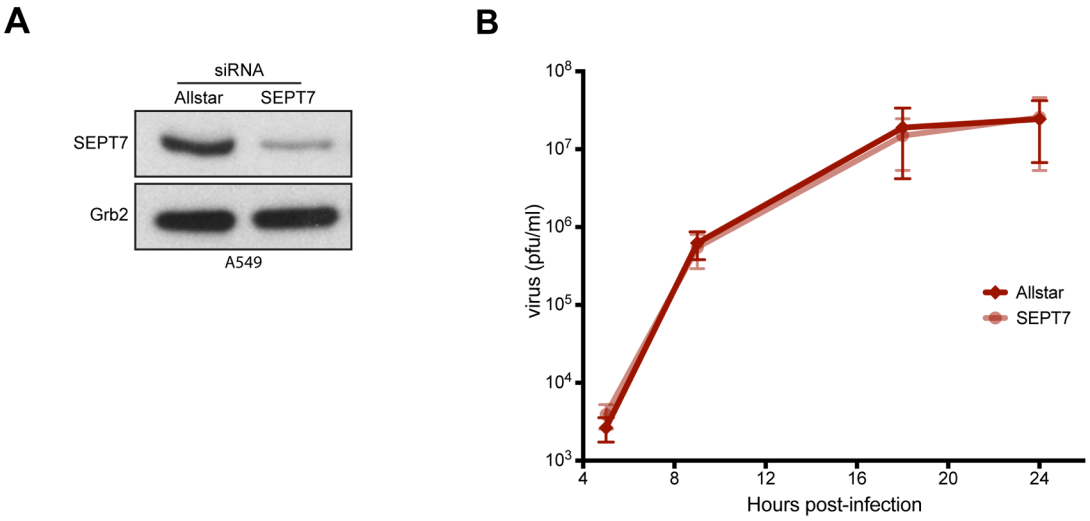

Figure 5.2 Depletion of SEPT7 does not impact on virus growth

A Western blot analysis confirming SEPT7 depletion in A549 cells after 72 hours of treatment; Grb2 was added as a loading control. **B** Virus titer during single step growth curve determined at 5, 9, 18 and 24 hours WR infection in A549 cells treated with control and SEPT7 siRNA. Error bars represent SEM from three independent experiments.

Since septins are found on cell associated virus particles after fusion with the plasma membrane, septin depletion might impact on virus release and/or spread. Virus spread can be measured performing a plaque assay on confluent cell monolayers. I therefore infected confluent monolayers of A549 cells at a very low multiplicity of infection (MOI=0.005). To maintain a substantial knockdown of septin 7 over the course of three days, I transfected the confluent cells with siRNA 72 and 5 hours before infecting them with vaccinia and confirmed the knockdown by immunoblot analysis (Figure 5.3A). In order to measure only cell-to-cell spread and inhibit diffusion of the virus through the media, I covered the cells with a semi-solid overlay of 1.5% methylcellulose. The infection was then allowed to progress for 72 hours before the cells were fixed. The plaques that formed in the cell monolayer were then visualized by immunostaining against the viral protein B5 (Figure 5.3B) and the diameter of the plaques was measured. In Allstar treated siRNA cells WR formed 1.56 ± 0.01 mm sized plaques whereas RNAi-mediated loss of SEPT7 led to larger 1.94 ± 0.02 mm sized plaques (Figure 5.3B). This data shows that loss of septins increases the cell-to-cell spread of the virus. In parallel, I also performed plaque assays using media as a liquid overlay allowing virus diffusion. Under these conditions WR formed plaques with a diameter of 1.60 ± 0.02 mm in control infected

cells and 2.23 ± 0.03 mm sized plaques in septin-depleted cells. In addition to significantly larger plaques, I observed also an increase in the number of the so called “comets”. Spontaneous flows in the media cause non-uniform diffusion of the virus, thereby allowing these trails of infected cells to form around the plaques, as seen in Figure 5.3C. Increased comet formation are indicative of higher levels of EEV release (Horsington et al., 2013, Mathew et al., 1999, McIntosh and Smith, 1996).
Given that septins and actin tails seem to compete with each other, I wanted to see if the observed increase in spread depends on the actin-based motility of the virus. To investigate this matter, I analysed the size of plaques formed by the A36-YdF virus, which is deficient in actin tail formation (Frischknecht et al., 1999b, Moreau et al., 2000, Rietdorf et al., 2001, Ward et al., 2003), in the presence and absence of SEPT7. Again, a significant increase in virus spread following septin depletion was observed under both the semi-solid and the liquid overlay (semi-solid overlay: Allstar 0.96 ± 0.01 mm, SEPT7 1.17 ± 0.01mm; liquid overlay: Allstar 0.91 ± 0.01 mm, SEPT7 1.40 ± 0.03 mm), see Figure 5.3D and E. These results demonstrate that the accelerated cell-to-cell spread of vaccinia upon septin depletion does not require vaccinia-induced actin tail formation.

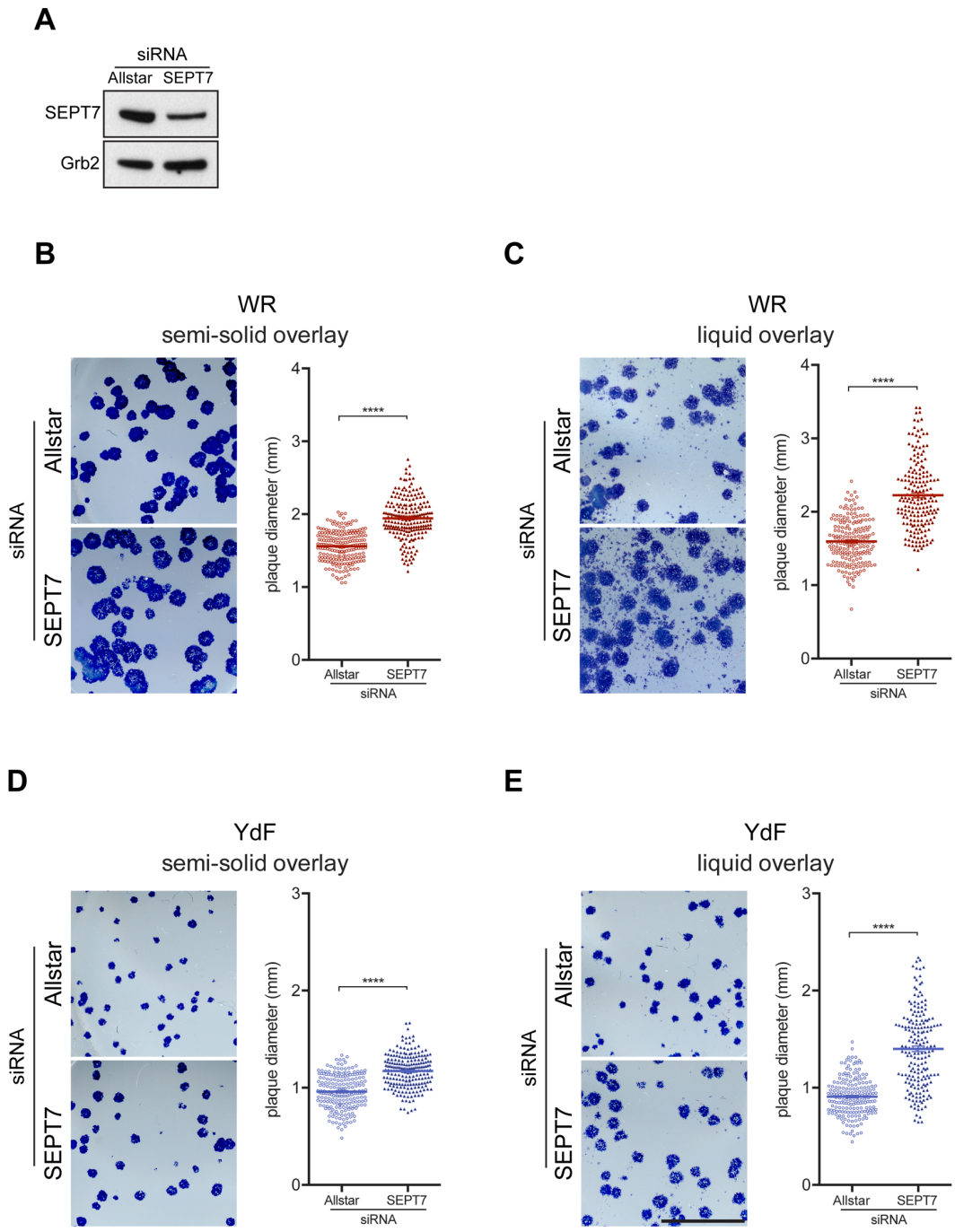

Figure 5.3 Septin depletion increases virus spread

Western blot analysis confirming the knockdown of SEPT7 in A549 cells at the terminal point of the plaque assay; Grb2 is included as a loading control **B** Virus plaques formed under semi-solid overlay in control and SEPT7-depleted A549 cells infected with WR for 72 hours. **C** Virus plaques formed under liquid overlay in control and SEPT7-depleted A549 cells infected with WR for three days. **D, E** Virus plaques formed under semi-solid or liquid overlay in control and SEPT7-depleted A549 cells infected with YdF for three days. All graphs show the quantification of plaque diameter. Scale bar = 1 cm. Error bars represent SEM from three independent experiments in which over 190 plaques were analysed; p-value of <0.0001 is indicated by ****.

Virus spread depends on several parameters, one of which is the amount of released virus. Extracellular enveloped virus particles (EEV) are released from the cell by fusion of intracellular enveloped viruses (IEV) with the plasma membrane from 6 hours post infection onwards (Payne, 1980, Payne and Kristenson, 1979, Smith and Law, 2004). To assess EEV release, I transfected A549 cells with Allstar and SEPT7 siRNA and subsequently infected them after 72 hours with a high multiplicity of infection (MOI=10) of WR or A36-YdF virus. After 1eight hours of infection the media containing the released EEV was collected and their titer determined using plaque assays. In parallel the infected cells were also harvested and the amount of intracellular and cell-associated virus was measured. Experiments were performed in duplicate in three independent experiments. Virus levels varied slightly between experiments on different days but the technical replicates were consistent. To account for these variations, I also calculated the relative amount of virus released in addition to the absolute number of virus particles released. Overall there was significantly more virus released from cells depleted of septin compared to the control, for both WR and YdF infected cells (Figure 5.4). The increase in virus release occurred despite a slight decrease in intracellular virus, indicating that while virus production is not increased, the process of virus egress is improved. Furthermore, it was worth noticing that in the case of WR the amount of released virus was three logs below the intracellular virus, consistent with previous observations (Smith and Law, 2004). In addition, a reduction in A36-YdF release was observed compared to the wild type virus (Figure 5.4), as previously reported (Horsington et al., 2013). Taken together, these data show that septins exert their anti-viral role by restricting vaccinia release and spread.

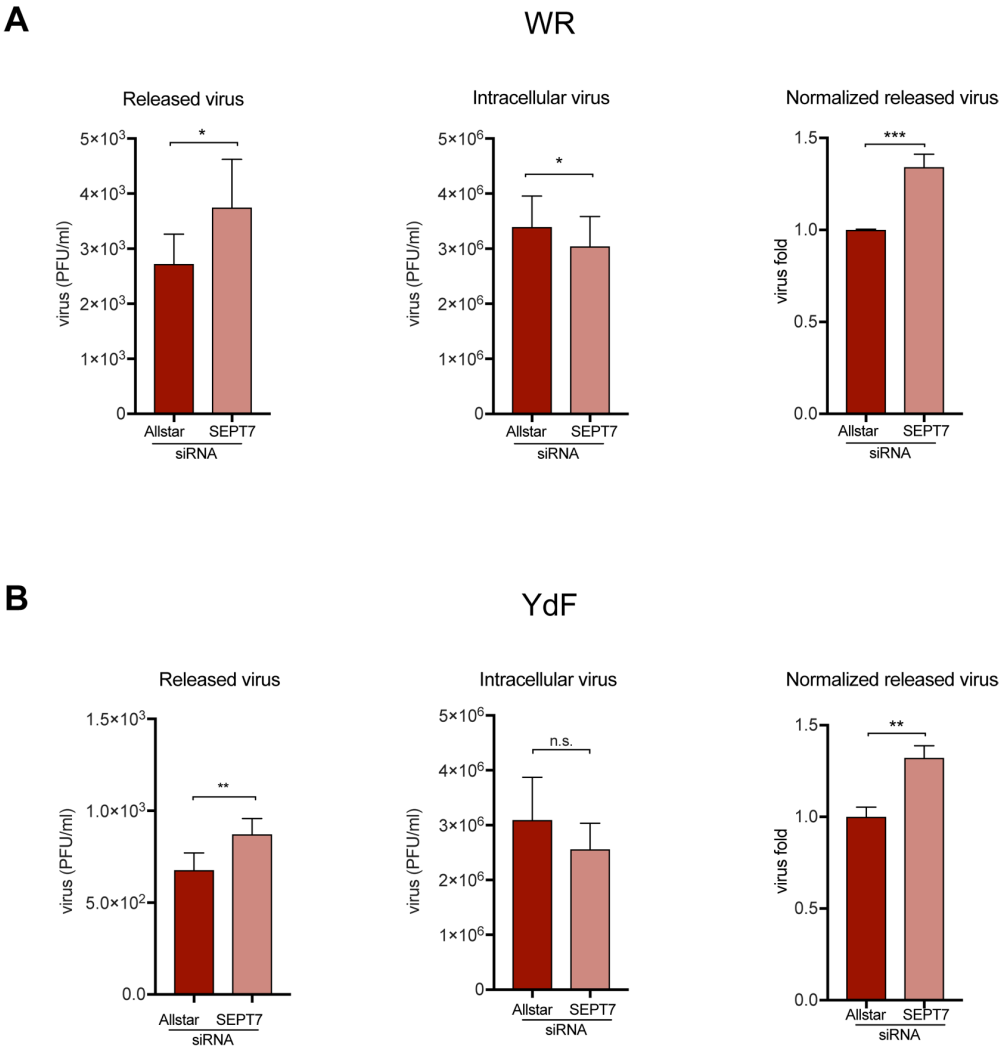

Figure 5.4 Depletion of SEPT7 increases virus release from infected A549 cells

A Quantification of WR virus titer released from control and SEPT7-depleted A549 cells after 18 hpi. Virus release is increased while the amount of intracellular virus is slightly decreased. **B** Quantification of YdF virus titer released from control and SEPT7-depleted A549 cells after 18 hpi. Virus release is increased while the amount of intracellular virus is not significantly changed. Error bars represent SEM from three independent experiments; n.s. p-value >0.05; * p-value < 0.05; ** p-value < 0.01; *** p-value < 0.001.

5.2.3 Dynamin has multiple roles during vaccinia replication

In the previous chapter I showed that the recruitment of dynamin to CEV leads to the displacement of septins. In this chapter, I found that septin depletion leads to increased virus release and spread (Figure 5.3 and Figure 5.4). I next set out to investigate whether I could revert this phenotype by removing dynamin from the cells. First, I repeated the EEV release assay in the Dyn +/+ and Dyn -/- cells. As septins inhibit virus release but are displaced by dynamin, virus release should be reduced in the absence of dynamin. This hypothesis was confirmed, as Dyn -/- cells release about 60% fewer EEV than Dyn+/+ parental cells 18 hours post-infection (Figure 5.5A). However, quantification of the intracellular virus revealed that dynamin knockout cells produced 70% less virus compared to the parental cells (Figure 5.5A). The decreased level of intracellular virus indicated that dynamin plays an additional role before virus release. It was not clear whether the decrease in virus release was due to lack of septins displacement by dynamin or due to the reduced number of total virus inside the cells.

To follow up on these release experiments, I also performed a single-step growth curve to examine virus replication by infecting the Dyn +/+ and Dyn -/- cells with WR at a high multiplicity of infection (MOI=10). Comparing total virus titers at 5, 9, 18 and 24 hours post-infection reveals that dynamin knockout cells consistently produced less virus than the dynamin parental control cells (Figure 5.5B). This confirms that dynamin impacts on an earlier step during virus replication prior to virus release.

A

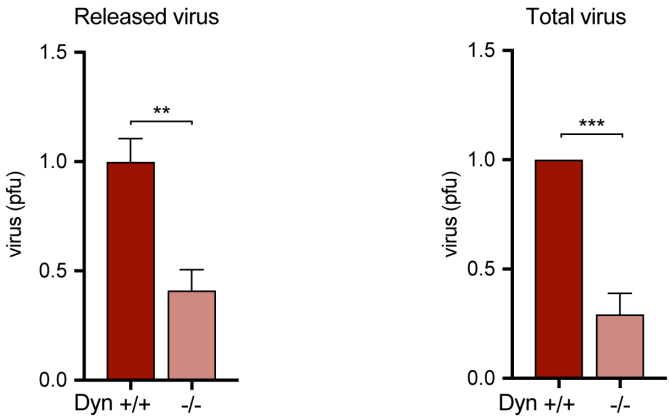

B

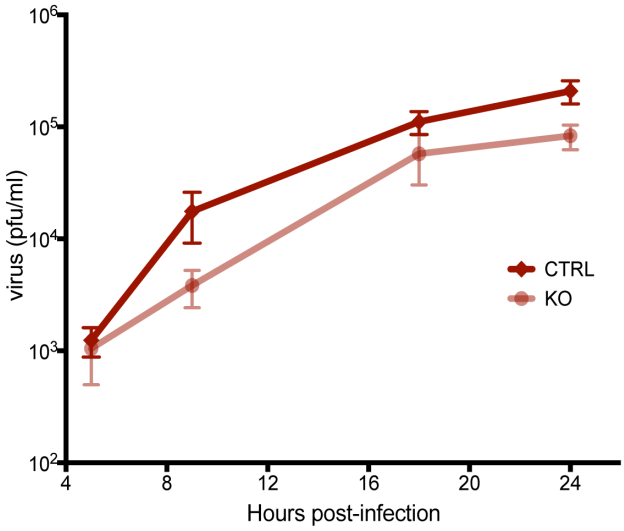

Figure 5.5 Virus release and replication is reduced in the absence of dynamin

A Quantification of released and intracellular WR virus in control and Dyn -/- cells after 18 hpi. Virus release is increased while the amount of intracellular virus is slightly decreased. **B** Virus titer during single step growth curve determined at 5, 9, 18 and 24 hpi from WR infected control and Dyn -/- cells. Error bars represent SEM from three independent experiments; ** p-value < 0.01; *** p-value < 0.001.

Reduced virus production and release should also result in smaller virus plaques. Plaque assays on confluent control and dynamin knockout fibroblasts revealed a significant decrease in plaque diameter in the absence of dynamin for both WR (Dyn+/+ 2.15 ± 0.02mm versus Dyn-/- 1.33 ± 0.03nm) and YdF infected cells (Dyn+/+ 1.32 ± 0.02mm versus Dyn-/- 0.79 ± 0.02nm) see Figure 5.6. Moreover, it was noticeable that in the dynamin knockout cells fewer plaques were also formed. Normalized to the parental cells only 48 ± 7 % and 30 ± 12% of WR and A36-YdF viruses respectively could establish an infection and go on to form a plaque (Figure 5.6). In order for a plaque to be detected more than one cell has to be infected. Hence it is not clear if loss of dynamin results in an entry defect or whether replication and spread are so severely impaired that the side of infection remains too small to be detected. Further experiments are needed to determine whether dynamin is involved in virus entry and/or replication. However, any effects of dynamin during virus egress are obscured by the earlier involvement of dynamin.

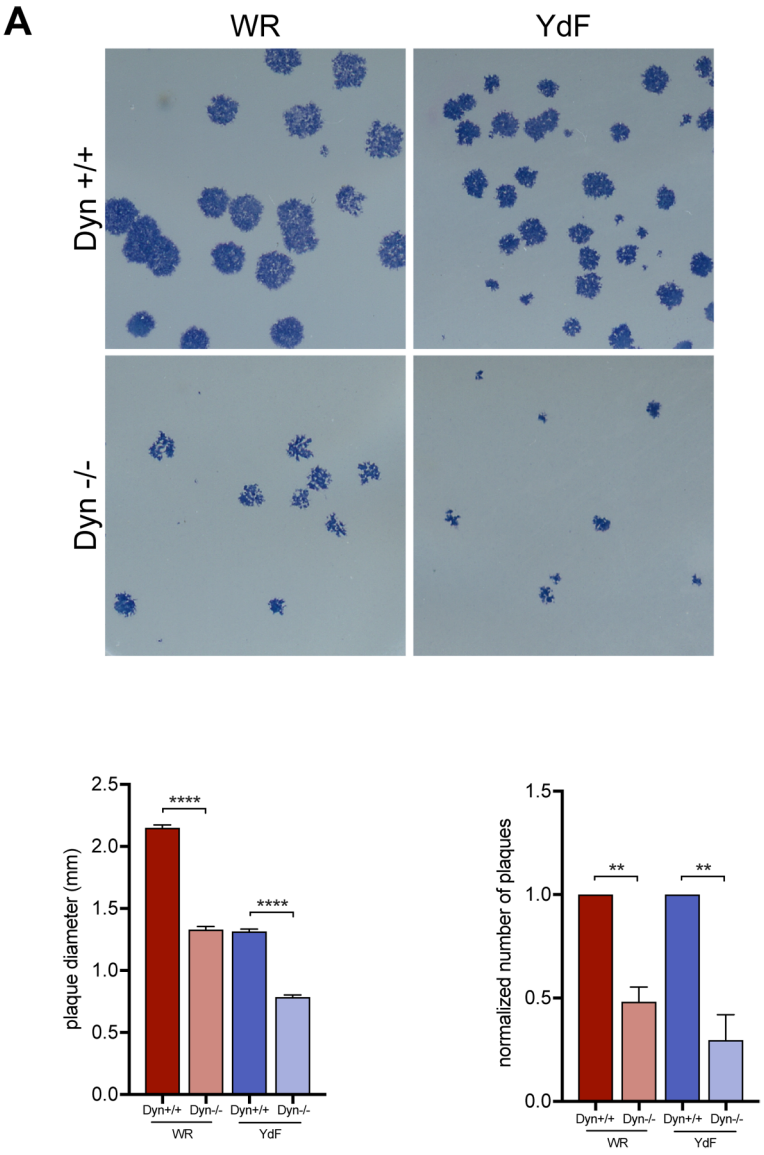

Figure 5.6 Absence of dynamin results in smaller and fewer plaques

A Virus plaques formed under semi-solid overlay in control and Dyn -/- cells infected with WR or YdF. Quantification of plaque diameter and amount. Fewer and smaller plaques are formed in the absence of dynamin. Error bars represent SEM from three independent experiments; ** p-value < 0.01; **** p-value < 0.0001.

5.2.4 Borg2 regulates septins at the CEV and has additional pro-viral effects on virus release and spread

Septins can be regulated in a variety of ways, for example by post translational modification such as phosphorylation (Cvrcková et al., 1995, Longtine et al., 1998, Versele and Thorner, 2004, Dobbelaere et al., 2003 Garcia, Garcia et al.) and SUMOlation (Johnson and Blobel, 1999, Johnson and Gupta, 2001, Makhnevych et al., 2007, Martin and Konopka, 2004). Since septins are GTPases, their guanine nucleotide binding states is also thought to impact on their behaviour (Kim et al., 2012, Mendoza et al., 2002, Sirajuddin et al., 2009). Alternatively, direct interaction with other proteins can influence their function. The Borgs, also named Cdc42 effector proteins (CDC42EP 1-5), are a family of proteins that regulate both septin and actin downstream of Cdc42 (Hirsch et al., 2001, Joberty et al., 1999, Joberty et al., 2001). Borg2 can act as “molecular glue” and connect actin and septin filaments (Calvo et al., 2015). I therefore decided to investigate the potential role of Borgs during vaccinia infection, since it is possible they are responsible for recruiting septins to the virus.

Given its ability to interact with actin and septin filaments, I focused on Borg2. Unfortunately, I was not able to find an antibody that was suited for immunofluorescence. Next, I expressed GFP-tagged Borg2, kindly provided by F.Calvo (Calvo et al., 2015) in HeLa cells stably expressing mCherry-SEPT6 and LifeAct-iRFP. I found that the localization of Borg2 very much resembles SEPT6 localization and Borg2 was also transiently recruited to vaccinia virus particles (Figure 5.7).

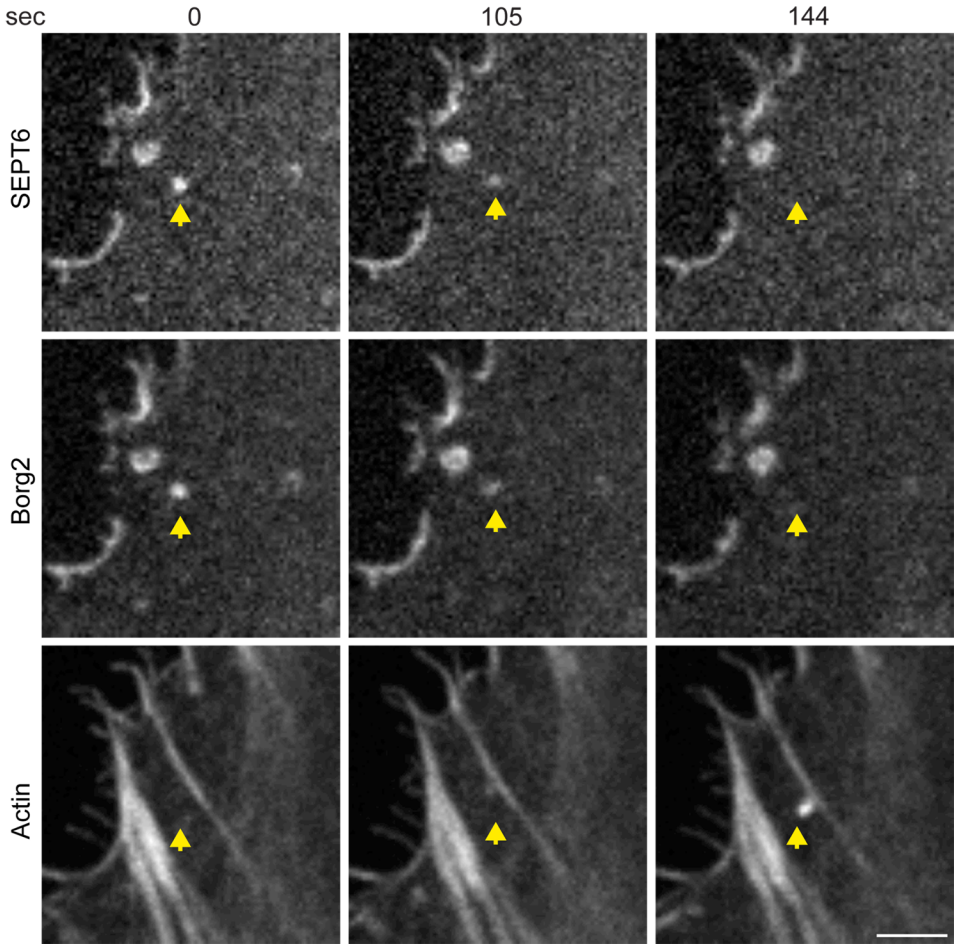

Figure 5.7 Borg2 co-localizes with SEPT6 and is also recruited to vaccinia

Stills from live cell imaging of an infected HeLa cell expressing mCherry-SEPT6, LifeAct-iRFP and GFP-Borg2. Yellow arrow highlights the displacement of Borg2 and SEPT6 by the forming actin tail. The time is indicated in seconds. Scale bar = 2µm.

As a next step, I used a pool of four different siRNA oligos to deplete Borg2. Cells were either treated with Allstar, SEPT7, Borg2 or Borg2 + SEPT7 siRNA and the knockdown efficiency was confirmed by immunoblot analysis on whole cell lysates (Figure 5.8A). Depletion of Borg2 did not change the overall level of SEPT7 or SEPT2 in the cell, neither did septin depletion alter the level of Borg2 expression. Nevertheless, Borg2 depletion reduces the number of functional septin structures in SETP7 stained cells. In the control 12.7 ± 2.8% of WR and 64.6 ± 6.2% of A36-YdF CEV co-localized with SEPT7 only 3.2 ± 2.2% of WR and 19.0 ± 4.5% of YdF CEV recruited septins in Borg2-depleted cells (Figure 5.8B). As expected SEPT7 siRNA treatment also led to reduced levels of septin recruitment (WR 1.5 ± 1.0% and YdF 10.4 ± 3.2%,). The double knockdown further decreased the number of septin

positive CEV (WR 1.3 ± 0.6% and YdF 5.9 ± 2.5%). These data suggest that Borg2 is involved in septin recruitment to the virus.

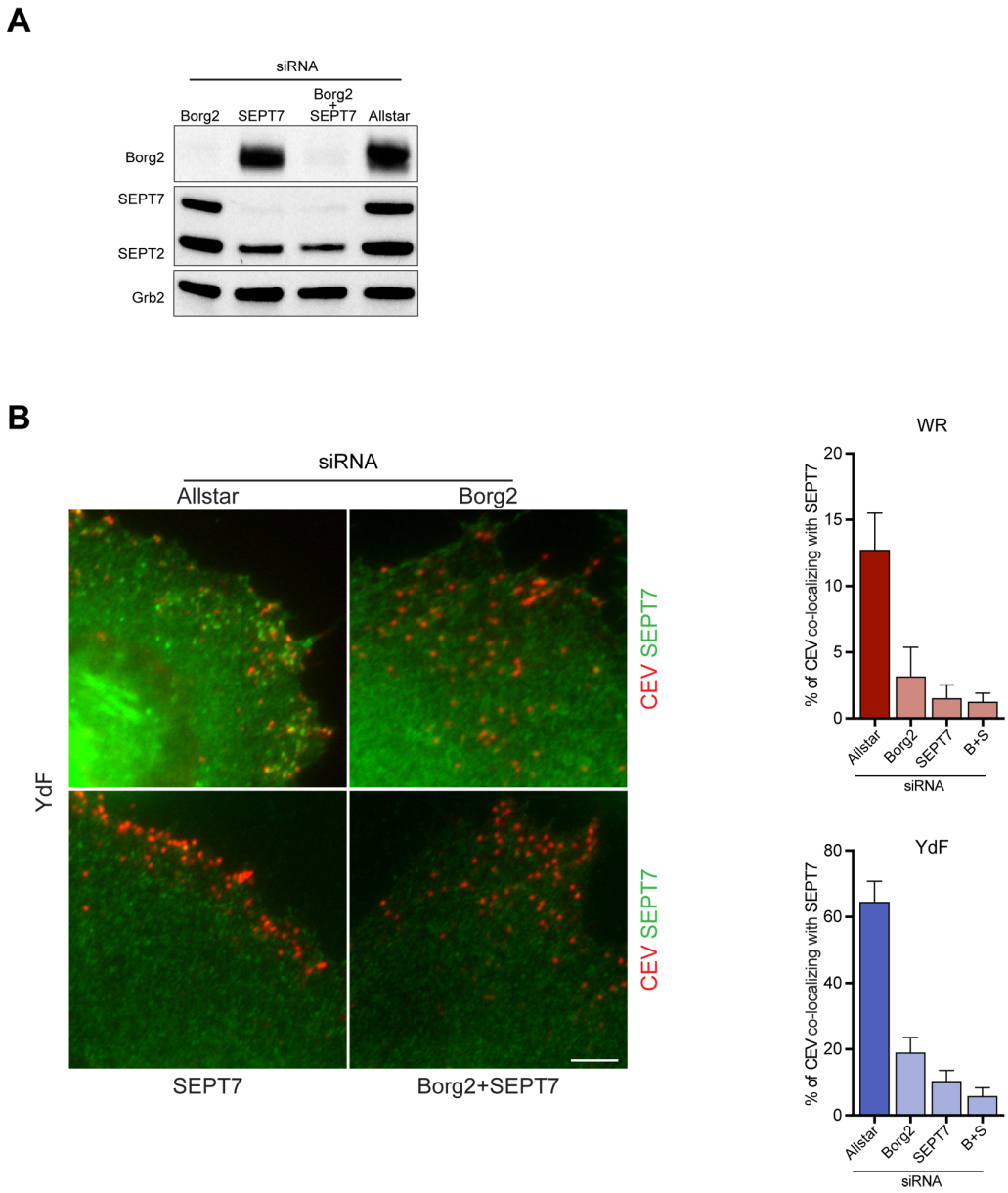

Figure 5.8 Depletion of Borg2 decreases septin recruitment to vaccinia

A Western blot analysis showing Borg2, SEPT2 and SEPT7 protein levels under the indicated knockdown conditions; Grb2 is included as a loading control. **B** Representative image of YdF infected HeLa cells stained for SEPT7 in green and CEV in red under the indicated knockdown conditions. Scale bar = 5 µm. The graph shows the % of CEV recruiting SEPT7. Error bars represent SEM from two and one independent experiments, in which 600 or 300 particles for WR and YdF infected cells were analysed, respectively.

In agreement with this, I also found that Borg2 and SEPT7 depletion had similar effects on actin tails (Figure 5.9A). Loss of Borg2 resulted in slightly more CEV inducing an actin tail (34.1 ± 5.6%) and the average tail length was significantly increased (4.1 ± 0.1 μm). The same effect was observed in the double knockdown (Figure 5.9A). The dynamics of actin tails, however, did not change upon either septin or Borg2 depletion compared with control cells. In the absence of Borg2 viruses moved with a speed of 183.2 ± 3.5 nm/sec and a directionality of 0.76 ± 0.01, whereas SEPT7 and Allstar knockdown led to speeds of 183.4 ± 3.1 and 176.3 ± 3.1 nm/sec and directionalities of 0.78 ± 0.01 and 0.79 ± 0.01 respectively. As seen with the septin depletion, knockdown of Borg2 significantly increased the life-time of actin tails (Allstar 2.9 ± 0.1min SEPT7 3.8 ± 0.1min Borg2 4.2 ± 0.1min Borg2+SEPT7 4.5 ± 0.2min). These data suggested that Borg2 and septins work together and influence vaccinia induced actin tails in a similar fashion.

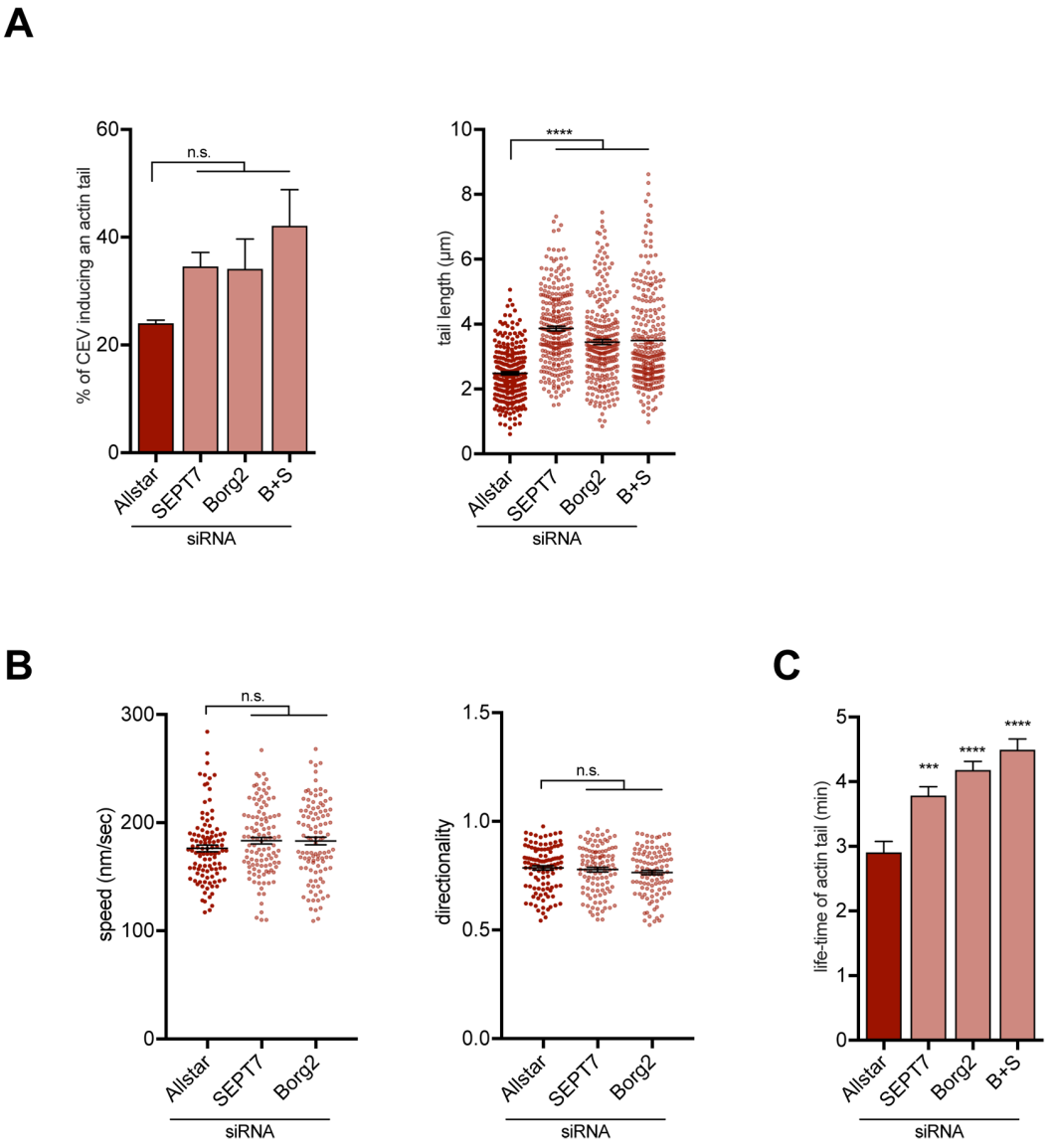

Figure 5.9 SEPT7 and Borg2 depletion enhance actin tail formation

A Quantification of number and length of actin tails in control cells and SEPT7, Borg2 and SEPT7+Borg2-depleted cells. **B** Quantification of virus speed and directionality during actin-based movement in WR infected HeLa cells. **C** Quantification of the life-time of vaccinia induced actin tails in control and SEPT7, Borg2 and SEPT7+Borg2 HeLa cells. Knockdown of Borg2 and SEPT7 have similar effects on actin tail formation. Error bars represent SEM from three independent experiments; n.s. p-value > 0.05; *** p-value < 0.001; **** p-value < 0.0001.

These data show that Borg2 is involved in septin recruitment at the CEV. Given septins-mediated inhibition of vaccinia spread, loss of Borg2 should increase the spread and release of vaccinia by reducing the amount of septins recruited to the CEV. To investigate if this is the case, I analysed the size of WR and YdF induced plaques in A549 cells depleted of SEPT7, Borg2 or both proteins. Surprisingly knockdown of Borg2 did not phenocopy septin depletion. While lack of septin increase virus spread, Borg2 depletion had the opposite effect and led to smaller plaques, (WR: Allstar 1.60 ± 0.02 μm, SEPT7 2.23 ± 0.03 μm Borg2 1.18 ± 0.02μm, YdF: Allstar 0.91 ± 0.01μm SEPT7 1.40 ± 0.03μm and Borg2 0.74 ± 0.02μm) see Figure 5.10A. Interestingly depletion of both proteins resulted in normal sized or larger plaques in WR and YdF infected cells respectively (WR 1.65 ± 0.03μm and YdF 1.06 ± 0.02μm). Similar results were obtained under semi-solid overlay conditions. The inhibitory effect of Borg2 knockdown was less pronounced under semi-solid condition and in YdF infected cells. In those cases, the combined knockdown lead to larger plaques (Figure 5.10B). One explanation could be that Borg2 is involved in virus release. Under condition where diffusion is prevented or only few virus particles can exit the cell, Borg2 depletion has less impact.

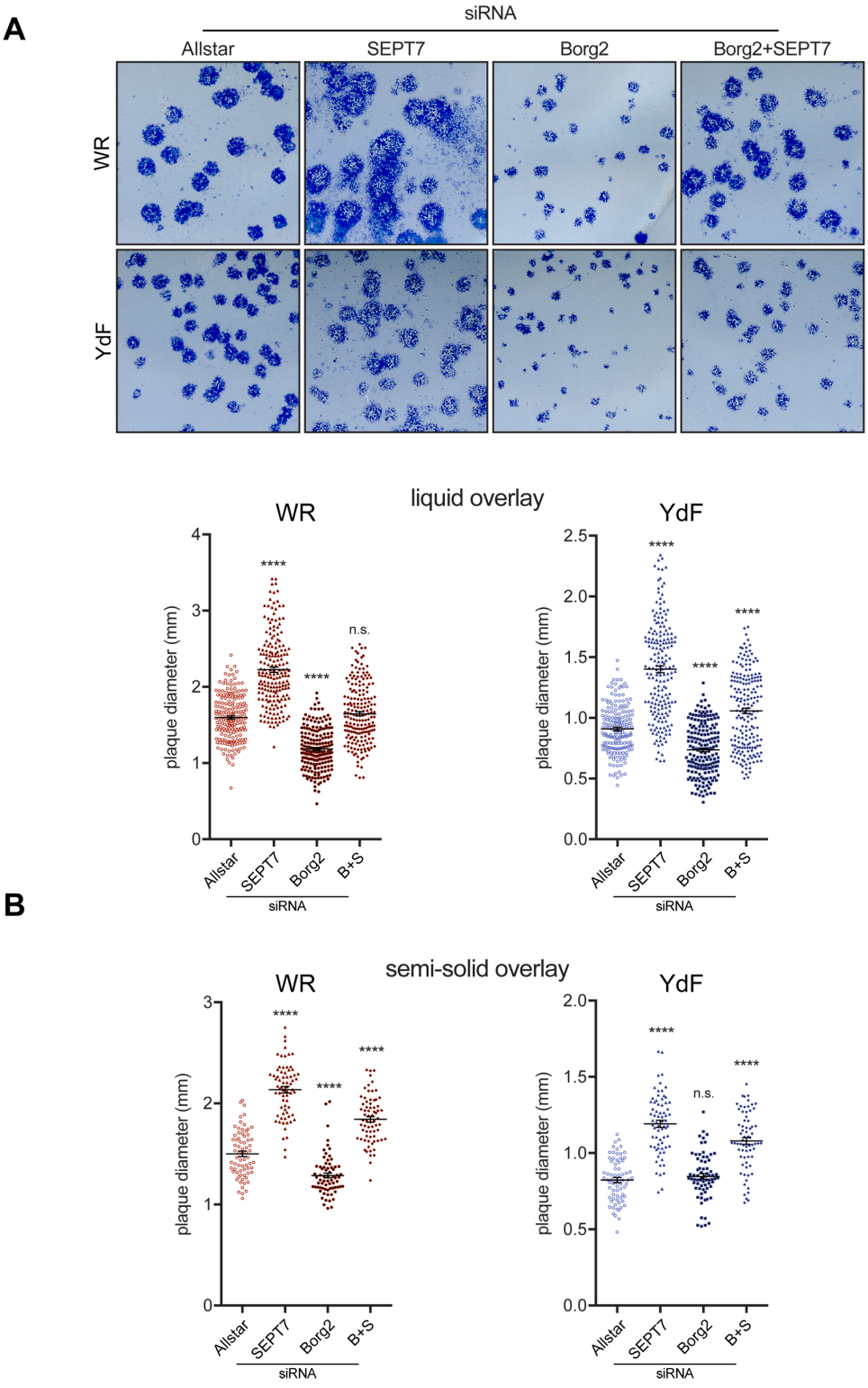

Figure 5.10 Septin and Borg2 depletion have opposing effects on virus spread

A Virus plaques formed under liquid overlay in WR and YdF infected A549 cells transfected with Allstar, SEPT7, Borg2 and SEPT7+Borg2 siRNA. Quantification of plaque diameter. **B** Quantification of plaque diameter in WR and YdF infected A549 cells under semi-solid overlay in control and SEPT7, Borg2 and SEPT7+Borg2-depleted conditions. Borg2 depletion increases virus spread, while SEPT7

knockdown has the opposite effect. Error bars represent SEM from three and one independent experiments in which over 190 and 70 plaques for semi-solid and liquid overlay respectively were analysed; n.s. p-value > 0.05; **** p-value < 0.0001.

These rather unexpected results showed that overall Borg2 facilitates cell-to-cell spread of vaccinia. Furthermore, in the case of simultaneous depletion of SEPT7 and Borg2 pro- and anti-viral effects could partially cancel each other out, resulting, in most cases, in a slight increase in plaque size. This would suggest that septins have a stronger impact on vaccinia spread than Borg2. However, Borg2 might also affect other parts of the viral replication cycle. Given that Borg2 is an effector of Cdc42, which in turn is regulated by the virus, vaccinia could indirectly influence Borgs to its advantage.

Next, I also compared virus release upon SEPT7 or Borg2 depletion. While septin depletion led to a 1.8-fold increase in virus release, Borg2 depletion decreased virus release by 54%. (Figure 5.11). In case of the YdF virus, the trend was the same but Borg2 knockdown did not significantly reduce virus release. These data indicate that the decrease of virus spread when depleting Borg2 is at least partially due to reduced levels of virus release. Furthermore, Borg2-mediated enhancement of virus release and spread is more pronounced in the WR virus.

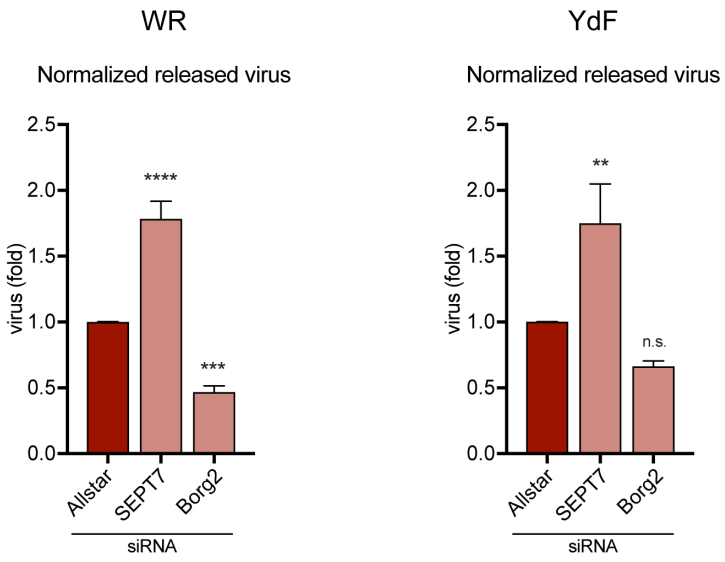

Figure 5.11 Borg depletion decreases virus release

Quantification of WR and YdF virus titer released from control, SEPT7 and Borg2-depleted A549 cells after 18 hours of infection. Error bars represent SEM from three independent experiments; n.s. > 0.05; ** p-value < 0.01; *** p-value < 0.001 **** p-value < 0.0001.

5.3 Summary

After investigating septin recruitment and loss from CEV I have now explored the effects of septins during virus egress and spread. Knockdown of SEPT7 leads to more and longer actin tails with an extended life-time. On a more macroscopic scale, septin depletion increases the cell-to-cell spread of vaccinia. The inhibitory effect of septin on virus release occurs regardless of whether the virus can form actin tails or diffuses through the media. While septin depletion does not significantly change the entry and replication of the virus, more EEV are released from infected cells. In WR infected cells dynamin efficiently displaces septins from the virus. Therefore, virus release and spread should be decreased in dynamin knockout cells. Indeed, in the absence of dynamin there are significantly fewer and smaller plaques formed confirming a role of dynamin during vaccinia spread. Single-step growth curves revealed a supportive role of dynamin during the virus replication cycle prior to virus egress. Unfortunately, this additional earlier involvement of dynamin obscures later effects during egress. Looking at another group of proteins that have the ability to regulate septins, I found that Borg2 is required for septin recruitment to virus particles. While Borg2 knockdown phenocopies septin depletion in terms of actin tail dynamics, it has opposing effects on virus release or spread. Furthermore, it seems as if Borg2-mediated enhancement of virus release and spread is more prominent in WR than YdF infected cells. Identifying the additional role of Borg2 during vaccinia infection and investigating if and how Borg2 mediates septin recruitment to the virus will be part of future work.

Chapter 6. Discussion

Septins are conserved components of the cytoskeleton that are involved in a variety of fundamental cellular processes including division, migration and membrane trafficking (Bridges and Gladfelter, 2015, Fung et al., 2014, Mostowy and Cossart, 2012, Saarikangas and Barral, 2011). In addition, septins can suppress bacterial infection by forming cage-like structures around pathogens such as *Shigella* or *Listeria* (Mostowy et al., 2009a, Mostowy et al., 2010, Mostowy et al., 2011, Sirianni et al., 2016). In this thesis, I investigated the role of septins during vaccinia virus infection. I demonstrate that septins are recruited to vaccinia during viral egress immediately following its fusion with the plasma membrane. RNAi-mediated depletion of septins results in increased virus release and accelerated cell-to-cell spread, as well as the formation of more and longer actin tails with prolonged life-times. Live cell imaging revealed that septins are displaced from the virus when vaccinia induces actin polymerization. I found that septin loss is dependent on the recruitment of the SH2/SH3 adaptor Nck, but not on Arp2/3-mediated actin polymerization. Moreover, it is the recruitment of dynamin by the third SH3 domain of Nck that is responsible for the displacement of septins from the virus. Furthermore, chemical inhibition of formins increases septin recruitment as seen with dynamin inhibition, indicating that formins are also involved in the displacement of septins. My work demonstrates that septins have an anti-viral effect and that dynamin is recruited to vaccinia to overcome septin “entrapment” to enhance virus release and spread.

6.1 Septins are recruited to vaccinia during viral egress

The aim of my thesis was to characterize the role of septins during vaccinia infection. Previous data from two siRNA screens demonstrated that knockdown of septins negatively impacts on replication and/or spread of vaccinia virus (Beard et al., 2014, Sivan et al., 2013). However, the experimental design did not define how or at which stage of the virus life-cycle septins exert their anti-viral effect. Given that septins are involved in the uptake and spread of several bacterial pathogens, including EPEC, *Shigella* and *Listeria* (Sirianni et al., 2016, Scholz et al., 2015, Mostowy et al., 2010, Mostowy et al., 2009a, Mostowy et al., 2009b), I started to explore the function of

septins in the context of vaccinia infection by visualizing endogenous SEPT7 in HeLa cells at various points of infection. Septins are recruited to vaccinia from 7 hours infection onwards when newly generated virus particles reach the plasma membrane and exit from the cell (Figure 3.2 and Figure 3.3). More specifically, septins co-localize with a subset of viruses that have already fused with the plasma membrane but remain attached to the cell. These virus particles are referred to as cell-associated enveloped viruses (CEV) (Figure 3.5). Live cell imaging revealed that septins are recruited to vaccinia just before the virus induces local actin polymerisation (Figure 3.8). These actin tails propel the virus onto neighbouring cells thereby greatly enhance virus spread (Frischknecht et al., 1999b, Rietdorf et al., 2001, Ward et al., 2003, Moreau et al., 2000, Welch and Way, 2013) and their formation marks the loss of septins from the virus.
A very similar behaviour has been observed previously for clathrin (Humphries et al., 2012, Snetkov et al., 2016). Prior to actin tail formation intersectin and Eps15 are recruited to vaccinia virus particles via three so-called NPF motifs in A36 and subsequently clathrin and AP-2 also localize to the virus (Humphries et al., 2012, Snetkov et al., 2016). Septin and clathrin accumulate at the virus approximately four and two minutes prior to actin tail formation respectively. Together both proteins are displaced by the newly formed actin tail. Their overlapping presence at the virus begged the question whether septin recruitment affects clathrin at the virus or vice versa. My work in chapter 3.2.3 showed that neither is the case, since, septin and clathrin are recruited independently of one another to vaccinia.

Using conventional fluorescence microscopy is limited by the diffraction limit of light and it is therefore only possible to separate two structures if they are spaced apart more 200-350 nm (Abbe, 1883, Coling and Kachar, 2001, Combs and Shroff, 2017). However, several “super-resolution” light microscopy techniques have been developed that achieve resolution far superior to traditional approaches. One of these methods is named structured illumination microscopy (SIM) and allows for lateral resolution of around 100nm (Schermelleh et al., 2008, Gustafsson, 2000, Gustafsson et al., 2008). Studying proteins located at vaccinia, which is 360x270x250nm in size (Cyrklaff et al., 2005), this advanced microscopy technique resulted in a sub-viral resolution (Gray et al., 2016, Horsington et al., 2012, Humphries et al., 2012). Imaging cells infected with a virus encoding a mutated A36R

gene encoding two tyrosine-to-phenylalanine substitutions (YdF) (Frischknecht et al., 1999b, Rietdorf et al., 2001, Ward et al., 2003, Moreau et al., 2000) that in addition expressed an RFP-tagged A3 core protein (RFP-A3L YdF) revealed that SEPT7 appears as a ring surrounding the virus. Looking at the orthogonal views, septins are found all along the length of the virus (Figure 3.10C and Figure 3.11B). However, with SIM the resolution in z is still expected to be between 250 and 350 nm, (Schermelleh et al., 2010, Huang et al., 2010) This is an improvement compared to confocal imaging with around 800nm z-resolution, but it still does not allow for any conclusion about the relative positioning of septin and the enclosed virus particle along the z-axis.

Therefore, I turned to scanning electron microscopy, which has a resolution of down to 50 pm (Erni et al., 2009) on “unroofed” cells, a method that has been successfully used to visualize clathrin-coated vesicle (see chapter 2.6.4) (Heuser, 1980, Heuser, 2000, Sochacki et al., 2017). Testing different “unroofing” and sample preparation protocols I was not able to preserve the structural features to the same extend as others had reported before. For example, I could not identify the typical clathrin lattice. Changing the drying step from air drying to critical point drying clearly improved the structural preservation, especially of actin filaments (Figure 3.16), however further adaptations will be required. One improvement may be to adapt the fixation step after the “unroofing”, such as using a combination of glutaraldehyde and PF followed by tannic acid and uranyl acetate, as performed by Sochacki and colleagues (Sochacki et al., 2017). Another option is to create platinum replica of the sample and image them with a transmission electron microscope (TEM), which could give better resolution than the platinum coat. However, my EM data indicates that some viruses are invaginated in a membrane pit and immunolabelling of SEPT7 suggests that septins surround the invaginated virus particle forming a cup-like structure that covers the “basolateral” sides of the virus (Figure 3.15). Given the cup-like structure, one can imagine how septins restrict the release of vaccinia by entrapping the virus particle. This could be achieved by a physical constriction of the membrane. Right after fusion, when the virus is still invaginated, septins might constrict the neck of the membrane pit and thereby the virus remains trapped in the invagination. Horsington and colleagues reported reduced levels of virus release in situations where actin polymerization is blocked, either by infecting with YdF virus or by using CytoD

treatment or Nck null cells or (Horsington et al., 2013). This work proposed that vaccinia virus particles remain trapped in a membrane pit and require local actin polymerization to be pushed outwards to successfully detach from the cell. It is tempting to suggest that septin entrapment contributes to the described retention during virus release.

Alternatively, the septin cup surrounding the virus could inhibit virus release and spread by masking the cytoplasmic parts of CEV proteins. Septins might sterically hinder Src and downstream proteins such as Nck, WIP and N-WASP from accessing A36. However, this speculation raises an interesting question. Namely, how are septins and clathrin arranged when both are present at the virus simultaneously? Clathrin was shown to form a coat underneath the CEV (Humphries et al., 2012). Since clathrin is recruited to the virus particle after septin, it might form an outer lattice surrounding the septin cup. Yet, this would require the cytoplasmic tail of A36 to extend through the septin layer to allow binding of Eps15/intersectin to the NPF motifs. Another possibility is that the clathrin lattice assembles between virus membrane and septin cup, which would require the triskelia to diffuse through the layer of septin. In chapter 4.2.4 I observed that septins are lost from the virus a few seconds before clathrin. If septins are indeed located between virus and clathrin coat, the disassembled septins would be required to diffuse through the clathrin coat. Alternatively, the delayed displacement of clathrin might be due to a slower disassembly rate of the clathrin coat compared with the septin “cup”. Additional high-resolution imaging is needed to resolve the precise arrangement of both proteins at the virus.

An invaginated virus particle has several parallels to the formation of a clathrin-coated vesicle. Although the virus is significantly larger than an average endocytic vesicle, which measures around 90nm (Heuser, 1980), they both recruit clathrin, AP-2, intersectin, Eps15, dynamin and the actin polymerization machinery, and both induce a branched actin network underneath (Kirchhausen et al., 2014, Robinson, 2015, Goode et al., 2015, Humphries et al., 2012, Snetkov et al., 2016). Yet in one case the actin polymerization drives the object inwards (clathrin-coated vesicle) and in the other case it pushes the object outwards (vaccinia virus). What determines the opposite outcome and which mechanisms apply to both systems? Would a larger

vesicle or a smaller virus go the opposite way? Certainly, the orientation of the actin filaments determines the direction of the exerted force. In case of the vesicle, filaments grow parallel to the plasma membrane towards the neck of the vesicle, as well as away from the plasma membrane towards the cell centre (Collins et al., 2011). In contrast, actin filaments associated with the CEV grow towards the plasma membrane pushing the virus outward (Cudmore et al., 1995, Cudmore et al., 1996). Yet how is the orientation of actin filaments determined? Might the formin-dependent actin burst seen on vaccinia viruses help polarize the actin outward? Formins, such as formin2 and mDia1, are involved in clathrin-independent endocytosis and phagocytosis, but not in clathrin-mediated endocytosis (Junemann et al., 2016, Brandt et al., 2007, Soykan et al., 2017, Lian et al., 2016). Does dynamin collaborate with formins during additional cellular processes? Is dynamin also preferentially recruited to the rim of the clathrin patch as seen during early steps of clathrin-mediated endocytosis and how does this correlate with Nck localization (Sodeik et al., 1993)?

Answering these questions will bring useful insights into the mechanistic similarities and differences between clathrin-coated vesicles and septin/clathrin-coated vaccinia virus particles, and may provide insights of wider cell biological significance.

6.2 How are septins recruited to the virus

Seeing that septins co-localize with CEV at the cell periphery raised the question of how septins are recruited to the virus particle. The drastic increase in septin recruitment to YdF viruses (Figure 4.1) led to our hypothesis that septins could be recruited to non-phosphorylated A36. A36 is found in the outer membrane of IEV and CEV and it gets phosphorylated by Src only on CEV prior to actin tail formation (Smith et al., 2002, Smith and Law, 2004). However, the recruiting signal of A36 would need to be in the context of the plasma membrane, since intracellular virions do not recruit septins. It has been shown that the largely disordered, cytoplasmic part of A36 has the ability to self-interact (Snetkov, 2015). This would allow intermolecular association between several A36 proteins, as well as adopting a closed conformation of the protein. It is not clear what could trigger the switch between closed and open conformation, but it would add another layer of regulation during viral egress

(Snetkov, 2015). Could it be possible that septins are only recruited to one of the two conformations? It had been speculated that the phosphorylation of A36 might impact on the open/closed conformation (Snetkov, 2015). Therefore, A36-YdF would only adopt one conformation and this might make it more efficient in recruiting septins. However, A36 was not required for septin recruitment and PP1 treatment in ΔA36 infected cells had no effect (Figure 4.7A) suggesting that the phosphorylation A36 triggers the displacement of septins from the virus. When the A36 gene was substituted with either the YLDV orthologue Y126 or a part of calsyntenin-1 to overcome the trafficking defect of the ΔA36 virus, high levels of septin recruitment were observed (Figure 4.7B,C) providing further evidence that A36 is not essential for septin recruitment.

Septins are often found at membranes and it was shown that they bind directly to PIP_2 (Bertin et al., 2010, Bridges and Gladfelter, 2015, Zhang et al., 1999). PIP_2 containing membranes can facilitate septin assembly (Bertin et al., 2010). In MDCK cells, septins are recruited to macropinosomes in a $PI_{(3,5)}P_2$-dependent manner (Dolat and Spiliotis, 2016). Conversely, it was shown that septins can redistribute PIP_2 on the plasma membrane (Sharma et al., 2013). In response to ER Ca^{2+} store depletion, septins and PIP_2 form clusters at ER-plasma membrane junctions to allow successful recruitment of ORAI1 Ca^{2+} channels to the septins and PIP_2 free regions (Sharma et al., 2013). In addition, in *Candida albicans* septins and PIP_2 are jointly redistributed at the plasma membrane in response to cell wall damage. Although it is not known whether septins recruit PIP2 or vice versa, a strong co-localization has been observed (Badrane et al., 2012, Badrane et al., 2016). Taken together these reports have given rise to the speculation that septins are recruited to PIP_2, which might be enriched at the plasma membrane underneath CEV. Interestingly, the Ebola virus protein VP40 was shown to enhance PIP_2 clustering (Johnson et al., 2016, Gc et al., 2016) and PIP_2 is also linked to Src and FAK signalling at focal adhesions (Goni et al., 2014). However, preliminary data using GFP-tagged PLCδ-PH domain, a PIP_2 reporter (Varnai and Balla, 1998, Stauffer et al., 1998), revealed that tagged PLCδ-PH is recruited to ~19, 25 and 7% CEV in WR, ΔNPF and YdF infected cells respectively. Less than 3% of all CEV show simultaneous recruitment of septins and the PIP_2 probe (Figure 6.1A,B).

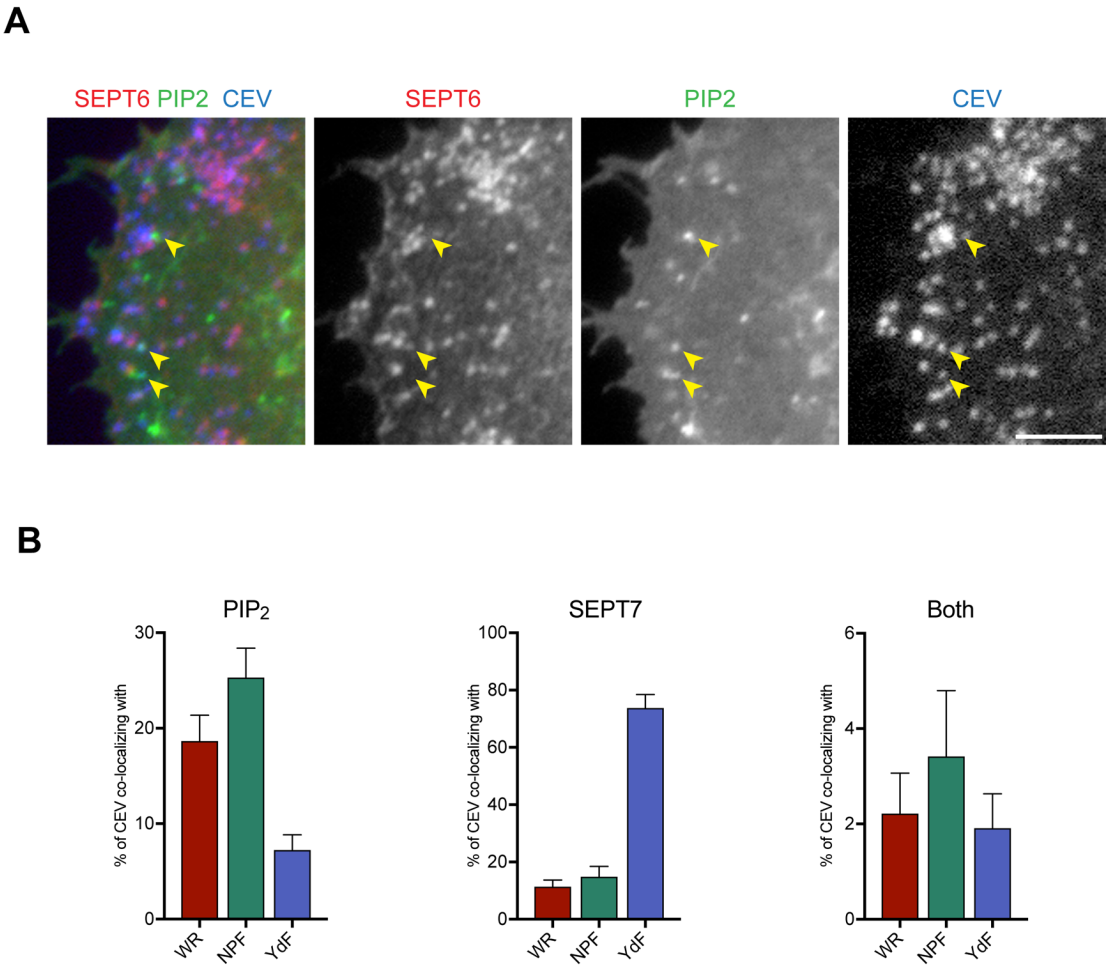

Figure 6.1 Septins and GFP-PLCδ-PH do not preferentially co-localize at the virus

A Immunofluorescence image of a HeLa cell infected with YdF for eight hours expressing GFP-PLCδ-PH as a marker for PIP_2 (green) and stained for SEPT7 (red) and CEV (blue). Yellow arrow heads indicate PIP_2-rich areas that are void of septins. Scale bar = 5 µm. **B** Quantification of CEV co-localizing with SEPT7, GFP-PLCδ-PH and both. Error bars represent SEM from over 30 particles counted in ten cells from one independent experiment.

This contrasts the studies of septins and PIP_2 surrounding ORAI1 channels, where a strong overlap of septins and the PIP_2 marker was reported (Sharma et al., 2013). However, given that both, the PLCδ-PH domain and septins, bind to PIP_2, they might be competing and this could result in a spatial anti-correlation. Using an antibody against PIP_2 may determine whether or not the membrane under the CEV is enriched in PIP_2. Further evidence for a competition between septins and PLCδ-PH domain may be gained by comparing recruitment of GFP-PLCδ-PH to vaccinia in control and septin-depleted cells. Alternatively, the levels of PIP_2 can be reduced at the plasma

membrane to determine the level of co-localisation of SEPT7 and CEV. Live cell imaging using the GFP-tagged PLCδ-PH domain will reveal if septins displace the marker from the virus or whether PIP_2 enrichment is linked to another specific step during viral egress.
However, the virus membrane is thought to be densely packed with viral proteins, and clathrin was shown to polarize A36 at the base of the virus (Humphries et al., 2012, Payne and Kristensson, 1990, Smith et al., 2002). Therefore, it is questionable how many lipids are exposed and accessible.

Another hypothesis to explain why septins accumulate at the virus could be that septins are recruited by the plasma membrane curvature at the CEV. Septins can induce tubulation and bending of membranes (Tanaka-Takiguchi et al., 2009), but more recent work has also shown that septin can sense positively curved membranes and show preferential binding to lipid-coated beads with a diameter of 1-3 µm (Bridges et al., 2016). Vaccinia is only 250-300nm in size, however, septins were also found on slightly smaller beads with similar dimensions as vaccinia (Bridges et al., 2016, Cyrklaff et al., 2005). Unfortunately, confirming that the membrane curvature is required and sufficient to recruit septins to the virus is experimentally challenging. As an initial test, I used latex beads with 250 nm diameter and added them on top of uninfected GFP-SEPT6 cells. Interestingly, I found that some of the beads recruited septins in a very similar fashion as CEV (Figure 6.2). Live cell imaging showed that septin recruitment can remain stable over several minutes. My current results do not yet prove that these beads really induce membrane curvature and it cannot be excluded that the beads induce any other reactions in the cell. However, the hypothesis that the membrane curvature surrounding the invaginated CEV is sensed by septins remains attractive. Combined with the finding that YdF viruses are more often found in membrane pits than WR viruses, which by contrast sit on a flatter patch of plasma membrane (Horsington et al., 2013) this could explain the increased levels of septin recruitment to YdF.

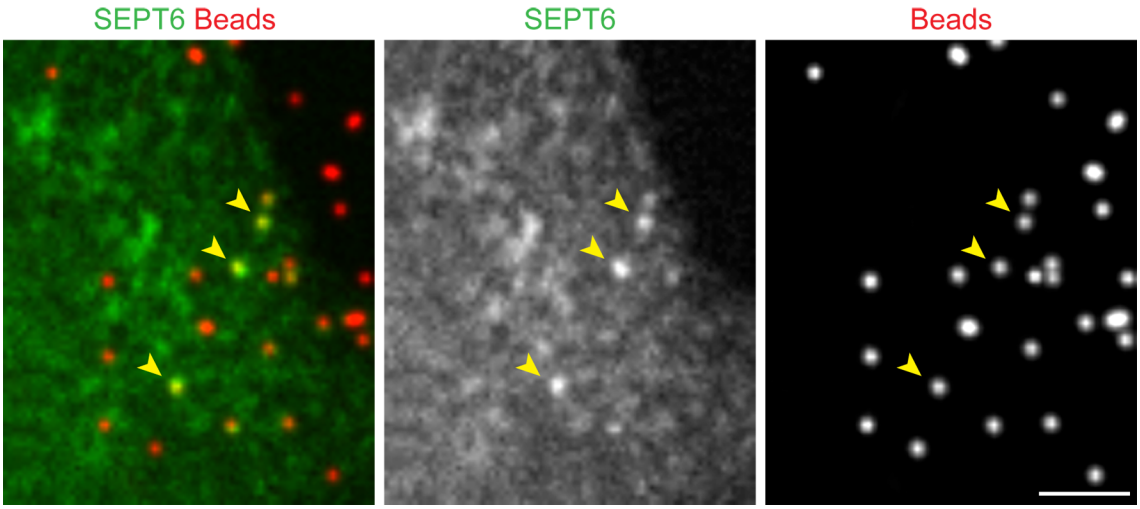

Figure 6.2 Latex beads can also recruit septins

Latex beads (red) were added on top of GFP-SEPT6 HeLa cells (green). Yellow arrow heads indicate the enrichment of septins associated with latex beads. Scale bar = 2μm.

6.3 What causes the loss of septins from the virus?

Given the similarities between the recruitment of clathrin and septin in respect to actin tail formation, I speculated that actin polymerization physically pushes the virus away from the septins which then disassemble, similarly to the clathrin coat (Humphries et al., 2012). This hypothesis was supported by experiments using the YdF virus, which is deficient in actin tail formation. I found that 85% of YdF CEV co-localized with septins and it was noticeable that CEV accumulated in clusters at the cell periphery (Figure 4.1). However, using the Arp2/3 inhibitor CK666 I found that WR still recruits septins to the same extent as in control cells (Figure 4.2A). In order to confirm that the absence of actin tails did not change septin recruitment, I took advantage of the N-WASP knockout MEFs. WR had low levels of septin recruitment, while YdF showed high levels in both the parental and knockout cells (Figure 4.2B). These results further demonstrated that it is not Arp2/3-mediated actin polymerization itself that impacts on septin recruitment. Additionally, neither WIP nor N-WASP recruitment, which are recruited to A36 as a complex (Donnelly et al., 2013, Moreau et al., 2000, Weisswange et al., 2009), changes septin levels at the CEV.

One hypothesis for the differential septin levels at WR and YdF viruses, was that the phosphorylation of A36 or subsequent events are responsible for the loss of septins from the virus. Given the role for Src-dependent phosphorylation of A36 (Leite and Way, 2015), I investigated the potential effects of Src on septins. From my experiments, I could conclude that roughly 3% of all WR CEV recruit Src and SEPT7 simultaneously and although YdF recruits five times more septin, the percentage of septin co-localizing with active Src is half of what is observed in WR infected cells (Figure 4.3A-C). Chemical inhibition of Src drastically increased septin levels at the CEV, mimicking the situation in YdF infected cells (Figure 4.4C). Furthermore, overexpression of Src-GFP strongly reduced the levels of septin recruitment at both WR and YdF CEV (Figure 4.4B). This lead to the hypothesis that septins might be regulated by phosphorylation. Unfortunately, pull-down experiments looking at potential phosphorylation of septins by Src could neither exclude nor confirm phosphorylation of septins by Src (Figure 4.5). Performing FRAP experiments on septins in the absence or presence of the Src inhibitor PP1 may be able to determine whether Src can change the dynamics of septins. To exclude indirect effects on septin phosphorylation and assembly from components in the cell lysate, in vitro experiments using purified septins and Src could in the future establish whether the kinase induces septin filament assembly/disassembly.
However subsequent experiments using the Nck and Dynamin knockout cells indicate that septin phosphorylation by Src is not the trigger for septin displacement (Figure 4.8A and Figure 4.12B). Moreover, septins are only reported to be phosphorylated on serine or histidine residues (Longtine et al., 1998, Sinha et al., 2007, Tang and Reed, 2002, Dobbelaere et al., 2003, Garcia et al., 2011, Egelhofer et al., 2008, Yu et al., 2009, Gonzalez-Novo et al., 2008, Meseroll et al., 2012, Meseroll et al., 2013, Cvrcková et al., 1995, She et al., 2004, Chi et al., 2007). Utilizing mass spectrometry comparing septins in infected and uninfected cells would give precise information about potential changes in septin phosphorylation.

In uninfected cells, I observe a striking absence of co-localization between active Src and septins (Figure 4.4A). Previously, septins were shown to enhance maturation of focal adhesions, which also depend on and co-localize with active Src. Yet septins have only been observed adjacent to, but not overlapping with the focal adhesion marker paxillin (Dolat et al., 2014). Hence it would be interesting to investigate what

underlies the mutual antagonism between Src and septins. Do Src and septins compete for the same binding site along the actin filament or are septins directly regulated by Src? And what are the implication of this spatial separation in the cell?

6.4 How can dynamin replace septins?

In chapter 4.2.3 showed that in the absence of Nck, WR and YdF CEV co-localize with SEPT7 at similarly high levels. Reintroduction of various Nck mutants, in which one or all SH3 binding sites were disrupted by a single amino acid substitution, showed that Nck needs its third SH3 domain to efficiently displace septins from the virus (Figure 4.8B). This indicated that steric hindrance by Nck was less likely to be the cause of low levels of SEPT7 and CEV co-localization, but rather a downstream binding partner of Nck. Following a literature review of proteins that have been reported to specifically bind to the third SH3 domain in Nck I pursued several potential candidates for their ability to displace septins from vaccinia.

I found that depletion of DIP/SPIN90/WISH and inhibition of casein kinase 1+2, respectively, had no effect on septin recruitment to CEV. Immunostaining for SOS, another protein that interacts with the third SH3 domain of Nck (Hu et al., 1995, Wunderlich et al., 1999), also indicated that the protein was not present at the CEV. A further interesting candidate was the GTPase dynamin, which also selectively binds to the third SH3 domain of Nck (Wunderlich et al., 1999). Dynamin has been reported several times to interact with a range of pathogens, often associated with clathrin or actin, both of which are present at CEV (Bonazzi et al., 2011, Veiga et al., 2007, Veiga and Cossart, 2005, Fukumatsu et al., 2012, Lee and De Camilli, 2002, Orth et al., 2002, Unsworth et al., 2007, Henmi et al., 2011). For instance, during Listeria entry, dynamin is required for successful uptake of the bacterium (Bonazzi et al., 2011, Veiga et al., 2007, Veiga and Cossart, 2005, Fukumatsu et al., 2012). There dynamin is thought to promote actin re-organization via cortactin, a regulator of actin which is also found in vaccinia actin tails (Abella et al., 2015, González-Jamett et al., 2013, Bonazzi et al., 2011, Veiga et al., 2007, Veiga and Cossart, 2005). Furthermore, dynamin is present at and promotes the formation of Listeria-induced actin tails, as well as EPEC actin pedestals (Lee and De Camilli, 2002, Orth et al.,

2002, Unsworth et al., 2007, Henmi et al., 2011). Interestingly, in the case of EPEC, dynamin recruitment depends on Nck and N-WASP (Unsworth et al., 2007). Because of these similarities to the vaccinia machinery, I investigated the potential role of dynamin in regulating septin recruitment to CEV. Previous work from our laboratory has shown that over-expressed GFP-dynamin II did not co-localize with vaccinia actin tails (Scaplehorn et al., 2002, Unsworth et al., 2007). Furthermore, over-expression of the dominant negative mutant Dyn K44A or ΔPRD had no effect on the number of infected cells displaying actin tails, suggesting that dynamin is not required for actin tail formation (Unsworth et al., 2007).

Staining for endogenous dynamin II, I found that roughly 13% of WR CEV recruited dynamin, whereas in YdF infected cells, where no Nck is recruited and high levels of septin are present, dynamin is only found on 3% of the CEV (Figure 4.9B). This, and the observation that in Nck-/- cells both WR and YdF CEV have high levels of septins and very low levels of dynamin (Figure 4.9C), supports the hypothesis that dynamin is recruited downstream of Nck and might be involved in displacing septins. However, viruses lacking the NPF motifs in A36 show a slight reduction in dynamin recruitment, ΔNPF ~7% and YdF ΔNPF ~1.5% (Figure 4.11E). This suggests that intersectin-1, a known binding partner of dynamin (Okamoto et al., 1999b, Roos and Kelly, 1998, Sengar et al., 1999, Yamabhai et al., 1998), also partially contributes to dynamin recruitment. Dynamin as well as clathrin have a preference for strongly, positively curved membranes (Zhao et al., 2017). It is conceivable that the membrane curvature induced by the invaginated virus further aids the recruitment of dynamin to the virus.

Live cell imaging revealed that dynamin is recruited to WR after septin and clathrin but slightly before onset of actin tail formation (Figure 4.10). Given the presence of actin, clathrin and dynamin, I compared the protein dynamics between virus egress and clathrin-mediated endocytosis in Figure 6.3.

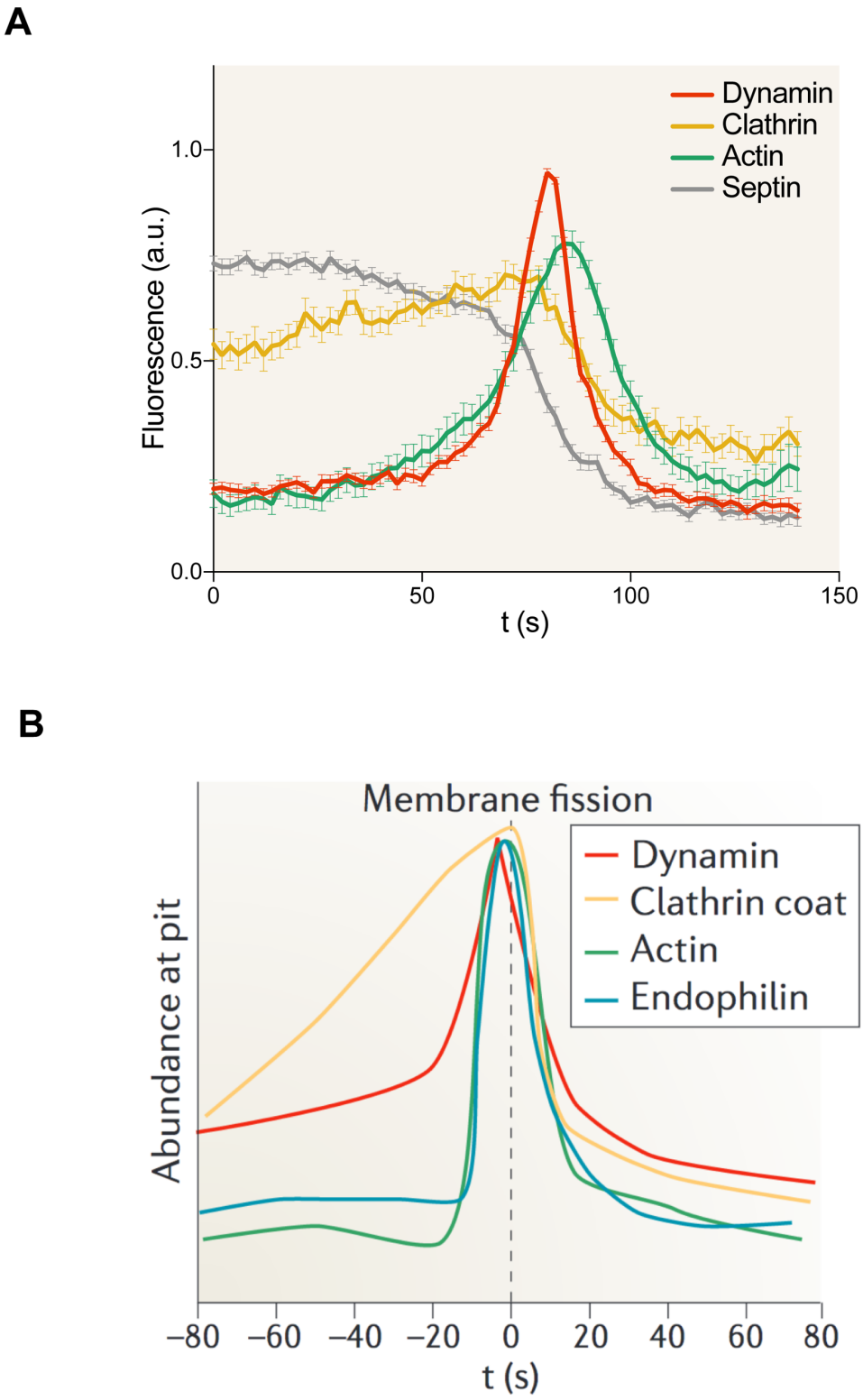

Figure 6.3 Comparing proteins at the CEV and on forming endocytic vesicles

Schematic of protein intensities at CEV (**A**) and during CME (**B**) over time. Clathrin accumulation is terminated by a transient recruitment of dynamin and actin. **B** Data from Taylor et al., 2011; picture taken from © Ferguson and De Camilli, 2012 originally published in Nat *Rev Mol Cell Biol* 1471-0080.

A transient recruitment of dynamin marks the loss of septins from the virus. Actin polymerization peaks shortly after dynamin recruitment and following the initial actin burst, a typical actin tail is initiated in most cases. Yet since the fluorescence intensity is monitored only locally in the ROI, actin intensity decreases as the virus is propelled away and the filaments disassemble. Septin is present at the virus on average 4 minutes prior to actin tail formation and clathrin is usually recruited 2 minutes before onset of actin tail formation. Interestingly, while septin intensity appears unchanged or slightly reduced, clathrin keeps accumulating until the arrival of dynamin marks the loss of both septin and clathrin. Dynamin is recruited for roughly 40 seconds to the virus. Actin accumulates together with dynamin but it reaches its peak intensity a few seconds after dynamin does. This might suggest that dynamin induces this actin polymerisation. Live cell imaging of infected Dyn knockout cells will determine if this actin burst relies on dynamin. Moreover, the requirement for Dynamin GTPase activity can be assessed by reintroduction of the GTPase-dead mutant into the knockout MEFs.

The accumulation of clathrin followed by a transient burst of actin concomitant with dynamin recruitment that I observed is also reported to occur during mammalian endocytosis (Taylor et al., 2011). Here, the linear accumulation of clathrin appears steeper, but is equally terminated by a transient recruitment of dynamin, lasting around 40 sec. In the case of endocytosis, the maxima of actin and dynamin coincide and their recruitment was shown to be interdependent (Taylor et al., 2012). To my knowledge septins have not been reported to localize to CME. While it is easy to see the similarities in the protein dynamics at the virus and on forming endocytic vesicles, it is less clear where the functional similarities lie, particularly for dynamin. For example, it seems unlikely that dynamin can fulfil its function as a membrane scission protein at the CEV. It will be interesting to see where precisely dynamin localizes at the virus. Given that dynamin is also found on the rim of clathrin patches prior to its localization at the neck of the vesicle (Sochacki et al., 2017), one might speculate that dynamin is equally found at the outer border of clathrin at the CEV. Super-resolution microscopy might be able determine the precise localization of dynamin at the virus. In an alternative approach, I plan to perform immunogold labelling of

“unroofed” cells using the dynamin antibody. However, the caveat in this experiment may be that the rather rare and transient nature of dynamin recruitment will be less advantageous when performing electron microscopy.

There are a variety of chemical inhibitors for dynamin available. Dynasore, for example, blocks the GTPase activity of dynamin (Macia et al., 2006) but it was shown to have additional off-target effects (Park et al., 2013, Preta et al., 2015). Therefore, data obtained with this drug must be interpreted with caution. Therefore, I decided to use the drug MiTMAB, which prevents localization of dynamin to the plasma membrane without impacting on its GTPase function (Hill et al., 2004, Quan et al., 2007). Treating the infected cells with this inhibitor significantly increased the percentage of CEV co-localising with SEPT7 (Figure 4.11A). Given the temporal order seen in live cell imaging, it suggests that dynamin can displace septins from the virus. However, the effect was not as prominent as with the Src inhibitor, which might either indicate that there is an additional factor involved that either acts in parallel to dynamin or has the capacity to compensate for the absence of dynamin at the CEV. Alternatively, it could suggest that the drug treatment only partially inhibits the function of dynamin. While PP1 blocks the kinase activity of Src, MiTMAB only prevents the recruitment of dynamin to the plasma membrane (Hanke et al., 1996, Hill et al., 2004, Quan et al., 2007).
In experiments using the tamoxifen-inducible dynamin triple knockout MEFs I showed that in the absence of any dynamin, WR and YdF CEV co-localized with septins to the same extent, whilst in the control cells WR showed low levels and YdF high levels of septin recruitment (Figure 4.12B). In agreement with the chemical inhibition experiment, actin tail formation was reduced in dynamin knockout cells, however, the average tail length was indistinguishably different (Figure 4.12C). Whether this difference is caused by cell type differences (HeLa vs MEFs) or whether increased tail length is a side effect of MiTMAB remains to be investigated. For example, it could also be that upon MiTMAB treatment, when dynamin is no longer recruited to the membrane but accumulates in the cytoplasm, it is still able to globally influence actin dynamics.

Overall, I conclude that dynamin displaces septins from the virus. However, the obstructive dynamics between septin and dynamin appears to be bi-directional

because dynamin recruitment to CEV is enhanced in septin-depleted cells (Figure 4.12D). This could be indicative of steric hindrance, as both proteins are recruited by different means to the virus but once there they would occupy the same space. In contrast to Nck, which is only around 50 kDa, dynamin is 100 kDa and importantly has the ability to self-assemble into spiral-shaped multimers, which might peel off the septins from the virus.

In addition, my data supports the idea that dynamin facilitates actin tail formation, as seen during EPEC and Listeria infection (Henmi et al., 2011, Unsworth et al., 2007, Orth et al., 2002). Whether septins suppress actin tail formation and dynamin alleviates this inhibition, or whether dynamin promotes actin polymerization in a more direct manner is the key question to be resolved.

6.5 Can dynamin induce formin-dependent actin polymerization?

Noticeably, the loss of septin and increase of dynamin at the virus always coincides with a burst of actin (Figure 4.10). This transient actin polymerization can either result in an Arp2/3 driven actin tail or it subsides and the virus remains stationary. So far it remains unclear, whether this transient actin burst is Arp2/3-driven or not. Could it be initiated by dynamin and, unlike the actin tail, be involved in the displacement of septins from vaccinia? Dynamin has the capacity to directly bind actin and promote its polymerisation (Schafer et al., 2002, Gu et al., 2010). I showed that blocking all actin polymerization with CytoD or only inhibiting formins with the drug SMIFH2 promotes septin recruitment to vaccinia (Figure 4.13). This suggests that formins are involved in septin displacement. Interestingly, combined inhibition of dynamin and formins had no additive effect, suggesting that they do not act independently of each other (Figure 4.13). However, up to now I have no proof that the observed effect of SMIFH2 is indeed due to local formin inhibition at the CEV, and not caused indirectly by global formin perturbation. Future experiments are needed to investigate whether the actin burst concomitant with dynamin recruitment is formin-driven, and whether formin activity at the CEV is dependent on dynamin.

It was reported that FHOD1 is present all along vaccinia induced actin tails and that it promotes downstream of the small GTPase Rac tail formation and virus spread by nucleating actin filaments from which Arp2/3 can branch of new daughter filaments (Alvarez and Agaisse, 2013). However, in my hands, knockdown of FHOD1 neither changed septin recruitment nor actin tail formation in WR and ΔNPF infected cells (Figure 6.4). However, in vitro experiments showed that FHOD1 only has capping activity and was neither nucleating nor elongating actin filaments (Schonichen et al., 2013). Equally there was no effect on virus associated septin or actin following a combined knockdown of mDia 1+2 (Figure 6.4). Hence more work is required to identify which of the 15 formins are capable of displacing septins.

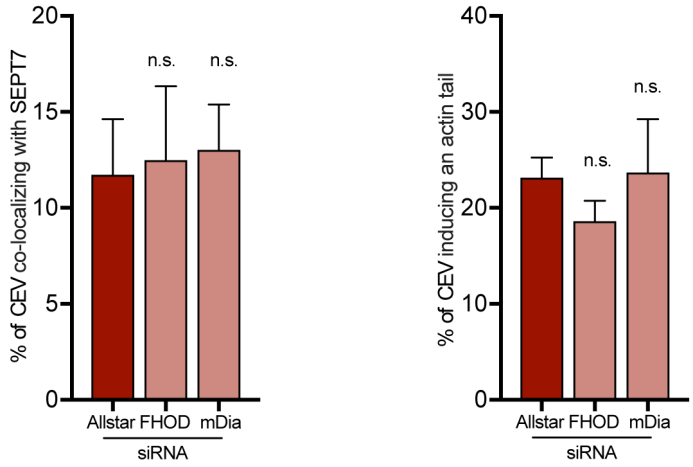

Figure 6.4 Knock-down of FHOD1 or mDia 1+2 has no effect on actin tail formation or septin recruitment

The graphs show the quantification of the % of CEV recruiting SEPT7 or inducing an actin tail. Error bars represent SEM from three independent experiments in which over 900 virus particles were analysed; n.s. indicates a p-value > 0.05.

Currently it is also unknown whether dynamin can directly interact with formins. Mitochondrial fission, for example, is another event where septins, dynamin-related proteins, formins and Arp2/3-dependent actin polymerization are present at a membrane (Pagliuso et al., 2017). However, the temporal order and functions differ because during mitochondria division actin was shown to precede and recruit Dynamin-related protein1 (Drp1) to the side of fission, while at vaccinia dynamin accumulates before actin (De Vos et al., 2005, Ji et al., 2015). Drp1 can directly bind to actin, which at the mitochondria is nucleated by Arp2/3, inverted formin 2 (INF2),

as well as Spire1C (Korobova et al., 2013, Manor et al., 2015, Li et al., 2015). Like actin, septins can also bind Drp1 and promote mitochondria fission by guiding Drp1 to the mitochondria (Pagliuso et al., 2016, Sirianni et al., 2016). Interestingly, Dyn II is transiently recruited to mitochondria downstream of Drp1 and required for the terminal abscission step (Lee et al., 2016). Overall, it appears that similar players are involved in different processes, however their interdependence and timings can vary.

Furthermore, dynamin has been reported to regulate and stabilize filopodia to promote cell migration (Chou et al., 2014, Yamada et al., 2013, Yamada et al., 2016). While in one study, dynamin was shown facilitate filopodia initiation by binding to IRSp53 (Chou et al., 2014), other work showed that dynamin and cortactin form a ring around actin filaments that bundles and stabilizes filopodia (Yamada et al., 2013, Yamada et al., 2016). Future experiments will determine how formins facilitate tail formation as well as septin displacement, and whether GFP-IRSp53 is recruited to the virus.

When using the formin inhibitor SMIFH2 in ΔNPF infected cells I made a surprising discovery (Figure 4.14). While septin recruitment was equally increased upon dynamin and formin inhibition as seen in WR infected cells, the effects on actin tails differed remarkably. Blocking formins during WR infection did not change the number of actin tails but slightly increased the average tail length. In contrast, in ΔNPF infected cells treatment with SMIFH induced the formation of many more but drastically shorter actin tails (Figure 4.14). This could indicate that that ΔNPF viruses become much more efficient in inducing an actin tail in the presence of SMIFH2, but the pool of available G-actin is limiting the tail length. It is currently still under debate whether or not monomeric actin can be a limiting factor for actin polymerization in the cell (Suarez and Kovar, 2016, Davidson and Wood, 2016, Raz-Ben Aroush et al., 2017). Alternatively, it could also be that ΔNPF is impaired in actin tail formation in the presence of SMIFH2, only weakly inducing actin clouds, similar to the structures seen in Y112F infected cells (Horsington et al., 2013, Scaplehorn et al., 2002). In either case, it will be interesting to investigate what underlies this distinct outcome to the same perturbation. We know that ΔNPF viruses cannot recruit AP-2, Eps15, clathrin, intersectin1 or active Cdc42 (Humphries et al., 2012, Snetkov et al., 2016). Cdc42 is activated by intersectin1 and in turn activates and stabilizes N-WASP at the virus (Humphries et al., 2014, Snetkov et al., 2016). Since formins need to be

activated by small GTPases, this would indicate that formins, which are only activated by Cdc42 (such as mDia3 or INF2) are not involved in actin tail formation because they would not be present in ΔNPF associated tail formation and hence SMIFH2 would not have an effect on those actin structures. However, if the inhibitor is only partially blocking formin activity and Cdc42 is helping but not essential for formins at the virus, then the combination of partial inhibition and reduced efficiency might cause the rather severe tail phenotype. To shed light onto this matter, in future work I will investigate septin recruitment to CEV in Cdc42 knockout cells to test whether Cdc42 is masking the effect of SMIFH in WR infected cells or whether other proteins cause the opposing effects of SMIFH on WR and ΔNPF induced tails. Furthermore, a systematic knockdown of all formins might also be a good way of identifying formins that affect actin tail formation in both WR and ΔNPF infected cells.

6.6 Septins suppress actin tail formation

Depletion of septins in infected cells results in more and longer actin tails (Figure 5.1A and B), while the time between microtubule-based transport and actin tail initiation is unchanged (Figure 5.1D). This suggests that the increased number of actin tails is not due to accelerated tail formation. It rather seems that once the tail is initiated, maintaining the actin polymerization is easier, since the average life-time of an actin tail is significantly prolonged in septin-depleted cells (Figure 5.1E). One possible explanation would be that the underlying architecture of the branched actin network is altered in a way that it leads to longer tails that are less sensitive to disassembly. For example, if the overall filament and/or branch density is increased, then there are more mother filaments available to propel the virus and allow the Arp2/3 complex to nucleate new daughter filaments. Increased filament density also slows down actin tail disassembly, since the network is less accessible to depolymerisation factors. Additionally, it takes longer to depolymerize all filaments simply due to their increased number (Pollard and Borisy, 2003, Carlsson, 2010, Lee and Dominguez, 2010, Svitkina and Borisy, 1999, Wachsstock et al., 1994). The very high density of actin filaments in a vaccinia actin tail made previous attempts to track and quantify the filaments unfeasible (Pfanzelter, 2013). Quantitative fluorescence

imaging might indicate whether the actin density along the actin tails changes (Abella et al., 2015).

Interestingly, although actin replaces clathrin and inhibition of actin tails in WR infected cells leads to an increase in CEV co-localising with clathrin (Humphries et al., 2012), I found that YdF has the same levels of clathrin recruitment as WR (% of CEV co-localizing with AP-2: WR 25.6 ± 2.3% YdF 21.5 ± 1.2%; p-value > 0.05 indicating no significant difference using over 900 particles from three independent experiments). This indicates that septin and clathrin are regulated in different ways at the virus.

It is slightly surprising that actin tails propel vaccinia with the same speed and directionality forward in control and septin-depleted cells despite their increased length. Previously it was shown that in some cases longer actin tails correlate with faster virus movement (Abella et al., 2015, Humphries et al., 2012, Snetkov et al., 2016). In one case, different isoforms with distinct branching abilities changed the actin dynamics in the tail (Abella et al., 2015). In the other case, it was shown that the clathrin coat formed under the virus prior to actin tail formation helps to cluster A36, thereby increasing the local density of binding sites for Nck, Grb2 and subsequently increased Arp2/3 activation (Humphries et al., 2012, Snetkov et al., 2016). Depletion of clathrin reduces the efficiency of actin tail initiation and results in longer and faster actin tails due to higher turnover of N-WASP at the CEV (Humphries et al., 2012, Snetkov et al., 2016).
It is possible that septins, similar to the clathrin coat change the dynamics of actin nucleators at the CEV through their presence prior to tail formation. Future FRAP experiments will determine if septin depletion changes the stability of Nck, Grb2 or N-WASP at the virus.

The cup-like septin structure underneath the CEV could also obstruct the recruitment of factors required for tail formation as well as phosphorylation of A36. Using MEFs only expressing GFP-tagged Nck or N-WASP, it should be possible to determine the number of these molecules at the virus by performing quantitative live-cell imaging (Verdaasdonk et al., 2014, Coffman and Wu, 2012).

My work demonstrates that septin depletion leads to an increased percentage of CEV co-localizing with dynamin (Figure 4.12D). Given that dynamin was shown to support local actin polymerization in other systems (Gu et al., 2010, Destaing et al., 2013, Palmer et al., 2015, Roux and Plastino, 2010, Krueger et al., 2003, Grassart et al., 2014) and dynamin might promote formin-driven actin polymerization, it is possible that the increase in dynamin recruitment, caused by septin depletion, also enhances actin tail formation.

However, since I do not know what recruits septins to the virus I cannot change the levels of septins at the virus without altering the total septin pool in the cell. Hence, I cannot exclude that the changes in actin tails are due to a global lack of septins and independent of the septin “cup” recruited to the CEV.

6.7 Septins inhibit virus release and spread

It has been previously observed, based on siRNA screens, that septin depletion changes the propagation of vaccinia through HeLa cells (Beard et al., 2014, Sivan et al., 2013). However, the experimental set up did not provide any mechanistic insight into how or where septins impact on the virus. I therefore set out to investigate the effects of septin depletion on virus entry, replication, release and spread. From single-step growth experiments, where the amount of produced virus after one replication cycle is measured, I concluded that virus entry and replication is not affected by septin knockdown (Figure 5.2B). Next, I determined in plaque assays how fast the virus can spread through a confluent monolayer of cells, in conditions where diffusion through the liquid media was prevented or allowed (semi-solid and liquid overlay respectively) (Figure 5.3). In liquid conditions vaccinia spread faster, forming so called plaque comets, indicative of increased virus release (Horsington et al., 2013, Mathew et al., 1999, McIntosh and Smith, 1996). Under semi-solid overlay situation increased plaque sizes were also observed, indicating that the direct cell-to-cell spread of the virus was also accelerated. Actin tails greatly enhance cell-to-cell spread (Doceul et al., 2012, Doceul et al., 2010, Horsington et al., 2013, Ward et al., 2003), therefore the increased number and life-time of actin tails might explain how septin knockdown increases virus spread. However, the same boost in

virus spread was also observed in YdF infected cells, where no actin tails are formed. Septins clearly have an additional negative impact on vaccinia egress that is independent of actin polymerization. Release assays revealed that more EEV are found in the media surrounding septin-depleted cells than control cells (Figure 5.4). Hence it is likely that the cup-like structure around the CEV might restrict their release from the cell into the supernatant.

6.8 Dynamin impacts on early steps of virus replication cycle

To test whether the absence of dynamin and subsequent increase in septin recruitment decrease virus release and spread I performed plaque and release assays on dynamin knockout cells. I found that the total amount of virus produced is significantly reduced, which results in decreased levels of virus release (Figure 5.5). Plaque assays revealed that significantly fewer and smaller plaques are formed (Figure 5.6). Since a plaque becomes only detectable after several rounds of infection it is unclear whether dynamin is involved in virus entry or later steps in replication. From previous work, it remained controversial whether dynamin was involved in vaccinia uptake or not. The chemical inhibitor dynasore was used at concentrations ranging from 40-160μM on HeLa cells and in some cases defects in vaccinia entry were reported (Huang et al., 2008a, Laliberte et al., 2011, Schroeder et al., 2012), while other studies saw no change in virus uptake even at high concentrations of dynasore (Mercer and Helenius, 2008, Mercer et al., 2010a). Overexpression of dominant-negative dynamin also had varying effects on virus entry (Mercer et al., 2010a, Huang et al., 2008a, Schroeder et al., 2012). Performing virus entry assays with the triple dynamin knockout cells would help to resolve this controversy.

6.9 How do Borgs affect vaccinia replication and spread?

Borgs are effectors of Cdc42 and can regulate septins (Hirsch et al., 2001, Joberty et al., 1999, Joberty et al., 2001). Borg3 for example was shown to bundle septin filaments and overexpression of Borgs can disrupt the septin network by aggregation of the septins (Joberty et al., 2001). In C. difficile infection, Borgs are required to

recruit septins to the future protrusion site of microtubule filled extensions (Nölke et al.). Borg2 can interact with both septins and actin (Calvo et al., 2015), I therefore investigated its role during vaccinia egress. Overexpressed Borg2 had a very similar location in the cell as septins and was also present at CEV (Figure 5.7). Knockdown of Borg2 did not affect the expression level of septins, however, it drastically reduced the percentage of WR and YdF CEV co-localizing with SEPT7 (Figure 5.8). In addition, I noticed that the overall septin cytoskeleton appears changed, with fewer distinct structures at the plasma membrane. Depletion of Borg2 and reduced septin levels at the virus also led to more and longer actin tails, as seen with SEPT7 knockdown (Figure 5.9). These data indicate that Borg2 acts upstream of septin. Similar effects were seen during Clostridium difficile entry, where Borgs recruit septins to the entry site (Nölke et al., 2016). However, virus release and spread assays in Borg2-depleted cells suggest that the situation is more complex. Whilst septins supress virus release, Borg2 enhances it (Figure 5.11). Similarly, plaques in Borg2-depleted cells are smaller, whereas septin knockdown increases plaque diameter (Figure 5.10). Combined knockdown results in slightly larger or wild-type plaques. However, the effect of Borg2 knockdown on plaque size is less pronounced in conditions where no diffusion or no actin tail formation occur (Figure 5.10). Taken together my data suggests that Borg2 has an additional septin-independent function during vaccinia infection. More work is needed to define the role of Borgs during vaccinia infection, since we don't know which Borgs are expressed in our HeLa cells and to which degree they act redundantly. From the plaque assay no strong implication of Borgs in virus entry could be deduced, since the number of formed plaques in Borg2-depleted cells was comparable to control cells. Single-step growth curves will tell if the reduced release in Borg2-depleted cells is caused by impaired virus replication. Given that Borgs are effectors of Cdc42, it will be interesting to see if, when and where the small GTPase has indirect effects on vaccinia through the regulation of Borg2 and subsequent changes in septin behaviour. Interestingly in the absence of Cdc42, virus plaques are smaller however they are also decreased in number (Snetkov et al., 2016), indicating that Cdc42 but not Borg2 affects virus uptake. Furthermore, future experiments will determine whether Borgs are recruited to ΔNPF CEV, where no active Cdc42 is present, or to WR in Cdc42 null cells. The role of the other Borgs and to which degree they are redundant in the context of vaccinia infection is another line of future investigation. In addition, it remains to be

established if Borgs are essential for septin recruitment to CEV or whether the reduced levels of CEV co-localizing with septin upon Borg2 knockdown are not due to recruitment defects but rather an indirect effect of global Borg2 depletion.

6.10 Future perspective

Work presented in my thesis has clarified the inhibitory role of septins on vaccinia egress and spread. My studies have also shed light on the mechanism by which the virus overcomes the restrictive effects of septin. I have uncovered a new potential link between septins, dynamin and formins. New mechanisms of septin regulation are of great interest to the wider septin and cell biology fields, since not much is known about how assembly and disassembly of septins is orchestrated in the cell.

An unresolved aspect of the role of septins during vaccinia infection is the mechanistic basis of septin recruitment. Further work is needed to examine whether the membrane under the CEV is enriched in PIP2 and whether this is responsible for recruiting septins. The alternative hypothesis that the membrane curvature at the invaginating virus attracts septin, will be experimentally challenging. More work is needed to characterize the actin burst that coincides with septin displacement by dynamin recruitment. Using live cell imaging to test the effects of formin or Arp2/3 inhibition will help to identify the responsible actin nucleator. Given the suggested involvement of formins in septin displacement, a small siRNA screen of formins can quickly identify the responsible formin. Preliminary data suggest that dynamin induces this formin-dependent actin burst. Clarifying whether dynamin directly facilitates actin filament formation or whether it can recruit or activate actin nucleation factors, such as formins, is another important future goal. Interestingly, dynamin is mostly associated with branched actin networks. Identifying a potential, new link between dynamin and formin-driven actin polymerization would bring new and exciting insights into the regulation of actin and might identify additional functions of dynamin.

The transient presence of formins prior to actin tail formation would also add to the current debate of how actin can convert between linear and branched networks and

whether one can support the other (Borinskaya et al., 2015, Carlier et al., 2015, Johnson et al., 2015b, Rotty and Bear, 2015). It has been previously proposed that formin derived filaments provide a template for the branched actin network to emerge and thereby facilitate vaccinia induced actin tail formation (Alvarez and Agaisse, 2013). However, in vitro FHOD only acts as a capping protein but has no actin nucleation or elongation activity (Schonichen et al., 2013). Hence, it will be useful to investigate why actin tails lacking clathrin:AP2, intersectin and active Cdc42 are more sensitive to formin inhibition than wild-type tails. The ΔNPF virus might help to identify the formin that is responsible for the transient actin burst and the subsequent displacement of septins.

Further research will also shed light on the involvement of Borgs during vaccinia replication. Dissecting septin-dependent and -independent effects of Borgs at different stages of the virus replication cycle will contribute to the understanding of this group of Cdc42 effectors.

Future structural work will determine the organization of septins, clathrin and dynamin at the virus. It will be useful to reveal how three components that all form higher ordered structures independently of one another are organized, and whether these networks are interconnected.

Chapter 7. Appendix

7.1 MATLAB script to measure septin ring diameter

```
clear all
close all
d = dir('*.csv');
d = {d.name};
dia=zeros(1,length(d));

for i = 1:length(d)
   b=readtable(d);
   [PKS,LOCS,W] = findpeaks(b.Y);
   doubleGauss = 'a*exp(-((x-b)/c)^2)+d*exp(-((x-e)/f)^2)';
   f1 = fit((1:length(b.Y))',b.Y,doubleGauss, 'Start', [PKS(1), LOCS(1), 2, PKS(2), LOCS(2), 2]);
   dia(i)=abs(f1.e-f1.b);

   % optionally plot fit and raw data to visually check the quality of the fit
   plot(1:length(b.Y),b.Y); hold on;
   plot(1:0.01:length(b.Y), f1(1:0.01:length(b.Y)));
end

dia_m=mean(dia);
```

7.2 MATLAB script to analyse protein intensities during virus egress

```
clear all
close all
e=NaN(1,600);
y=(0:2:600);
pic=44;

c1_col = 'r';
c2_col = 'g';
c3_col = 'b';

for j = 1 : pic

p(j).c1 = tiffread2(['D',num2str(j), '.tif']);
p(j).c2 = tiffread2(['S',num2str(j), '.tif']);
p(j).c3 = tiffread2(['A',num2str(j), '.tif']);

len = length(p(j).c1);
sz = size(p(j).c1(1).data);
c1_data = zeros(sz(1), sz(2), len);
c2_data = zeros(sz(1), sz(2), len);
c3_data = zeros(sz(1), sz(2), len);
c1_data_mean = zeros(1, len);
c2_data_mean = zeros(1, len);
c3_data_mean = zeros(1, len);
for i = 1:len
   c1_data(:, :, i) = p(j).c1(i).data;
   c1_data_mean(i) = mean(p(j).c1(i).data(:));

   c2_data(:, :, i) = p(j).c2(i).data;
   c2_data_mean(i) = mean(p(j).c2(i).data(:));

   c3_data(:, :, i) = p(j).c3(i).data;
   c3_data_mean(i) = mean(p(j).c3(i).data(:));
end

order = 5;
framelength = 11;
gol = @(x) sgolayfilt(x, order, framelength);
nor = @(x) (x-min(x))/(max(x)-min(x));
```

```
p(j).c1_mean = nor(c1_data_mean);
p(j).c2_mean = nor(c2_data_mean);
p(j).c3_mean = nor(c3_data_mean);

p(j).c1_filt = nor(gol(c1_data_mean));
p(j).c2_filt = nor(gol(c2_data_mean));
p(j).c3_filt = nor(gol(c3_data_mean));

[m, in] = max(p(j).c1_filt);
p(j).in = in;

q(j).c1_m_align=e;
q(j).c2_m_align=e;
q(j).c3_m_align=e;

for k = 1:len
q(j).c1_m_align(250-p(j).in+k)=p(j).c1_mean(k);
q(j).c2_m_align(250-p(j).in+k)=p(j).c2_mean(k);
q(j).c3_m_align(250-p(j).in+k)=p(j).c3_mean(k);
end


Dm(:,j)= q(j).c1_m_align;
Sm(:,j)= q(j).c2_m_align;
Am(:,j)= q(j).c3_m_align;


% optionally plot normalized intensity profiles of each movie

% figure
% hold on;
% plot(p(j).c1_mean, c1_col, 'LineWidth', 3)
% plot(p(j).c2_mean, c2_col, 'LineWidth', 3)
% plot(p(j).c3_mean, c3_col, 'LineWidth', 3)
%
% pause
end

Actm=nanmean(Am,2);
Dynm=nanmean(Dm,2);
Septm=nanmean(Sm,2);

Actme=nanstd(Am');
Dynme=nanstd(Dm');
Septme=nanstd(Sm');

figure
hold on;

errorbar(y(1:71),Dynm(210:280),Dynme(210:280), 'k','LineWidth', 1)
errorbar(y(1:71),Septm(210:280),Septme(210:280), 'k', 'LineWidth', 1)
errorbar(y(1:71),Actm(210:280),Actme(210:280),'k', 'LineWidth', 1)
xlabel('sec')
ylabel('intensity [a.u.]')

plot(y(1:71),Dynm(210:280), c1_col,'LineWidth', 3)
plot(y(1:71),Septm(210:280),c2_col, 'LineWidth', 3)
plot(y(1:71),Actm(210:280), c3_col, 'LineWidth', 3)
xlabel('sec')
ylabel('intensity [a.u.]')
legend('Dynamin','Septin', 'Actin')
```

Reference List

ABBE, E. 1883. XV.-The Relation of Aperture and Power in the Microscope (continued)*. *Journal of the Royal Microscopical Society,* 3**,** 790-812.

ABELLA, J. V. G., GALLONI, C., PERNIER, J., BARRY, D. J., KJÆR, S., CARLIER, M.-F. & WAY, M. 2015. Isoform diversity in the Arp2/3 complex determines actin filament dynamics. *Nat Cell Biol,* 18**,** 76-86.

AGETA-ISHIHARA, N., MIYATA, T., OHSHIMA, C., WATANABE, M., SATO, Y., HAMAMURA, Y., HIGASHIYAMA, T., MAZITSCHEK, R., BITO, H. & KINOSHITA, M. 2013a. Septins promote dendrite and axon development by negatively regulating microtubule stability via HDAC6-mediated deacetylation. *Nat Commun,* 4**,** 2532.

AGETA-ISHIHARA, N., YAMAKADO, H., MORITA, T., HATTORI, S., TAKAO, K., MIYAKAWA, T., TAKAHASHI, R. & KINOSHITA, M. 2013b. Chronic overload of SEPT4, a parkin substrate that aggregates in Parkinson's disease, causes behavioral alterations but not neurodegeneration in mice. *Mol Brain,* 6**,** 35.

AGHAMOHAMMADZADEH, S. & AYSCOUGH, K. R. 2009. Differential requirements for actin during yeast and mammalian endocytosis. *Nat Cell Biol,* 11**,** 1039-42.

AHUJA, R., PINYOL, R., REICHENBACH, N., CUSTER, L., KLINGENSMITH, J., KESSELS, M. M. & QUALMANN, B. 2007. Cordon-bleu is an actin nucleation factor and controls neuronal morphology. *Cell,* 131**,** 337-50.

AKIL, A., PENG, J., OMRANE, M., GONDEAU, C., DESTERKE, C., MARIN, M., TRONCHÈRE, H., TAVENEAU, C., SAR, S., BRIOLOTTI, P., BENJELLOUN, S., BENJOUAD, A., MAUREL, P., THIERS, V., BRESSANELLI, S., SAMUEL, D., BRÉCHOT, C. & GASSAMA-DIAGNE, A. 2016. Septin 9 induces lipid droplets growth by a phosphatidylinositol-5-phosphate and microtubule-dependent mechanism hijacked by HCV. *Nat Commun,* 7**,** 12203-12203.

ALKAM, D., FELDMAN, E. Z., SINGH, A. & KIAEI, M. 2017. Profilin1 biology and its mutation, actin(g) in disease. *Cell Mol Life Sci,* 74**,** 967-981.

ALLERBERGER, F. & WAGNER, M. 2010. Listeriosis: a resurgent foodborne infection. *Clin Microbiol Infect,* 16**,** 16-23.

ALVAREZ, D. E. & AGAISSE, H. 2012. Casein kinase 2 regulates vaccinia virus actin tail formation. *Virology,* 423**,** 143-51.

ALVAREZ, D. E. & AGAISSE, H. 2013. The formin FHOD1 and the small GTPase Rac1 promote vaccinia virus actin-based motility. *J Cell Biol,* 202**,** 1075-90.

AMARA, A. & MERCER, J. 2015. Viral apoptotic mimicry. *Nat Rev Microbiol,* 13**,** 461-9.

AMIN, N. D., ZHENG, Y.-L., KESAVAPANY, S., KANUNGO, J., GUSZCZYNSKI, T., SIHAG, R. K., RUDRABHATLA, P., ALBERS, W., GRANT, P. & PANT, H. C. 2008. Cyclin-dependent kinase 5 phosphorylation of human septin SEPT5 (hCDCrel-1) modulates exocytosis. *The Journal of neuroscience,* 28**,** 3631-43.

ANTOKU, S., SAKSELA, K., RIVERA, G. M. & MAYER, B. J. 2008. A crucial role in cell spreading for the interaction of Abl PxxP motifs with Crk and Nck adaptors. *J Cell Sci,* 121**,** 3071-82.

ANTON, I. M., JONES, G. E., WANDOSELL, F., GEHA, R. & RAMESH, N. 2007. WASP-interacting protein (WIP): working in polymerisation and much more. *Trends Cell Biol,* 17**,** 555-62.

ANTONESCU, C. N., AGUET, F., DANUSER, G. & SCHMID, S. L. 2011. Phosphatidylinositol-(4,5)-bisphosphate regulates clathrin-coated pit initiation, stabilization, and size. *Mol Biol Cell,* 22**,** 2588-600.

ANTONNY, B., BURD, C., DE CAMILLI, P., CHEN, E., DAUMKE, O., FAELBER, K., FORD, M., FROLOV, V. A., FROST, A., HINSHAW, J. E., KIRCHHAUSEN, T., KOZLOV, M. M., LENZ, M., LOW, H. H., MCMAHON, H., MERRIFIELD, C., POLLARD, T. D., ROBINSON, P. J., ROUX, A. & SCHMID, S. 2016. Membrane fission by dynamin: what we know and what we need to know. *EMBO J,* 35**,** 2270-2284.

APPLEYARD, G., HAPEL, A. J. & BOULTER, E. A. 1971. An antigenic difference between intracellular and extracellular rabbitpox virus. *J Gen Virol,* 13**,** 9-17.

ARAKAWA, Y., CORDEIRO, J. V., SCHLEICH, S., NEWSOME, T. P. & WAY, M. 2007a. The Release of Vaccinia Virus from Infected Cells Requires RhoA-mDia Modulation of Cortical Actin. *Cell Host Microbe,* 1**,** 227-240.

ARAKAWA, Y., CORDEIRO, J. V. & WAY, M. 2007b. F11L-Mediated Inhibition of RhoA-mDia Signaling Stimulates Microtubule Dynamics during Vaccinia Virus Infection. *Cell Host Microbe,* 1**,** 213-226.

ARAKI, Y., KAWANO, T., TARU, H., SAITO, Y., WADA, S., MIYAMOTO, K., KOBAYASHI, H., ISHIKAWA, H. O., OHSUGI, Y., YAMAMOTO, T., MATSUNO, K., KINJO, M. & SUZUKI, T. 2007. The novel cargo Alcadein induces vesicle association of kinesin-1 motor components and activates axonal transport. *EMBO J,* 26**,** 1475-86.

ARISAKA, F., NODA, H. & MARUYAMA, K. 1975. Kinetic analysis of the polymerization process of actin. *Biochim Biophys Acta,* 400**,** 263-74.

ARSLAN, D., LEGENDRE, M., SELTZER, V., ABERGEL, C. & CLAVERIE, J. M. 2011. Distant Mimivirus relative with a larger genome highlights the fundamental features of Megaviridae. *Proc Natl Acad Sci U S A,* 108**,** 17486-91.

ASSARSSON, E., GREENBAUM, J. A., SUNDSTROM, M., SCHAFFER, L., HAMMOND, J. A., PASQUETTO, V., OSEROFF, C., HENDRICKSON, R. C., LEFKOWITZ, E. J., TSCHARKE, D. C., SIDNEY, J., GREY, H. M., HEAD, S. R., PETERS, B. & SETTE, A. 2008. Kinetic analysis of a complete poxvirus transcriptome reveals an immediate-early class of genes. *Proc Natl Acad Sci U S A,* 105**,** 2140-5.

AVINOAM, O., SCHORB, M., BEESE, C. J., BRIGGS, J. A. & KAKSONEN, M. 2015. ENDOCYTOSIS. Endocytic sites mature by continuous bending and remodeling of the clathrin coat. *Science,* 348**,** 1369-72.

AYSCOUGH, K. R. 2000. Endocytosis and the development of cell polarity in yeast require a dynamic F-actin cytoskeleton. *Curr Biol,* 10**,** 1587-90.

AYSCOUGH, K. R., STRYKER, J., POKALA, N., SANDERS, M., CREWS, P. & DRUBIN, D. G. 1997. High rates of actin filament turnover in budding yeast and roles for actin in establishment and maintenance of cell polarity revealed using the actin inhibitor latrunculin-A. *J Cell Biol,* 137**,** 399-416.

BABA, T., DAMKE, H., HINSHAW, J. E., IKEDA, K., SCHMID, S. L. & WARNOCK, D. E. 1995. Role of dynamin in clathrin-coated vesicle formation. *Cold Spring Harb Symp Quant Biol,* 60**,** 235-42.

BABKIN, I. V. & BABKINA, I. N. 2015. The origin of the variola virus. *Viruses,* 7**,** 1100-12.

BABLANIAN, R., BAXT, B., SONNABEND, J. A. & ESTEBAN, M. 1978. Studies on the Mechanisms of Vaccinia Virus Cytopathic Effects. II. Early Cell Rounding is Associated with Virus Polypeptide Synthesis: II. Early Cell Rounding is Associated with Virus Polypeptide Synthesis. *The Journal of general virology,* 39**,** 403-413.

BADRANE, H., NGUYEN, M. H., BLANKENSHIP, J. R., CHENG, S., HAO, B., MITCHELL, A. P. & CLANCY, C. J. 2012. Rapid redistribution of phosphatidylinositol-(4,5)-bisphosphate and septins during the Candida albicans response to caspofungin. *Antimicrob Agents Chemother,* 56**,** 4614-24.

BADRANE, H., NGUYEN, M. H. & CLANCY, C. J. 2016. Highly Dynamic and Specific Phosphatidylinositol 4,5-Bisphosphate, Septin, and Cell Wall Integrity Pathway Responses Correlate with Caspofungin Activity against Candida albicans. *Antimicrob Agents Chemother,* 60**,** 3591-600.

BAI, X., BOWEN, J. R., KNOX, T. K., ZHOU, K., PENDZIWIAT, M., KUHLENBAUMER, G., SINDELAR, C. V. & SPILIOTIS, E. T. 2013. Novel septin 9 repeat motifs altered in neuralgic amyotrophy bind and bundle microtubules. *J Cell Biol,* 203**,** 895-905.

BAI, X., KARASMANIS, E. P. & SPILIOTIS, E. T. 2016. Septin 9 interacts with kinesin KIF17 and interferes with the mechanism of NMDA receptor cargo binding and transport. *Mol Biol Cell,* 27**,** 897-906.

BALDASSARRE, M., POMPEO, A., BEZNOUSSENKO, G., CASTALDI, C., CORTELLINO, S., MCNIVEN, M. A., LUINI, A. & BUCCIONE, R. 2003. Dynamin participates in focal extracellular matrix degradation by invasive cells. *Mol Biol Cell,* 14**,** 1074-84.

BALDICK, C. J., JR. & MOSS, B. 1993. Characterization and temporal regulation of mRNAs encoded by vaccinia virus intermediate-stage genes. *J Virol,* 67**,** 3515-27.

BARQUET, N. & DOMINGO, P. 1997. Smallpox: the triumph over the most terrible of the ministers of death. *Annals of internal medicine,* 127**,** 635-42.

BARRAL, Y. & KINOSHITA, M. 2008. Structural insights shed light onto septin assemblies and function. *Curr Opin Cell Biol,* 20**,** 12-8.

BARRAL, Y., MERMALL, V., MOOSEKER, M. S. & SNYDER, M. 2000. Compartmentalization of the cell cortex by septins is required for maintenance of cell polarity in yeast. *Mol Cell,* 5**,** 841-51.

BARRY, D. J., DURKIN, C. H., ABELLA, J. V. & WAY, M. 2015. Open source software for quantification of cell migration, protrusions, and fluorescence intensities. *J Cell Biol,* 209**,** 163-80.

BARTLETT, J. G. 2017. Clostridium difficile Infection. *Infect Dis Clin North Am,* 31**,** 489-495.

BARTSCH, I., SANDROCK, K., LANZA, F., NURDEN, P., HAINMANN, I., PAVLOVA, A., GREINACHER, A., TACKE, U., BARTH, M., BUSSE, A., OLDENBURG, J., BOMMER, M., STRAHM, B., SUPERTI-FURGA, A. & ZIEGER, B. 2011. Deletion of human GP1BB and SEPT5 is associated with Bernard-Soulier syndrome, platelet secretion defect, polymicrogyria, and developmental delay. *Thromb Haemost,* 106**,** 475-83.

BARTUZI, P., BILLADEAU, D. D., FAVIER, R., RONG, S., DEKKER, D., FEDOSEIENKO, A., FIETEN, H., WIJERS, M., LEVELS, J. H., HUIJKMAN, N., KLOOSTERHUIS, N., VAN DER MOLEN, H., BRUFAU, G., GROEN, A. K., ELLIOTT, A. M., KUIVENHOVEN, J. A., PLECKO, B., GRANGL, G., MCGAUGHRAN, J., HORTON, J. D., BURSTEIN, E., HOFKER, M. H. & VAN DE SLUIS, B. 2016. CCC- and WASH-mediated endosomal sorting of LDLR is required for normal clearance of circulating LDL. *Nat Commun,* 7**,** 10961.

BATCHELDER, E. M. & YARAR, D. 2010. Differential requirements for clathrin-dependent endocytosis at sites of cell-substrate adhesion. *Mol Biol Cell,* 21**,** 3070-9.

BAXBY, D. 1975. Identification and interrelationships of the variola/vaccinia subgroup of poxviruses. *Prog Med Virol,* 19**,** 215-46.

BAXBY, D. 1977. The origins of vaccinia virus. *J Infect Dis,* 136**,** 453-5.

BEAR, J. E., RAWLS, J. F. & SAXE, C. L., 3RD 1998. SCAR, a WASP-related protein, isolated as a suppressor of receptor defects in late Dictyostelium development. *J Cell Biol,* 142**,** 1325-35.

BEARD, P. M., GRIFFITHS, S. J., GONZALEZ, O., HAGA, I. R., PECHENICK JOWERS, T., REYNOLDS, D. K., WILDENHAIN, J., TEKOTTE, H., AUER, M., TYERS, M., GHAZAL, P., ZIMMER, R. & HAAS, J. 2014. A Loss of Function Analysis of Host Factors Influencing Vaccinia virus Replication by RNA Interference. *PLoS One,* 9**,** e98431-e98431.

BECK, K. A. & KEEN, J. H. 1991a. Interaction of phosphoinositide cycle intermediates with the plasma membrane-associated clathrin assembly protein AP-2. *J Biol Chem,* 266**,** 4442-7.

BECK, K. A. & KEEN, J. H. 1991b. Self-association of the plasma membrane-associated clathrin assembly protein AP-2. *J Biol Chem,* 266**,** 4437-41.

BEISE, N. & TRIMBLE, W. 2011. Septins at a glance. *J Cell Sci,* 124**,** 4141-6.

BEITES, C. L., CAMPBELL, K. A. & TRIMBLE, W. S. 2005. The septin Sept5/CDCrel-1 competes with alpha-SNAP for binding to the SNARE complex. *Biochem J,* 385**,** 347-53.

BEITES, C. L., XIE, H., BOWSER, R. & TRIMBLE, W. S. 1999. The septin CDCrel-1 binds syntaxin and inhibits exocytosis. *Nature neuroscience,* 2**,** 434-9.

BENANTI, E. L., NGUYEN, C. M. & WELCH, M. D. 2015. Virulent Burkholderia species mimic host actin polymerases to drive actin-based motility. *Cell,* 161**,** 348-60.

BENESCH, S., POLO, S., LAI, F. P. L., ANDERSON, K. I., STRADAL, T. E. B., WEHLAND, J. & ROTTNER, K. 2005. N-WASP deficiency impairs EGF internalization and actin assembly at clathrin-coated pits. *J Cell Sci,* 118**,** 3103-3115.

BENGALI, Z., SATHESHKUMAR, P. S., YANG, Z., WEISBERG, A. S., PARAN, N. & MOSS, B. 2011. Drosophila S2 cells are non-permissive for vaccinia virus DNA replication following entry via low pH-dependent endocytosis and early transcription. *PLoS One,* 6**,** e17248.

BENGALI, Z., TOWNSLEY, A. C. & MOSS, B. 2009. Vaccinia virus strain differences in cell attachment and entry. *Virology,* 389**,** 132-40.

BENMERAH, A., LAMAZE, C., BEGUE, B., SCHMID, S. L., DAUTRY-VARSAT, A. & CERF-BENSUSSAN, N. 1998. AP-2/Eps15 interaction is required for receptor-mediated endocytosis. *J Cell Biol,* 140**,** 1055-62.

BERNARDINI, M. L., MOUNIER, J., D'HAUTEVILLE, H., COQUIS-RONDON, M. & SANSONETTI, P. J. 1989. Identification of icsA, a plasmid locus of Shigella flexneri that governs bacterial intra- and intercellular spread through interaction with F-actin. *Proc Natl Acad Sci U S A,* 86**,** 3867-71.

BERTIN, A., MCMURRAY, M. A., GROB, P., PARK, S.-S., GARCIA, G., PATANWALA, I., NG, H.-L., ALBER, T., THORNER, J. & NOGALES, E. 2008. Saccharomyces cerevisiae septins: supramolecular organization of heterooligomers and the mechanism of filament assembly. *Proc Natl Acad Sci U S A,* 105**,** 8274-9.

BERTIN, A., MCMURRAY, M. A., THAI, L., GARCIA, G., 3RD, VOTIN, V., GROB, P., ALLYN, T., THORNER, J. & NOGALES, E. 2010. Phosphatidylinositol-4,5-bisphosphate promotes budding yeast septin filament assembly and organization. *J Mol Biol,* 404**,** 711-31.

BHATTACHARYA, N., GHOSH, S., SEPT, D. & COOPER, J. A. 2006. Binding of myotrophin/V-1 to actin-capping protein: implications for how capping protein binds to the filament barbed end. *J Biol Chem,* 281**,** 31021-30.

BIDGOOD, S. R. & MERCER, J. 2015. Cloak and Dagger: Alternative Immune Evasion and Modulation Strategies of Poxviruses. *Viruses,* 7**,** 4800-25.

BISHT, H., WEISBERG, A. S. & MOSS, B. 2008. Vaccinia virus I1 protein is required for cell entry and membrane fusion. *J Virol,* 82**,** 8687-94.

BLADT, F., AIPPERSBACH, E., GELKOP, S., STRASSER, G. A., NASH, P., TAFURI, A., GERTLER, F. B. & PAWSON, T. 2003. The murine Nck SH2/SH3 adaptors

are important for the development of mesoderm-derived embryonic structures and for regulating the cellular actin network. *Mol Cell Biol,* 23**,** 4586-97.
BLANCHOIN, L., BOUJEMAA-PATERSKI, R., SYKES, C. & PLASTINO, J. 2014. Actin dynamics, architecture, and mechanics in cell motility. *Physiol Rev,* 94**,** 235-63.
BLANCHOIN, L. & MICHELOT, A. 2012. Actin cytoskeleton: a team effort during actin assembly. *Curr Biol,* 22**,** R643-5.
BLANCHOIN, L. & POLLARD, T. D. 1998. Interaction of actin monomers with Acanthamoeba actophorin (ADF/cofilin) and profilin. *J Biol Chem,* 273**,** 25106-11.
BLANCHOIN, L. & POLLARD, T. D. 1999. Mechanism of interaction of Acanthamoeba actophorin (ADF/Cofilin) with actin filaments. *J Biol Chem,* 274**,** 15538-46.
BLASCO, R. & MOSS, B. 1992. Role of cell-associated enveloped vaccinia virus in cell-to-cell spread. *J Virol,* 66**,** 4170-9.
BOMMARIUS, B., MAXWELL, D., SWIMM, A., LEUNG, S., CORBETT, A., BORNMANN, W. & KALMAN, D. 2007. Enteropathogenic Escherichia coli Tir is an SH2/3 ligand that recruits and activates tyrosine kinases required for pedestal formation. *Mol Microbiol,* 63**,** 1748-68.
BONAZZI, M., KUHBACHER, A., TOLEDO-ARANA, A., MALLET, A., VASUDEVAN, L., PIZARRO-CERDA, J., BRODSKY, F. M. & COSSART, P. 2012. A common clathrin-mediated machinery co-ordinates cell-cell adhesion and bacterial internalization. *Traffic,* 13**,** 1653-66.
BONAZZI, M., VASUDEVAN, L., MALLET, A., SACHSE, M., SARTORI, A., PREVOST, M. C., ROBERTS, A., TANER, S. B., WILBUR, J. D., BRODSKY, F. M. & COSSART, P. 2011. Clathrin phosphorylation is required for actin recruitment at sites of bacterial adhesion and internalization. *J Cell Biol,* 195**,** 525-36.
BONJARDIM, C. A. 2017. Viral exploitation of the MEK/ERK pathway - A tale of vaccinia virus and other viruses. *Virology,* 507**,** 267-275.
BORINSKAYA, S., VELLE, K. B., CAMPELLONE, K. G., TALMAN, A., ALVAREZ, D., AGAISSE, H., WU, Y. I., LOEW, L. M. & MAYER, B. J. 2015. Integration of Linear and Dendritic Actin Nucleation in Nck-Induced Actin Comets. *Mol Biol Cell*.
BOULANT, S., KURAL, C., ZEEH, J. C., UBELMANN, F. & KIRCHHAUSEN, T. 2011. Actin dynamics counteract membrane tension during clathrin-mediated endocytosis. *Nat Cell Biol,* 13**,** 1124-31.
BOWEN, J. R., HWANG, D., BAI, X., ROY, D. & SPILIOTIS, E. T. 2011. Septin GTPases spatially guide microtubule organization and plus end dynamics in polarizing epithelia. *J Cell Biol,* 194**,** 187-97.
BRANDT, D. T., MARION, S., GRIFFITHS, G., WATANABE, T., KAIBUCHI, K. & GROSSE, R. 2007. Dia1 and IQGAP1 interact in cell migration and phagocytic cup formation. *J Cell Biol,* 178**,** 193-200.
BRAVO-CORDERO, J. J., MAGALHAES, M. A., EDDY, R. J., HODGSON, L. & CONDEELIS, J. 2013. Functions of cofilin in cell locomotion and invasion. *Nat Rev Mol Cell Biol,* 14**,** 405-15.
BREITBACH, K., ROTTNER, K., KLOCKE, S., ROHDE, M., JENZORA, A., WEHLAND, J. & STEINMETZ, I. 2003. Actin-based motility of Burkholderia pseudomallei involves the Arp 2/3 complex, but not N-WASP and Ena/VASP proteins. *Cell Microbiol,* 5**,** 385-93.
BREITSPRECHER, D. & GOODE, B. L. 2013. Formins at a glance. *J Cell Sci,* 126**,** 1-7.
BREITSPRECHER, D., JAISWAL, R., BOMBARDIER, J. P., GOULD, C. J., GELLES, J. & GOODE, B. L. 2012. Rocket launcher mechanism of collaborative actin assembly defined by single-molecule imaging. *Science,* 336**,** 1164-8.
BRIDGES, A. A. & GLADFELTER, A. S. 2015. Septin Form and Function at the Cell Cortex. *The Journal of biological chemistry*.

BRIDGES, A. A., JENTZSCH, M. S., OAKES, P. W., OCCHIPINTI, P. & GLADFELTER, A. S. 2016. Micron-scale plasma membrane curvature is recognized by the septin cytoskeleton. *J Cell Biol*, jcb.201512029-jcb.201512029.

BRIDGES, A. A., ZHANG, H., MEHTA, S. B., OCCHIPINTI, P., TANI, T. & GLADFELTER, A. S. 2014. Septin assemblies form by diffusion-driven annealing on membranes. *Proc Natl Acad Sci U S A,* 111**,** 2146-51.

BRIEHER, W. M., COUGHLIN, M. & MITCHISON, T. J. 2004. Fascin-mediated propulsion of Listeria monocytogenes independent of frequent nucleation by the Arp2/3 complex. *J Cell Biol,* 165**,** 233-42.

BRODSKY, F. M. 1988. Living with clathrin: its role in intracellular membrane traffic. *Science,* 242**,** 1396-402.

BRODSKY, F. M., CHEN, C. Y., KNUEHL, C., TOWLER, M. C. & WAKEHAM, D. E. 2001. Biological basket weaving: formation and function of clathrin-coated vesicles. *Annu Rev Cell Dev Biol,* 17**,** 517-68.

BRODSKY, F. M., SOSA, R. T., YBE, J. A. & O'HALLORAN, T. J. 2014. Unconventional functions for clathrin, ESCRTs, and other endocytic regulators in the cytoskeleton, cell cycle, nucleus, and beyond: links to human disease. *Cold Spring Harb Perspect Biol,* 6**,** a017004.

BROWN, E., SENKEVICH, T. G. & MOSS, B. 2006. Vaccinia virus F9 virion membrane protein is required for entry but not virus assembly, in contrast to the related L1 protein. *J Virol,* 80**,** 9455-64.

BROWN, J. L., JAQUENOUD, M., GULLI, M. P., CHANT, J. & PETER, M. 1997. Novel Cdc42-binding proteins Gic1 and Gic2 control cell polarity in yeast. *Genes Dev,* 11**,** 2972-82.

BROYLES, S. S. 2003. Vaccinia virus transcription. *J Gen Virol,* 84**,** 2293-303.

BUCKLEY, C. M., GOPALDASS, N., BOSMANI, C., JOHNSTON, S. A., SOLDATI, T., INSALL, R. H. & KING, J. S. 2016. WASH drives early recycling from macropinosomes and phagosomes to maintain surface phagocytic receptors. *Proc Natl Acad Sci U S A,* 113**,** E5906-E5915.

BUDAY, L. 1999. Membrane-targeting of signalling molecules by SH2/SH3 domain-containing adaptor proteins. *Biochim Biophys Acta,* 1422**,** 187-204.

BUDAY, L., WUNDERLICH, L. & TAMÁS, P. 2002. The Nck family of adapter proteins: Regulators of actin cytoskeleton. *Cellular Signalling,* 14**,** 723-731.

BUGALHÃO, J. N., MOTA, L. J. & FRANCO, I. S. 2015. Bacterial nucleators: actin' on actin. *Pathogens and Disease,* 73**,** ftv078-ftv078.

BUGYI, B. & CARLIER, M.-F. 2010. Control of actin filament treadmilling in cell motility. *Annu Rev Biophys,* 39**,** 449-70.

BUIJS, P. R., VERHAGEN, J. H., VAN EIJCK, C. H. & VAN DEN HOOGEN, B. G. 2015. Oncolytic viruses: From bench to bedside with a focus on safety. *Hum Vaccin Immunother,* 11**,** 1573-84.

BURBELO, P. D., DRECHSEL, D. & HALL, A. 1995. A conserved binding motif defines numerous candidate target proteins for both Cdc42 and Rac GTPases. *J Biol Chem,* 270**,** 29071-4.

BURBELO, P. D., SNOW, D. M., BAHOU, W. & SPIEGEL, S. 1999. MSE55, a Cdc42 effector protein, induces long cellular extensions in fibroblasts. *Proc Natl Acad Sci U S A,* 96**,** 9083-8.

BURNETTE, W. N. 1992. Vaccine development: necessity as the mother of invention. *New Biol,* 4**,** 269-73.

BYERS, B. & GOETSCH, L. 1976. A highly ordered ring of membrane-associated filaments in budding yeast. *J Cell Biol,* 69**,** 717-21.

CALVO, F., EGE, N., GRANDE-GARCIA, A., HOOPER, S., JENKINS, R. P., CHAUDHRY, S. I., HARRINGTON, K., WILLIAMSON, P., MOEENDARBARY, E., CHARRAS, G. & SAHAI, E. 2013. Mechanotransduction and YAP-dependent

matrix remodelling is required for the generation and maintenance of cancer-associated fibroblasts. *Nat Cell Biol,* 15**,** 637-46.

CALVO, F., RANFTL, R., HOOPER, S., FARRUGIA, A. J., MOEENDARBARY, E., BRUCKBAUER, A., BATISTA, F., CHARRAS, G. & SAHAI, E. 2015. Cdc42EP3/BORG2 and Septin Network Enables Mechano-transduction and the Emergence of Cancer-Associated Fibroblasts. *Cell Reports,* 13**,** 2699-714.

CAMPELLONE, K. G., RANKIN, S., PAWSON, T., KIRSCHNER, M. W., TIPPER, D. J. & LEONG, J. M. 2004a. Clustering of Nck by a 12-residue Tir phosphopeptide is sufficient to trigger localized actin assembly. *J Cell Biol,* 164**,** 407-16.

CAMPELLONE, K. G., ROBBINS, D. & LEONG, J. M. 2004b. EspFU is a translocated EHEC effector that interacts with Tir and N-WASP and promotes Nck-independent actin assembly. *Developmental Cell,* 7**,** 217-28.

CAMPELLONE, K. G., WEBB, N. J., ZNAMEROSKI, E. A. & WELCH, M. D. 2008. WHAMM is an Arp2/3 complex activator that binds microtubules and functions in ER to Golgi transport. *Cell,* 134**,** 148-61.

CAMPELLONE, K. G. & WELCH, M. D. 2010. A nucleator arms race: cellular control of actin assembly. *Nat Rev Mol Cell Biol,* 11**,** 237-51.

CAO, H., GARCIA, F. & MCNIVEN, M. A. 1998. Differential distribution of dynamin isoforms in mammalian cells. *Mol Biol Cell,* 9**,** 2595-609.

CAO, L., DING, X., YU, W., YANG, X., SHEN, S. & YU, L. 2007. Phylogenetic and evolutionary analysis of the septin protein family in metazoan. *FEBS Lett,* 581**,** 5526-32.

CAO, W., GOODARZI, J. P. & DE LA CRUZ, E. M. 2006. Energetics and kinetics of cooperative cofilin-actin filament interactions. *J Mol Biol,* 361**,** 257-67.

CARLIER, M. F., DUCRUIX, A. & PANTALONI, D. 1999. Signalling to actin: the Cdc42-N-WASP-Arp2/3 connection. *Chem Biol,* 6**,** R235-40.

CARLIER, M. F., HUSSON, C., RENAULT, L. & DIDRY, D. 2011. Control of actin assembly by the WH2 domains and their multifunctional tandem repeats in Spire and Cordon-Bleu. *Int Rev Cell Mol Biol,* 290**,** 55-85.

CARLIER, M. F., NIOCHE, P., BROUTIN-L'HERMITE, I., BOUJEMAA, R., LE CLAINCHE, C., EGILE, C., GARBAY, C., DUCRUIX, A., SANSONETTI, P. & PANTALONI, D. 2000. GRB2 links signaling to actin assembly by enhancing interaction of neural Wiskott-Aldrich syndrome protein (N-WASp) with actin-related protein (ARP2/3) complex. *J Biol Chem,* 275**,** 21946-52.

CARLIER, M. F. & PANTALONI, D. 1986. Direct evidence for ADP-Pi-F-actin as the major intermediate in ATP-actin polymerization. Rate of dissociation of Pi from actin filaments. *Biochemistry,* 25**,** 7789-92.

CARLIER, M. F., PANTALONI, D., EVANS, J. A., LAMBOOY, P. K., KORN, E. D. & WEBB, M. R. 1988. The hydrolysis of ATP that accompanies actin polymerization is essentially irreversible. *FEBS Lett,* 235**,** 211-4.

CARLIER, M. F., PERNIER, J., MONTAVILLE, P., SHEKHAR, S., KUHN, S., CYTOSKELETON, D. & MOTILITY, G. 2015. Control of polarized assembly of actin filaments in cell motility. *Cell Mol Life Sci,* 72**,** 3051-67.

CARLSSON, A. E. 2010. Actin dynamics: from nanoscale to microscale. *Annu Rev Biophys,* 39**,** 91-110.

CARLSSON, F. & BROWN, E. J. 2006. Actin-based motility of intracellular bacteria, and polarized surface distribution of the bacterial effector molecules. *J Cell Physiol,* 209**,** 288-96.

CARLSSON, L., NYSTROM, L. E., LINDBERG, U., KANNAN, K. K., CID-DRESDNER, H. & LOVGREN, S. 1976. Crystallization of a non-muscle actin. *J Mol Biol,* 105**,** 353-66.

CARLSSON, L., NYSTROM, L. E., SUNDKVIST, I., MARKEY, F. & LINDBERG, U. 1977. Actin polymerizability is influenced by profilin, a low molecular weight protein in non-muscle cells. *J Mol Biol,* 115**,** 465-83.

CARNELL, M., ZECH, T., CALAMINUS, S. D., URA, S., HAGEDORN, M., JOHNSTON, S. A., MAY, R. C., SOLDATI, T., MACHESKY, L. M. & INSALL, R. H. 2011. Actin polymerization driven by WASH causes V-ATPase retrieval and vesicle neutralization before exocytosis. *J Cell Biol,* 193**,** 831-9.

CARPENTIER, D. C., GAO, W. N., EWLES, H., MORGAN, G. W. & SMITH, G. L. 2015. Vaccinia virus protein complex F12/E2 interacts with kinesin light chain isoform 2 to engage the kinesin-1 motor complex. *PLoS Pathog,* 11**,** e1004723.

CARPENTIER, D. C. J., VAN LOGGERENBERG, A., DIECKMANN, N. M. G. & SMITH, G. L. 2017. Vaccinia virus egress mediated by virus protein A36 is reliant on the F12 protein. *J Gen Virol,* 98**,** 1500-1514.

CARTER, G. C., LAW, M., HOLLINSHEAD, M. & SMITH, G. L. 2005. Entry of the vaccinia virus intracellular mature virion and its interactions with glycosaminoglycans. *J Gen Virol,* 86**,** 1279-90.

CARTER, G. C., RODGER, G., MURPHY, B. J., LAW, M., KRAUSS, O., HOLLINSHEAD, M. & SMITH, G. L. 2003. Vaccinia virus cores are transported on microtubules. *J Gen Virol,* 84**,** 2443-58.

CASAMAYOR, A. & SNYDER, M. 2003. Molecular dissection of a yeast septin: distinct domains are required for septin interaction, localization, and function. *Mol Cell Biol,* 23**,** 2762-77.

CAUDRON, F. & BARRAL, Y. 2009. Septins and the lateral compartmentalization of eukaryotic membranes. *Developmental Cell,* 16**,** 493-506.

CEPEDA, V. & ESTEBAN, M. 2014. Novel insights on the progression of intermediate viral forms in the morphogenesis of vaccinia virus. *Virus Res,* 183**,** 23-9.

CHACKO, A. D., HYLAND, P. L., MCDADE, S. S., HAMILTON, P. W., RUSSELL, S. H. & HALL, P. A. 2005. SEPT9_v4 expression induces morphological change, increased motility and disturbed polarity. *J Pathol,* 206**,** 458-65.

CHAKI, S. P. & RIVERA, G. M. 2013. Integration of signaling and cytoskeletal remodeling by Nck in directional cell migration. *Bioarchitecture,* 3**,** 57-63.

CHANG, S. J., CHANG, Y. X., IZMAILYAN, R., TANG, Y. L. & CHANG, W. 2010. Vaccinia virus A25 and A26 proteins are fusion suppressors for mature virions and determine strain-specific virus entry pathways into HeLa, CHO-K1, and L cells. *J Virol,* 84**,** 8422-32.

CHAO, J. T., WONG, A. K. O., TAVASSOLI, S., YOUNG, B. P., CHRUSCICKI, A., FANG, N. N., HOWE, L. J., MAYOR, T., FOSTER, L. J. & LOEWEN, C. J. R. 2014. Polarization of the endoplasmic reticulum by ER-septin tethering. *Cell,* 158**,** 620-32.

CHAPPIE, J. S., ACHARYA, S., LEONARD, M., SCHMID, S. L. & DYDA, F. 2010. G domain dimerization controls dynamin's assembly-stimulated GTPase activity. *Nature,* 465**,** 435-40.

CHARRAS, G. T. 2008. A short history of blebbing. *J Microsc,* 231**,** 466-78.

CHEN, G. C., KIM, Y. J. & CHAN, C. S. 1997. The Cdc42 GTPase-associated proteins Gic1 and Gic2 are required for polarized cell growth in Saccharomyces cerevisiae. *Genes Dev,* 11**,** 2958-71.

CHEN, H., FRE, S., SLEPNEV, V. I., CAPUA, M. R., TAKEI, K., BUTLER, M. H., DI FIORE, P. P. & DE CAMILLI, P. 1998. Epsin is an EH-domain-binding protein implicated in clathrin-mediated endocytosis. *Nature,* 394**,** 793-7.

CHEN, X. J., SQUARR, A. J., STEPHAN, R., CHEN, B., HIGGINS, T. E., BARRY, D. J., MARTIN, M. C., ROSEN, M. K., BOGDAN, S. & WAY, M. 2014. Ena/VASP proteins cooperate with the WAVE complex to regulate the actin cytoskeleton. *Developmental Cell,* 30**,** 569-84.

CHEN, Y. J., ZHANG, P., EGELMAN, E. H. & HINSHAW, J. E. 2004. The stalk region of dynamin drives the constriction of dynamin tubes. *Nat Struct Mol Biol,* 11**,** 574-5.

CHENG, L., CHEN, S., ZHOU, Z. H. & ZHANG, J. 2007. Structure comparisons of Aedes albopictus densovirus with other parvoviruses. *Sci China C Life Sci,* 50**,** 70-4.

CHEREAU, D., KERFF, F., GRACEFFA, P., GRABAREK, Z., LANGSETMO, K. & DOMINGUEZ, R. 2005. Actin-bound structures of Wiskott-Aldrich syndrome protein (WASP)-homology domain 2 and the implications for filament assembly. *Proc Natl Acad Sci U S A,* 102**,** 16644-9.

CHESARONE, M. A., DUPAGE, A. G. & GOODE, B. L. 2010. Unleashing formins to remodel the actin and microtubule cytoskeletons. *Nature reviews. Molecular cell biology,* 11**,** 62-74.

CHI, A., HUTTENHOWER, C., GEER, L. Y., COON, J. J., SYKA, J. E. P., BAI, D. L., SHABANOWITZ, J., BURKE, D. J., TROYANSKAYA, O. G. & HUNT, D. F. 2007. Analysis of phosphorylation sites on proteins from Saccharomyces cerevisiae by electron transfer dissociation (ETD) mass spectrometry. *Proc Natl Acad Sci U S A,* 104**,** 2193-8.

CHI, R. J., LIU, J., WEST, M., WANG, J., ODORIZZI, G. & BURD, C. G. 2014. Fission of SNX-BAR-coated endosomal retrograde transport carriers is promoted by the dynamin-related protein Vps1. *J Cell Biol,* 204**,** 793-806.

CHI, S., CAO, H., CHEN, J. & MCNIVEN, M. A. 2008. Eps15 mediates vesicle trafficking from the trans-Golgi network via an interaction with the clathrin adaptor AP-1. *Mol Biol Cell,* 19**,** 3564-75.

CHIN, E., KIRKER, K., ZUCK, M., JAMES, G. & HYBISKE, K. 2012. Actin recruitment to the Chlamydia inclusion is spatiotemporally regulated by a mechanism that requires host and bacterial factors. *PLoS One,* 7**,** e46949.

CHIU, W. L., LIN, C. L., YANG, M. H., TZOU, D. L. & CHANG, W. 2007. Vaccinia virus 4c (A26L) protein on intracellular mature virus binds to the extracellular cellular matrix laminin. *J Virol,* 81**,** 2149-57.

CHOE, J. E. & WELCH, M. D. 2016. Actin-based motility of bacterial pathogens: mechanistic diversity and its impact on virulence. *Pathogens and disease*.

CHOU, A. M., SEM, K. P., WRIGHT, G. D., SUDHAHARAN, T. & AHMED, S. 2014. Dynamin1 is a novel target for IRSp53 protein and works with mammalian enabled (Mena) protein and Eps8 to regulate filopodial dynamics. *J Biol Chem,* 289**,** 24383-96.

CHUNG, C. S., HSIAO, J. C., CHANG, Y. S. & CHANG, W. 1998. A27L protein mediates vaccinia virus interaction with cell surface heparan sulfate. *J Virol,* 72**,** 1577-85.

CLEMENT, C., TIWARI, V., SCANLAN, P. M., VALYI-NAGY, T., YUE, B. Y. & SHUKLA, D. 2006. A novel role for phagocytosis-like uptake in herpes simplex virus entry. *J Cell Biol,* 174**,** 1009-21.

COCUCCI, E., AGUET, F., BOULANT, S. & KIRCHHAUSEN, T. 2012. The first five seconds in the life of a clathrin-coated pit. *Cell,* 150**,** 495-507.

CODA, L., SALCINI, A. E., CONFALONIERI, S., PELICCI, G., SORKINA, T., SORKIN, A., PELICCI, P. G. & DI FIORE, P. P. 1998. Eps15R is a tyrosine kinase substrate with characteristics of a docking protein possibly involved in coated pits-mediated internalization. *J Biol Chem,* 273**,** 3003-12.

COFFMAN, V. C. & WU, J. Q. 2012. Counting protein molecules using quantitative fluorescence microscopy. *Trends Biochem Sci,* 37**,** 499-506.

COLING, D. & KACHAR, B. 2001. Theory and application of fluorescence microscopy. *Curr Protoc Neurosci,* Chapter 2**,** Unit 2 1.

COLLETT, M. S., PURCHIO, A. F. & ERIKSON, R. L. 1980. Avian sarcoma virus-transforming protein, pp60src shows protein kinase activity specific for tyrosine. *Nature,* 285**,** 167-9.

COLLINS, A., WARRINGTON, A., TAYLOR, K. A. & SVITKINA, T. 2011. Structural organization of the actin cytoskeleton at sites of clathrin-mediated endocytosis. *Curr Biol,* 21**,** 1167-75.

COLLINS, B. M., MCCOY, A. J., KENT, H. M., EVANS, P. R. & OWEN, D. J. 2002. Molecular architecture and functional model of the endocytic AP2 complex. *Cell,* 109**,** 523-35.

COLONNE, P. M., WINCHELL, C. G. & VOTH, D. E. 2016. Hijacking Host Cell Highways: Manipulation of the Host Actin Cytoskeleton by Obligate Intracellular Bacterial Pathogens. *Front Cell Infect Microbiol,* 6**,** 107.

COMBS, C. A. & SHROFF, H. 2017. Fluorescence Microscopy: A Concise Guide to Current Imaging Methods. *Curr Protoc Neurosci,* 79**,** 2 1 1-2 1 25.

CONDIT, R. C., MOUSSATCHE, N. & TRAKTMAN, P. 2006. In a nutshell: structure and assembly of the vaccinia virion. *Adv Virus Res,* 66**,** 31-124.

COOK, T., MESA, K. & URRUTIA, R. 1996. Three dynamin-encoding genes are differentially expressed in developing rat brain. *Journal of neurochemistry,* 67**,** 927-31.

COOPER, J. A. & SEPT, D. 2008. New Insights into Mechanism and Regulation of Actin Capping Protein. 267**,** 183-206.

CORDEIRO, J. V., GUERRA, S., ARAKAWA, Y., DODDING, M. P., ESTEBAN, M. & WAY, M. 2009. F11-mediated inhibition of RhoA signalling enhances the spread of vaccinia virus in vitro and in vivo in an intranasal mouse model of infection. *PLoS One,* 4**,** e8506.

COURTEMANCHE, N. & POLLARD, T. D. 2013. Interaction of profilin with the barbed end of actin filaments. *Biochemistry,* 52**,** 6456-66.

COUTTS, A. S. & LA THANGUE, N. B. 2015. Actin nucleation by WH2 domains at the autophagosome. *Nat Commun,* 6**,** 7888.

COUTTS, A. S., WESTON, L. & LA THANGUE, N. B. 2009. A transcription co-factor integrates cell adhesion and motility with the p53 response. *Proc Natl Acad Sci U S A,* 106**,** 19872-7.

CROWTHER, R. A., FINCH, J. T. & PEARSE, B. M. 1976. On the structure of coated vesicles. *J Mol Biol,* 103**,** 785-98.

CUDMORE, S., COSSART, P., GRIFFITHS, G. & WAY, M. 1995. Actin-based motility of vaccinia virus. *Nature,* 378**,** 636-8.

CUDMORE, S., RECKMANN, I., GRIFFITHS, G. & WAY, M. 1996. Vaccinia virus: a model system for actin-membrane interactions. *J Cell Sci,* 109 (Pt 7**,** 1739-47.

CUPERS, P., TER HAAR, E., BOLL, W. & KIRCHHAUSEN, T. 1997. Parallel dimers and anti-parallel tetramers formed by epidermal growth factor receptor pathway substrate clone 15. *J Biol Chem,* 272**,** 33430-4.

CURETON, D. K., MASSOL, R. H., WHELAN, S. P. & KIRCHHAUSEN, T. 2010. The length of vesicular stomatitis virus particles dictates a need for actin assembly during clathrin-dependent endocytosis. *PLoS Pathog,* 6**,** e1001127.

CVRCKOVÁ, F., DE VIRGILIO, C., MANSER, E., PRINGLE, J. R. & NASMYTH, K. 1995. Ste20-like protein kinases are required for normal localization of cell growth and for cytokinesis in budding yeast. *Genes Dev,* 9**,** 1817-30.

CYRKLAFF, M., RISCO, C., FERNANDEZ, J. J., JIMENEZ, M. V., ESTEBAN, M., BAUMEISTER, W. & CARRASCOSA, J. L. 2005. Cryo-electron tomography of vaccinia virus. *Proc Natl Acad Sci U S A,* 102**,** 2772-7.

DA COSTA, S. R., SOU, E., XIE, J., YARBER, F. A., OKAMOTO, C. T., PIDGEON, M., KESSELS, M. M., MIRCHEFF, A. K., SCHECHTER, J. E., QUALMANN, B. & HAMM-ALVAREZ, S. F. 2003. Impairing Actin Filament or Syndapin Functions Promotes Accumulation of Clathrin-coated Vesicles at the Apical Plasma Membrane of Acinar Epithelial Cells. *Mol Biol Cell,* 14**,** 4397-4413.

DALES, S. 1963. The uptake and development of vaccinia virus in strain L cells followed with labeled viral deoxyribonucleic acid. *J Cell Biol,* 18**,** 51-72.

DALES, S. & MOSBACH, E. H. 1968. Vaccinia as a model for membrane biogenesis. *Virology,* 35**,** 564-83.

DALHAIMER, P. & POLLARD, T. D. 2010. Molecular dynamics simulations of Arp2/3 complex activation. *Biophysical Journal,* 99**,** 2568-76.

DAMKE, H., BABA, T., WARNOCK, D. E. & SCHMID, S. L. 1994. Induction of mutant dynamin specifically blocks endocytic coated vesicle formation. *J Cell Biol,* 127**,** 915-34.

DANINO, D., MOON, K. H. & HINSHAW, J. E. 2004. Rapid constriction of lipid bilayers by the mechanochemical enzyme dynamin. *J Struct Biol,* 147**,** 259-67.

DAVIDSON, A. J. & WOOD, W. 2016. Unravelling the Actin Cytoskeleton: A New Competitive Edge? *Trends Cell Biol,* 26**,** 569-76.

DE LA FUENTE, M. A., SASAHARA, Y., CALAMITO, M., ANTON, I. M., ELKHAL, A., GALLEGO, M. D., SURESH, K., SIMINOVITCH, K., OCHS, H. D., ANDERSON, K. C., ROSEN, F. S., GEHA, R. S. & RAMESH, N. 2007. WIP is a chaperone for Wiskott-Aldrich syndrome protein (WASP). *Proc Natl Acad Sci U S A,* 104**,** 926-31.

DE VOS, K. J., ALLAN, V. J., GRIERSON, A. J. & SHEETZ, M. P. 2005. Mitochondrial function and actin regulate dynamin-related protein 1-dependent mitochondrial fission. *Curr Biol,* 15**,** 678-83.

DEMAY, B. S., MESEROLL, R. A., OCCHIPINTI, P. & GLADFELTER, A. S. 2009. Regulation of distinct septin rings in a single cell by Elm1p and Gin4p kinases. *Mol Biol Cell,* 20**,** 2311-26.

DEN OTTER, W. K. & BRIELS, W. J. 2011. The generation of curved clathrin coats from flat plaques. *Traffic,* 12**,** 1407-16.

DENG, L., FAN, J., DING, Y., ZHANG, J., ZHOU, B., ZHANG, Y. & HUANG, B. 2017. Oncolytic efficacy of thymidine kinase-deleted vaccinia virus strain Guang9. *Oncotarget,* 8**,** 40533-40543.

DERIVERY, E., SOUSA, C., GAUTIER, J. J., LOMBARD, B., LOEW, D. & GAUTREAU, A. 2009. The Arp2/3 activator WASH controls the fission of endosomes through a large multiprotein complex. *Developmental Cell,* 17**,** 712-23.

DESTAING, O., FERGUSON, S. M., GRICHINE, A., ODDOU, C., DE CAMILLI, P., ALBIGES-RIZO, C. & BARON, R. 2013. Essential function of dynamin in the invasive properties and actin architecture of v-Src induced podosomes/invadosomes. *PLoS One,* 8**,** e77956.

DING, Z., BAE, Y. H. & ROY, P. Molecular insights on context-specific role of profilin-1 in cell migration. *Cell adhesion & migration,* 6**,** 442-9.

DIXON, C. W. 1962. *Smallpox,* London, Churchill.

DOBBELAERE, J., GENTRY, M. S., HALLBERG, R. L. & BARRAL, Y. 2003. Phosphorylation-Dependent Regulation of Septin Dynamics during the Cell Cycle. *Developmental Cell,* 4**,** 345-357.

DOCEUL, V., HOLLINSHEAD, M., BREIMAN, A., LAVAL, K. & SMITH, G. L. 2012. Protein B5 is required on extracellular enveloped vaccinia virus for repulsion of superinfecting virions. *J Gen Virol,* 93**,** 1876-86.

DOCEUL, V., HOLLINSHEAD, M., VAN DER LINDEN, L. & SMITH, G. L. 2010. Repulsion of superinfecting virions: a mechanism for rapid virus spread. *Science,* 327**,** 873-6.

DODDING, M. P., MITTER, R., HUMPHRIES, A. C. & WAY, M. 2011. A kinesin-1 binding motif in vaccinia virus that is widespread throughout the human genome. *EMBO J,* 30**,** 4523-38.

DODDING, M. P., NEWSOME, T. P., COLLINSON, L. M., EDWARDS, C. & WAY, M. 2009. An E2-F12 complex is required for intracellular enveloped virus morphogenesis during vaccinia infection. *Cell Microbiol,* 11**,** 808-24.

DODDING, M. P. & WAY, M. 2009. Nck- and N-WASP-dependent actin-based motility is conserved in divergent vertebrate poxviruses. *Cell Host Microbe,* 6**,** 536-50.

DODDING, M. P. & WAY, M. 2011. Coupling viruses to dynein and kinesin-1. *EMBO J,* 30**,** 3527-39.

DOLAT, L., HUNYARA, J. L., BOWEN, J. R., KARASMANIS, E. P., ELGAWLY, M., GALKIN, V. E. & SPILIOTIS, E. T. 2014. Septins promote stress fiber-mediated maturation of focal adhesions and renal epithelial motility. *J Cell Biol,* 207**,** 225-235.

DOLAT, L. & SPILIOTIS, E. T. 2016. Septins promote macropinosome maturation and traffic to the lysosome by facilitating membrane fusion. *J Cell Biol,* 214.

DOMINGUEZ, R. 2016. The WH2 Domain and Actin Nucleation: Necessary but Insufficient. *Trends Biochem Sci,* 41**,** 478-490.

DOMINGUEZ, R. & HOLMES, K. C. 2011. Actin structure and function. *Annu Rev Biophys,* 40**,** 169-86.

DONNELLY, S. K., WEISSWANGE, I., ZETTL, M. & WAY, M. 2013. WIP provides an essential link between Nck and N-WASP during Arp2/3-dependent actin polymerization. *Curr Biol,* 23**,** 999-1006.

DORSEY, J. F., JOVE, R., KRAKER, A. J. & WU, J. 2000. The pyrido[2,3-d]pyrimidine derivative PD180970 inhibits p210Bcr-Abl tyrosine kinase and induces apoptosis of K562 leukemic cells. *Cancer Res,* 60**,** 3127-31.

DUGGAN, A. T., PERDOMO, M. F., PIOMBINO-MASCALI, D., MARCINIAK, S., POINAR, D., EMERY, M. V., BUCHMANN, J. P., DUCHENE, S., JANKAUSKAS, R., HUMPHREYS, M., GOLDING, G. B., SOUTHON, J., DEVAULT, A., ROUILLARD, J. M., SAHL, J. W., DUTOUR, O., HEDMAN, K., SAJANTILA, A., SMITH, G. L., HOLMES, E. C. & POINAR, H. N. 2016. 17th Century Variola Virus Reveals the Recent History of Smallpox. *Curr Biol,* 26**,** 3407-3412.

DURKIN, C. H., LEITE, F., CORDEIRO, J. V., HANDA, Y., ARAKAWA, Y., VALDERRAMA, F. & WAY, M. 2017. RhoD Inhibits RhoC-ROCK-Dependent Cell Contraction via PAK6. *Developmental Cell,* 41**,** 315-329.e7.

EARLEY, A. K., CHAN, W. M. & WARD, B. M. 2008. The vaccinia virus B5 protein requires A34 for efficient intracellular trafficking from the endoplasmic reticulum to the site of wrapping and incorporation into progeny virions. *J Virol,* 82**,** 2161-9.

EDELING, M. A., SMITH, C. & OWEN, D. 2006. Life of a clathrin coat: insights from clathrin and AP structures. *Nat Rev Mol Cell Biol,* 7**,** 32-44.

EDWARDS, M., ZWOLAK, A., SCHAFER, D. A., SEPT, D., DOMINGUEZ, R. & COOPER, J. A. 2014. Capping protein regulators fine-tune actin assembly dynamics. *Nat Rev Mol Cell Biol,* 15**,** 677-89.

EGELHOFER, T. A., VILLEN, J., MCCUSKER, D., GYGI, S. P. & KELLOGG, D. R. 2008. The septins function in G1 pathways that influence the pattern of cell growth in budding yeast. *PLoS One,* 3**,** e2022.

EGILE, C., LOISEL, T. P., LAURENT, V., LI, R., PANTALONI, D., SANSONETTI, P. J. & CARLIER, M. F. 1999. Activation of the CDC42 effector N-WASP by the Shigella flexneri IcsA protein promotes actin nucleation by Arp2/3 complex and bacterial actin-based motility. *J Cell Biol,* 146**,** 1319-32.

EGILE, C., ROUILLER, I., XU, X. P., VOLKMANN, N., LI, R. & HANEIN, D. 2005. Mechanism of filament nucleation and branch stability revealed by the structure of the Arp2/3 complex at actin branch junctions. *PLoS Biology,* 3**,** e383.

EHRLICH, M., BOLL, W., VAN OIJEN, A., HARIHARAN, R., CHANDRAN, K., NIBERT, M. L. & KIRCHHAUSEN, T. 2004. Endocytosis by random initiation and stabilization of clathrin-coated pits. *Cell,* 118**,** 591-605.

ENGELSTAD, M. & SMITH, G. L. 1993. The vaccinia virus 42-kDa envelope protein is required for the envelopment and egress of extracellular virus and for virus virulence. *Virology,* 194**,** 627-37.

ENGQVIST-GOLDSTEIN, A. E. & DRUBIN, D. G. 2003. Actin assembly and endocytosis: from yeast to mammals. *Annu Rev Cell Dev Biol,* 19**,** 287-332.

ERNI, R., ROSSELL, M. D., KISIELOWSKI, C. & DAHMEN, U. 2009. Atomic-resolution imaging with a sub-50-pm electron probe. *Phys Rev Lett,* 102**,** 096101.

FARBER, J. M. & PETERKIN, P. I. 1991. Listeria monocytogenes, a food-borne pathogen. *Microbiol Rev,* 55**,** 476-511.

FARKASOVSKY, M., HERTER, P., VOSS, B. & WITTINGHOFER, A. 2005. Nucleotide binding and filament assembly of recombinant yeast septin complexes. *Biol Chem,* 386**,** 643-56.

FARRUGIA, A. J. & CALVO, F. 2016a. The Borg family of Cdc42 effector proteins Cdc42EP1-5. *Biochemical Society Transactions,* 44**,** 1709-1716.

FARRUGIA, A. J. & CALVO, F. 2016b. Cdc42 regulates Cdc42EP3 function in Cancer-Associated Fibroblasts. *Small GTPases*.

FAZIOLI, F., MINICHIELLO, L., MATOSKOVA, B., WONG, W. T. & DI FIORE, P. P. 1993. eps15, a novel tyrosine kinase substrate, exhibits transforming activity. *Mol Cell Biol,* 13**,** 5814-28.

FENNER, F., HENDERSON, D. A., ARITA, I., JEZEK, Z., LADNYI, I. D. & ORGANIZATION, W. H. 1988. Smallpox and its eradication. *Geneva : World Health Organization.*

FERGUSON, S. M., FERGUSON, S., RAIMONDI, A., PARADISE, S., SHEN, H., MESAKI, K., FERGUSON, A., DESTAING, O., KO, G., TAKASAKI, J., CREMONA, O., O' TOOLE, E. & DE CAMILLI, P. 2009. Coordinated actions of actin and BAR proteins upstream of dynamin at endocytic clathrin-coated pits. *Developmental Cell,* 17**,** 811-22.

FERNANDEZ-CHACON, R., ACHIRILOAIE, M., JANZ, R., ALBANESI, J. P. & SUDHOF, T. C. 2000. SCAMP1 function in endocytosis. *J Biol Chem,* 275**,** 12752-6.

FIELD, C. M., AL-AWAR, O., ROSENBLATT, J., WONG, M. L., ALBERTS, B. & MITCHISON, T. J. 1996. A purified Drosophila septin complex forms filaments and exhibits GTPase activity. *J Cell Biol,* 133**,** 605-16.

FLETCHER, D. A. & MULLINS, R. D. 2010. Cell mechanics and the cytoskeleton. *Nature,* 463**,** 485-92.

FOSTER-BARBER, A. & BISHOP, J. M. 1998. Src interacts with dynamin and synapsin in neuronal cells. *Proc Natl Acad Sci U S A,* 95**,** 4673-7.

FRAZIER, J. A., WONG, M. L., LONGTINE, M. S., PRINGLE, J. R., MANN, M., MITCHISON, T. J. & FIELD, C. 1998. Polymerization of purified yeast septins: evidence that organized filament arrays may not be required for septin function. *J Cell Biol,* 143**,** 737-49.

FRESE, S., SCHUBERT, W. D., FINDEIS, A. C., MARQUARDT, T., ROSKE, Y. S., STRADAL, T. E. & HEINZ, D. W. 2006. The phosphotyrosine peptide binding specificity of Nck1 and Nck2 Src homology 2 domains. *J Biol Chem,* 281**,** 18236-45.

FRISCHKNECHT, F., CUDMORE, S., MOREAU, V., RECKMANN, I., RÖTTGER, S. & WAY, M. 1999a. Tyrosine phosphorylation is required for actin-based motility of vaccinia but not Listeria or Shigella. *Curr Biol,* 9**,** 89-92.

FRISCHKNECHT, F., MOREAU, V., ROTTGER, S., GONFLONI, S., RECKMANN, I., SUPERTI-FURGA, G. & WAY, M. 1999b. Actin-based motility of vaccinia virus mimics receptor tyrosine kinase signalling. *Nature,* 401**,** 926-9.

FRISCHKNECHT, F. & WAY, M. 2001. Surfing pathogens and the lessons learned for actin polymerization. *Trends Cell Biol,* 11**,** 30-38.

FROIDEVAUX-KLIPFEL, L., TARGA, B., CANTALOUBE, I., AHMED-ZAID, H., POUS, C. & BAILLET, A. 2015. Septin cooperation with tubulin polyglutamylation contributes to cancer cell adaptation to taxanes. *Oncotarget,* 6**,** 36063-80.

FUCHTBAUER, A., LASSEN, L. B., JENSEN, A. B., HOWARD, J., QUIROGA ADE, S., WARMING, S., SORENSEN, A. B., PEDERSEN, F. S. & FUCHTBAUER, E. M. 2011. Septin9 is involved in septin filament formation and cellular stability. *Biol Chem,* 392**,** 769-77.

FUJIWARA, I., TAKAHASHI, S., TADAKUMA, H., FUNATSU, T. & ISHIWATA, S. 2002. Microscopic analysis of polymerization dynamics with individual actin filaments. *Nat Cell Biol,* 4**,** 666-73.

FUKUHARA, H., INO, Y. & TODO, T. 2016. Oncolytic virus therapy: A new era of cancer treatment at dawn. *Cancer Science,* 107**,** 1373-1379.

FUKUMATSU, M., OGAWA, M., ARAKAWA, S., SUZUKI, M., NAKAYAMA, K., SHIMIZU, S., KIM, M., MIMURO, H. & SASAKAWA, C. 2012. Shigella targets epithelial tricellular junctions and uses a noncanonical clathrin-dependent endocytic pathway to spread between cells. *Cell Host Microbe,* 11**,** 325-36.

FUNG, K. Y. Y., DAI, L. & TRIMBLE, W. S. 2014. Cell and molecular biology of septins. *International review of cell and molecular biology,* 310**,** 289-339.

GANDHI, M., GOODE, B. L. & CHAN, C. S. 2006. Four novel suppressors of gic1 gic2 and their roles in cytokinesis and polarized cell growth in Saccharomyces cerevisiae. *Genetics,* 174**,** 665-78.

GAO, L., LIU, W. & BRETSCHER, A. 2010. The yeast formin Bnr1p has two localization regions that show spatially and temporally distinct association with septin structures. *Mol Biol Cell,* 21**,** 1253-62.

GARCIA, G., 3RD, BERTIN, A., LI, Z., SONG, Y., MCMURRAY, M. A., THORNER, J. & NOGALES, E. 2011. Subunit-dependent modulation of septin assembly: budding yeast septin Shs1 promotes ring and gauze formation. *J Cell Biol,* 195**,** 993-1004.

GARCIA, G., FINNIGAN, G. C., HEASLEY, L. R., STERLING, S. M., AGGARWAL, A., PEARSON, C. G., NOGALES, E., MCMURRAY, M. A. & THORNER, J. 2016. Assembly, molecular organization, and membrane-binding properties of development-specific septins. *J Cell Biol,* 212**,** 515-29.

GARMENDIA, J., PHILLIPS, A. D., CARLIER, M. F., CHONG, Y., SCHULLER, S., MARCHES, O., DAHAN, S., OSWALD, E., SHAW, R. K., KNUTTON, S. & FRANKEL, G. 2004. TccP is an enterohaemorrhagic Escherichia coli O157:H7 type III effector protein that couples Tir to the actin-cytoskeleton. *Cell Microbiol,* 6**,** 1167-83.

GASMAN, S., CHASSEROT-GOLAZ, S., MALACOMBE, M., WAY, M. & BADER, M. F. 2004. Regulated exocytosis in neuroendocrine cells: a role for subplasmalemmal Cdc42/N-WASP-induced actin filaments. *Mol Biol Cell,* 15**,** 520-31.

GAYTAN, M. O., MARTINEZ-SANTOS, V. I., SOTO, E. & GONZALEZ-PEDRAJO, B. 2016. Type Three Secretion System in Attaching and Effacing Pathogens. *Front Cell Infect Microbiol,* 6**,** 129.

GC, J. B., GERSTMAN, B. S., STAHELIN, R. V. & CHAPAGAIN, P. P. 2016. The Ebola virus protein VP40 hexamer enhances the clustering of PI(4,5)P2 lipids in the plasma membrane. *Phys Chem Chem Phys,* 18**,** 28409-28417.

GEADA, M. M., GALINDO, I., LORENZO, M. M., PERDIGUERO, B. & BLASCO, R. 2001. Movements of vaccinia virus intracellular enveloped virions with GFP tagged to the F13L envelope protein. *The Journal of general virology,* 82**,** 2747-60.

GEEVES, M. A. 1991. The dynamics of actin and myosin association and the crossbridge model of muscle contraction. *Biochem J,* 274 (Pt 1)**,** 1-14.

GELI, M. I. & RIEZMAN, H. 1998. Endocytic internalization in yeast and animal cells: similar and different. *J Cell Sci,* 111 (Pt 8)**,** 1031-7.

GER, M., ZITKUS, Z. & VALIUS, M. 2011. Adaptor protein Nck1 interacts with p120 Ras GTPase-activating protein and regulates its activity. *Cell Signal,* 2**3,** 1651-8.

GHIGO, E., KARTENBECK, J., LIEN, P., PELKMANS, L., CAPO, C., MEGE, J. L. & RAOULT, D. 2008. Ameobal pathogen mimivirus infects macrophages through phagocytosis. *PLoS Pathog,* 4**,** e1000087.

GILBERT, H. R. & FRIEDEN, C. 1983. Preparation, purification and properties of a crosslinked trimer of G-actin. *Biochem Biophys Res Commun,* 111**,** 404-8.

GILDEN, J. K., PECK, S., CHEN, Y.-C. M. & KRUMMEL, M. F. 2012. The septin cytoskeleton facilitates membrane retraction during motility and blebbing. *J Cell Biol,* 196**,** 103-14.

GIUBELLINO, A., BURKE, T. R., JR. & BOTTARO, D. P. 2008. Grb2 signaling in cell motility and cancer. *Expert Opin Ther Targets,* 12**,** 1021-33.

GOLEBIEWSKA, U., KAY, J. G., MASTERS, T., GRINSTEIN, S., IM, W., PASTOR, R. W., SCARLATA, S. & MCLAUGHLIN, S. 2011. Evidence for a fence that impedes the diffusion of phosphatidylinositol 4,5-bisphosphate out of the forming phagosomes of macrophages. *Mol Biol Cell,* 22**,** 3498-507.

GOLEY, E. D., OHKAWA, T., MANCUSO, J., WOODRUFF, J. B., D'ALESSIO, J. A., CANDE, W. Z., VOLKMAN, L. E. & WELCH, M. D. 2006. Dynamic nuclear actin assembly by Arp2/3 complex and a baculovirus WASP-like protein. *Science,* 314**,** 464-7.

GOLEY, E. D., RODENBUSCH, S. E., MARTIN, A. C. & WELCH, M. D. 2004. Critical conformational changes in the Arp2/3 complex are induced by nucleotide and nucleation promoting factor. *Mol Cell,* 16**,** 269-79.

GOLEY, E. D. & WELCH, M. D. 2006. The ARP2/3 complex: an actin nucleator comes of age. *Nature reviews. Molecular cell biology,* 7**,** 713-26.

GÓMEZ, C. E., NÁJERA, J. L., KRUPA, M., PERDIGUERO, B. & ESTEBAN, M. 2011. MVA and NYVAC as vaccines against emergent infectious diseases and cancer. *Current gene therapy,* 11**,** 189-217.

GONI, G. M., EPIFANO, C., BOSKOVIC, J., CAMACHO-ARTACHO, M., ZHOU, J., BRONOWSKA, A., MARTIN, M. T., ECK, M. J., KREMER, L., GRATER, F., GERVASIO, F. L., PEREZ-MORENO, M. & LIETHA, D. 2014. Phosphatidylinositol 4,5-bisphosphate triggers activation of focal adhesion kinase by inducing clustering and conformational changes. *Proc Natl Acad Sci U S A,* 111**,** E3177-86.

GONZÁLEZ-JAMETT, A. M., MOMBOISSE, F., HARO-ACUÑA, V., BEVILACQUA, J. A., CAVIEDES, P. & CÁRDENAS, A. M. 2013. Dynamin-2 Function and Dysfunction Along the Secretory Pathway. *Frontiers in Endocrinology,* 4**,** 126-126.

GONZALEZ-NOVO, A., CORREA-BORDES, J., LABRADOR, L., SANCHEZ, M., VAZQUEZ DE ALDANA, C. R. & JIMENEZ, J. 2008. Sep7 is essential to modify septin ring dynamics and inhibit cell separation during Candida albicans hyphal growth. *Mol Biol Cell,* 19**,** 1509-18.

GOODE, B. L., ESKIN, J. A. & WENDLAND, B. 2015. Actin and endocytosis in budding yeast. *Genetics,* 199**,** 315-58.

GOTTLIEB, T. A., IVANOV, I. E., ADESNIK, M. & SABATINI, D. D. 1993. Actin microfilaments play a critical role in endocytosis at the apical but not the basolateral surface of polarized epithelial cells. *J Cell Biol,* 120**,** 695-710.

GOUIN, E., EGILE, C., DEHOUX, P., VILLIERS, V., ADAMS, J., GERTLER, F., LI, R. & COSSART, P. 2004. The RickA protein of Rickettsia conorii activates the Arp2/3 complex. *Nature,* 427**,** 457-61.

GOULD, C. J., MAITI, S., MICHELOT, A., GRAZIANO, B. R., BLANCHOIN, L. & GOODE, B. L. 2011. The formin DAD domain plays dual roles in autoinhibition and actin nucleation. *Curr Biol,* 21**,** 384-90.

GOUT, I., DHAND, R., HILES, I. D., FRY, M. J., PANAYOTOU, G., DAS, P., TRUONG, O., TOTTY, N. F., HSUAN, J., BOOKER, G. W. & ET AL. 1993. The GTPase dynamin binds to and is activated by a subset of SH3 domains. *Cell,* 75**,** 25-36.

GOZAL, Y. M., SEYFRIED, N. T., GEARING, M., GLASS, J. D., HEILMAN, C. J., WUU, J., DUONG, D. M., CHENG, D., XIA, Q., REES, H. D., FRITZ, J. J., COOPER, D. S., PENG, J., LEVEY, A. I. & LAH, J. J. 2011. Aberrant septin 11 is associated with sporadic frontotemporal lobar degeneration. *Mol Neurodegener,* 6**,** 82.

GRASSART, A., CHENG, A. T., HONG, S. H., ZHANG, F., ZENZER, N., FENG, Y., BRINER, D. M., DAVIS, G. D., MALKOV, D. & DRUBIN, D. G. 2014. Actin and dynamin2 dynamics and interplay during clathrin-mediated endocytosis. *J Cell Biol,* 205**,** 721-35.

GRAY, R. D., BEERLI, C., PEREIRA, P. M., SCHERER, K. M., SAMOLEJ, J., BLECK, C. K., MERCER, J. & HENRIQUES, R. 2016. VirusMapper: open-source nanoscale mapping of viral architecture through super-resolution microscopy. *Sci Rep,* 6**,** 29132.

GREENE, B., LIU, S. H., WILDE, A. & BRODSKY, F. M. 2000. Complete reconstitution of clathrin basket formation with recombinant protein fragments: adaptor control of clathrin self-assembly. *Traffic,* 1**,** 69-75.

GRIFFITHS, G., ROOS, N., SCHLEICH, S. & LOCKER, J. K. 2001. Structure and assembly of intracellular mature vaccinia virus: thin-section analyses. *J Virol,* 75**,** 11056-70.

GRIGG, P., TITONG, A., JONES, L. A., YILMA, T. D. & VERARDI, P. H. 2013. Safety mechanism assisted by the repressor of tetracycline (SMART) vaccinia virus vectors for vaccines and therapeutics. *Proc Natl Acad Sci U S A,* 110**,** 15407-15412.

GROSS, C. P. & SEPKOWITZ, K. A. 1998. The myth of the medical breakthrough: smallpox, vaccination, and Jenner reconsidered. *Int J Infect Dis,* 3**,** 54-60.

GRUENHEID, S., DEVINNEY, R., BLADT, F., GOOSNEY, D., GELKOP, S., GISH, G. D., PAWSON, T. & FINLAY, B. B. 2001. Enteropathogenic E. coli Tir binds Nck to initiate actin pedestal formation in host cells. *Nat Cell Biol,* 3**,** 856-9.

GU, C., YADDANAPUDI, S., WEINS, A., OSBORN, T., REISER, J., POLLAK, M., HARTWIG, J. & SEVER, S. 2010. Direct dynamin-actin interactions regulate the actin cytoskeleton. *EMBO J,* 29**,** 3593-606.

GUIPPONI, M., SCOTT, H. S., HATTORI, M., ISHII, K., SAKAKI, Y. & ANTONARAKIS, S. E. 1998. Genomic structure, sequence, and refined mapping of the human intersectin gene (ITSN), which encompasses 250 kb on chromosome 21q22.1-->q22.2. *Cytogenet Cell Genet,* 83**,** 218-20.

GUPTA, Y. K., DAGDAS, Y. F., MARTINEZ-ROCHA, A. L., KERSHAW, M. J., LITTLEJOHN, G. R., RYDER, L. S., SKLENAR, J., MENKE, F. & TALBOT, N. J. 2015. Septin-Dependent Assembly of the Exocyst Is Essential for Plant Infection by Magnaporthe oryzae. *Plant Cell,* 27**,** 3277-89.

GUSTAFSSON, M. G. 2000. Surpassing the lateral resolution limit by a factor of two using structured illumination microscopy. *J Microsc,* 198**,** 82-7.

GUSTAFSSON, M. G., SHAO, L., CARLTON, P. M., WANG, C. J., GOLUBOVSKAYA, I. N., CANDE, W. Z., AGARD, D. A. & SEDAT, J. W. 2008. Three-dimensional resolution doubling in wide-field fluorescence microscopy by structured illumination. *Biophysical Journal,* 94**,** 4957-70.

GUTTMAN, J. A., LIN, A. E., VEIGA, E., COSSART, P. & FINLAY, B. B. 2010. Role for CD2AP and other endocytosis-associated proteins in enteropathogenic Escherichia coli pedestal formation. *Infect Immun,* 78**,** 3316-22.

HAARER, B. K. & PRINGLE, J. R. 1987. Immunofluorescence localization of the Saccharomyces cerevisiae CDC12 gene product to the vicinity of the 10-nm filaments in the mother-bud neck. *Mol Cell Biol,* 7**,** 3678-87.

HAGLUND, C. M., CHOE, J. E., SKAU, C. T., KOVAR, D. R. & WELCH, M. D. 2010. Rickettsia Sca2 is a bacterial formin-like mediator of actin-based motility. *Nat Cell Biol,* 12**,** 1057-63.

HAMMARSTEN, J. F., TATTERSALL, W. & HAMMARSTEN, J. E. 1979. Who discovered smallpox vaccination? Edward Jenner or Benjamin Jesty? *Trans Am Clin Climatol Assoc,* 90**,** 44-55.

HAMMERSCHLAG, M. R. 2002. The intracellular life of chlamydiae. *Semin Pediatr Infect Dis,* 13**,** 239-48.

HANAI, N., NAGATA, K., KAWAJIRI, A., SHIROMIZU, T., SAITOH, N., HASEGAWA, Y., MURAKAMI, S. & INAGAKI, M. 2004. Biochemical and cell biological characterization of a mammalian septin, Sept11. *FEBS Lett,* 568**,** 83-8.

HANKE, J. H., GARDNER, J. P., DOW, R. L., CHANGELIAN, P. S., BRISSETTE, W. H., WERINGER, E. J., POLLOK, B. A. & CONNELLY, P. A. 1996. Discovery of a novel, potent, and Src family-selective tyrosine kinase inhibitor. Study of Lck- and FynT-dependent T cell activation. *The Journal of biological chemistry,* 271**,** 695-701.

HANSON, J. & LOWY, J. 1964. The Structure of Actin Filaments and the Origin of the Axial Periodicity in the I-Substance of Vertebrate Striated Muscle. *Proc R Soc Lond B Biol Sci,* 160**,** 449-60.

HARTWELL, L. H. 1971. Genetic control of the cell division cycle in yeast. IV. Genes controlling bud emergence and cytokinesis. *Experimental cell research,* 69**,** 265-76.

HASSINGER, J. E., OSTER, G., DRUBIN, D. G. & RANGAMANI, P. 2017. Design principles for robust vesiculation in clathrin-mediated endocytosis. *Proc Natl Acad Sci U S A,* 114**,** E1118-E1127.

HAYWARD, R. D., LEONG, J. M., KORONAKIS, V. & CAMPELLONE, K. G. 2006. Exploiting pathogenic Escherichia coli to model transmembrane receptor signalling. *Nat Rev Microbiol,* 4**,** 358-70.

HEIMSATH, E. G., JR. & HIGGS, H. N. 2012. The C terminus of formin FMNL3 accelerates actin polymerization and contains a WH2 domain-like sequence that binds both monomers and filament barbed ends. *J Biol Chem,* 287**,** 3087-98.

HENDERSON, D. A. Smallpox: clinical and epidemiologic features. *Emerging infectious diseases,* 5**,** 537-9.

HENMI, Y., TANABE, K. & TAKEI, K. 2011. Disruption of microtubule network rescues aberrant actin comets in dynamin2-depleted cells. *PLoS One,* 6**,** e28603.

HENNE, W. M., BOUCROT, E., MEINECKE, M., EVERGREN, E., VALLIS, Y., MITTAL, R. & MCMAHON, H. T. 2010. FCHo proteins are nucleators of clathrin-mediated endocytosis. *Science,* 328**,** 1281-4.

HERNANDEZ-RODRIGUEZ, Y. & MOMANY, M. 2012. Posttranslational modifications and assembly of septin heteropolymers and higher-order structures. *Curr Opin Microbiol,* 15**,** 660-8.

HERRERO-MARTINEZ, E., ROBERTS, K. L., HOLLINSHEAD, M. & SMITH, G. L. 2005. Vaccinia virus intracellular enveloped virions move to the cell periphery on microtubules in the absence of the A36R protein. *J Gen Virol,* 86**,** 2961-8.

HETRICK, B., HAN, M. S., HELGESON, L. A. & NOLEN, B. J. 2013. Small molecules CK-666 and CK-869 inhibit actin-related protein 2/3 complex by blocking an activating conformational change. *Chem Biol,* 20**,** 701-12.

HEUSER, J. 1980. Three-dimensional visualization of coated vesicle formation in fibroblasts. *J Cell Biol,* 84**,** 560-83.

HEUSER, J. 2000. The production of 'cell cortices' for light and electron microscopy. *Traffic,* 1**,** 545-52.

HEUSER, J. 2005. Deep-etch EM reveals that the early poxvirus envelope is a single membrane bilayer stabilized by a geodetic "honeycomb" surface coat. *J Cell Biol,* 169**,** 269-83.

HEYMANN, J. A. & HINSHAW, J. E. 2009. Dynamins at a glance. *J Cell Sci,* 122**,** 3427-31.

HILL, T. A., ODELL, L. R., QUAN, A., ABAGYAN, R., FERGUSON, G., ROBINSON, P. J. & MCCLUSKEY, A. 2004. Long chain amines and long chain ammonium salts as novel inhibitors of dynamin GTPase activity. *Bioorganic & Medicinal Chemistry Letters,* 14**,** 3275-3278.

HILLER, G., JUNGWIRTH, C. & WEBER, K. 1981. Fluorescence microscopical analysis of the life cycle of vaccinia virus in chick embryo fibroblasts. Virus-cytoskeleton interactions. *Exp Cell Res,* 132**,** 81-7.

HILLER, G. & WEBER, K. 1985. Golgi-derived membranes that contain an acylated viral polypeptide are used for vaccinia virus envelopment. *J Virol,* 55**,** 651-9.

HILLER, G., WEBER, K., SCHNEIDER, L., PARAJSZ, C. & JUNGWIRTH, C. 1979. Interaction of assembled progeny pox viruses with the cellular cytoskeleton. *Virology,* 98**,** 142-53.

HINSHAW, J. E. & SCHMID, S. L. 1995. Dynamin self-assembles into rings suggesting a mechanism for coated vesicle budding. *Nature,* 374**,** 190-2.

HIRSCH, D. S., PIRONE, D. M. & BURBELO, P. D. 2001. A new family of Cdc42 effector proteins, CEPs, function in fibroblast and epithelial cell shape changes. *The Journal of biological chemistry,* 276**,** 875-83.

HO, C. W., CHEN, H. T. & HWANG, J. 2011. UBC9 autosumoylation negatively regulates sumoylation of septins in Saccharomyces cerevisiae. *J Biol Chem,* 286**,** 21826-34.

HO, H. Y., ROHATGI, R., LEBENSOHN, A. M., LE, M., LI, J., GYGI, S. P. & KIRSCHNER, M. W. 2004. Toca-1 mediates Cdc42-dependent actin nucleation by activating the N-WASP-WIP complex. *Cell,* 118**,** 203-16.

HOFFMANN, P. R., DECATHELINEAU, A. M., OGDEN, C. A., LEVERRIER, Y., BRATTON, D. L., DALEKE, D. L., RIDLEY, A. J., FADOK, V. A. & HENSON, P. M. 2001. Phosphatidylserine (PS) induces PS receptor-mediated macropinocytosis and promotes clearance of apoptotic cells. *J Cell Biol,* 155**,** 649-59.

HOLLINSHEAD, M., RODGER, G., VAN EIJL, H., LAW, M., HOLLINSHEAD, R., VAUX, D. J. & SMITH, G. L. 2001. Vaccinia virus utilizes microtubules for movement to the cell surface. *J Cell Biol,* 154**,** 389-402.

HOLLINSHEAD, M., VANDERPLASSCHEN, A., SMITH, G. L. & VAUX, D. J. 1999. Vaccinia virus intracellular mature virions contain only one lipid membrane. *J Virol,* 73**,** 1503-17.

HOPKINS, D. R. 1985. Smallpox entombed. *Lancet,* 1**,** 175-175.

HORSINGTON, J., LYNN, H., TURNBULL, L., CHENG, D., BRAET, F., DIEFENBACH, R. J., WHITCHURCH, C. B., KARUPIAH, G. & NEWSOME, T. P. 2013. A36-dependent actin filament nucleation promotes release of vaccinia virus. *PLoS Pathog,* 9**,** e1003239-e1003239.

HORSINGTON, J., TURNBULL, L., WHITCHURCH, C. B. & NEWSOME, T. P. 2012. Sub-viral imaging of vaccinia virus using super-resolution microscopy. *J Virol Methods,* 186**,** 132-6.

HSIAO, J. C., CHUNG, C. S. & CHANG, W. 1999. Vaccinia virus envelope D8L protein binds to cell surface chondroitin sulfate and mediates the adsorption of intracellular mature virions to cells. *J Virol,* 73**,** 8750-61.

HSU, S. C., HAZUKA, C. D., ROTH, R., FOLETTI, D. L., HEUSER, J. & SCHELLER, R. H. 1998. Subunit composition, protein interactions, and structures of the mammalian brain sec6/8 complex and septin filaments. *Neuron,* 20**,** 1111-22.

HU, Q., MILENKOVIC, L., JIN, H., SCOTT, M. P., NACHURY, M. V., SPILIOTIS, E. T. & NELSON, W. J. 2010. A septin diffusion barrier at the base of the primary cilium maintains ciliary membrane protein distribution. *Science,* 329**,** 436-9.

HU, Q., MILFAY, D. & WILLIAMS, L. T. 1995. Binding of NCK to SOS and activation of ras-dependent gene expression. *Mol Cell Biol,* 15**,** 1169-74.

HUANG, B., BABCOCK, H. & ZHUANG, X. 2010. Breaking the diffraction barrier: super-resolution imaging of cells. *Cell,* 143**,** 1047-58.

HUANG, C. Y., LU, T. Y., BAIR, C. H., CHANG, Y. S., JWO, J. K. & CHANG, W. 2008a. A Novel Cellular Protein, VPEF, Facilitates Vaccinia Virus Penetration into HeLa Cells through Fluid Phase Endocytosis. *J Virol,* 82**,** 7988-7999.

HUANG, Y.-W., SURKA, M. C., REYNAUD, D., PACE-ASCIAK, C. & TRIMBLE, W. S. 2006. GTP binding and hydrolysis kinetics of human septin 2. *The FEBS journal,* 273**,** 3248-60.

HUANG, Y.-W., YAN, M., COLLINS, R. F., DICICCIO, J. E., GRINSTEIN, S. & TRIMBLE, W. S. 2008b. Mammalian septins are required for phagosome formation. *Mol Biol Cell,* 19**,** 1717-26.

HUFNER, K., HIGGS, H. N., POLLARD, T. D., JACOBI, C., AEPFELBACHER, M. & LINDER, S. 2001. The verprolin-like central (vc) region of Wiskott-Aldrich syndrome protein induces Arp2/3 complex-dependent actin nucleation. *J Biol Chem,* 276**,** 35761-7.

HUMPHRIES, A. C., DODDING, M. P., BARRY, D. J., COLLINSON, L. M., DURKIN, C. H. & WAY, M. 2012. Clathrin potentiates vaccinia-induced actin polymerization to facilitate viral spread. *Cell Host Microbe,* 12**,** 346-59.

HUMPHRIES, A. C., DONNELLY, S. K. & WAY, M. 2014. Cdc42 and the Rho GEF intersectin-1 collaborate with Nck to promote N-WASP-dependent actin polymerisation. *J Cell Sci,* 127**,** 673-85.

HUMPHRIES, A. C. & WAY, M. 2013. The non-canonical roles of clathrin and actin in pathogen internalization, egress and spread. *Nat Rev Microbiol,* 11**,** 551-60.

HUSAIN, M. & MOSS, B. 2003. Intracellular trafficking of a palmitoylated membrane-associated protein component of enveloped vaccinia virus. *J Virol,* 77**,** 9008-19.

HUSAIN, M. & MOSS, B. 2005. Role of receptor-mediated endocytosis in the formation of vaccinia virus extracellular enveloped particles. *J Virol,* 79**,** 4080-9.

HUSAIN, M., WEISBERG, A. S. & MOSS, B. 2006. Existence of an operative pathway from the endoplasmic reticulum to the immature poxvirus membrane. *Proc Natl Acad Sci U S A,* 103**,** 19506-11.

HUSSAIN, N. K., JENNA, S., GLOGAUER, M., QUINN, C. C., WASIAK, S., GUIPPONI, M., ANTONARAKIS, S. E., KAY, B. K., STOSSEL, T. P., LAMARCHE-VANE, N. & MCPHERSON, P. S. 2001. Endocytic protein intersectin-l regulates actin assembly via Cdc42 and N-WASP. *Nat Cell Biol,* 3**,** 927-32.

HUSSAIN, N. K., YAMABHAI, M., RAMJAUN, A. R., GUY, A. M., BARANES, D., O'BRYAN, J. P., DER, C. J., KAY, B. K. & MCPHERSON, P. S. 1999. Splice variants of intersectin are components of the endocytic machinery in neurons and nonneuronal cells. *J Biol Chem,* 274**,** 15671-7.

HUXLEY, H. E. 1963. Electron Microscope Studies on the Structure of Natural and Synthetic Protein Filaments from Striated Muscle. *J Mol Biol,* 7**,** 281-308.

IBORRA, S., IZQUIERDO, H. M., MARTINEZ-LOPEZ, M., BLANCO-MENENDEZ, N., REIS E SOUSA, C. & SANCHO, D. 2012. The DC receptor DNGR-1 mediates cross-priming of CTLs during vaccinia virus infection in mice. *J Clin Invest,* 122**,** 1628-43.

ICHIHASHI, Y., MATSUMOTO, S. & DALES, S. 1971. Biogenesis of poxviruses: role of A-type inclusions and host cell membranes in virus dissemination. *Virology,* 46**,** 507-32.

ICHIHASHI, Y. & OIE, M. 1983. The activation of vaccinia virus infectivity by the transfer of phosphatidylserine from the plasma membrane. *Virology,* 130**,** 306-17.

IDRISSI, F. Z. & GELI, M. I. 2014. Zooming in on the molecular mechanisms of endocytic budding by time-resolved electron microscopy. *Cell Mol Life Sci,* 71**,** 641-57.

IHARA, M., KINOSHITA, A., YAMADA, S., TANAKA, H., TANIGAKI, A., KITANO, A., GOTO, M., OKUBO, K., NISHIYAMA, H., OGAWA, O., TAKAHASHI, C., ITOHARA, S., NISHIMUNE, Y., NODA, M. & KINOSHITA, M. 2005. Cortical organization by the septin cytoskeleton is essential for structural and mechanical integrity of mammalian spermatozoa. *Developmental Cell,* 8**,** 343-52.

INGERMAN, E., PERKINS, E. M., MARINO, M., MEARS, J. A., MCCAFFERY, J. M., HINSHAW, J. E. & NUNNARI, J. 2005. Dnm1 forms spirals that are structurally tailored to fit mitochondria. *J Cell Biol,* 170**,** 1021-7.

INNOCENTI, M., GERBOTH, S., ROTTNER, K., LAI, F. P. L., HERTZOG, M., STRADAL, T. E. B., FRITTOLI, E., DIDRY, D., POLO, S., DISANZA, A., BENESCH, S., FIORE, P. P. D., CARLIER, M.-F. & SCITA, G. 2005. Abi1 regulates the activity of N-WASP and WAVE in distinct actin-based processes. *Nat Cell Biol,* 7**,** 969-976.

IRETON, K. 2013. Molecular mechanisms of cell-cell spread of intracellular bacterial pathogens. *Open Biology,* 3**,** 130079-130079.

ISENBERG, G., AEBI, U. & POLLARD, T. D. 1980. An actin-binding protein from Acanthamoeba regulates actin filament polymerization and interactions. *Nature,* 288**,** 455-9.

IYER, S. S. & AMARA, R. R. 2014. DNA/MVA Vaccines for HIV/AIDS. *Vaccines (Basel),* 2**,** 160-78.

IZMAILYAN, R. A., HUANG, C. Y., MOHAMMAD, S., ISAACS, S. N. & CHANG, W. 2006. The envelope G3L protein is essential for entry of vaccinia virus into host cells. *J Virol,* 80**,** 8402-10.

JACKSON, L. P., KELLY, B. T., MCCOY, A. J., GAFFRY, T., JAMES, L. C., COLLINS, B. M., HONING, S., EVANS, P. R. & OWEN, D. J. 2010. A large-scale conformational change couples membrane recruitment to cargo binding in the AP2 clathrin adaptor complex. *Cell,* 141**,** 1220-9.

JANMEY, P. A., HVIDT, S., OSTER, G. F., LAMB, J., STOSSEL, T. P. & HARTWIG, J. H. 1990. Effect of ATP on actin filament stiffness. *Nature,* 347**,** 95-9.

JANSSEN, E., TOHME, M., HEDAYAT, M., LEICK, M., KUMARI, S., RAMESH, N., MASSAAD, M. J., ULLAS, S., AZCUTIA, V., GOODNOW, C. C., RANDALL, K. L., QIAO, Q., WU, H., AL-HERZ, W., COX, D., HARTWIG, J., IRVINE, D. J., LUSCINSKAS, F. W. & GEHA, R. S. 2016. A DOCK8-WIP-WASp complex links T cell receptors to the actin cytoskeleton. *J Clin Invest,* 126**,** 3837-3851.

JEFFERSON, A., CADET, V. E. & HIELSCHER, A. 2015. The mechanisms of genetically modified vaccinia viruses for the treatment of cancer. *Critical Reviews in Oncology/Hematology,* 95**,** 407-416.

JENG, R. L., GOLEY, E. D., D'ALESSIO, J. A., CHAGA, O. Y., SVITKINA, T. M., BORISY, G. G., HEINZEN, R. A. & WELCH, M. D. 2004. A Rickettsia WASP-like protein activates the Arp2/3 complex and mediates actin-based motility. *Cell Microbiol,* 6**,** 761-9.

JI, W. K., HATCH, A. L., MERRILL, R. A., STRACK, S. & HIGGS, H. N. 2015. Actin filaments target the oligomeric maturation of the dynamin GTPase Drp1 to mitochondrial fission sites. *Elife,* 4**,** e11553.

JOBERTY, G., PERLUNGHER, R. R. & MACARA, I. G. 1999. The Borgs, a new family of Cdc42 and TC10 GTPase-interacting proteins. *Molecular and cellular biology,* 19**,** 6585-97.

JOBERTY, G., PERLUNGHER, R. R., SHEFFIELD, P. J., KINOSHITA, M., NODA, M., HAYSTEAD, T. & MACARA, I. G. 2001. Borg proteins control septin organization and are negatively regulated by Cdc42. *Nat Cell Biol,* 3**,** 861-866.

JOHANNSDOTTIR, H. K., MANCINI, R., KARTENBECK, J., AMATO, L. & HELENIUS, A. 2009. Host cell factors and functions involved in vesicular stomatitis virus entry. *J Virol,* 83**,** 440-53.

JOHNSON, C. R., WEEMS, A. D., BREWER, J. M., THORNER, J. & MCMURRAY, M. A. 2015a. Cytosolic chaperones mediate quality control of higher-order septin assembly in budding yeast. *Mol Biol Cell,* 26**,** 1323-44.

JOHNSON, E. S. & BLOBEL, G. 1999. Cell cycle-regulated attachment of the ubiquitin-related protein SUMO to the yeast septins. *J Cell Biol,* 147**,** 981-94.

JOHNSON, E. S. & GUPTA, A. A. 2001. An E3-like factor that promotes SUMO conjugation to the yeast septins. *Cell,* 106**,** 735-44.

JOHNSON, H. E., KING, S. J., ASOKAN, S. B., ROTTY, J. D., BEAR, J. E. & HAUGH, J. M. 2015b. F-actin bundles direct the initiation and orientation of lamellipodia through adhesion-based signaling. *J Cell Biol,* 208**,** 443-55.

JOHNSON, K. A., TAGHON, G. J., SCOTT, J. L. & STAHELIN, R. V. 2016. The Ebola Virus matrix protein, VP40, requires phosphatidylinositol 4,5-bisphosphate (PI(4,5)P2) for extensive oligomerization at the plasma membrane and viral egress. *Sci Rep,* 6**,** 19125.

JOO, E., SURKA, M. C. & TRIMBLE, W. S. 2007. Mammalian SEPT2 is required for scaffolding nonmuscle myosin II and its kinases. *Developmental Cell,* 13**,** 677-90.

JUNEMANN, A., FILIC, V., WINTERHOFF, M., NORDHOLZ, B., LITSCHKO, C., SCHWELLENBACH, H., STEPHAN, T., WEBER, I. & FAIX, J. 2016. A Diaphanous-related formin links Ras signaling directly to actin assembly in macropinocytosis and phagocytosis. *Proc Natl Acad Sci U S A,* 113**,** E7464-E7473.

KAKSONEN, M., SUN, Y. & DRUBIN, D. G. 2003. A pathway for association of receptors, adaptors, and actin during endocytic internalization. *Cell,* 115**,** 475-87.

KAKSONEN, M., TORET, C. P. & DRUBIN, D. G. 2005. A modular design for the clathrin- and actin-mediated endocytosis machinery. *Cell,* 123**,** 305-20.

KANASEKI, T. & KADOTA, K. 1969. The "vesicle in a basket". A morphological study of the coated vesicle isolated from the nerve endings of the guinea pig brain, with special reference to the mechanism of membrane movements. *J Cell Biol,* 42**,** 202-20.

KAST, D. J., ZAJAC, A. L., HOLZBAUR, E. L., OSTAP, E. M. & DOMINGUEZ, R. 2015. WHAMM Directs the Arp2/3 Complex to the ER for Autophagosome Biogenesis through an Actin Comet Tail Mechanism. *Curr Biol,* 25**,** 1791-7.

KELLEHER, J. F., ATKINSON, S. J. & POLLARD, T. D. 1995. Sequences, structural models, and cellular localization of the actin-related proteins Arp2 and Arp3 from Acanthamoeba. *J Cell Biol,* 131**,** 385-97.

KELLY, B. T., GRAHAM, S. C., LISKA, N., DANNHAUSER, P. N., HONING, S., UNGEWICKELL, E. J. & OWEN, D. J. 2014. Clathrin adaptors. AP2 controls clathrin polymerization with a membrane-activated switch. *Science,* 345**,** 459-63.

KENNY, B. 1999. Phosphorylation of tyrosine 474 of the enteropathogenic Escherichia coli (EPEC) Tir receptor molecule is essential for actin nucleating activity and is preceded by additional host modifications. *Mol Microbiol,* 31**,** 1229-41.

KENNY, B., DEVINNEY, R., STEIN, M., REINSCHEID, D. J., FREY, E. A. & FINLAY, B. B. 1997. Enteropathogenic E. coli (EPEC) transfers its receptor for intimate adherence into mammalian cells. *Cell,* 91**,** 511-20.

KENT, R. 1989. Transcription in vaccinia virus. *Microbiologia,* 5**,** 69-77.

KIKYO, M., TANAKA, K., KAMEI, T., OZAKI, K., FUJIWARA, T., INOUE, E., TAKITA, Y., OHYA, Y. & TAKAI, Y. 1999. An FH domain-containing Bnr1p is a multifunctional protein interacting with a variety of cytoskeletal proteins in Saccharomyces cerevisiae. *Oncogene,* 18**,** 7046-54.

KILCHER, S., SCHMIDT, F. I., SCHNEIDER, C., KOPF, M., HELENIUS, A. & MERCER, J. 2014. siRNA screen of early poxvirus genes identifies the AAA+ ATPase D5 as the virus genome-uncoating factor. *Cell Host Microbe,* 15**,** 103-12.

KIM, A. S., KAKALIS, L. T., ABDUL-MANAN, N., LIU, G. A. & ROSEN, M. K. 2000. Autoinhibition and activation mechanisms of the Wiskott-Aldrich syndrome protein. *Nature,* 404**,** 151-8.

KIM, C. S., SEOL, S. K., SONG, O.-K., PARK, J. H. & JANG, S. K. 2007. An RNA-binding protein, hnRNP A1, and a scaffold protein, septin 6, facilitate hepatitis C virus replication. *J Virol,* 81**,** 3852-65.

KIM, H. B., HAARER, B. K. & PRINGLE, J. R. 1991. Cellular morphogenesis in the Saccharomyces cerevisiae cell cycle: localization of the CDC3 gene product and the timing of events at the budding site. *J Cell Biol,* 112**,** 535-44.

KIM, M. S., FROESE, C. D., ESTEY, M. P. & TRIMBLE, W. S. 2011. SEPT9 occupies the terminal positions in septin octamers and mediates polymerization-dependent functions in abscission. *J Cell Biol,* 195**,** 815-26.

KIM, M. S., FROESE, C. D., XIE, H. & TRIMBLE, W. S. 2012. Uncovering principles that control septin-septin interactions. *The Journal of biological chemistry,* 287**,** 30406-13.

KIM, S. K., SHINDO, A., PARK, T. J., OH, E. C., GHOSH, S., GRAY, R. S., LEWIS, R. A., JOHNSON, C. A., ATTIE-BITTACH, T., KATSANIS, N. & WALLINGFORD, J. B. 2010. Planar cell polarity acts through septins to control collective cell movement and ciliogenesis. *Science,* 329**,** 1337-40.

KINOSHITA, M., FIELD, C. M., COUGHLIN, M. L., STRAIGHT, A. F. & MITCHISON, T. J. 2002. Self- and actin-templated assembly of Mammalian septins. *Developmental Cell,* 3**,** 791-802.

KINOSHITA, M., KUMAR, S., MIZOGUCHI, A., IDE, C., KINOSHITA, A., HARAGUCHI, T., HIRAOKA, Y. & NODA, M. 1997. Nedd5, a mammalian septin, is a novel cytoskeletal component interacting with actin-based structures. *Genes Dev,* 11**,** 1535-47.

KIRCHHAUSEN, T. 2009. Imaging endocytic clathrin structures in living cells. *Trends Cell Biol,* 19**,** 596-605.

KIRCHHAUSEN, T. & HARRISON, S. C. 1981. Protein organization in clathrin trimers. *Cell,* 23**,** 755-61.

KIRCHHAUSEN, T., HARRISON, S. C., CHOW, E. P., MATTALIANO, R. J., RAMACHANDRAN, K. L., SMART, J. & BROSIUS, J. 1987a. Clathrin heavy chain: molecular cloning and complete primary structure. *Proc Natl Acad Sci U S A,* 84**,** 8805-9.

KIRCHHAUSEN, T., OWEN, D. & HARRISON, S. C. 2014. Molecular structure, function, and dynamics of clathrin-mediated membrane traffic. *Cold Spring Harb Perspect Biol,* 6**,** a016725.

KIRCHHAUSEN, T., SCARMATO, P., HARRISON, S. C., MONROE, J. J., CHOW, E. P., MATTALIANO, R. J., RAMACHANDRAN, K. L., SMART, J. E., AHN, A. H. & BROSIUS, J. 1987b. Clathrin light chains LCA and LCB are similar, polymorphic, and share repeated heptad motifs. *Science,* 236**,** 320-4.

KISSEL, H., GEORGESCU, M.-M., LARISCH, S., MANOVA, K., HUNNICUTT, G. R. & STELLER, H. 2005. The Sept4 septin locus is required for sperm terminal differentiation in mice. *Developmental Cell,* 8**,** 353-64.

KLEBA, B., CLARK, T. R., LUTTER, E. I., ELLISON, D. W. & HACKSTADT, T. 2010. Disruption of the Rickettsia rickettsii Sca2 autotransporter inhibits actin-based motility. *Infect Immun,* 78**,** 2240-7.

KOCH, S., ACEBRON, S. P., HERBST, J., HATIBOGLU, G. & NIEHRS, C. 2015. Post-transcriptional Wnt Signaling Governs Epididymal Sperm Maturation. *Cell,* 163**,** 1225-36.

KOCKS, C., GOUIN, E., TABOURET, M., BERCHE, P., OHAYON, H. & COSSART, P. 1992. L. monocytogenes-induced actin assembly requires the actA gene product, a surface protein. *Cell,* 68**,** 521-31.

KOESTLER, S. A., ROTTNER, K., LAI, F., BLOCK, J., VINZENZ, M. & SMALL, J. V. 2009. F- and G-actin concentrations in lamellipodia of moving cells. *PLoS One,* 4**,** e4810.

KOIRALA, S., GUO, Q., KALIA, R., BUI, H. T., ECKERT, D. M., FROST, A. & SHAW, J. M. 2013. Interchangeable adaptors regulate mitochondrial dynamin assembly for membrane scission. *Proc Natl Acad Sci U S A,* 110**,** E1342-51.

KONECNA, A., FRISCHKNECHT, R., KINTER, J., LUDWIG, A., STEUBLE, M., MESKENAITE, V., INDERMUHLE, M., ENGEL, M., CEN, C., MATEOS, J. M., STREIT, P. & SONDEREGGER, P. 2006. Calsyntenin-1 docks vesicular cargo to kinesin-1. *Mol Biol Cell,* 17**,** 3651-63.

KORN, E. D., CARLIER, M. F. & PANTALONI, D. 1987. Actin polymerization and ATP hydrolysis. *Science,* 238**,** 638-44.

KOROBOVA, F., RAMABHADRAN, V. & HIGGS, H. N. 2013. An actin-dependent step in mitochondrial fission mediated by the ER-associated formin INF2. *Science,* 339**,** 464-7.

KOVAR, D. R. 2006. Molecular details of formin-mediated actin assembly. *Curr Opin Cell Biol,* 18**,** 11-7.

KOVAR, D. R., HARRIS, E. S., MAHAFFY, R., HIGGS, H. N. & POLLARD, T. D. 2006. Control of the assembly of ATP- and ADP-actin by formins and profilin. *Cell,* 124**,** 423-35.

KOVAR, D. R., KUHN, J. R., TICHY, A. L. & POLLARD, T. D. 2003. The fission yeast cytokinesis formin Cdc12p is a barbed end actin filament capping protein gated by profilin. *J Cell Biol,* 161**,** 875-87.

KRAKER, A. J., HARTL, B. G., AMAR, A. M., BARVIAN, M. R., SHOWALTER, H. D. & MOORE, C. W. 2000. Biochemical and cellular effects of c-Src kinase-selective pyrido[2, 3-d]pyrimidine tyrosine kinase inhibitors. *Biochem Pharmacol,* 60**,** 885-98.

KRAUS, F. & RYAN, M. T. 2017. The constriction and scission machineries involved in mitochondrial fission. *J Cell Sci,* 130**,** 2953-2960.

KRAUSE, M., DENT, E. W., BEAR, J. E., LOUREIRO, J. J. & GERTLER, F. B. 2003. Ena/VASP proteins: regulators of the actin cytoskeleton and cell migration. *Annu Rev Cell Dev Biol,* 19**,** 541-64.

KREMER, B. E., ADANG, L. A. & MACARA, I. G. 2007. Septins regulate actin organization and cell-cycle arrest through nuclear accumulation of NCK mediated by SOCS7. *Cell,* 130**,** 837-50.

KREMER, B. E., HAYSTEAD, T. & MACARA, I. G. 2005. Mammalian septins regulate microtubule stability through interaction with the microtubule-binding protein MAP4. *Mol Biol Cell,* 16**,** 4648-59.

KREMPIEN, U., SCHNEIDER, L., HILLER, G., WEBER, K., KATZ, E. & JUNGWIRTH, C. 1981. Conditions for pox virus-specific microvilli formation studied during synchronized virus assembly. *Virology,* 113**,** 556-64.

KRUEGER, E. W., ORTH, J. D., CAO, H. & MCNIVEN, M. A. 2003. A dynamin-cortactin-Arp2/3 complex mediates actin reorganization in growth factor-stimulated cells. *Mol Biol Cell,* 14**,** 1085-96.

KULAK, N. A., PICHLER, G., PARON, I., NAGARAJ, N. & MANN, M. 2014. Minimal, encapsulated proteomic-sample processing applied to copy-number estimation in eukaryotic cells. *Nat Methods,* 11**,** 319-24.

KUMARI, S., MG, S. & MAYOR, S. 2010. Endocytosis unplugged: multiple ways to enter the cell. *Cell Res,* 20**,** 256-75.

KWITNY, S., KLAUS, A. V. & HUNNICUTT, G. R. 2010. The annulus of the mouse sperm tail is required to establish a membrane diffusion barrier that is engaged during the late steps of spermiogenesis. *Biol Reprod,* 82**,** 669-78.

KZHYSHKOWSKA, J. & KRUSELL, L. 2009. Cross-talk between endocytic clearance and secretion in macrophages. *Immunobiology,* 214**,** 576-93.

LAI, Y., ROSENSHINE, I., LEONG, J. M. & FRANKEL, G. 2013. Intimate host attachment: enteropathogenic and enterohaemorrhagic Escherichia coli. *Cell Microbiol,* 15**,** 1796-808.

LALIBERTE, J. P. & MOSS, B. 2009. Appraising the apoptotic mimicry model and the role of phospholipids for poxvirus entry. *Proc Natl Acad Sci U S A,* 106**,** 17517-21.

LALIBERTE, J. P., WEISBERG, A. S. & MOSS, B. 2011. The Membrane Fusion Step of Vaccinia Virus Entry Is Cooperatively Mediated by Multiple Viral Proteins and Host Cell Components. *PLoS Pathog,* 7**,** e1002446-e1002446.

LAMASON, R. L., BASTOUNIS, E., KAFAI, N. M., SERRANO, R., DEL ALAMO, J. C., THERIOT, J. A. & WELCH, M. D. 2016. Rickettsia Sca4 Reduces Vinculin-Mediated Intercellular Tension to Promote Spread. *Cell,* 167**,** 670-683 e10.

LAMAZE, C., FUJIMOTO, L. M., YIN, H. L. & SCHMID, S. L. 1997. The actin cytoskeleton is required for receptor-mediated endocytosis in mammalian cells. *J Biol Chem,* 272**,** 20332-5.

LAMMERMANN, T. & SIXT, M. 2009. Mechanical modes of 'amoeboid' cell migration. *Curr Opin Cell Biol,* 21**,** 636-44.

LAMPE, M., VASSILOPOULOS, S. & MERRIFIELD, C. 2016. Clathrin coated pits, plaques and adhesion. *J Struct Biol,* 196**,** 48-56.

LANIER, L. M. & VOLKMAN, L. E. 1998. Actin binding and nucleation by Autographa california M nucleopolyhedrovirus. *Virology,* 243**,** 167-77.

LARKIN, J. M., DONZELL, W. C. & ANDERSON, R. G. 1986. Potassium-dependent assembly of coated pits: new coated pits form as planar clathrin lattices. *J Cell Biol,* 103**,** 2619-27.

LAW, M., CARTER, G. C., ROBERTS, K. L., HOLLINSHEAD, M. & SMITH, G. L. 2006. Ligand-induced and nonfusogenic dissolution of a viral membrane. *Proc Natl Acad Sci U S A,* 103**,** 5989-94.

LAW, M., HOLLINSHEAD, R. & SMITH, G. L. 2002. Antibody-sensitive and antibody-resistant cell-to-cell spread by vaccinia virus: role of the A33R protein in antibody-resistant spread. *J Gen Virol,* 83**,** 209-22.

LEE, E. & DE CAMILLI, P. 2002. Dynamin at actin tails. *Proc Natl Acad Sci U S A,* 99**,** 161-166.

LEE, J. E., WESTRATE, L. M., WU, H., PAGE, C. & VOELTZ, G. K. 2016. Multiple dynamin family members collaborate to drive mitochondrial division. *Nature,* 540**,** 139-143.

LEE, S. H. & DOMINGUEZ, R. 2010. Regulation of actin cytoskeleton dynamics in cells. *Mol Cell,* 29**,** 311-25.

LEGESSE-MILLER, A., MASSOL, R. H. & KIRCHHAUSEN, T. 2003. Constriction and Dnm1p recruitment are distinct processes in mitochondrial fission. *Mol Biol Cell,* 14**,** 1953-63.

LEHMANN, J. M., RIETHMULLER, G. & JOHNSON, J. P. 1990. Nck, a melanoma cDNA encoding a cytoplasmic protein consisting of the src homology units SH2 and SH3. *Nucleic Acids Res,* 18**,** 1048.

LEITE, F. & WAY, M. 2015. The role of signalling and the cytoskeleton during Vaccinia Virus egress. *Virus Res,* 209**,** 87-99.

LETT, M. C., SASAKAWA, C., OKADA, N., SAKAI, T., MAKINO, S., YAMADA, M., KOMATSU, K. & YOSHIKAWA, M. 1989. virG, a plasmid-coded virulence gene of Shigella flexneri: identification of the virG protein and determination of the complete coding sequence. *J Bacteriol,* 171**,** 353-9.

LEYTON-PUIG, D., ISOGAI, T., ARGENZIO, E., VAN DEN BROEK, B., KLARENBEEK, J., JANSSEN, H., JALINK, K. & INNOCENTI, M. 2017. Flat clathrin lattices are dynamic actin-controlled hubs for clathrin-mediated endocytosis and signalling of specific receptors. *Nat Commun,* 8**,** 16068.

LI, B., DING, S., FENG, N., MOONEY, N., OOI, Y. S., REN, L., DIEP, J., KELLY, M. R., YASUKAWA, L. L., PATTON, J. T., YAMAZAKI, H., SHIRAO, T., JACKSON, P. K. & GREENBERG, H. B. 2017. Drebrin restricts rotavirus entry by inhibiting dynamin-mediated endocytosis. *Proc Natl Acad Sci U S A,* 114**,** E3642-E3651.

LI, F. & HIGGS, H. N. 2003. The mouse Formin mDia1 is a potent actin nucleation factor regulated by autoinhibition. *Curr Biol,* 13**,** 1335-40.

LI, S., XU, S., ROELOFS, B. A., BOYMAN, L., LEDERER, W. J., SESAKI, H. & KARBOWSKI, M. 2015. Transient assembly of F-actin on the outer mitochondrial membrane contributes to mitochondrial fission. *J Cell Biol,* 208**,** 109-23.

LI, W., FAN, J. & WOODLEY, D. T. 2001. Nck/Dock: an adapter between cell surface receptors and the actin cytoskeleton. *Oncogene,* 20**,** 6403-17.

LIAN, G., DETTENHOFER, M., LU, J., DOWNING, M., CHENN, A., WONG, T. & SHEEN, V. 2016. Filamin A- and formin 2-dependent endocytosis regulates proliferation via the canonical Wnt pathway. *Development,* 143**,** 4509-4520.

LIM, C. S., PARK, E. S., KIM, D. J., SONG, Y. H., EOM, S. H., CHUN, J.-S., KIM, J. H., KIM, J.-K., PARK, D. & SONG, W. K. 2001. SPIN90 (SH3 ProteinInteracting with Nck, 90 kDa), an Adaptor Protein That Is Developmentally Regulated during Cardiac Myocyte Differentiation. *Journal of Biological Chemistry,* 276**,** 12871-12878.

LIN, A. E., BENMERAH, A. & GUTTMAN, J. A. 2011. Eps15 and Epsin1 are crucial for enteropathogenic Escherichia coli pedestal formation despite the absence of adaptor protein 2. *J Infect Dis,* 204**,** 695-703.

LIN, C. L., CHUNG, C. S., HEINE, H. G. & CHANG, W. 2000. Vaccinia virus envelope H3L protein binds to cell surface heparan sulfate and is important for intracellular mature virion morphogenesis and virus infection in vitro and in vivo. *J Virol,* 74**,** 3353-65.

LINARDOPOULOU, E. V., PARGHI, S. S., FRIEDMAN, C., OSBORN, G. E., PARKHURST, S. M. & TRASK, B. J. 2007. Human subtelomeric WASH genes encode a new subclass of the WASP family. *PLoS Genet,* 3**,** e237.

LIU, A. P., LOERKE, D., SCHMID, S. L. & DANUSER, G. 2009. Global and local regulation of clathrin-coated pit dynamics detected on patterned substrates. *Biophysical Journal,* 97**,** 1038-47.

LIU, S. H., WONG, M. L., CRAIK, C. S. & BRODSKY, F. M. 1995. Regulation of clathrin assembly and trimerization defined using recombinant triskelion hubs. *Cell,* 83**,** 257-67.

LIU, T., DAI, A., CAO, Y., ZHANG, R., DONG, M. Q. & WANG, H. W. 2017. Structural Insights of WHAMM's Interaction with Microtubules by Cryo-EM. *J Mol Biol,* 429**,** 1352-1363.

LIU, Y. W., MATTILA, J. P. & SCHMID, S. L. 2013. Dynamin-catalyzed membrane fission requires coordinated GTP hydrolysis. *PLoS One,* 8**,** e55691.

LIU, Z., VONG, Q. P., LIU, C. & ZHENG, Y. 2014. Borg5 is required for angiogenesis by regulating persistent directional migration of the cardiac microvascular endothelial cells. *Mol Biol Cell,* 25**,** 841-51.

LIVERMAN, A. D., CHENG, H. C., TROSKY, J. E., LEUNG, D. W., YARBROUGH, M. L., BURDETTE, D. L., ROSEN, M. K. & ORTH, K. 2007. Arp2/3-independent assembly of actin by Vibrio type III effector VopL. *Proc Natl Acad Sci U S A,* 104**,** 17117-22.

LOCKER, J. K., KUEHN, A., SCHLEICH, S., RUTTER, G., HOHENBERG, H., WEPF, R. & GRIFFITHS, G. 2000. Entry of the two infectious forms of vaccinia virus at the plasma membane is signaling-dependent for the IMV but not the EEV. *Mol Biol Cell,* 11**,** 2497-511.

LOISEL, T. P., BOUJEMAA, R., PANTALONI, D. & CARLIER, M. F. 1999. Reconstitution of actin-based motility of Listeria and Shigella using pure proteins. *Nature,* 401**,** 613-6.

LONGTINE, M. S., FARES, H. & PRINGLE, J. R. 1998. Role of the yeast Gin4p protein kinase in septin assembly and the relationship between septin assembly and septin function. *J Cell Biol,* 143**,** 719-36.

LOUSBERG, E. L., DIENER, K. R., BROWN, M. P. & HAYBALL, J. D. 2011. Innate immune recognition of poxviral vaccine vectors. *Expert Rev Vaccines,* 10**,** 1435-49.

LOWENSTEIN, E. J., DALY, R. J., BATZER, A. G., LI, W., MARGOLIS, B., LAMMERS, R., ULLRICH, A., SKOLNIK, E. Y., BAR-SAGI, D. & SCHLESSINGER, J. 1992. The SH2 and SH3 domain-containing protein GRB2 links receptor tyrosine kinases to ras signaling. *Cell,* 70**,** 431-42.

LU, J. & POLLARD, T. D. 2001. Profilin binding to poly-L-proline and actin monomers along with ability to catalyze actin nucleotide exchange is required for viability of fission yeast. *Mol Biol Cell,* 12**,** 1161-75.

LU, R., DRUBIN, D. G. & SUN, Y. 2016. Clathrin-mediated endocytosis in budding yeast at a glance. *J Cell Sci,* 129**,** 1531-6.

LUEDEKE, C., FREI, S. B., SBALZARINI, I., SCHWARZ, H., SPANG, A. & BARRAL, Y. 2005. Septin-dependent compartmentalization of the endoplasmic reticulum during yeast polarized growth. *J Cell Biol,* 169**,** 897-908.

LUSSIER, G. & LAROSE, L. 1997. A casein kinase I activity is constitutively associated with Nck. *J Biol Chem,* 272**,** 2688-94.

MA, L., UMASANKAR, P. K., WROBEL, A. G., LYMAR, A., MCCOY, A. J., HOLKAR, S. S., JHA, A., PRADHAN-SUNDD, T., WATKINS, S. C., OWEN, D. J. & TRAUB, L. M. 2016. Transient Fcho1/2Eps15/RAP-2 Nanoclusters Prime the AP-2 Clathrin Adaptor for Cargo Binding. *Developmental Cell,* 37**,** 428-43.

MACHESKY, L. M., ATKINSON, S. J., AMPE, C., VANDEKERCKHOVE, J. & POLLARD, T. D. 1994. Purification of a cortical complex containing two unconventional actins from Acanthamoeba by affinity chromatography on profilin-agarose. *J Cell Biol,* 127**,** 107-15.

MACHESKY, L. M. & INSALL, R. H. 1998. Scar1 and the related Wiskott-Aldrich syndrome protein, WASP, regulate the actin cytoskeleton through the Arp2/3 complex. *Curr Biol,* 8**,** 1347-56.

MACHESKY, L. M., INSALL, R. H. & VOLKMAN, L. E. 2001. WASP homology sequences in baculoviruses. *Trends Cell Biol,* 11**,** 286-7.

MACHESKY, L. M., MULLINS, R. D., HIGGS, H. N., KAISER, D. A., BLANCHOIN, L., MAY, R. C., HALL, M. E. & POLLARD, T. D. 1999. Scar, a WASp-related protein, activates nucleation of actin filaments by the Arp2/3 complex. *Proc Natl Acad Sci U S A,* 96**,** 3739-44.

MACIA, E., EHRLICH, M., MASSOL, R., BOUCROT, E., BRUNNER, C. & KIRCHHAUSEN, T. 2006. Dynasore, a Cell-Permeable Inhibitor of Dynamin. *Developmental Cell,* 10**,** 839-850.

MADDOX, A. S., LEWELLYN, L., DESAI, A. & OEGEMA, K. 2007. Anillin and the septins promote asymmetric ingression of the cytokinetic furrow. *Developmental Cell,* 12**,** 827-35.

MAIB, H., SMYTHE, E. & AYSCOUGH, K. 2017. Forty years on: clathrin-coated pits continue to fascinate. *Mol Biol Cell,* 28**,** 843-847.

MAIMAITIYIMING, M., KOBAYASHI, Y., KUMANOGOH, H., NAKAMURA, S., MORITA, M. & MAEKAWA, S. 2013. Identification of dynamin as a septin-binding protein.

MAITI, S., MICHELOT, A., GOULD, C., BLANCHOIN, L., SOKOLOVA, O. & GOODE, B. L. 2012. Structure and activity of full-length formin mDia1. *Cytoskeleton (Hoboken),* 69**,** 393-405.

MAKHNEVYCH, T., PTAK, C., LUSK, C. P., AITCHISON, J. D. & WOZNIAK, R. W. 2007. The role of karyopherins in the regulated sumoylation of septins. *J Cell Biol,* 177**,** 39-49.

MAKINO, S., SASAKAWA, C., KAMATA, K., KURATA, T. & YOSHIKAWA, M. 1986. A genetic determinant required for continuous reinfection of adjacent cells on large plasmid in S. flexneri 2a. *Cell,* 46**,** 551-5.

MALLARDO, M., SCHLEICH, S. & KRIJNSE LOCKER, J. 2001. Microtubule-dependent organization of vaccinia virus core-derived early mRNAs into distinct cytoplasmic structures. *Mol Biol Cell,* 12**,** 3875-91.

MANOR, U., BARTHOLOMEW, S., GOLANI, G., CHRISTENSON, E., KOZLOV, M., HIGGS, H., SPUDICH, J. & LIPPINCOTT-SCHWARTZ, J. 2015. A mitochondria-anchored isoform of the actin-nucleating spire protein regulates mitochondrial division. *Elife,* 4.

MARCHAND, J. B., KAISER, D. A., POLLARD, T. D. & HIGGS, H. N. 2001. Interaction of WASP/Scar proteins with actin and vertebrate Arp2/3 complex. *Nat Cell Biol,* 3**,** 76-82.

MARKS, B., STOWELL, M. H., VALLIS, Y., MILLS, I. G., GIBSON, A., HOPKINS, C. R. & MCMAHON, H. T. 2001. GTPase activity of dynamin and resulting conformation change are essential for endocytosis. *Nature,* 410**,** 231-5.

MARTIN, S. W. & KONOPKA, J. B. 2004. SUMO Modification of Septin-interacting Proteins in Candida albicans. *Journal of Biological Chemistry,* 279**,** 40861-40867.

MARTINEZ, C., CORRAL, J., DENT, J. A., SESMA, L., VICENTE, V. & WARE, J. 2006. Platelet septin complexes form rings and associate with the microtubular network. *J Thromb Haemost,* 4**,** 1388-95.

MARTINEZ-QUILES, N., ROHATGI, R., ANTON, I. M., MEDINA, M., SAVILLE, S. P., MIKI, H., YAMAGUCHI, H., TAKENAWA, T., HARTWIG, J. H., GEHA, R. S. & RAMESH, N. 2001. WIP regulates N-WASP-mediated actin polymerization and filopodium formation. *Nat Cell Biol,* 3**,** 484-91.

MARTTINEN, M., KURKINEN, K. M., SOININEN, H., HAAPASALO, A. & HILTUNEN, M. 2015. Synaptic dysfunction and septin protein family members in neurodegenerative diseases. *Mol Neurodegener,* 10**,** 16.

MATHEW, E. C., SANDERSON, C. M., HOLLINSHEAD, R., HOLLINSHEAD, M., GRIMLEY, R. & SMITH, G. L. 1999. The effects of targeting the vaccinia virus B5R protein to the endoplasmic reticulum on virus morphogenesis and dissemination. *Virology,* 265**,** 131-46.

MATTILA, J.-P., SHNYROVA, A. V., SUNDBORGER, A. C., HORTELANO, E. R., FUHRMANS, M., NEUMANN, S., MÜLLER, M., HINSHAW, J. E., SCHMID, S. L. & FROLOV, V. A. 2015. A hemi-fission intermediate links two mechanistically distinct stages of membrane fission. *Nature,* 524**,** 109-113.

MAURICIO, R. P., JEFFRIES, C. M., SVERGUN, D. I. & DEANE, J. E. 2017. The Shigella Virulence Factor IcsA Relieves N-WASP Autoinhibition by Displacing the Verprolin Homology/Cofilin/Acidic (VCA) Domain. *J Biol Chem,* 292**,** 134-145.

MAVRAKIS, M., AZOU-GROS, Y., TSAI, F.-C., ALVARADO, J., BERTIN, A., IV, F., KRESS, A., BRASSELET, S., KOENDERINK, G. H. & LECUIT, T. 2014. Septins promote F-actin ring formation by crosslinking actin filaments into curved bundles. *Nat Cell Biol,* 16**,** 322-34.

MAZON-MOYA, M. J., WILLIS, A. R., TORRACA, V., BOUCONTET, L., SHENOY, A. R., COLUCCI-GUYON, E. & MOSTOWY, S. 2017. Septins restrict inflammation and protect zebrafish larvae from Shigella infection. *PLoS Pathog,* 13**,** e1006467.

MCCARTY, J. H. 1998. The Nck SH2/SH3 adaptor protein: a regulator of multiple intracellular signal transduction events. *Bioessays,* 20**,** 913-21.

MCCLUSKEY, A., DANIEL, J. A., HADZIC, G., CHAU, N., CLAYTON, E. L., MARIANA, A., WHITING, A., GORGANI, N. N., LLOYD, J., QUAN, A., MOSHKANBARYANS, L., KRISHNAN, S., PERERA, S., CHIRCOP, M., VON KLEIST, L., MCGEACHIE, A. B., HOWES, M. T., PARTON, R. G., CAMPBELL, M., SAKOFF, J. A., WANG, X., SUN, J.-Y., ROBERTSON, M. J., DEANE, F. M., NGUYEN, T. H., MEUNIER, F. A., COUSIN, M. A. & ROBINSON, P. J. 2013. Building a Better Dynasore: The Dyngo Compounds Potently Inhibit Dynamin and Endocytosis. *Traffic,* 14**,** 1272-1289.

MCGAVIN, M. K., BADOUR, K., HARDY, L. A., KUBISESKI, T. J., ZHANG, J. & SIMINOVITCH, K. A. 2001. The intersectin 2 adaptor links Wiskott Aldrich Syndrome protein (WASp)-mediated actin polymerization to T cell antigen receptor endocytosis. *J Exp Med,* 194**,** 1777-87.

MCGOUGH, A., POPE, B., CHIU, W. & WEEDS, A. 1997. Cofilin changes the twist of F-actin: implications for actin filament dynamics and cellular function. *J Cell Biol,* 138**,** 771-81.

MCINTOSH, A. A. & SMITH, G. L. 1996. Vaccinia virus glycoprotein A34R is required for infectivity of extracellular enveloped virus. *J Virol,* 70**,** 272-81.

MCMAHON, H. T. & BOUCROT, E. 2011. Molecular mechanism and physiological functions of clathrin-mediated endocytosis. *Nat Rev Mol Cell Biol,* 12**,** 517-33.

MCNIVEN, M. A., KIM, L., KRUEGER, E. W., ORTH, J. D., CAO, H. & WONG, T. W. 2000. Regulated Interactions between Dynamin and the Actin-Binding Protein Cortactin Modulate Cell Shape. *J Cell Biol,* 151.

MEARS, J. A., LACKNER, L. L., FANG, S., INGERMAN, E., NUNNARI, J. & HINSHAW, J. E. 2011. Conformational changes in Dnm1 support a contractile mechanism for mitochondrial fission. *Nat Struct Mol Biol,* 18**,** 20-6.

MEARS, J. A., RAY, P. & HINSHAW, J. E. 2007. A corkscrew model for dynamin constriction. *Structure,* 15**,** 1190-202.

MENDOZA, M., HYMAN, A. A. & GLOTZER, M. 2002. GTP binding induces filament assembly of a recombinant septin. *Curr Biol,* 12**,** 1858-63.

MERCER, J. 2011. Viral apoptotic mimicry party: P.S. Bring your own Gas6. *Cell Host Microbe,* 9**,** 255-7.

MERCER, J. & HELENIUS, A. 2008. Vaccinia virus uses macropinocytosis and apoptotic mimicry to enter host cells. *Science,* 320**,** 531-5.

MERCER, J. & HELENIUS, A. 2009. Virus entry by macropinocytosis. *Nat Cell Biol,* 11**,** 510-20.

MERCER, J. & HELENIUS, A. 2010. Apoptotic mimicry: phosphatidylserine-mediated macropinocytosis of vaccinia virus. *Ann N Y Acad Sci,* 1209**,** 49-55.

MERCER, J., KNEBEL, S., SCHMIDT, F. I., CROUSE, J., BURKARD, C. & HELENIUS, A. 2010a. Vaccinia virus strains use distinct forms of macropinocytosis for host-cell entry. *Proc Natl Acad Sci U S A,* 107**,** 9346-51.

MERCER, J., SCHELHAAS, M. & HELENIUS, A. 2010b. Virus entry by endocytosis. *Annu Rev Biochem,* 79**,** 803-33.

MERCER, J., SNIJDER, B., SACHER, R., BURKARD, C., BLECK, C. K. E., STAHLBERG, H., PELKMANS, L. & HELENIUS, A. 2012. RNAi Screening Reveals Proteasome- and Cullin3-Dependent Stages in Vaccinia Virus Infection. *Cell Reports,* 2**,** 1036-1047.

MERRIFIELD, C., QUALMANN, B., KESSELS, M. M. & ALMERS, W. 2004. Neural Wiskott Aldrich Syndrome Protein (N-WASP) and the Arp2/3 complex are recruited to sites of clathrin-mediated endocytosis in cultured fibroblasts. *European Journal of Cell Biology,* 83**,** 13-18.

MESEROLL, R. A., HOWARD, L. & GLADFELTER, A. S. 2012. Septin ring size scaling and dynamics require the coiled-coil region of Shs1p. *Mol Biol Cell,* 23**,** 3391-406.

MESEROLL, R. A., OCCHIPINTI, P. & GLADFELTER, A. S. 2013. Septin phosphorylation and coiled-coil domains function in cell and septin ring morphology in the filamentous fungus Ashbya gossypii. *Eukaryotic cell,* 12**,** 182-93.

MIKI, H., MIURA, K., MATUOKA, K., NAKATA, T., HIROKAWA, N., ORITA, S., KAIBUCHI, K., TAKAI, Y. & TAKENAWA, T. 1994. Association of Ash/Grb-2 with dynamin through the Src homology 3 domain. *J Biol Chem,* 269**,** 5489-92.

MIKI, H., MIURA, K. & TAKENAWA, T. 1996. N-WASP, a novel actin-depolymerizing protein, regulates the cortical cytoskeletal rearrangement in a PIP2-dependent manner downstream of tyrosine kinases. *EMBO J,* 15**,** 5326-35.

MIKI, H., SASAKI, T., TAKAI, Y. & TAKENAWA, T. 1998a. Induction of filopodium formation by a WASP-related actin-depolymerizing protein N-WASP. *Nature,* 391**,** 93-6.

MIKI, H., SUETSUGU, S. & TAKENAWA, T. 1998b. WAVE, a novel WASP-family protein involved in actin reorganization induced by Rac. *EMBO J,* 17**,** 6932-41.

MINER, J. N. & HRUBY, D. E. 1990. Vaccinia virus: a versatile tool for molecular biologists. *Trends Biotechnol,* 8**,** 20-5.

MITCHELL, L., LAU, A., LAMBERT, J. P., ZHOU, H., FONG, Y., COUTURE, J. F., FIGEYS, D. & BAETZ, K. 2011. Regulation of septin dynamics by the Saccharomyces cerevisiae lysine acetyltransferase NuA4. *PLoS One,* 6**,** e25336.

MOGILNER, A. & OSTER, G. 1996. Cell motility driven by actin polymerization. *Biophysical Journal,* 71**,** 3030-45.

MOGILNER, A. & OSTER, G. 2003. Force Generation by Actin Polymerization II: The Elastic Ratchet and Tethered Filaments. *Biophysical Journal,* 84**,** 1591-1605.

MONTAVILLE, P., KUHN, S., COMPPER, C. & CARLIER, M. F. 2016. Role of the C-terminal Extension of Formin 2 in Its Activation by Spire Protein and Processive Assembly of Actin Filaments. *J Biol Chem,* 291**,** 3302-18.

MOON, I. S., LEE, H. & WALIKONIS, R. S. 2013. Septin 6 localizes to microtubules in neuronal dendrites. *Cytotechnology,* 65**,** 179-86.

MOOREN, O. L., GALLETTA, B. J. & COOPER, J. A. 2012. Roles for actin assembly in endocytosis. *Annu Rev Biochem,* 81**,** 661-86.

MOREAU, V., FRISCHKNECHT, F., RECKMANN, I., VINCENTELLI, R., RABUT, G., STEWART, D. & WAY, M. 2000. A complex of N-WASP and WIP integrates signalling cascades that lead to actin polymerization. *Nat Cell Biol,* 2**,** 441-8.

MORENO-RUIZ, E., GALAN-DIEZ, M., ZHU, W., FERNANDEZ-RUIZ, E., D'ENFERT, C., FILLER, S. G., COSSART, P. & VEIGA, E. 2009. Candida albicans internalization by host cells is mediated by a clathrin-dependent mechanism. *Cell Microbiol,* 11**,** 1179-89.

MORGAN, C. 1976. The insertion of DNA into vaccinia virus. *Science,* 193**,** 591-2.

MORGAN, G. W., HOLLINSHEAD, M., FERGUSON, B. J., MURPHY, B. J., CARPENTIER, D. C. & SMITH, G. L. 2010. Vaccinia protein F12 has structural similarity to kinesin light chain and contains a motor binding motif required for virion export. *PLoS Pathog,* 6**,** e1000785.

MORLOT, S., GALLI, V., KLEIN, M., CHIARUTTINI, N., MANZI, J., HUMBERT, F., DINIS, L., LENZ, M., CAPPELLO, G. & ROUX, A. 2012. Membrane shape at the edge of the dynamin helix sets location and duration of the fission reaction. *Cell,* 151**,** 619-29.

MORTENSEN, E. M., MCDONALD, H., YATES, J., 3RD & KELLOGG, D. R. 2002. Cell cycle-dependent assembly of a Gin4-septin complex. *Mol Biol Cell,* 13**,** 2091-105.

MOSELEY, J. B., SAGOT, I., MANNING, A. L., XU, Y., ECK, M. J., PELLMAN, D. & GOODE, B. L. 2004. A conserved mechanism for Bni1- and mDia1-induced actin assembly and dual regulation of Bni1 by Bud6 and profilin. *Mol Biol Cell,* 15**,** 896-907.

MOSER, B., ROTH, G., BRUNNER, M., LILAJ, T., DEICHER, R., WOLNER, E., KOVARIK, J., BOLTZ-NITULESCU, G., VYCHYTIL, A. & ANKERSMIT, H. J. 2003. Aberrant T cell activation and heightened apoptotic turnover in end-stage renal failure patients: a comparative evaluation between non-dialysis, haemodialysis, and peritoneal dialysis. *Biochem Biophys Res Commun,* 308**,** 581-5.

MOSS, B. 1968. Inhibition of HeLa cell protein synthesis by the vaccinia virion. *J Virol,* 2**,** 1028-37.

MOSS, B. 2007. *Poxviridae: The Viruses and Their Replication*.

MOSS, B. 2013. Poxvirus DNA replication. *Cold Spring Harb Perspect Biol,* 5.

MOSS, B. 2016. Membrane fusion during poxvirus entry. *Semin Cell Dev Biol,* 60**,** 89-96.

MOSS, B. & ROSENBLUM, E. N. 1973. Letter: Protein cleavage and poxvirus morphogenesis: tryptic peptide analysis of core precursors accumulated by blocking assembly with rifampicin. *J Mol Biol,* 81**,** 267-9.

MOSTOWY, S., BONAZZI, M., HAMON, M. A., THAM, T. N., MALLET, A., LELEK, M., GOUIN, E., DEMANGEL, C., BROSCH, R., ZIMMER, C., SARTORI, A., KINOSHITA, M., LECUIT, M. & COSSART, P. 2010. Entrapment of intracytosolic bacteria by septin cage-like structures. *Cell Host Microbe,* 8**,** 433-44.

MOSTOWY, S. & COSSART, P. 2012. Septins: the fourth component of the cytoskeleton. *Nature reviews. Molecular cell biology,* 13**,** 183-94.

MOSTOWY, S., DANCKAERT, A., THAM, T. N., MACHU, C., GUADAGNINI, S., PIZARRO-CERDÁ, J. & COSSART, P. 2009a. Septin 11 restricts InlB-mediated invasion by Listeria. *The Journal of biological chemistry,* 284**,** 11613-21.

MOSTOWY, S., JANEL, S., FORESTIER, C., RODUIT, C., KASAS, S., PIZARRO-CERDÁ, J., COSSART, P. & LAFONT, F. 2011. A role for septins in the interaction between the Listeria monocytogenes INVASION PROTEIN InlB and the Met receptor. *Biophysical Journal,* 100**,** 1949-59.

MOSTOWY, S., NAM THAM, T., DANCKAERT, A., GUADAGNINI, S., BOISSON-DUPUIS, S., PIZARRO-CERDÁ, J. & COSSART, P. 2009b. Septins regulate bacterial entry into host cells. *PLoS One,* 4**,** e4196-e4196.

MUELLER, J., PFANZELTER, J., WINKLER, C., NARITA, A., LE CLAINCHE, C., NEMETHOVA, M., CARLIER, M.-F., MAEDA, Y., WELCH, M. D., OHKAWA, T., SCHMEISER, C., RESCH, G. P. & SMALL, J. V. 2014. Electron Tomography and Simulation of Baculovirus Actin Comet Tails Support a Tethered Filament Model of Pathogen Propulsion. *PLoS Biology,* 12**,** e1001765-e1001765.

MULLINS, R. D., HEUSER, J. A. & POLLARD, T. D. 1998a. The interaction of Arp2/3 complex with actin: nucleation, high affinity pointed end capping, and formation of branching networks of filaments. *Proc Natl Acad Sci U S A,* 95**,** 6181-6.

MULLINS, R. D., KELLEHER, J. F., XU, J. & POLLARD, T. D. 1998b. Arp2/3 complex from Acanthamoeba binds profilin and cross-links actin filaments. *Mol Biol Cell,* 9**,** 841-52.

MURALIDHAR, S., PUMFERY, A. M., HASSANI, M., SADAIE, M. R., KISHISHITA, M., BRADY, J. N., DONIGER, J., MEDVECZKY, P. & ROSENTHAL, L. J. 1998. Identification of kaposin (open reading frame K12) as a human herpesvirus 8 (Kaposi's sarcoma-associated herpesvirus) transforming gene. *J Virol,* 72**,** 4980-8.

MURALIDHAR, S., VEYTSMANN, G., CHANDRAN, B., ABLASHI, D., DONIGER, J. & ROSENTHAL, L. J. 2000. Characterization of the human herpesvirus 8 (Kaposi's sarcoma-associated herpesvirus) oncogene, kaposin (ORF K12). *J Clin Virol,* 16**,** 203-13.

NAGARAJ, S., RAJENDRAN, A., JACKSON, C. E. & LONGTINE, M. S. 2008. Role of nucleotide binding in septin-septin interactions and septin localization in Saccharomyces cerevisiae. *Mol Cell Biol,* 28**,** 5120-37.

NAGATA, K.-I., KAWAJIRI, A., MATSUI, S., TAKAGISHI, M., SHIROMIZU, T., SAITOH, N., IZAWA, I., KIYONO, T., ITOH, T. J., HOTANI, H. & INAGAKI, M. 2003. Filament formation of MSF-A, a mammalian septin, in human mammary epithelial cells depends on interactions with microtubules. *The Journal of biological chemistry,* 278**,** 18538-43.

NAGHAVI, M. H. & WALSH, D. 2017. Microtubule Regulation and Function during Virus Infection. *J Virol,* 91.

NAKAHIRA, M., MACEDO, J. N. A., SERAPHIM, T. V., CAVALCANTE, N., SOUZA, T. A. C. B., DAMALIO, J. C. P., REYES, L. F., ASSMANN, E. M., ALBORGHETTI, M. R., GARRATT, R. C., ARAUJO, A. P. U., ZANCHIN, N. I. T., BARBOSA, J. A. R. G. & KOBARG, J. 2010. A draft of the human septin interactome. *PLoS One,* 5**,** e13799-e13799.

NAKATA, T., TAKEMURA, R. & HIROKAWA, N. 1993. A novel member of the dynamin family of GTP-binding proteins is expressed specifically in the testis. *J Cell Sci,* 105.

NEWMARK, P. 1980. Smallpox: gone for good? *Nature,* 285**,** 62.

NEWSOME, T. P. & MARZOOK, N. B. 2015. Viruses that ride on the coat-tails of actin nucleation. *Semin Cell Dev Biol,* 46**,** 155-63.

NEWSOME, T. P., SCAPLEHORN, N. & WAY, M. 2004. SRC mediates a switch from microtubule- to actin-based motility of vaccinia virus. *Science,* 306**,** 124-9.

NEWSOME, T. P., WEISSWANGE, I., FRISCHKNECHT, F. & WAY, M. 2006. Abl collaborates with Src family kinases to stimulate actin-based motility of vaccinia virus. *Cellular microbiology,* 8**,** 233-41.

NEZAMI, A. G., POY, F. & ECK, M. J. 2006. Structure of the autoinhibitory switch in formin mDia1. *Structure,* 14**,** 257-63.

NICHOLS, D. B., DE MARTINI, W. & COTTRELL, J. 2017. Poxviruses Utilize Multiple Strategies to Inhibit Apoptosis. *Viruses,* 9.

NICHOLS, R. J., STANITSA, E., UNGER, B. & TRAKTMAN, P. 2008. The vaccinia virus gene I2L encodes a membrane protein with an essential role in virion entry. *J Virol,* 82**,** 10247-61.

NISHIDA, E. & SAKAI, H. 1983. Kinetic analysis of actin polymerization. *J Biochem,* 93**,** 1011-20.

NOLEN, B. J., TOMASEVIC, N., RUSSELL, A., PIERCE, D. W., JIA, Z., MCCORMICK, C. D., HARTMAN, J., SAKOWICZ, R. & POLLARD, T. D. 2009. Characterization of two classes of small molecule inhibitors of Arp2/3 complex. *Nature,* 460**,** 1031-4.

NÖLKE, T., SCHWAN, C., LEHMANN, F., ØSTEVOLD, K., PERTZ, O. & AKTORIES, K. 2016. Septins guide microtubule protrusions induced by actin-depolymerizing toxins like Clostridium difficile transferase (CDT). *Proc Natl Acad Sci U S A*.

NOVOKHATSKA, O., DERGAI, M., HOUSSIN, N., TSYBA, L., MOREAU, J. & RYNDITCH, A. 2011. Intersectin 2 nucleotide exchange factor regulates Cdc42 activity during Xenopus early development. *Biochem Biophys Res Commun,* 408**,** 663-8.

NUNEZ, D., ANTONESCU, C., METTLEN, M., LIU, A., SCHMID, S. L., LOERKE, D. & DANUSER, G. 2011. Hotspots organize clathrin-mediated endocytosis by efficient recruitment and retention of nucleating resources. *Traffic,* 12**,** 1868-78.

O'BRYAN, J. P. 2010. Intersecting pathways in cell biology. *Sci Signal,* 3**,** re10.

OCHOA, G. C., SLEPNEV, V. I., NEFF, L., RINGSTAD, N., TAKEI, K., DANIELL, L., KIM, W., CAO, H., MCNIVEN, M., BARON, R. & DE CAMILLI, P. 2000. A functional link between dynamin and the actin cytoskeleton at podosomes. *J Cell Biol,* 150**,** 377-89.

OEGEMA, K., SAVOIAN, M. S., MITCHISON, T. J. & FIELD, C. M. 2000. Functional analysis of a human homologue of the Drosophila actin binding protein anillin suggests a role in cytokinesis. *J Cell Biol,* 150**,** 539-52.

OHIMAIN, E. I. 2016. Recent advances in the development of vaccines for Ebola virus disease. *Virus Res,* 211**,** 174-85.

OHKAWA, T., VOLKMAN, L. E. & WELCH, M. D. 2010. Actin-based motility drives baculovirus transit to the nucleus and cell surface. *J Cell Biol,* 190**,** 187-95.

OHNO, H., STEWART, J., FOURNIER, M. C., BOSSHART, H., RHEE, I., MIYATAKE, S., SAITO, T., GALLUSSER, A., KIRCHHAUSEN, T. & BONIFACINO, J. S. 1995. Interaction of tyrosine-based sorting signals with clathrin-associated proteins. *Science,* 269**,** 1872-5.

OJEDA, S., DOMI, A. & MOSS, B. 2006a. Vaccinia virus G9 protein is an essential component of the poxvirus entry-fusion complex. *J Virol,* 80**,** 9822-30.

OJEDA, S., SENKEVICH, T. G. & MOSS, B. 2006b. Entry of vaccinia virus and cell-cell fusion require a highly conserved cysteine-rich membrane protein encoded by the A16L gene. *J Virol,* 80**,** 51-61.

OKAMOTO, M., SCHOCH, S. & SUDHOF, T. C. 1999a. EHSH1/intersectin, a protein that contains EH and SH3 domains and binds to dynamin and SNAP-25. A protein connection between exocytosis and endocytosis? *J Biol Chem,* 274**,** 18446-54.

OKAMOTO, M., SCHOCH, S. & SÜDHOF, T. C. 1999b. EHSH1/intersectin, a protein that contains EH and SH3 domains and binds to dynamin and SNAP-25. A protein connection between exocytosis and endocytosis? *The Journal of biological chemistry,* 274**,** 18446-54.

OKREGLAK, V. & DRUBIN, D. G. 2007. Cofilin recruitment and function during actin-mediated endocytosis dictated by actin nucleotide state. *J Cell Biol,* 178**,** 1251-64.

ONG, K., WLOKA, C., OKADA, S., SVITKINA, T. & BI, E. 2014. Architecture and dynamic remodelling of the septin cytoskeleton during the cell cycle. *Nat Commun,* 5**,** 5698.

ORLOVA, A. & EGELMAN, E. H. 1992. Structural basis for the destabilization of F-actin by phosphate release following ATP hydrolysis. *J Mol Biol,* 227**,** 1043-53.

ORR, M. W. & MCNEILL, W. H. 1988. Plagues and peoples, William H. McNeill. *Touchstone (Nashv)***,** 3-5.

ORTH, J. D., KRUEGER, E. W., CAO, H. & MCNIVEN, M. A. 2002. The large GTPase dynamin regulates actin comet formation and movement in living cells. *Proc Natl Acad Sci U S A,* 99**,** 167-172.

OSZ-PAPAI, J., RADU, L., ABDULRAHMAN, W., KOLB-CHEYNEL, I., TROFFER-CHARLIER, N., BIRCK, C. & POTERSZMAN, A. 2015. Insect cells-baculovirus system for the production of difficult to express proteins. *Methods Mol Biol,* 1258**,** 181-205.

OWEN, D. J. & EVANS, P. R. 1998. A structural explanation for the recognition of tyrosine-based endocytotic signals. *Science,* 282**,** 1327-32.

PADRICK, S. B., CHENG, H. C., ISMAIL, A. M., PANCHAL, S. C., DOOLITTLE, L. K., KIM, S., SKEHAN, B. M., UMETANI, J., BRAUTIGAM, C. A., LEONG, J. M. & ROSEN, M. K. 2008. Hierarchical regulation of WASP/WAVE proteins. *Mol Cell,* 32**,** 426-38.

PADRON, D., WANG, Y. J., YAMAMOTO, M., YIN, H. & ROTH, M. G. 2003. Phosphatidylinositol phosphate 5-kinase Ibeta recruits AP-2 to the plasma membrane and regulates rates of constitutive endocytosis. *J Cell Biol,* 162**,** 693-701.

PAGLIUSO, A., COSSART, P. & STAVRU, F. 2017. The ever-growing complexity of the mitochondrial fission machinery. *Cell Mol Life Sci*.

PAGLIUSO, A., THAM, T. N., STEVENS, J. K., LAGACHE, T., PERSSON, R., SALLES, A., OLIVO-MARIN, J.-C., ODDOS, S., SPANG, A., COSSART, P. & STAVRU, F. 2016. A role for septin 2 in Drp1-mediated mitochondrial fission. *EMBO reports*.

PALMER, S. E., SMACZYNSKA-DE, R., II, MARKLEW, C. J., ALLWOOD, E. G., MISHRA, R., JOHNSON, S., GOLDBERG, M. W. & AYSCOUGH, K. R. 2015. A dynamin-actin interaction is required for vesicle scission during endocytosis in yeast. *Curr Biol,* 25**,** 868-78.

PAN, F., MALMBERG, R. L. & MOMANY, M. 2007. Analysis of septins across kingdoms reveals orthology and new motifs. *BMC Evol Biol,* 7**,** 103.

PANCHAL, S. C., KAISER, D. A., TORRES, E., POLLARD, T. D. & ROSEN, M. K. 2003. A conserved amphipathic helix in WASP/Scar proteins is essential for activation of Arp2/3 complex. *Nat Struct Mol Biol,* 10**,** 591-8.

PAOLUZI, S., CASTAGNOLI, L., LAURO, I., SALCINI, A. E., CODA, L., FRE, S., CONFALONIERI, S., PELICCI, P. G., DI FIORE, P. P. & CESARENI, G. 1998. Recognition specificity of individual EH domains of mammals and yeast. *EMBO J,* 17**,** 6541-50.

PARK, R. J., SHEN, H., LIU, L., LIU, X., FERGUSON, S. M. & DE CAMILLI, P. 2013. Dynamin triple knockout cells reveal off target effects of commonly used dynamin inhibitors. *J Cell Sci,* 126**,** 5305-12.

PARKINSON, J. E. & SMITH, G. L. 1994. Vaccinia virus gene A36R encodes a M(r) 43-50 K protein on the surface of extracellular enveloped virus. *Virology,* 204**,** 376-90.

PAUL, A. S. & POLLARD, T. D. 2008. The role of the FH1 domain and profilin in formin-mediated actin-filament elongation and nucleation. *Curr Biol,* 18**,** 9-19.

PAYNE, L. G. 1980. Significance of extracellular enveloped virus in the in vitro and in vivo dissemination of vaccinia. *The Journal of general virology,* 50**,** 89-100.

PAYNE, L. G. & KRISTENSON, K. 1979. Mechanism of vaccinia virus release and its specific inhibition by N1-isonicotinoyl-N2-3-methyl-4-chlorobenzoylhydrazine. *J Virol,* 32**,** 614-22.

PAYNE, L. G. & KRISTENSSON, K. 1982. The effect of cytochalasin D and monensin on enveloped vaccinia virus release. *Arch Virol,* 74**,** 11-20.

PAYNE, L. G. & KRISTENSSON, K. 1990. The polypeptide composition of vaccinia-infected cell membranes and rifampicin bodies. *Virus Res,* 17**,** 15-30.

PEARSE, B. M. 1975. Coated vesicles from pig brain: purification and biochemical characterization. *J Mol Biol,* 97**,** 93-8.

PEARSE, B. M. 1982. Structure of coated pits and vesicles. *Ciba Found Symp***,** 246-65.

PEARSE, B. M. & ROBINSON, M. S. 1984. Purification and properties of 100-kd proteins from coated vesicles and their reconstitution with clathrin. *EMBO J,* 3**,** 1951-7.

PECHLIVANIS, M., SAMOL, A. & KERKHOFF, E. 2009. Identification of a short Spir interaction sequence at the C-terminal end of formin subgroup proteins. *J Biol Chem,* 284**,** 25324-33.

PECHSTEIN, A., BACETIC, J., VAHEDI-FARIDI, A., GROMOVA, K., SUNDBORGER, A., TOMLIN, N., KRAINER, G., VORONTSOVA, O., SCHAFER, J. G., OWE, S. G., COUSIN, M. A., SAENGER, W., SHUPLIAKOV, O. & HAUCKE, V. 2010. Regulation of synaptic vesicle recycling by complex formation between intersectin 1 and the clathrin adaptor complex AP2. *Proc Natl Acad Sci U S A,* 107**,** 4206-11.

PEDERSEN, K., SNIJDER, E. J., SCHLEICH, S., ROOS, N., GRIFFITHS, G. & LOCKER, J. K. 2000. Characterization of vaccinia virus intracellular cores: implications for viral uncoating and core structure. *J Virol,* 74**,** 3525-36.

PELKMANS, L., PUNTENER, D. & HELENIUS, A. 2002. Local actin polymerization and dynamin recruitment in SV40-induced internalization of caveolae. *Science,* 296**,** 535-9.

PERNIGO, S., LAMPRECHT, A., STEINER, R. A. & DODDING, M. P. 2013. Structural basis for kinesin-1:cargo recognition. *Science,* 340**,** 356-9.

PERSON-FERNANDEZ, A. & BEAUD, G. 1986. Purification and characterization of a protein synthesis inhibitor associated with vaccinia virus. *J Biol Chem,* 261**,** 8283-9.

PETERS, C., BAARS, T. L., BUHLER, S. & MAYER, A. 2004. Mutual control of membrane fission and fusion proteins. *Cell,* 119**,** 667-78.

PFANZELTER, J. 2013. *Development of a structural and mathematical model of actin tails propelling pathogens.* University of Vienna.

PHAN, Q. T., ENG, D. K., MOSTOWY, S., PARK, H., COSSART, P. & FILLER, S. G. 2013. Role of endothelial cell septin 7 in the endocytosis of Candida albicans. *MBio,* 4**,** e00542-13.

PICCO, A., MUND, M., RIES, J., NEDELEC, F. & KAKSONEN, M. 2015. Visualizing the functional architecture of the endocytic machinery. *Elife,* 4.

PINOT, M., VANNI, S., PAGNOTTA, S., LACAS-GERVAIS, S., PAYET, L. A., FERREIRA, T., GAUTIER, R., GOUD, B., ANTONNY, B. & BARELLI, H. 2014. Lipid cell biology. Polyunsaturated phospholipids facilitate membrane deformation and fission by endocytic proteins. *Science,* 345**,** 693-7.

PIOTROWSKI, J. T., GOMEZ, T. S., SCHOON, R. A., MANGALAM, A. K. & BILLADEAU, D. D. 2013. WASH knockout T cells demonstrate defective receptor trafficking, proliferation, and effector function. *Mol Cell Biol,* 33**,** 958-73.

PIZARRO-CERDA, J., JONQUIERES, R., GOUIN, E., VANDEKERCKHOVE, J., GARIN, J. & COSSART, P. 2002. Distinct protein patterns associated with Listeria monocytogenes InlA- or InlB-phagosomes. *Cell Microbiol,* 4**,** 101-15.

PIZARRO-CERDA, J., KUHBACHER, A. & COSSART, P. 2012. Entry of Listeria monocytogenes in mammalian epithelial cells: an updated view. *Cold Spring Harb Perspect Med,* 2.

PLETT, P. C. 2006. [Peter Plett and other discoverers of cowpox vaccination before Edward Jenner]. *Sudhoffs Arch,* 90**,** 219-32.

PLOUBIDOU, A., MOREAU, V., ASHMAN, K., RECKMANN, I., GONZALEZ, C. & WAY, M. 2000. Vaccinia virus infection disrupts microtubule organization and centrosome function. *EMBO J,* 19**,** 3932-44.

POLLARD, T. D. 1977. Actin, myosin and cofactor from motile cells. *J Mechanochem Cell Motil,* 4**,** 15-30.

POLLARD, T. D. 1983. Measurement of rate constants for actin filament elongation in solution. *Anal Biochem,* 134**,** 406-12.

POLLARD, T. D. 2016. Actin and Actin-Binding Proteins. *Cold Spring Harb Perspect Biol,* 8.

POLLARD, T. D. & BORISY, G. G. 2003. Cellular motility driven by assembly and disassembly of actin filaments. *Cell,* 112**,** 453-65.

POLLARD, T. D. & COOPER, J. A. 1984. Quantitative analysis of the effect of Acanthamoeba profilin on actin filament nucleation and elongation. *Biochemistry,* 23**,** 6631-41.

POLLARD, T. D. & COOPER, J. A. 1986. Actin and actin-binding proteins. A critical evaluation of mechanisms and functions. *Annu Rev Biochem,* 55**,** 987-1035.

POLLARD, T. D. & COOPER, J. A. 2009. Actin, a central player in cell shape and movement. *Science,* 326**,** 1208-12.

POLLARD, T. D. & MOOSEKER, M. S. 1981. Direct measurement of actin polymerization rate constants by electron microscopy of actin filaments nucleated by isolated microvillus cores. *J Cell Biol,* 88**,** 654-9.

POLLARD, T. D. & WEEDS, A. G. 1984. The rate constant for ATP hydrolysis by polymerized actin. *FEBS Lett,* 170**,** 94-8.

POPOVA, N. V., DEYEV, I. E. & PETRENKO, A. G. 2013. Clathrin-mediated endocytosis and adaptor proteins. *Acta Naturae,* 5**,** 62-73.

PORTA, J. C. & BORGSTAHL, G. E. 2012. Structural basis for profilin-mediated actin nucleotide exchange. *J Mol Biol,* 418**,** 103-16.

POSTIGO, A. & FERRER, P. E. 2009. Viral inhibitors reveal overlapping themes in regulation of cell death and innate immunity. *Microbes Infect,* 11**,** 1071-8.

POSTIGO, A., MARTIN, M. C., DODDING, M. P. & WAY, M. 2009. Vaccinia-induced epidermal growth factor receptor-MEK signalling and the anti-apoptotic protein F1L synergize to suppress cell death during infection. *Cell Microbiol,* 11**,** 1208-18.

POSTIGO, A., RAMSDEN, A. E., HOWELL, M. & WAY, M. 2017. Cytoplasmic ATR Activation Promotes Vaccinia Virus Genome Replication. *Cell Reports,* 19**,** 1022-1032.

PRAEFCKE, G. J. & MCMAHON, H. T. 2004. The dynamin superfamily: universal membrane tubulation and fission molecules? *Nat Rev Mol Cell Biol,* 5**,** 133-47.

PREHODA, K. E., SCOTT, J. A., MULLINS, R. D. & LIM, W. A. 2000. Integration of multiple signals through cooperative regulation of the N-WASP-Arp2/3 complex. *Science,* 290**,** 801-6.

PRETA, G., CRONIN, J. G. & SHELDON, I. M. 2015. Dynasore - not just a dynamin inhibitor. *Cell communication and signaling : CCS,* 13**,** 24-24.

PRING, M., EVANGELISTA, M., BOONE, C., YANG, C. & ZIGMOND, S. H. 2003. Mechanism of formin-induced nucleation of actin filaments. *Biochemistry,* 42**,** 486-96.

PRUITT, W. M., KARNOUB, A. E., RAKAUSKAS, A. C., GUIPPONI, M., ANTONARAKIS, S. E., KURAKIN, A., KAY, B. K., SONDEK, J., SIDEROVSKI, D. P. & DER, C. J. 2003. Role of the pleckstrin homology domain in intersectin-L Dbl homology domain activation of Cdc42 and signaling. *Biochim Biophys Acta,* 1640**,** 61-8.

PRUYNE, D., EVANGELISTA, M., YANG, C., BI, E., ZIGMOND, S., BRETSCHER, A. & BOONE, C. 2002. Role of formins in actin assembly: nucleation and barbed-end association. *Science,* 297**,** 612-5.

QUALMANN, B. & KESSELS, M. M. 2009. New players in actin polymerization--WH2-domain-containing actin nucleators. *Trends Cell Biol,* 19**,** 276-85.

QUALMANN, B., KESSELS, M. M. & KELLY, R. B. 2000. Molecular links between endocytosis and the actin cytoskeleton. *J Cell Biol,* 150**,** F111-6.

QUAN, A., MCGEACHIE, A. B., KEATING, D. J., VAN DAM, E. M., RUSAK, J., CHAU, N., MALLADI, C. S., CHEN, C., MCCLUSKEY, A., COUSIN, M. A. & ROBINSON, P. J. 2007. Myristyl Trimethyl Ammonium Bromide and Octadecyl Trimethyl

Ammonium Bromide Are Surface-Active Small Molecule Dynamin Inhibitors that Block Endocytosis Mediated by Dynamin I or Dynamin II. *Molecular Pharmacology,* 72**,** 1425-1439.

QUINLAN, M. E., HEUSER, J. E., KERKHOFF, E. & MULLINS, R. D. 2005. Drosophila Spire is an actin nucleation factor. *Nature,* 433**,** 382-8.

QUINLAN, M. E., HILGERT, S., BEDROSSIAN, A., MULLINS, R. D. & KERKHOFF, E. 2007. Regulatory interactions between two actin nucleators, Spire and Cappuccino. *J Cell Biol,* 179**,** 117-28.

RADETSKY, M. 1999. Smallpox: a history of its rise and fall. *Pediatr Infect Dis J,* 18**,** 85-93.

RAMACHANDRAN, R. 2017. Mitochondrial dynamics: The dynamin superfamily and execution by collusion. *Semin Cell Dev Biol*.

RAMACHANDRAN, R., PUCADYIL, T. J., LIU, Y. W., ACHARYA, S., LEONARD, M., LUKIYANCHUK, V. & SCHMID, S. L. 2009. Membrane insertion of the pleckstrin homology domain variable loop 1 is critical for dynamin-catalyzed vesicle scission. *Mol Biol Cell,* 20**,** 4630-9.

RAMESH, N., ANTON, I. M., HARTWIG, J. H. & GEHA, R. S. 1997. WIP, a protein associated with wiskott-aldrich syndrome protein, induces actin polymerization and redistribution in lymphoid cells. *Proc Natl Acad Sci U S A,* 94**,** 14671-6.

RAMEZANPOUR, B., HAAN, I., OSTERHAUS, A. & CLAASSEN, E. 2016. Vector-based genetically modified vaccines: Exploiting Jenner's legacy. *Vaccine,* 34**,** 6436-6448.

RAPOPORT, I., MIYAZAKI, M., BOLL, W., DUCKWORTH, B., CANTLEY, L. C., SHOELSON, S. & KIRCHHAUSEN, T. 1997. Regulatory interactions in the recognition of endocytic sorting signals by AP-2 complexes. *EMBO J,* 16**,** 2240-50.

RAZ-BEN AROUSH, D., OFER, N., ABU-SHAH, E., ALLARD, J., KRICHEVSKY, O., MOGILNER, A. & KEREN, K. 2017. Actin Turnover in Lamellipodial Fragments. *Curr Biol,* 27**,** 2963-2973 e14.

REED, S. C., LAMASON, R. L., RISCA, V. I., ABERNATHY, E. & WELCH, M. D. 2014. Rickettsia actin-based motility occurs in distinct phases mediated by different actin nucleators. *Curr Biol,* 24**,** 98-103.

REEVES, P. M., BOMMARIUS, B., LEBEIS, S., MCNULTY, S., CHRISTENSEN, J., SWIMM, A., CHAHROUDI, A., CHAVAN, R., FEINBERG, M. B., VEACH, D., BORNMANN, W., SHERMAN, M. & KALMAN, D. 2005. Disabling poxvirus pathogenesis by inhibition of Abl-family tyrosine kinases. *Nature medicine,* 11**,** 731-9.

REIDER, A., BARKER, S. L., MISHRA, S. K., IM, Y. J., MALDONADO-BAEZ, L., HURLEY, J. H., TRAUB, L. M. & WENDLAND, B. 2009. Syp1 is a conserved endocytic adaptor that contains domains involved in cargo selection and membrane tubulation. *EMBO J,* 28**,** 3103-16.

RENA, G., BAIN, J., ELLIOTT, M. & COHEN, P. 2004. D4476, a cell-permeant inhibitor of CK1, suppresses the site-specific phosphorylation and nuclear exclusion of FOXO1a. *EMBO reports,* 5**,** 60-5.

RIETDORF, J., PLOUBIDOU, A., RECKMANN, I., HOLMSTROM, A., FRISCHKNECHT, F., ZETTL, M., ZIMMERMANN, T. & WAY, M. 2001. Kinesin-dependent movement on microtubules precedes actin-based motility of vaccinia virus. *Nat Cell Biol,* 3**,** 992-1000.

RISCO, C., RODRIGUEZ, J. R., LOPEZ-IGLESIAS, C., CARRASCOSA, J. L., ESTEBAN, M. & RODRIGUEZ, D. 2002. Endoplasmic reticulum-Golgi intermediate compartment membranes and vimentin filaments participate in vaccinia virus assembly. *J Virol,* 76**,** 1839-55.

RIVERO-LEZCANO, O. M., MARCILLA, A., SAMESHIMA, J. H. & ROBBINS, K. C. 1995. Wiskott-Aldrich syndrome protein physically associates with Nck through Src homology 3 domains. *Mol Cell Biol,* 15**,** 5725-31.

RIZVI, S. A., NEIDT, E. M., CUI, J., FEIGER, Z., SKAU, C. T., GARDEL, M. L., KOZMIN, S. A. & KOVAR, D. R. 2009. Identification and Characterization of a Small Molecule Inhibitor of Formin-Mediated Actin Assembly. *Chemistry & Biology,* 16**,** 1158-1168.

ROBBINS, J. R., MONACK, D., MCCALLUM, S. J., VEGAS, A., PHAM, E., GOLDBERG, M. B. & THERIOT, J. A. 2001. The making of a gradient: IcsA (VirG) polarity in Shigella flexneri. *Mol Microbiol,* 41**,** 861-72.

ROBERTS, K. L. & SMITH, G. L. 2008. Vaccinia virus morphogenesis and dissemination. *Trends Microbiol,* 16**,** 472-9.

ROBINSON, L. C., BRADLEY, C., BRYAN, J. D., JEROME, A., KWEON, Y. & PANEK, H. R. 1999. The Yck2 yeast casein kinase 1 isoform shows cell cycle-specific localization to sites of polarized growth and is required for proper septin organization. *Mol Biol Cell,* 10**,** 1077-92.

ROBINSON, M. S. 1987. 100-kD coated vesicle proteins: molecular heterogeneity and intracellular distribution studied with monoclonal antibodies. *J Cell Biol,* 104**,** 887-95.

ROBINSON, M. S. 2015. Forty Years of Clathrin-coated Vesicles. *Traffic,* 16**,** 1210-38.

ROBINSON, R. C., TURBEDSKY, K., KAISER, D. A., MARCHAND, J. B., HIGGS, H. N., CHOE, S. & POLLARD, T. D. 2001. Crystal structure of Arp2/3 complex. *Science,* 294**,** 1679-84.

RODAL, A. A., KOZUBOWSKI, L., GOODE, B. L., DRUBIN, D. G. & HARTWIG, J. H. 2005a. Actin and septin ultrastructures at the budding yeast cell cortex. *Mol Biol Cell,* 16**,** 372-84.

RODAL, A. A., SOKOLOVA, O., ROBINS, D. B., DAUGHERTY, K. M., HIPPENMEYER, S., RIEZMAN, H., GRIGORIEFF, N. & GOODE, B. L. 2005b. Conformational changes in the Arp2/3 complex leading to actin nucleation. *Nat Struct Mol Biol,* 12**,** 26-31.

RODRIGUEZ, D., RODRIGUEZ, J. R., OJAKIAN, G. K. & ESTEBAN, M. 1991. Vaccinia virus preferentially enters polarized epithelial cells through the basolateral surface. *J Virol,* 65**,** 494-8.

RODRIGUEZ, J. R., RISCO, C., CARRASCOSA, J. L., ESTEBAN, M. & RODRIGUEZ, D. 1998. Vaccinia virus 15-kilodalton (A14L) protein is essential for assembly and attachment of viral crescents to virosomes. *J Virol,* 72**,** 1287-96.

RODRIGUEZ-ESCUDERO, I., HARDWIDGE, P. R., NOMBELA, C., CID, V. J., FINLAY, B. B. & MOLINA, M. 2005. Enteropathogenic Escherichia coli type III effectors alter cytoskeletal function and signalling in Saccharomyces cerevisiae. *Microbiology,* 151**,** 2933-45.

ROGERS, L. D., BROWN, N. F., FANG, Y., PELECH, S. & FOSTER, L. J. 2011. Phosphoproteomic analysis of Salmonella-infected cells identifies key kinase regulators and SopB-dependent host phosphorylation events. *Sci Signal,* 4**,** rs9.

ROHATGI, R., HO, H. Y. & KIRSCHNER, M. W. 2000. Mechanism of N-WASP activation by CDC42 and phosphatidylinositol 4, 5-bisphosphate. *J Cell Biol,* 150**,** 1299-310.

ROHATGI, R., MA, L., MIKI, H., LOPEZ, M., KIRCHHAUSEN, T., TAKENAWA, T. & KIRSCHNER, M. W. 1999. The interaction between N-WASP and the Arp2/3 complex links Cdc42-dependent signals to actin assembly. *Cell,* 97**,** 221-31.

ROHATGI, R., NOLLAU, P., HO, H. Y., KIRSCHNER, M. W. & MAYER, B. J. 2001. Nck and phosphatidylinositol 4,5-bisphosphate synergistically activate actin polymerization through the N-WASP-Arp2/3 pathway. *J Biol Chem,* 276**,** 26448-52.

ROLHION, N. & COSSART, P. 2017. How the study of Listeria monocytogenes has led to new concepts in biology. *Future Microbiol,* 12**,** 621-638.

ROOS, J. & KELLY, R. B. 1998. Dap160, a neural-specific Eps15 homology and multiple SH3 domain-containing protein that interacts with Drosophila dynamin. *The Journal of biological chemistry,* 273**,** 19108-19.

ROSALES-NIEVES, A. E., JOHNDROW, J. E., KELLER, L. C., MAGIE, C. R., PINTO-SANTINI, D. M. & PARKHURST, S. M. 2006. Coordination of microtubule and microfilament dynamics by Drosophila Rho1, Spire and Cappuccino. *Nat Cell Biol,* 8**,** 367-76.

ROSE, R., WEYAND, M., LAMMERS, M., ISHIZAKI, T., AHMADIAN, M. R. & WITTINGHOFER, A. 2005. Structural and mechanistic insights into the interaction between Rho and mammalian Dia. *Nature,* 435**,** 513-8.

ROSEL, J. & MOSS, B. 1985. Transcriptional and translational mapping and nucleotide sequence analysis of a vaccinia virus gene encoding the precursor of the major core polypeptide 4b. *J Virol,* 56**,** 830-8.

ROTH, T. F. & PORTER, K. R. 1964. Yolk Protein Uptake in the Oocyte of the Mosquito Aedes Aegypti. L. *J Cell Biol,* 20**,** 313-32.

ROTTNER, K. & STRADAL, T. E. 2011. Actin dynamics and turnover in cell motility. *Curr Opin Cell Biol,* 23**,** 569-78.

ROTTY, J. D. & BEAR, J. E. 2015. Competition and collaboration between different actin assembly pathways allows for homeostatic control of the actin cytoskeleton. *Bioarchitecture,* 5**,** 27-34.

ROTTY, J. D., WU, C. & BEAR, J. E. 2013. New insights into the regulation and cellular functions of the ARP2/3 complex. *Nature reviews. Molecular cell biology,* 14**,** 7-12.

ROUILLER, I., XU, X.-P., AMANN, K. J., EGILE, C., NICKELL, S., NICASTRO, D., LI, R., POLLARD, T. D., VOLKMANN, N. & HANEIN, D. 2008. The structural basis of actin filament branching by the Arp2/3 complex. *J Cell Biol,* 180**,** 887-95.

ROUX, A. 2014. Reaching a consensus on the mechanism of dynamin? *F1000Prime Rep,* 6**,** 86.

ROUX, A., KOSTER, G., LENZ, M., SORRE, B., MANNEVILLE, J. B., NASSOY, P. & BASSEREAU, P. 2010. Membrane curvature controls dynamin polymerization. *Proc Natl Acad Sci U S A,* 107**,** 4141-6.

ROUX, A. & PLASTINO, J. 2010. Actin takes its hat off to dynamin. *EMBO J,* 29**,** 3591-2.

ROUX, A., UYHAZI, K., FROST, A. & DE CAMILLI, P. 2006. GTP-dependent twisting of dynamin implicates constriction and tension in membrane fission. *Nature,* 441**,** 528-31.

ROYLE, S. J., BRIGHT, N. A. & LAGNADO, L. 2005. Clathrin is required for the function of the mitotic spindle. *Nature,* 434**,** 1152-7.

RUST, M. J., LAKADAMYALI, M., ZHANG, F. & ZHUANG, X. 2004. Assembly of endocytic machinery around individual influenza viruses during viral entry. *Nat Struct Mol Biol,* 11**,** 567-73.

SAARIKANGAS, J. & BARRAL, Y. 2011. The emerging functions of septins in metazoans. *EMBO reports,* 12**,** 1118-26.

SADIAN, Y., GATSOGIANNIS, C., PATASI, C., HOFNAGEL, O., GOODY, R. S., FARKASOVSKÝ, M. & RAUNSER, S. 2013. The role of Cdc42 and Gic1 in the regulation of septin filament formation and dissociation. *Elife,* 2**,** e01085-e01085.

SAFFARIAN, S., COCUCCI, E. & KIRCHHAUSEN, T. 2009. Distinct dynamics of endocytic clathrin-coated pits and coated plaques. *PLoS Biology,* 7**,** e1000191.

SALCINI, A. E., CONFALONIERI, S., DORIA, M., SANTOLINI, E., TASSI, E., MINENKOVA, O., CESARENI, G., PELICCI, P. G. & DI FIORE, P. P. 1997.

Binding specificity and in vivo targets of the EH domain, a novel protein-protein interaction module. *Genes Dev,* 11**,** 2239-49.

SALZMAN, N. P. 1960. The rate of formation of vaccinia deoxyribonucleic acid and vaccinia virus. *Virology,* 10**,** 150-2.

SANDERSON, C. M., HOLLINSHEAD, M. & SMITH, G. L. 2000. The vaccinia virus A27L protein is needed for the microtubule-dependent transport of intracellular mature virus particles. *J Gen Virol,* 81**,** 47-58.

SANDGREN, K. J., WILKINSON, J., MIRANDA-SAKSENA, M., MCINERNEY, G. M., BYTH-WILSON, K., ROBINSON, P. J. & CUNNINGHAM, A. L. 2010. A differential role for macropinocytosis in mediating entry of the two forms of vaccinia virus into dendritic cells. *PLoS Pathog,* 6**,** e1000866.

SANDROCK, K., BARTSCH, I., BLASER, S., BUSSE, A., BUSSE, E. & ZIEGER, B. 2011. Characterization of human septin interactions. *Biol Chem,* 392**,** 751-61.

SARNO, S., REDDY, H., MEGGIO, F., RUZZENE, M., DAVIES, S. P., DONELLA-DEANA, A., SHUGAR, D. & PINNA, L. A. 2001. Selectivity of 4,5,6,7-tetrabromobenzotriazole, an ATP site-directed inhibitor of protein kinase CK2 ('casein kinase-2'). *FEBS Lett,* 496**,** 44-8.

SCAIFE, R. & MARGOLIS, R. L. 1990. Biochemical and immunochemical analysis of rat brain dynamin interaction with microtubules and organelles in vivo and in vitro. *J Cell Biol,* 111**,** 3023-33.

SCAPLEHORN, N., HOLMSTRÖM, A., MOREAU, V., FRISCHKNECHT, F., RECKMANN, I. & WAY, M. 2002. Grb2 and Nck act cooperatively to promote actin-based motility of vaccinia virus. *Curr Biol,* 12**,** 740-5.

SCHAECHTER, M., BOZEMAN, F. M. & SMADEL, J. E. 1957. Study on the growth of Rickettsiae. II. Morphologic observations of living Rickettsiae in tissue culture cells. *Virology,* 3**,** 160-72.

SCHAFER, D. A., JENNINGS, P. B. & COOPER, J. A. 1996. Dynamics of capping protein and actin assembly in vitro: uncapping barbed ends by polyphosphoinositides. *J Cell Biol,* 135**,** 169-79.

SCHAFER, D. A., WEED, S. A., BINNS, D., KARGINOV, A. V., PARSONS, J. T. & COOPER, J. A. 2002. Dynamin2 and cortactin regulate actin assembly and filament organization. *Curr Biol,* 12**,** 1852-7.

SCHERMELLEH, L., CARLTON, P. M., HAASE, S., SHAO, L., WINOTO, L., KNER, P., BURKE, B., CARDOSO, M. C., AGARD, D. A., GUSTAFSSON, M. G., LEONHARDT, H. & SEDAT, J. W. 2008. Subdiffraction multicolor imaging of the nuclear periphery with 3D structured illumination microscopy. *Science,* 320**,** 1332-6.

SCHERMELLEH, L., HEINTZMANN, R. & LEONHARDT, H. 2010. A guide to super-resolution fluorescence microscopy. *J Cell Biol,* 190**,** 165-75.

SCHLIWA, M. 1982. Action of cytochalasin D on cytoskeletal networks. *J Cell Biol,* 92.

SCHLOSSMAN, D. M., SCHMID, S. L., BRAELL, W. A. & ROTHMAN, J. E. 1984. An enzyme that removes clathrin coats: purification of an uncoating ATPase. *J Cell Biol,* 99**,** 723-33.

SCHLUNCK, G., DAMKE, H., KIOSSES, W. B., RUSK, N., SYMONS, M. H., WATERMAN-STORER, C. M., SCHMID, S. L. & SCHWARTZ, M. A. 2004. Modulation of Rac localization and function by dynamin. *Mol Biol Cell,* 15**,** 256-67.

SCHMELZ, M., SODEIK, B., ERICSSON, M., WOLFFE, E. J., SHIDA, H., HILLER, G. & GRIFFITHS, G. 1994. Assembly of vaccinia virus: the second wrapping cisterna is derived from the trans Golgi network. *J Virol,* 68**,** 130-47.

SCHMIDT, F. I., BLECK, C. K., HELENIUS, A. & MERCER, J. 2011. Vaccinia extracellular virions enter cells by macropinocytosis and acid-activated membrane rupture. *EMBO J,* 30**,** 3647-61.

SCHMIDT, F. I., BLECK, C. K. E. & MERCER, J. 2012. Poxvirus host cell entry. *Current opinion in virology,* 2**,** 20-7.

SCHMIDT, F. I., BLECK, C. K. E., REH, L., NOVY, K., WOLLSCHEID, B., HELENIUS, A., STAHLBERG, H. & MERCER, J. 2013. Vaccinia virus entry is followed by core activation and proteasome-mediated release of the immunomodulatory effector VH1 from lateral bodies. *Cell Reports,* 4**,** 464-76.

SCHMIDT, K. & NICHOLS, B. J. 2004. Functional interdependence between septin and actin cytoskeleton. *BMC cell biology,* 5**,** 43-43.

SCHMUTZ, C., AHRNE, E., KASPER, C. A., TSCHON, T., SORG, I., DREIER, R. F., SCHMIDT, A. & ARRIEUMERLOU, C. 2013. Systems-level overview of host protein phosphorylation during Shigella flexneri infection revealed by phosphoproteomics. *Mol Cell Proteomics,* 12**,** 2952-68.

SCHOLZ, R., IMAMI, K., SCOTT, N. E., TRIMBLE, W. S., FOSTER, L. J. & FINLAY, B. B. 2015. Novel Host Proteins and Signaling Pathways in Enteropathogenic E. coli Pathogenesis Identified by Global Phosphoproteome Analysis. *Mol Cell Proteomics,* 14**,** 1927-45.

SCHONICHEN, A. & GEYER, M. 2010. Fifteen formins for an actin filament: a molecular view on the regulation of human formins. *Biochim Biophys Acta,* 1803**,** 152-63.

SCHONICHEN, A., MANNHERZ, H. G., BEHRMANN, E., MAZUR, A. J., KUHN, S., SILVAN, U., SCHOENENBERGER, C. A., FACKLER, O. T., RAUNSER, S., DEHMELT, L. & GEYER, M. 2013. FHOD1 is a combined actin filament capping and bundling factor that selectively associates with actin arcs and stress fibers. *J Cell Sci,* 126**,** 1891-901.

SCHRAMM, B., DE HAAN, C. A., YOUNG, J., DOGLIO, L., SCHLEICH, S., REESE, C., POPOV, A. V., STEFFEN, W., SCHROER, T. & LOCKER, J. K. 2006. Vaccinia-virus-induced cellular contractility facilitates the subcellular localization of the viral replication sites. *Traffic,* 7**,** 1352-67.

SCHROEDER, N., CHUNG, C. S., CHEN, C. H., LIAO, C. L. & CHANG, W. 2012. The lipid raft-associated protein CD98 is required for vaccinia virus endocytosis. *J Virol,* 86**,** 4868-82.

SCHUMACHER, N., BORAWSKI, J. M., LEBERFINGER, C. B., GESSLER, M. & KERKHOFF, E. 2004. Overlapping expression pattern of the actin organizers Spir-1 and formin-2 in the developing mouse nervous system and the adult brain. *Gene Expr Patterns,* 4**,** 249-55.

SCHWAN, C. & AKTORIES, K. 2017. Formation of Nanotube-Like Protrusions, Regulation of Septin Organization and Re-guidance of Vesicle Traffic by Depolymerization of the Actin Cytoskeleton Induced by Binary Bacterial Protein Toxins. *Curr Top Microbiol Immunol,* 399**,** 35-51.

SCHWAN, C., KRUPPKE, A. S., NOLKE, T., SCHUMACHER, L., KOCH-NOLTE, F., KUDRYASHEV, M., STAHLBERG, H. & AKTORIES, K. 2014. Clostridium difficile toxin CDT hijacks microtubule organization and reroutes vesicle traffic to increase pathogen adherence. *Proc Natl Acad Sci U S A,* 111**,** 2313-8.

SEEDORF, K., KOSTKA, G., LAMMERS, R., BASHKIN, P., DALY, R., BURGESS, W. H., VAN DER BLIEK, A. M., SCHLESSINGER, J. & ULLRICH, A. 1994. Dynamin binds to SH3 domains of phospholipase C gamma and GRB-2. *J Biol Chem,* 269**,** 16009-14.

SELDEN, L. A., KINOSIAN, H. J., ESTES, J. E. & GERSHMAN, L. C. 1999. Impact of profilin on actin-bound nucleotide exchange and actin polymerization dynamics. *Biochemistry,* 38**,** 2769-78.

SELLIN, M. E., HOLMFELDT, P., STENMARK, S. & GULLBERG, M. 2011a. Microtubules support a disk-like septin arrangement at the plasma membrane of mammalian cells. *Mol Biol Cell,* 22**,** 4588-601.

SELLIN, M. E., SANDBLAD, L., STENMARK, S. & GULLBERG, M. 2011b. Deciphering the rules governing assembly order of mammalian septin complexes. *Mol Biol Cell,* 22**,** 3152-64.

SENGAR, A. S., WANG, W., BISHAY, J., COHEN, S. & EGAN, S. E. 1999. The EH and SH3 domain Ese proteins regulate endocytosis by linking to dynamin and Eps15. *EMBO J,* 18**,** 1159-1171.

SENKEVICH, T. G., WARD, B. M. & MOSS, B. 2004a. Vaccinia virus A28L gene encodes an essential protein component of the virion membrane with intramolecular disulfide bonds formed by the viral cytoplasmic redox pathway. *J Virol,* 78**,** 2348-56.

SENKEVICH, T. G., WARD, B. M. & MOSS, B. 2004b. Vaccinia virus entry into cells is dependent on a virion surface protein encoded by the A28L gene. *J Virol,* 78**,** 2357-66.

SEPT, D. & MCCAMMON, J. A. 2001. Thermodynamics and kinetics of actin filament nucleation. *Biophysical Journal,* 81**,** 667-74.

SERIO, A. W., JENG, R. L., HAGLUND, C. M., REED, S. C. & WELCH, M. D. 2010. Defining a core set of actin cytoskeletal proteins critical for actin-based motility of Rickettsia. *Cell Host Microbe,* 7**,** 388-98.

SETO, E. S., BELLEN, H. J. & LLOYD, T. E. 2002. When cell biology meets development: endocytic regulation of signaling pathways. *Genes Dev,* 16**,** 1314-36.

SHAHHOSEINI, M., AZAD, M., SABBAGHIAN, M., SHAFIPOUR, M., AKHOOND, M. R., SALMAN-YAZDI, R., SADIGHI GILANI, M. A. & GOURABI, H. 2015. New single nucleotide polymorphism G5508A in the SEPT12 gene may be associated with idiopathic male infertility in Iranian men. *Iran J Reprod Med,* 13**,** 503-6.

SHARMA, S., QUINTANA, A., FINDLAY, G. M., METTLEN, M., BAUST, B., JAIN, M., NILSSON, R., RAO, A. & HOGAN, P. G. 2013. An siRNA screen for NFAT activation identifies septins as coordinators of store-operated Ca2+ entry. *Nature,* 499**,** 238-42.

SHE, Y.-M., HUANG, Y.-W., ZHANG, L. & TRIMBLE, W. S. 2004. Septin 2 phosphorylation: theoretical and mass spectrometric evidence for the existence of a single phosphorylation site in vivo. *Rapid communications in mass spectrometry : RCM,* 18**,** 1123-30.

SHEFFIELD, P. J., OLIVER, C. J., KREMER, B. E., SHENG, S., SHAO, Z. & MACARA, I. G. 2003. Borg/septin interactions and the assembly of mammalian septin heterodimers, trimers, and filaments. *The Journal of biological chemistry,* 278**,** 3483-8.

SHEKHAR, S., PERNIER, J. & CARLIER, M. F. 2016. Regulators of actin filament barbed ends at a glance. *J Cell Sci,* 129**,** 1085-91.

SHEN, Q. T., HSIUE, P. P., SINDELAR, C. V., WELCH, M. D., CAMPELLONE, K. G. & WANG, H. W. 2012. Structural insights into WHAMM-mediated cytoskeletal coordination during membrane remodeling. *J Cell Biol,* 199**,** 111-24.

SHEN, Y. R., WANG, H. Y., KUO, Y. C., SHIH, S. C., HSU, C. H., CHEN, Y. R., WU, S. R., WANG, C. Y. & KUO, P. L. 2017. SEPT12 phosphorylation results in loss of the septin ring/sperm annulus, defective sperm motility and poor male fertility. *PLoS Genet,* 13**,** e1006631.

SHIBATA, T., TAKESHIMA, F., CHEN, F., ALT, F. W. & SNAPPER, S. B. 2002. Cdc42 facilitates invasion but not the actin-based motility of Shigella. *Curr Biol,* 12**,** 341-5.

SHIH, W., GALLUSSER, A. & KIRCHHAUSEN, T. 1995. A clathrin-binding site in the hinge of the beta 2 chain of mammalian AP-2 complexes. *J Biol Chem,* 270**,** 31083-90.

SHIKAMA, N., LEE, C. W., FRANCE, S., DELAVAINE, L., LYON, J., KRSTIC-DEMONACOS, M. & LA THANGUE, N. B. 1999. A novel cofactor for p300 that regulates the p53 response. *Mol Cell,* 4**,** 365-76.

SHNYROVA, A. V., BASHKIROV, P. V., AKIMOV, S. A., PUCADYIL, T. J., ZIMMERBERG, J., SCHMID, S. L. & FROLOV, V. A. 2013. Geometric catalysis of membrane fission driven by flexible dynamin rings. *Science,* 339**,** 1433-6.

SHPETNER, H. S. & VALLEE, R. B. 1989. Identification of dynamin, a novel mechanochemical enzyme that mediates interactions between microtubules. *Cell,* 59**,** 421-32.

SHPETNER, H. S. & VALLEE, R. B. 1992. Dynamin is a GTPase stimulated to high levels of activity by microtubules. *Nature,* 355**,** 733-5.

SINCLAIR, D. A. & GUARENTE, L. 1997. Extrachromosomal rDNA circles--a cause of aging in yeast. *Cell,* 91**,** 1033-42.

SINHA, I., WANG, Y. M., PHILP, R., LI, C. R., YAP, W. H. & WANG, Y. 2007. Cyclin-dependent kinases control septin phosphorylation in Candida albicans hyphal development. *Developmental Cell,* 13**,** 421-32.

SIRAJUDDIN, M., FARKASOVSKY, M., HAUER, F., KUHLMANN, D., MACARA, I. G., WEYAND, M., STARK, H. & WITTINGHOFER, A. 2007. Structural insight into filament formation by mammalian septins. *Nature,* 449**,** 311-5.

SIRAJUDDIN, M., FARKASOVSKY, M., ZENT, E. & WITTINGHOFER, A. 2009. GTP-induced conformational changes in septins and implications for function. *Proc Natl Acad Sci U S A,* 106**,** 16592-7.

SIRIANNI, A., KROKOWSKI, S., LOBATO-MÁRQUEZ, D., BURANYI, S., PFANZELTER, J., GALEA, D., WILLIS, A., CULLEY, S., HENRIQUES, R., LARROUY-MAUMUS, G., HOLLINSHEAD, M., SANCHO-SHIMIZU, V., WAY, M. & MOSTOWY, S. 2016. Mitochondria mediate septin cage assembly to promote autophagy of Shigella. *EMBO reports*.

SISSON, J. C., FIELD, C., VENTURA, R., ROYOU, A. & SULLIVAN, W. 2000. Lava lamp, a novel peripheral golgi protein, is required for Drosophila melanogaster cellularization. *J Cell Biol,* 151**,** 905-18.

SITTHIDET, C., STEVENS, J. M., FIELD, T. R., LAYTON, A. N., KORBSRISATE, S. & STEVENS, M. P. 2010. Actin-based motility of Burkholderia thailandensis requires a central acidic domain of BimA that recruits and activates the cellular Arp2/3 complex. *J Bacteriol,* 192**,** 5249-52.

SIVAN, G., MARTIN, S. E., MYERS, T. G., BUEHLER, E., SZYMCZYK, K. H., ORMANOGLU, P. & MOSS, B. 2013. Human genome-wide RNAi screen reveals a role for nuclear pore proteins in poxvirus morphogenesis. *Proc Natl Acad Sci U S A,* 110**,** 3519-24.

SMALL, J. V. 2015. Pushing with actin: from cells to pathogens. *Biochemical Society transactions,* 43**,** 84-91.

SMITH, G. L. & LAW, M. 2004. The exit of vaccinia virus from infected cells. *Virus Res,* 106**,** 189-97.

SMITH, G. L., VANDERPLASSCHEN, A. & LAW, M. 2002. The formation and function of extracellular enveloped vaccinia virus. *The Journal of general virology,* 83**,** 2915-31.

SMITH, J. L., CAMPOS, S. K. & OZBUN, M. A. 2007. Human papillomavirus type 31 uses a caveolin 1- and dynamin 2-mediated entry pathway for infection of human keratinocytes. *J Virol,* 81**,** 9922-31.

SMITH, K. A. 2011. Edward jenner and the small pox vaccine. *Front Immunol,* 2**,** 21.

SNAPPER, S. B., TAKESHIMA, F., ANTÓN, I., LIU, C. H., THOMAS, S. M., NGUYEN, D., DUDLEY, D., FRASER, H., PURICH, D., LOPEZ-ILASACA, M., KLEIN, C., DAVIDSON, L., BRONSON, R., MULLIGAN, R. C., SOUTHWICK, F., GEHA, R., GOLDBERG, M. B., ROSEN, F. S., HARTWIG, J. H. & ALT, F. W. 2001. N-

WASP deficiency reveals distinct pathways for cell surface projections and microbial actin-based motility. *Nat Cell Biol,* 3**,** 897-904.

SNETKOV, X. 2015. *The role of endocytic machinery during Vaccinia Virus egress and spread.* PhD Thesis, University College London.

SNETKOV, X., WEISSWANGE, I., PFANZELTER, J., HUMPHRIES, A. C. & WAY, M. 2016. NPF motifs in the vaccinia virus protein A36 recruit intersectin-1 to promote Cdc42:N-WASP-mediated viral release from infected cells. *Nature Microbiology,* 1**,** 16141-16141.

SOCHACKI, K. A., DICKEY, A. M., STRUB, M.-P. & TARASKA, J. W. 2017. Endocytic proteins are partitioned at the edge of the clathrin lattice in mammalian cells. *Nat Cell Biol*.

SODEIK, B., DOMS, R. W., ERICSSON, M., HILLER, G., MACHAMER, C. E., VAN 'T HOF, W., VAN MEER, G., MOSS, B. & GRIFFITHS, G. 1993. Assembly of vaccinia virus: role of the intermediate compartment between the endoplasmic reticulum and the Golgi stacks. *J Cell Biol,* 121**,** 521-41.

SODEIK, B. & KRIJNSE-LOCKER, J. 2002. Assembly of vaccinia virus revisited: de novo membrane synthesis or acquisition from the host? *Trends Microbiol,* 10**,** 15-24.

SONG, K., RUSSO, G. & KRAUSS, M. 2016. Septins As Modulators of Endo-Lysosomal Membrane Traffic. *Front Cell Dev Biol,* 4**,** 124-124.

SONGYANG, Z. & CANTLEY, L. C. 1995. Recognition and specificity in protein tyrosine kinase-mediated signalling. *Trends Biochem Sci,* 20**,** 470-5.

SONGYANG, Z., SHOELSON, S. E., CHAUDHURI, M., GISH, G., PAWSON, T., HASER, W. G., KING, F., ROBERTS, T., RATNOFSKY, S., LECHLEIDER, R. J. & ET AL. 1993. SH2 domains recognize specific phosphopeptide sequences. *Cell,* 72**,** 767-78.

SOYKAN, T., KAEMPF, N., SAKABA, T., VOLLWEITER, D., GOERDELER, F., PUCHKOV, D., KONONENKO, N. L. & HAUCKE, V. 2017. Synaptic Vesicle Endocytosis Occurs on Multiple Timescales and Is Mediated by Formin-Dependent Actin Assembly. *Neuron,* 93**,** 854-866 e4.

SPILIOTIS, E. T., HUNT, S. J., HU, Q., KINOSHITA, M. & NELSON, W. J. 2008. Epithelial polarity requires septin coupling of vesicle transport to polyglutamylated microtubules. *J Cell Biol,* 180**,** 295-303.

SPILIOTIS, E. T., KARASMANIS, E. P. & DOLAT, L. 2016. Chapter 14 – Fluorescence microscopy of actin- and microtubule-associated septins in mammalian cells. *Methods Cell Biol,* 136**,** 243-268.

SPILIOTIS, E. T., KINOSHITA, M. & NELSON, W. J. 2005. A mitotic septin scaffold required for Mammalian chromosome congression and segregation. *Science,* 307**,** 1781-5.

SPILIOTIS, E. T. & NELSON, W. J. 2006. Here come the septins: novel polymers that coordinate intracellular functions and organization. *J Cell Sci,* 119**,** 4-10.

SPIRO, Z., THYAGARAJAN, K., DE SIMONE, A., TRAGER, S., AFSHAR, K. & GONCZY, P. 2014. Clathrin regulates centrosome positioning by promoting acto-myosin cortical tension in C. elegans embryos. *Development,* 141**,** 2712-23.

STAMM, L. M., MORISAKI, J. H., GAO, L. Y., JENG, R. L., MCDONALD, K. L., ROTH, R., TAKESHITA, S., HEUSER, J., WELCH, M. D. & BROWN, E. J. 2003. Mycobacterium marinum escapes from phagosomes and is propelled by actin-based motility. *J Exp Med,* 198**,** 1361-8.

STAMM, L. M., PAK, M. A., MORISAKI, J. H., SNAPPER, S. B., ROTTNER, K., LOMMEL, S. & BROWN, E. J. 2005. Role of the WASP family proteins for Mycobacterium marinum actin tail formation. *Proc Natl Acad Sci U S A,* 102**,** 14837-42.

STAUFFER, T. P., AHN, S. & MEYER, T. 1998. Receptor-induced transient reduction in plasma membrane PtdIns(4,5)P2 concentration monitored in living cells. *Curr Biol,* 8**,** 343-6.

STEINMETZ, M. O., STOFFLER, D., HOENGER, A., BREMER, A. & AEBI, U. 1997. Actin: from cell biology to atomic detail. *Journal of structural biology,* 119**,** 295-320.

STEVENS, M. P., STEVENS, J. M., JENG, R. L., TAYLOR, L. A., WOOD, M. W., HAWES, P., MONAGHAN, P., WELCH, M. D. & GALYOV, E. E. 2005. Identification of a bacterial factor required for actin-based motility of Burkholderia pseudomallei. *Mol Microbiol,* 56**,** 40-53.

STOKES, G. V. 1976. High-voltage electron microscope study of the release of vaccinia virus from whole cells. *J Virol,* 18**,** 636-43.

STOWELL, M. H., MARKS, B., WIGGE, P. & MCMAHON, H. T. 1999. Nucleotide-dependent conformational changes in dynamin: evidence for a mechanochemical molecular spring. *Nat Cell Biol,* 1**,** 27-32.

STRADAL, T. E. & SCITA, G. 2006. Protein complexes regulating Arp2/3-mediated actin assembly. *Curr Opin Cell Biol,* 18**,** 4-10.

STRNADOVA, P., REN, H., VALENTINE, R., MAZZON, M., SWEENEY, T. R., BRIERLEY, I. & SMITH, G. L. 2015. Inhibition of Translation Initiation by Protein 169: A Vaccinia Virus Strategy to Suppress Innate and Adaptive Immunity and Alter Virus Virulence. *PLoS Pathog,* 11**,** e1005151.

SUAREZ, C., CARROLL, R. T., BURKE, T. A., CHRISTENSEN, J. R., BESTUL, A. J., SEES, J. A., JAMES, M. L., SIROTKIN, V. & KOVAR, D. R. 2015. Profilin regulates F-actin network homeostasis by favoring formin over Arp2/3 complex. *Developmental Cell,* 32**,** 43-53.

SUAREZ, C. & KOVAR, D. R. 2016. Internetwork competition for monomers governs actin cytoskeleton organization. *Nat Rev Mol Cell Biol,* 17**,** 799-810.

SUN, Y., LEONG, N. T., JIANG, T., TANGARA, A., DARZACQ, X. & DRUBIN, D. G. 2017. Switch-like Arp2/3 activation upon WASP and WIP recruitment to an apparent threshold level by multivalent linker proteins in vivo. *Elife,* 6.

SUN, Y., LEONG, N. T., WONG, T. & DRUBIN, D. G. 2015. A Pan1/End3/Sla1 complex links Arp2/3-mediated actin assembly to sites of clathrin-mediated endocytosis. *Mol Biol Cell,* 26**,** 3841-56.

SUNDBORGER, A. C., FANG, S., HEYMANN, J. A., RAY, P., CHAPPIE, J. S. & HINSHAW, J. E. 2014. A dynamin mutant defines a superconstricted prefission state. *Cell Reports,* 8**,** 734-42.

SUNDBORGER, A. C. & HINSHAW, J. E. 2014. Regulating dynamin dynamics during endocytosis. *F1000Prime Rep,* 6**,** 85-85.

SURKA, M. C., TSANG, C. W. & TRIMBLE, W. S. 2002. The mammalian septin MSF localizes with microtubules and is required for completion of cytokinesis. *Mol Biol Cell,* 13**,** 3532-45.

SUZUKI, R., TOSHIMA, J. Y. & TOSHIMA, J. 2012. Regulation of clathrin coat assembly by Eps15 homology domain-mediated interactions during endocytosis. *Mol Biol Cell,* 23**,** 687-700.

SUZUKI, T., MIKI, H., TAKENAWA, T. & SASAKAWA, C. 1998. Neural Wiskott-Aldrich syndrome protein is implicated in the actin-based motility of Shigella flexneri. *EMBO J,* 17**,** 2767-76.

SUZUKI, T., MIMURO, H., SUETSUGU, S., MIKI, H., TAKENAWA, T. & SASAKAWA, C. 2002. Neural Wiskott-Aldrich syndrome protein (N-WASP) is the specific ligand for Shigella VirG among the WASP family and determines the host cell type allowing actin-based spreading. *Cell Microbiol,* 4**,** 223-33.

SVITKINA, T. M. & BORISY, G. G. 1999. Arp2/3 complex and actin depolymerizing factor/cofilin in dendritic organization and treadmilling of actin filament array in lamellipodia. *J Cell Biol,* 145**,** 1009-26.

SWEITZER, S. M. & HINSHAW, J. E. 1998. Dynamin undergoes a GTP-dependent conformational change causing vesiculation. *Cell,* 93**,** 1021-9.

SWIMM, A., BOMMARIUS, B., REEVES, P., SHERMAN, M. & KALMAN, D. 2004. Complex kinase requirements for EPEC pedestal formation. *Nat Cell Biol,* 6**,** 795; author reply 795-6.

SYMONS, M., DERRY, J. M., KARLAK, B., JIANG, S., LEMAHIEU, V., MCCORMICK, F., FRANCKE, U. & ABO, A. 1996. Wiskott-Aldrich syndrome protein, a novel effector for the GTPase CDC42Hs, is implicated in actin polymerization. *Cell,* 84**,** 723-34.

TADA, T., SIMONETTA, A., BATTERTON, M., KINOSHITA, M., EDBAUER, D. & SHENG, M. 2007. Role of Septin cytoskeleton in spine morphogenesis and dendrite development in neurons. *Curr Biol,* 17**,** 1752-8.

TAKAHASHI, Y., IWASE, M., KONISHI, M., TANAKA, M., TOH-E, A. & KIKUCHI, Y. 1999. Smt3, a SUMO-1 homolog, is conjugated to Cdc3, a component of septin rings at the mother-bud neck in budding yeast. *Biochem Biophys Res Commun,* 259**,** 582-7.

TAKAHASHI, Y., TOH, E. A. & KIKUCHI, Y. 2003. Comparative analysis of yeast PIAS-type SUMO ligases in vivo and in vitro. *J Biochem,* 133**,** 415-22.

TAKEI, K., SLEPNEV, V. I., HAUCKE, V. & DE CAMILLI, P. 1999. Functional partnership between amphiphysin and dynamin in clathrin-mediated endocytosis. *Nat Cell Biol,* 1**,** 33-9.

TAKIZAWA, P. A., DERISI, J. L., WILHELM, J. E. & VALE, R. D. 2000. Plasma membrane compartmentalization in yeast by messenger RNA transport and a septin diffusion barrier. *Science,* 290**,** 341-4.

TAM, V. C., SERRUTO, D., DZIEJMAN, M., BRIEHER, W. & MEKALANOS, J. J. 2007. A type III secretion system in Vibrio cholerae translocates a formin/spire hybrid-like actin nucleator to promote intestinal colonization. *Cell Host Microbe,* 1**,** 95-107.

TANABE, K. & TAKEI, K. 2009. Dynamic instability of microtubules requires dynamin 2 and is impaired in a Charcot-Marie-Tooth mutant. *J Cell Biol,* 185**,** 939-48.

TANAKA, M., GUPTA, R. & MAYER, B. J. 1995. Differential inhibition of signaling pathways by dominant-negative SH2/SH3 adapter proteins. *Mol Cell Biol,* 15**,** 6829-37.

TANAKA-TAKIGUCHI, Y., KINOSHITA, M. & TAKIGUCHI, K. 2009. Septin-mediated uniform bracing of phospholipid membranes. *Curr Biol,* 19**,** 140-5.

TANG, C. S. & REED, S. I. 2002. Phosphorylation of the septin cdc3 in g1 by the cdc28 kinase is essential for efficient septin ring disassembly. *Cell Cycle,* 1**,** 42-9.

TAUNTON, J., ROWNING, B. A., COUGHLIN, M. L., WU, M., MOON, R. T., MITCHISON, T. J. & LARABELL, C. A. 2000. Actin-dependent propulsion of endosomes and lysosomes by recruitment of N-WASP. *J Cell Biol,* 148**,** 519-30.

TAYLOR, M. J., LAMPE, M. & MERRIFIELD, C. J. 2012. A feedback loop between dynamin and actin recruitment during clathrin-mediated endocytosis. *PLoS Biology,* 10**,** e1001302-e1001302.

TAYLOR, M. J., PERRAIS, D., MERRIFIELD, C. J., NAKATSU, F. & CHEN, H. 2011. A High Precision Survey of the Molecular Dynamics of Mammalian Clathrin-Mediated Endocytosis. *PLoS Biology,* 9**,** e1000604-e1000604.

TEBAR, F., SORKINA, T., SORKIN, A., ERICSSON, M. & KIRCHHAUSEN, T. 1996. Eps15 is a component of clathrin-coated pits and vesicles and is located at the rim of coated pits. *J Biol Chem,* 271**,** 28727-30.

TILNEY, L. G., BONDER, E. M., COLUCCIO, L. M. & MOOSEKER, M. S. 1983. Actin from Thyone sperm assembles on only one end of an actin filament: a behavior regulated by profilin. *J Cell Biol,* 97**,** 112-24.

TILNEY, L. G., CONNELLY, P. S. & PORTNOY, D. A. 1990. Actin filament nucleation by the bacterial pathogen, Listeria monocytogenes. *J Cell Biol,* 111**,** 2979-88.

TILNEY, L. G. & PORTNOY, D. A. 1989. Actin filaments and the growth, movement, and spread of the intracellular bacterial parasite, Listeria monocytogenes. *J Cell Biol,* 109**,** 1597-608.

TILNEY, L. G. & TILNEY, M. S. 1993. The wily ways of a parasite: induction of actin assembly by Listeria. *Trends Microbiol,* 1**,** 25-31.

TOKHTAEVA, E., CAPRI, J., MARCUS, E. A., WHITELEGGE, J. P., KHUZAKHMETOVA, V., BUKHARAEVA, E., DEISS-YEHIELY, N., DADA, L. A., SACHS, G., FERNANDEZ-SALAS, E. & VAGIN, O. 2015. Septin dynamics are essential for exocytosis. *The Journal of biological chemistry*.

TOLONEN, N., DOGLIO, L., SCHLEICH, S. & KRIJNSE LOCKER, J. 2001. Vaccinia virus DNA replication occurs in endoplasmic reticulum-enclosed cytoplasmic mini-nuclei. *Mol Biol Cell,* 12**,** 2031-46.

TOMKOWICZ, B., SINGH, S. P., LAI, D., SINGH, A., MAHALINGHAM, S., JOSEPH, J., SRIVASTAVA, S. & SRINIVASAN, A. 2005. Mutational analysis reveals an essential role for the LXXLL motif in the transformation function of the human herpesvirus-8 oncoprotein, kaposin. *DNA Cell Biol,* 24**,** 10-20.

TOOLEY, A. J., GILDEN, J., JACOBELLI, J., BEEMILLER, P., TRIMBLE, W. S., KINOSHITA, M. & KRUMMEL, M. F. 2009. Amoeboid T lymphocytes require the septin cytoskeleton for cortical integrity and persistent motility. *Nat Cell Biol,* 11**,** 17-26.

TOOZE, J., HOLLINSHEAD, M., REIS, B., RADSAK, K. & KERN, H. 1993. Progeny vaccinia and human cytomegalovirus particles utilize early endosomal cisternae for their envelopes. *Eur J Cell Biol,* 60**,** 163-78.

TORRACA, V. & MOSTOWY, S. 2016. Septins and Bacterial Infection. *Front Cell Dev Biol,* 4**,** 127.

TOWNSLEY, A. C. & MOSS, B. 2007. Two distinct low-pH steps promote entry of vaccinia virus. *J Virol,* 81**,** 8613-20.

TOWNSLEY, A. C., SENKEVICH, T. G. & MOSS, B. 2005. Vaccinia virus A21 virion membrane protein is required for cell entry and fusion. *J Virol,* 79**,** 9458-69.

TOWNSLEY, A. C., WEISBERG, A. S., WAGENAAR, T. R. & MOSS, B. 2006. Vaccinia virus entry into cells via a low-pH-dependent endosomal pathway. *J Virol,* 80**,** 8899-908.

TRAKTMAN, P. 1990. Poxviruses: an emerging portrait of biological strategy. *Cell,* 62**,** 621-6.

TU, Y., LI, F. & WU, C. 1998. Nck-2, a novel Src homology2/3-containing adaptor protein that interacts with the LIM-only protein PINCH and components of growth factor receptor kinase-signaling pathways. *Mol Biol Cell,* 9**,** 3367-82.

TURNBULL, S., WEST, E. J., SCOTT, K. J., APPLETON, E., MELCHER, A. & RALPH, C. 2015. Evidence for Oncolytic Virotherapy: Where Have We Got to and Where Are We Going? *Viruses,* 7**,** 6291-312.

TWETEN, D. J., BAYLY, P. V. & CARLSSON, A. E. 2017. Actin growth profile in clathrin-mediated endocytosis. *Phys Rev E,* 95**,** 052414.

TYLER, J. J., ALLWOOD, E. G. & AYSCOUGH, K. R. 2016. WASP family proteins, more than Arp2/3 activators. *Biochem Soc Trans,* 44**,** 1339-1345.

UNGEWICKELL, E. & BRANTON, D. 1981. Assembly units of clathrin coats. *Nature,* 289**,** 420-2.

UNGEWICKELL, E., UNGEWICKELL, H., HOLSTEIN, S. E., LINDNER, R., PRASAD, K., BAROUCH, W., MARTIN, B., GREENE, L. E. & EISENBERG, E. 1995. Role of auxilin in uncoating clathrin-coated vesicles. *Nature,* 378**,** 632-5.

UNSWORTH, K. E., MAZURKIEWICZ, P., SENF, F., ZETTL, M., MCNIVEN, M., WAY, M. & HOLDEN, D. W. 2007. Dynamin is required for F-actin assembly and pedestal formation by enteropathogenic Escherichia coli (EPEC). *Cellular microbiology,* 9**,** 438-49.

URBANIK, E. & WARE, B. R. 1989. Actin filament capping and cleaving activity of cytochalasins B, D, E, and H. *Archives of biochemistry and biophysics,* 269**,** 181-7.

URRUTIA, R., HENLEY, J. R., COOK, T. & MCNIVEN, M. A. 1997. The dynamins: redundant or distinct functions for an expanding family of related GTPases? *Proc Natl Acad Sci U S A,* 94**,** 377-84.

VALDERRAMA, F., CORDEIRO, J. V., SCHLEICH, S., FRISCHKNECHT, F. & WAY, M. 2006. Vaccinia virus-induced cell motility requires F11L-mediated inhibition of RhoA signaling. *Science,* 311**,** 377-81.

VAN DELFT, S., SCHUMACHER, C., HAGE, W., VERKLEIJ, A. J. & VAN BERGEN EN HENEGOUWEN, P. M. 1997. Association and colocalization of Eps15 with adaptor protein-2 and clathrin. *J Cell Biol,* 136**,** 811-21.

VAN DER BLIEK, A. M., REDELMEIER, T. E., DAMKE, H., TISDALE, E. J., MEYEROWITZ, E. M. & SCHMID, S. L. 1993. Mutations in human dynamin block an intermediate stage in coated vesicle formation. *J Cell Biol,* 122**,** 553-63.

VAN DER SCHAAR, H. M., RUST, M. J., CHEN, C., VAN DER ENDE-METSELAAR, H., WILSCHUT, J., ZHUANG, X. & SMIT, J. M. 2008. Dissecting the cell entry pathway of dengue virus by single-particle tracking in living cells. *PLoS Pathog,* 4**,** e1000244.

VAN EIJL, H., HOLLINSHEAD, M., RODGER, G., ZHANG, W. H. & SMITH, G. L. 2002. The vaccinia virus F12L protein is associated with intracellular enveloped virus particles and is required for their egress to the cell surface. *J Gen Virol,* 83**,** 195-207.

VAN EIJL, H., HOLLINSHEAD, M. & SMITH, G. L. 2000. The vaccinia virus A36R protein is a type Ib membrane protein present on intracellular but not extracellular enveloped virus particles. *Virology,* 271**,** 26-36.

VAN NHIEU, G. T., KRUKONIS, E. S., RESZKA, A. A., HORWITZ, A. F. & ISBERG, R. R. 1996. Mutations in the cytoplasmic domain of the integrin beta1 chain indicate a role for endocytosis factors in bacterial internalization. *J Biol Chem,* 271**,** 7665-72.

VAN OERS, M. M., PIJLMAN, G. P. & VLAK, J. M. 2015. Thirty years of baculovirus-insect cell protein expression: from dark horse to mainstream technology. *J Gen Virol,* 96**,** 6-23.

VARNAI, P. & BALLA, T. 1998. Visualization of phosphoinositides that bind pleckstrin homology domains: calcium- and agonist-induced dynamic changes and relationship to myo-[3H]inositol-labeled phosphoinositide pools. *J Cell Biol,* 143**,** 501-10.

VEGA, I. E. & HSU, S. C. 2003. The septin protein Nedd5 associates with both the exocyst complex and microtubules and disruption of its GTPase activity promotes aberrant neurite sprouting in PC12 cells. *Neuroreport,* 14**,** 31-7.

VEIGA, E. & COSSART, P. 2005. Listeria hijacks the clathrin-dependent endocytic machinery to invade mammalian cells. *Nat Cell Biol,* 7**,** 894-900.

VEIGA, E. & COSSART, P. 2006. The role of clathrin-dependent endocytosis in bacterial internalization. *Trends Cell Biol,* 16**,** 499-504.

VEIGA, E., GUTTMAN, J. A., BONAZZI, M., BOUCROT, E., TOLEDO-ARANA, A., LIN, A. E., ENNINGA, J., PIZARRO-CERDA, J., FINLAY, B. B., KIRCHHAUSEN, T.

& COSSART, P. 2007. Invasive and adherent bacterial pathogens co-Opt host clathrin for infection. *Cell Host Microbe,* 2**,** 340-51.

VELLE, K. B. & CAMPELLONE, K. G. 2017. Extracellular motility and cell-to-cell transmission of enterohemorrhagic E. coli is driven by EspFU-mediated actin assembly. *PLoS Pathog,* 13**,** e1006501.

VERDAASDONK, J. S., LAWRIMORE, J. & BLOOM, K. 2014. Determining absolute protein numbers by quantitative fluorescence microscopy. *Methods Cell Biol,* 123**,** 347-65.

VERMEER, P. D., MCHUGH, J., ROKHLINA, T., VERMEER, D. W., ZABNER, J. & WELSH, M. J. 2007. Vaccinia virus entry, exit, and interaction with differentiated human airway epithelia. *J Virol,* 81**,** 9891-9.

VERSELE, M., GULLBRAND, B., SHULEWITZ, M. J., CID, V. J., BAHMANYAR, S., CHEN, R. E., BARTH, P., ALBER, T. & THORNER, J. 2004. Protein-protein interactions governing septin heteropentamer assembly and septin filament organization in Saccharomyces cerevisiae. *Mol Biol Cell,* 15**,** 4568-83.

VERSELE, M. & THORNER, J. 2004. Septin collar formation in budding yeast requires GTP binding and direct phosphorylation by the PAK, Cla4. *J Cell Biol,* 164**,** 701-15.

VOIGT, E. A., KENNEDY, R. B. & POLAND, G. A. 2016. Defending against smallpox: a focus on vaccines. *Expert Rev Vaccines,* 15**,** 1197-211.

VOLCEANOV, L., HERBST, K., BINIOSSEK, M., SCHILLING, O., HALLER, D., NÖLKE, T., SUBBARAYAL, P., RUDEL, T., ZIEGER, B. & HÄCKER, G. 2014. Septins Arrange F-Actin-Containing Fibers on the Chlamydia trachomatis Inclusion and Are Required for Normal Release of the Inclusion by Extrusion. *mBio,* 5.

VOLZ, A. & SUTTER, G. 2017. Modified Vaccinia Virus Ankara: History, Value in Basic Research, and Current Perspectives for Vaccine Development. *Adv Virus Res,* 97**,** 187-243.

WACHSSTOCK, D. H., SCHWARZ, W. H. & POLLARD, T. D. 1994. Cross-linker dynamics determine the mechanical properties of actin gels. *Biophysical Journal,* 66**,** 801-9.

WAKEHAM, D. E., ABI-RACHED, L., TOWLER, M. C., WILBUR, J. D., PARHAM, P. & BRODSKY, F. M. 2005. Clathrin heavy and light chain isoforms originated by independent mechanisms of gene duplication during chordate evolution. *Proc Natl Acad Sci U S A,* 102**,** 7209-14.

WALSH, C. T. 2006. *Posttranslational modification of proteins : expanding nature's inventor,* United States, Ben Roberts.

WANG, L., JOHNSON, A., HANNA, M. & AUDHYA, A. 2016. Eps15 membrane-binding and -bending activity acts redundantly with Fcho1 during clathrin-mediated endocytosis. *Mol Biol Cell,* 27**,** 2675-87.

WANG, Y., WANG, Q., LIANG, C., SONG, J., LI, N., SHI, H. & CHEN, X. 2008. Autographa californica multiple nucleopolyhedrovirus nucleocapsid protein BV/ODV-C42 mediates the nuclear entry of P78/83. *J Virol,* 82**,** 4554-61.

WARD, B. M. 2005. Visualization and characterization of the intracellular movement of vaccinia virus intracellular mature virions. *J Virol,* 79**,** 4755-63.

WARD, B. M. & MOSS, B. 2000. Golgi network targeting and plasma membrane internalization signals in vaccinia virus B5R envelope protein. *J Virol,* 74**,** 3771-80.

WARD, B. M. & MOSS, B. 2001a. Vaccinia virus intracellular movement is associated with microtubules and independent of actin tails. *J Virol,* 75**,** 11651-63.

WARD, B. M. & MOSS, B. 2001b. Visualization of intracellular movement of vaccinia virus virions containing a green fluorescent protein-B5R membrane protein chimera. *J Virol,* 75**,** 4802-13.

WARD, B. M. & MOSS, B. 2004. Vaccinia virus A36R membrane protein provides a direct link between intracellular enveloped virions and the microtubule motor kinesin. *J Virol,* 78**,** 2486-93.

WARD, B. M., WEISBERG, A. S. & MOSS, B. 2003. Mapping and functional analysis of interaction sites within the cytoplasmic domains of the vaccinia virus A33R and A36R envelope proteins. *J Virol,* 77**,** 4113-26.

WEAR, M. A., YAMASHITA, A., KIM, K., MAEDA, Y. & COOPER, J. A. 2003. How capping protein binds the barbed end of the actin filament. *Curr Biol,* 13**,** 1531-7.

WEE, P. & WANG, Z. 2017. Epidermal Growth Factor Receptor Cell Proliferation Signaling Pathways. *Cancers (Basel),* 9.

WEEMS, A. & MCMURRAY, M. 2017. The step-wise pathway of septin hetero-octamer assembly in budding yeast. *Elife,* 6.

WEEMS, A. D., JOHNSON, C. R., ARGUESO, J. L. & MCMURRAY, M. A. 2014. Higher-order septin assembly is driven by GTP-promoted conformational changes: evidence from unbiased mutational analysis in Saccharomyces cerevisiae. *Genetics,* 196**,** 711-27.

WEGNER, A. 1976. Head to tail polymerization of actin. *J Mol Biol,* 108**,** 139-50.

WEISS, C. L. & SCHULTZ, J. 2015. Identification of divergent WH2 motifs by HMM-HMM alignments. *BMC Res Notes,* 8**,** 18.

WEISS, S. M., LADWEIN, M., SCHMIDT, D., EHINGER, J., LOMMEL, S., STADING, K., BEUTLING, U., DISANZA, A., FRANK, R., JANSCH, L., SCITA, G., GUNZER, F., ROTTNER, K. & STRADAL, T. E. 2009. IRSp53 links the enterohemorrhagic E. coli effectors Tir and EspFU for actin pedestal formation. *Cell Host Microbe,* 5**,** 244-58.

WEISSWANGE, I., NEWSOME, T. P., SCHLEICH, S. & WAY, M. 2009. The rate of N-WASP exchange limits the extent of ARP2/3-complex-dependent actin-based motility. *Nature,* 458**,** 87-91.

WELCH, M. D. 2015. Why should cell biologists study microbial pathogens? *Mol Biol Cell,* 26**,** 4295-301.

WELCH, M. D., DEPACE, A. H., VERMA, S., IWAMATSU, A. & MITCHISON, T. J. 1997a. The human Arp2/3 complex is composed of evolutionarily conserved subunits and is localized to cellular regions of dynamic actin filament assembly. *J Cell Biol,* 138**,** 375-84.

WELCH, M. D., IWAMATSU, A. & MITCHISON, T. J. 1997b. Actin polymerization is induced by Arp2/3 protein complex at the surface of Listeria monocytogenes. *Nature,* 385**,** 265-9.

WELCH, M. D. & MULLINS, R. D. 2002. Cellular control of actin nucleation. *Annu Rev Cell Dev Biol,* 18**,** 247-88.

WELCH, M. D., ROSENBLATT, J., SKOBLE, J., PORTNOY, D. A. & MITCHISON, T. J. 1998. Interaction of human Arp2/3 complex and the Listeria monocytogenes ActA protein in actin filament nucleation. *Science,* 281**,** 105-8.

WELCH, M. D. & WAY, M. 2013. Arp2/3-mediated actin-based motility: a tail of pathogen abuse. *Cell Host Microbe,* 14**,** 242-55.

WENDLAND, B. & EMR, S. D. 1998. Pan1p, yeast eps15, functions as a multivalent adaptor that coordinates protein-protein interactions essential for endocytosis. *J Cell Biol,* 141**,** 71-84.

WHITBECK, J. C., FOO, C. H., PONCE DE LEON, M., EISENBERG, R. J. & COHEN, G. H. 2009. Vaccinia virus exhibits cell-type-dependent entry characteristics. *Virology,* 385**,** 383-91.

WHO 1972. Expert Committee on Smallpox Eradication. Second report. *World Health Organization technical report series,* 493**,** 1-64.

WIGGE, P., VALLIS, Y. & MCMAHON, H. T. 1997. Inhibition of receptor-mediated endocytosis by the amphiphysin SH3 domain. *Curr Biol,* 7**,** 554-60.

WILBUR, J. D., HWANG, P. K., YBE, J. A., LANE, M., SELLERS, B. D., JACOBSON, M. P., FLETTERICK, R. J. & BRODSKY, F. M. 2010. Conformation switching of clathrin light chain regulates clathrin lattice assembly. *Developmental Cell,* 18**,** 841-8.

WINTER, D., LECHLER, T. & LI, R. 1999. Activation of the yeast Arp2/3 complex by Bee1p, a WASP-family protein. *Curr Biol,* 9**,** 501-4.

WISNIEWSKI, D., LAMBEK, C. L., LIU, C., STRIFE, A., VEACH, D. R., NAGAR, B., YOUNG, M. A., SCHINDLER, T., BORNMANN, W. G., BERTINO, J. R., KURIYAN, J. & CLARKSON, B. 2002. Characterization of potent inhibitors of the Bcr-Abl and the c-kit receptor tyrosine kinases. *Cancer Res,* 62**,** 4244-55.

WITKE, W., PODTELEJNIKOV, A. V., DI NARDO, A., SUTHERLAND, J. D., GURNIAK, C. B., DOTTI, C. & MANN, M. 1998. In mouse brain profilin I and profilin II associate with regulators of the endocytic pathway and actin assembly. *EMBO J,* 17**,** 967-76.

WOLFE, C. L., OJEDA, S. & MOSS, B. 2012. Transcriptional repression and RNA silencing act synergistically to demonstrate the function of the eleventh component of the vaccinia virus entry-fusion complex. *J Virol,* 86**,** 293-301.

WOLFFE, E. J., ISAACS, S. N. & MOSS, B. 1993. Deletion of the vaccinia virus B5R gene encoding a 42-kilodalton membrane glycoprotein inhibits extracellular virus envelope formation and dissemination. *J Virol,* 67**,** 4732-41.

WONG, A. R., PEARSON, J. S., BRIGHT, M. D., MUNERA, D., ROBINSON, K. S., LEE, S. F., FRANKEL, G. & HARTLAND, E. L. 2011. Enteropathogenic and enterohaemorrhagic Escherichia coli: even more subversive elements. *Mol Microbiol,* 80**,** 1420-38.

WONG, W. T., KRAUS, M. H., CARLOMAGNO, F., ZELANO, A., DRUCK, T., CROCE, C. M., HUEBNER, K. & DI FIORE, P. P. 1994. The human eps15 gene, encoding a tyrosine kinase substrate, is conserved in evolution and maps to 1p31-p32. *Oncogene,* 9**,** 1591-7.

WONG, W. T., SCHUMACHER, C., SALCINI, A. E., ROMANO, A., CASTAGNINO, P., PELICCI, P. G. & DI FIORE, P. P. 1995. A protein-binding domain, EH, identified in the receptor tyrosine kinase substrate Eps15 and conserved in evolution. *Proc Natl Acad Sci U S A,* 92**,** 9530-4.

WOODRUM, D. T., RICH, S. A. & POLLARD, T. D. 1975. Evidence for biased bidirectional polymerization of actin filaments using heavy meromyosin prepared by an improved method. *J Cell Biol,* 67**,** 231-7.

WUNDERLICH, L., FARAGÓ, A. & BUDAY, L. 1999. Characterization of interactions of Nck with Sos and dynamin. *Cellular Signalling,* 11**,** 25-9.

XU, Y., MOSELEY, J. B., SAGOT, I., POY, F., PELLMAN, D., GOODE, B. L. & ECK, M. J. 2004. Crystal structures of a Formin Homology-2 domain reveal a tethered dimer architecture. *Cell,* 116**,** 711-23.

XUE, J., TSANG, C. W., GAI, W. P., MALLADI, C. S., TRIMBLE, W. S., ROSTAS, J. A. & ROBINSON, P. J. 2004. Septin 3 (G-septin) is a developmentally regulated phosphoprotein enriched in presynaptic nerve terminals. *J Neurochem,* 91**,** 579-90.

XUE, J., WANG, X., MALLADI, C. S., KINOSHITA, M., MILBURN, P. J., LENGYEL, I., ROSTAS, J. A. & ROBINSON, P. J. 2000. Phosphorylation of a new brain-specific septin, G-septin, by cGMP-dependent protein kinase. *J Biol Chem,* 275**,** 10047-56.

YAMABHAI, M., HOFFMAN, N. G., HARDISON, N. L., MCPHERSON, P. S., CASTAGNOLI, L., CESARENI, G. & KAY, B. K. 1998. Intersectin, a novel adaptor protein with two Eps15 homology and five Src homology 3 domains. *The Journal of biological chemistry,* 273**,** 31401-7.

YAMADA, H., ABE, T., SATOH, A., OKAZAKI, N., TAGO, S., KOBAYASHI, K., YOSHIDA, Y., ODA, Y., WATANABE, M., TOMIZAWA, K., MATSUI, H. & TAKEI, K. 2013. Stabilization of actin bundles by a dynamin 1/cortactin ring complex is necessary for growth cone filopodia. *The Journal of neuroscience,* 33**,** 4514-26.

YAMADA, H., TAKEDA, T., MICHIUE, H., ABE, T. & TAKEI, K. 2016. Actin bundling by dynamin 2 and cortactin is implicated in cell migration by stabilizing filopodia in human non-small cell lung carcinoma cells. *International journal of oncology,* 49**,** 877-86.

YAMAUCHI, Y. & HELENIUS, A. 2013. Virus entry at a glance. *J Cell Sci,* 126**,** 1289-95.

YAMAZAKI, D., SUETSUGU, S., MIKI, H., KATAOKA, Y., NISHIKAWA, S., FUJIWARA, T., YOSHIDA, N. & TAKENAWA, T. 2003. WAVE2 is required for directed cell migration and cardiovascular development. *Nature,* 424**,** 452-6.

YANG, Z. & MOSS, B. 2009. Interaction of the vaccinia virus RNA polymerase-associated 94-kilodalton protein with the early transcription factor. *J Virol,* 83**,** 12018-26.

YANG, Z., REYNOLDS, S. E., MARTENS, C. A., BRUNO, D. P., PORCELLA, S. F. & MOSS, B. 2011. Expression profiling of the intermediate and late stages of poxvirus replication. *J Virol,* 85**,** 9899-908.

YARAR, D., TO, W., ABO, A. & WELCH, M. D. 1999. The Wiskott-Aldrich syndrome protein directs actin-based motility by stimulating actin nucleation with the Arp2/3 complex. *Curr Biol,* 9**,** 555-8.

YARMOLA, E. G. & BUBB, M. R. 2006. Profilin: emerging concepts and lingering misconceptions. *Trends Biochem Sci,* 31**,** 197-205.

YBE, J. A. 2014. Novel clathrin activity: developments in health and disease. *Biomol Concepts,* 5**,** 175-82.

YU, J., ZHANG, W., TANG, H., QIAN, H., YANG, J., ZHU, Z., REN, P. & LU, B. 2016. Septin 2 accelerates the progression of biliary tract cancer and is negatively regulated by mir-140-5p. *Gene,* 589**,** 20-26.

YU, L., CHEN, Y. & TOOZE, S. A. 2017. Autophagy pathway: cellular and molecular mechanisms. *Autophagy***,** 0.

YU, W., DING, X., CHEN, F., LIU, M., SHEN, S., GU, X. & YU, L. 2009. The phosphorylation of SEPT2 on Ser218 by casein kinase 2 is important to hepatoma carcinoma cell proliferation. *Mol Cell Biochem,* 325**,** 61-7.

ZAMANIAN, J. L. & KELLY, R. B. 2003. Intersectin 1L guanine nucleotide exchange activity is regulated by adjacent src homology 3 domains that are also involved in endocytosis. *Mol Biol Cell,* 14**,** 1624-37.

ZARRINPAR, A., BHATTACHARYYA, R. P. & LIM, W. A. 2003. The structure and function of proline recognition domains. *Sci STKE,* 2003**,** RE8.

ZECH, T., CALAMINUS, S. D., CASWELL, P., SPENCE, H. J., CARNELL, M., INSALL, R. H., NORMAN, J. & MACHESKY, L. M. 2011. The Arp2/3 activator WASH regulates alpha5beta1-integrin-mediated invasive migration. *J Cell Sci,* 124**,** 3753-9.

ZENT, E., VETTER, I. & WITTINGHOFER, A. 2011. Structural and biochemical properties of Sept7, a unique septin required for filament formation. *Biol Chem,* 392**,** 791-7.

ZENT, E. & WITTINGHOFER, A. 2014. Human septin isoforms and the GDP-GTP cycle. *Biol Chem,* 395**,** 169-80.

ZETTL, M. & WAY, M. 2002. The WH1 and EVH1 domains of WASP and Ena/VASP family members bind distinct sequence motifs. *Curr Biol,* 12**,** 1617-22.

ZHANG, J., KONG, C., XIE, H., MCPHERSON, P. S., GRINSTEIN, S. & TRIMBLE, W. S. 1999. Phosphatidylinositol polyphosphate binding to the mammalian septin H5 is modulated by GTP. *Curr Biol,* 9**,** 1458-67.

ZHANG, Y., KECK, J. G. & MOSS, B. 1992. Transcription of viral late genes is dependent on expression of the viral intermediate gene G8R in cells infected with an inducible conditional-lethal mutant vaccinia virus. *J Virol,* 66**,** 6470-9.

ZHANG, Y. & MOSS, B. 1992. Immature viral envelope formation is interrupted at the same stage by lac operator-mediated repression of the vaccinia virus D13L gene and by the drug rifampicin. *Virology,* 187**,** 643-53.

ZHAO, W., HANSON, L., LOU, H. Y., AKAMATSU, M., CHOWDARY, P. D., SANTORO, F., MARKS, J. R., GRASSART, A., DRUBIN, D. G., CUI, Y. & CUI, B. 2017. Nanoscale manipulation of membrane curvature for probing endocytosis in live cells. *Nat Nanotechnol,* 12**,** 750-756.

ZHAO, X. & ROTENBERG, S. A. 2014. Phosphorylation of Cdc42 effector protein-4 (CEP4) by protein kinase C promotes motility of human breast cells. *J Biol Chem,* 289**,** 25844-54.

ZHUANG, X., CHEN, Z., HE, C., WANG, L., ZHOU, R., YAN, D. & GE, B. 2017. Modulation of host signaling in the inflammatory response by enteropathogenic Escherichia coli virulence proteins. *Cell Mol Immunol,* 14**,** 237-244.

ZUCHERO, J. B., BELIN, B. & MULLINS, R. D. 2012. Actin binding to WH2 domains regulates nuclear import of the multifunctional actin regulator JMY. *Mol Biol Cell,* 23**,** 853-63.

ZUCHERO, J. B., COUTTS, A. S., QUINLAN, M. E., THANGUE, N. B. & MULLINS, R. D. 2009. p53-cofactor JMY is a multifunctional actin nucleation factor. *Nat Cell Biol,* 11**,** 451-9.

ZWARTOUW, H. T. 1964. The Chemical Composition of Vaccinia Virus. *J Gen Microbiol,* 34**,** 115-23.